The Role of TAM Receptors in Immuneparesis in Tissue Compartments in Liver Failure Syndromes

Arjuna Singanayagam

Imperial College London

Department of Metabolism, Digestion and Reproduction

September 2019

Thesis submitted for the degree of Doctor of Philosophy
Imperial College London

Imperial College London
Department of Metabolism, Digestion and Reproduction
Division of Digestive Diseases

Declaration of Originality

I declare that the work in this thesis is my own and all else is appropriately referenced.

Copyright Declaration

The copyright of this thesis rests with the author. Unless otherwise indicated, its contents are licensed under a Creative Commons Attribution-Non-Commercial 4.0 International Licence (CC BY-NC).

Under this licence, you may copy and redistribute the material in any medium or format. You may also create and distribute modified versions of the work. This is on the condition that: you credit the author and do not use it, or any derivative works, for a commercial purpose.

When reusing or sharing this work, ensure you make the licence terms clear to others by naming the licence and linking to the licence text. Where a work has been adapted, you should indicate that the work has been changed and describe those changes.

Please seek permission from the copyright holder for uses of this work that are not included in this licence or permitted under UK Copyright Law.

Dedication

To my father, Jeganath and my late mother Kamala Singanayagam

To my late mentor and supervisor, Harry Antoniades

Acknowledgements

I am grateful and indebted to a number of people for their support and contribution throughout the period of my studies. Firstly, words cannot express my gratitude and reverence for my original primary supervisor, the late Dr Harry Antoniades, who sadly died in April 2018. His encouragement, approachability, experience and mentorship knew no bounds, and has inspired me to pursue a career in academic hepatology. I am truly honoured to have been part of this research group under his guidance and leadership. I would like to thank Professor Mark Thursz, who took over the role as primary supervisor at a late stage in my PhD but, even prior to that as sponsor, provided useful intellectual input and has been very supportive. Special thanks go to my co-supervisor Professor David Adams for the opportunity to conduct a year of research at the National Institute for Health Research (NIHR) Birmingham Biomedical Research Unit (BRU), part of the University of Birmingham. I am grateful for his crucial advice and support as I prepared for my application to the Wellcome Trust Research Training Fellowship and his supervision during my year in Birmingham. Likewise, I would also like to acknowledge the resolute backing from my other co-supervisor Professor Julia Wendon, who originally took me on as a clinical research fellow at King's College Hospital, giving me the opportunity to undertake research in the field and ultimately join the Liver Failure research group.

I feel privileged to have worked at three different institutions during my PhD programme: Imperial College London, the Institute of Liver Studies at King's College Hospital and the NIHR Birmingham BRU in the University of Birmingham. Each place had its unique strengths and all exposed me to a strong research culture, where I was surrounded by dedicated and knowledgeable basic scientists and clinician researchers. It was from this experience that I learnt how successful laboratories functioned, and how to work well collaboratively. In Birmingham, I wish to thank Dr Chris Weston for his practical and intellectual support with immunological techniques and experiments. I also thank Dr Stuart Curbishley for his methodological support, Gill Muirhead for her assistance with principles of culture of hepatic sinusoidal endothelial cells, and Bridgette Gunson for help with management of the Monocyte study administration and due diligence at the Queen Elizabeth Hospital site.

In the Institute of Liver Studies (King's College Hospital), I would express my sincere gratitude to Dr Christine Bernsmeier and Dr Vishal Patel. Both are clinician scientists that already worked within the research group and taught me a great deal on patient consent and recruitment, data management, sample acquisition and storage and the basics of immunological experiments and flow cytometry. Without their initial teachings and encouragement, this thesis would not be possible. Similarly, Dr Evangelos Triantafyllou has been a constant support across all locations, both practically with laboratory experiments, and intellectually with data analysis and presentation. Dr Oltin Pop provided invaluable assistance with immunohistocytochemistry, especially prior to the Wellcome Fellowship application, for which I am thankful. Special thanks go to Dr Mark McPhail who towards the end of my thesis, guided me through metabonomic experiments and statistics amongst other things, and who since the death of my original primary supervisor, has been tremendously supportive and encouraging. Finally, I give thanks to Dr Francesca Trovato who continues to manage the Monocyte study infrastructure admirably.

In the Division of Digestive Diseases, Dr Wafa Khamri has taught and guided me through many aspects of my research. A multitude of others at Imperial College have helped in a variety of ways: Drs Rooshi Nathwani, Sujit Mukherjee, Naveenta Kumar and Fanny Lebossé (patient recruitment, laboratory maintenance, reagents and experimental support); Dr Lucia Possamai (intellectual support); Professor Julian Marchesi, Drs Julie McDonald, Benjamin Mullish, Jesús Miguéns Blanco and Rocio Castro Seoane (assistance in 16S bacterial DNA determination in ascites); Claire Parsonage, Celia Diaz-Moore, Thomas Barbera (help with Monocyte study management at the St. Mary's Hospital site or sample acquisition). It has been a sheer privilege to work with the aforementioned dedicated and talented individuals, and I look forward to working with them on future collaborative projects.

I wish to thank my parents Jeganath and Kamala Singanayagam, who have instilled in me a work ethic and determination which has served me well during this study period, and extended family and friends whose words of encouragement have kept me going in tough times. My fiancée Elaine Burrell deserves

my eternal thanks and praise for her support, patience and understanding during the trials and tribulations of a laboratory-based immunology PhD across three sites.

Finally, I would like to acknowledge the Wellcome Trust for the wonderful opportunity to undertake this period of funded-research.

Abstract

Background: Decompensated liver cirrhosis and acute-on-chronic liver failure (ACLF) – liver failure syndromes - are associated with increased incidence of bacterial infection, often spontaneous bacterial peritonitis (SBP), and a subsequent higher mortality. Within a model of pathological bacterial translocation, immuneparesis increases the susceptibility to infection. TAM receptor MerTK, expressed on monocytes and macrophages, mediates apoptotic cell clearance and attenuates responses to microbial challenge. Whilst MerTK+ circulating monocytes are expanded in ACLF, its role in conjunction with other TAM receptors, Axl and Tyro3, is not known in tissue compartments, such as the peritoneum and liver. In this thesis, I describe the tissue compartmental macrophage phenotype and function in cirrhosis and ACLF, focusing on TAM receptors, and the relationship to microenvironmental mediators.

Methods: Combinations of flow cytometry, gene expression analyses and live cell imaging determined the phenotypic, functional and transcriptomic profile of MerTK+ monocytes/macrophages in cirrhosis and ACLF, in the circulation, peritoneum and liver. The composition of the ascitic microenviroment was determined by enzyme-linked immunosorbent assay (ELISA) and ^{1}H-NMR metabonomics.

Results: Circulating monocyte MerTK expression in ACLF was markedly elevated whilst Axl was low-level and Tyro3 variable. The peritoneum in cirrhosis was immunotolerant, characterized by $MerTK^{high}Axl^{low}$ macrophages primed for apoptotic cell clearance, with impaired antimicrobial cytokine and oxidative burst responses but preserved phagocytosis. In ACLF, ascites contained pro-inflammatory cytokines, metabolites from anaerobic and lipid metabolism and increased apoptotic/necrotic cell death markers in conjunction with higher TAM receptor expression. Hepatic macrophages displayed intermediate MerTK expression.

Conclusions: The work presented in this thesis has determined the TAM receptor expression across tissue compartments, the ascitic microenvironment in cirrhosis and ACLF and identified MerTK as a promising immunotherapeutic target to restore innate immune function in the evolution of ACLF.

List of abbreviations

AC, ascitic cell

ACLF, acute-on-chronic liver failure

ALF, acute liver failure

ALD, alcoholic liver disease

APACHE II, acute physiology and chronic health evaluation II score

AST, aspartate transaminase

Axl, Axl tyrosine kinase receptor

BT, bacterial translocation

CARS, compensatory anti-inflammatory response syndrome

CCR, chemokine (C-C motif) receptor

CD, cluster of differentiation

CPMG, Carr-Purcell-Meiboom-Gill

CRIg, complement receptor of immunoglobulin superfamily

CRP, C-reactive protein

CTP, Child-Turcotte-Pugh

DAMP, damage-associated molecular pattern

DC, dendritic cell

DMSO, dimethyl sulfoxide

EASIA, enzyme amplified sensitivity immunoassay

ELISA, enzyme-linked immunosorbent assay

FACS, fluorescence-activated cell sorting

FVD, fixed viability dye

Gas6, growth-arrest-specific 6

GATA6, GATA-binding factor 6

GM-CSF, granulocyte macrophage colony stimulating factor

HBV, hepatitis B virus

HC, healthy control

HCV, hepatitis C virus

HFE, haemochromatosis

HGF, hepatocyte growth factor

HLA-DR, human leukocyte antigen-DR

HSC, hepatic stellate cell

HSEC, hepatic sinusoidal endothelial cell

HVPG, hepatic venous pressure gradient

IFN, interferon

IL, interleukin

INR, international normalized ratio

ITU, intensive therapy unit

JAK, Janus kinase

KC, Kupffer Cell

LPS, lipopolysaccharide

LTA, lipoteichoic acid

MAPK, mitogen-activated protein kinase

MDR, multi-drug resistant

MDSC, myeloid-derived suppressor cell

MELD, model for end stage liver disease

$MerTK^{-/-}$, Mer tyrosine kinase receptor deficient mice

MerTK, Mer tyrosine kinase receptor

MFI, median fluorescence intensity

MoMF, monocyte-derived macrophage

MPO, myeloperoxidase

NAFLD, non-alcoholic fatty liver disease

NASH, non-alcoholic steatohepatitis

NF-κB, nuclear factor NF-kappa B

NL, normal liver

NS, not significant

OF, organ failure

OPLS-DA, orthogonal projections to latent structures discriminant analysis

PAMP, pathogen-associated molecular pattern

PBC, primary biliary cholangitis

PBMC, peripheral blood mononuclear cell(s)

PBS, phosphate-buffered saline

PCA, principal component analysis

PCR, polymerase chain reaction

PGE_2, prostaglandin E2

PI3K, phosphoinositide 3 kinase

PICD, paracentesis-induced circulatory dysfunction

PMA, phorbol myristate acetate

PMN, polymorphonuclear leucocyte

PPI, proton pump inhibitor

Pros1, protein S

PtdSer, phosphatidylserine

PSC, primary sclerosing cholangitis

PtdSer, phosphatidylserine

ROS, reactive oxygen species

RTK, receptor tyrosine kinase

SALF, seronegative acute liver failure

SBP, spontaneous bacterial peritonitis

SIRS, systemic inflammatory response syndrome

SLE, systemic lupus erythromatosus

SOCS, suppressor of cytokine signaling protein

SOFA, sequential organ failure assessment score

TAM, (Tyro3-Axl-MerTK)

TEM, transendothelial migration

TLR, toll-like receptor

TNF-α, tumor necrosis factor-alpha

VCAM-1, vascular cell adhesion molecule-1

WCC, white cell count

Abstracts and publications related to this work

Publications:

- C. Bernsmeier, O.T. Pop, **A. Singanayagam**, E. Triantafyllou, V.C. Patel, C.J. Weston, S. Curbishley, F. Sadiq, N. Vergis, W. Khamri, W. Bernal, G. Auzinger, M. Heneghan, Y. Ma, W. Jassem, N.D. Heaton, D.H. Adams, A. Quaglia, M.R. Thursz, J. Wendon, C.G. Antoniades. *Patients with acute-on-chronic-liver failure have increased numbers of regulatory immune cells expressing the receptor tyrosine kinase MERTK*. Gastroenterology. 2015. 148:603-615; DOI: 10.1053/j.gastro.2014.11.045
- C. Bernsmeier, E. Triantafyllou, R. Brenig, F.J. Lebosse, **A. Singanayagam**, V.C. Patel, O.T. Pop, W. Khamri, R. Nathwani, R. Tidswell, C.J. Weston, D.H. Adams, M. Thursz, J. Wendon, C.G. Antoniades. *CD14+ CD15- HLA-DR- Myeloid Derived Suppressor Cells Impair Antimicrobial Responses in Patients with Acute-on-Chronic Liver Failure.* Gut. 2018. 6; 1155-1167; DOI: 10.1136/gutjnl-2017-314184

Published Abstracts:

- **A. Singanayagam**, D. Erminelli, E. Triantafyllou, C. Bernsmeier, E Tunc, M. Krasniqi, V.C. Patel, F. Lebosse, R. Nathwani, A. Atkinson, A. Dhar, M. Heneghan, G. Auzinger, W. Khamri, D.H. Adams, J. Wendon, M.R. Thursz, M.J. McPhail, C.G. Antoniades. *Immunometabolic Profiling of Ascites from Patients with Acute-on-Chronic Liver Failure Reveals Increased MerTK+ Immunosuppressive Myeloid Cells and Cell Death Markers with Preferential Lipid Metabolism Compared to Cirrhosis without Organ Failure.* Journal of Hepatology. 2019 April; (70); S1:183
- **A Singanayagam**, E. Triantafyllou, V.C. Patel, C. Bernsmeier, C. Weston, S. Curbishley, C. Willars, W. Bernal, G. Auzinger, M. Heneghan, A. Dhar, D.H. Adams , M. Thursz, J. Wendon, C.G. Antoniades. *Mer Tyrosine Kinase Regulates the Activation of Myeloid Cells and Innate Immune Responses in Acute-on-Chronic Liver Failure.* Journal of Hepatology. 2016; (64); S2: S143

Table of Contents

Declaration of Originality **2**

Copyright Declaration **2**

Dedication **3**

Acknowledgements **4**

Abstract **7**

List of abbreviations **8**

Abstracts and publications related to this work **12**

Table of Contents **13**

Table of Figures **24**

List of Tables **27**

1. Introduction **30**

1.1. Liver Failure Syndromes **30**

1.1.1. Liver Cirrhosis: Definition 30

1.1.2. Liver Cirrhosis: Epidemiology and Aetiology 30

1.1.3. Decompensation of Liver Cirrhosis 31

1.1.4. Acute-on-chronic Liver Failure (ACLF) 31

1.1.5. Acute Liver Failure 32

1.2. Acute-On-Chronic Liver Failure **32**

1.2.1. Definition 32

1.2.2. Prevalence and Prognosis 33

1.2.3. Pathophysiology and Systemic Inflammation 34

1.2.4. Scoring Systems in ACLF 36

1.2.5. Management of ACLF 37

1.3. Infections in Cirrhosis 37

1.3.1. Prevalence, Incidence and Outcomes of Infections in Cirrhosis 37

1.3.2. Second Infections in Hospitalized Cirrhotic Patients 38

1.3.3. Characteristics of Infections and Multi-Drug Resistance in Cirrhosis 38

1.3.4. Clinical Risk Factors for Infection in Cirrhosis 39

1.3.5. Bacterial Infection as a Precipitant for ACLF 39

1.3.6. Development of Infection in ACLF 40

1.4. Spontaneous Bacterial Peritonitis 40

1.4.1. Diagnosis and Sequelae of SBP 40

1.4.2. Risk Factors for Development of SBP 41

1.4.3. Empirical and Prophylactic Antibiotic Treatment for SBP 42

1.5. Pathogenesis of Bacterial Infections in Cirrhosis 43

1.5.1. Alterations to the Gut Microbiome 44

1.5.2. Intestinal Barrier Dysfunction 44

1.5.3. Gut-Associated Lymphoid Tissue and Mesenteric Lymph Nodes 45

1.6. Cirrhosis-Associated Immune Dysfunction 45

1.6.1. Inflammation: Basic Concepts 46

1.6.2. Concepts of Inflammation in Cirrhosis and ACLF 47

1.6.2.1. Systemic Inflammation in Cirrhosis and ACLF 47

1.6.2.2. Immuneparesis in Cirrhosis and ACLF 49

1.6.2.3. Monocyte Dysfunction in ACLF 49

1.6.2.4. Myeloid-Derived Suppressor Cells in ACLF 49

1.6.2.5. Neutrophil Dysfunction in Cirrhosis and ACLF 50

1.6.2.6. Adaptive Immune Defects in Cirrhosis and ACLF 50

1.6.2.7. Mechanisms of Immuneparesis in CAID and ACLF 51

1.6.2.8. Metabolic and Neuroendocrine Factors 51

1.7. Tissue Compartmental Immune Dysfunction in Cirrhosis 52

1.7.1. Role of the Liver in Cirrhosis-Associated Immune Dysfunction 53

1.7.1.1. Immune Functions of the Liver in Steady-State 53

1.7.1.2. Role of the Liver in the Systemic Immune Response 54

1.7.1.3. Impaired Liver Immune Function in Cirrhosis 56

1.7.2. Peritoneal Immunity in Cirrhosis-associated Immune Dysfunction 56

1.7.2.1. The Peritoneal Cavity 56

1.7.2.2. Characterisation of Peritoneal Macrophages & Ontogeny 57

1.7.2.3. Peritoneal Macrophage Function at Steady-State 58

1.7.2.4. Peritoneal Immunity in Cirrhosis 59

1.7.2.5. Dysregulated Ascitic Microenvironment 60

1.8. Monocyte and Macrophage Dysfunction in Liver Disease 60

1.8.1. Monocytes in Health 60

1.8.1.1. Monocyte Classification 61

1.8.1.2. Monocyte Recruitment to Sites of Injury or Infection 61

1.8.2. Monocyte Dysfunction in Cirrhosis and ACLF 62

1.8.3. Macrophage Biology 63

1.8.4. Resolution Responses and the Role of Macrophages 64

1.9. TAM Receptors 65

1.9.1. Immunobiology of TAM Receptors 65

1.9.2. TAM Receptor Structure and Expression 66

1.9.3. TAM Receptor Ligands 67

1.9.4. Signal Transduction of the TAM Receptors in Immune Regulation 67

1.9.4.1. Differential Expression of TAM Receptors 69

1.9.5. TAM Receptors and Autoimmunity 70

1.9.6. TAM Receptors in Viral Infection 70

1.9.7. TAM Receptors in Cancer Immunopathology 71

1.9.8. TAM Receptors in Liver Disease 71

1.9.8.1. Steady State 71

1.9.8.2. Acute and Chronic Liver Injury 72

1.10. Summary and Aims 73

2. Phenotype and Function of Circulating Monocytes in Acute-on-Chronic Liver Failure 76

2.1. Background and Aims 76

2.2. Materials and Methods 78

2.2.1. Patient recruitment 78

2.2.2. Clinical Data 78

2.2.3. Isolation of Peripheral Blood Mononuclear Cells 79

2.2.4. Isolation of CD14+ Monocytes by Magnetic Bead Separation 79

2.2.5. Isolation of Healthy Neutrophils by Density-Gradient Separation 80

2.2.6. Immunophenotyping of Monocytes by Flow Cytometry 81

2.2.7. Intracellular Cytokine Staining of PBMCs 81

2.2.8. Fluorescence Activated Cell Sorting of Live Cells 82

2.2.9. Gene Expression Analysis..... 83

2.2.10. Phagocytosis Imaging of Monocytes Conditioned in ACLF Plasma by Cell-IQ® 84

2.2.11. Statistical Analysis 85

2.3. Results 86

2.3.1. Clinical Summary of Recruited Patients 86

2.3.2. Immunophenotype of Circulating Monocytes 88

2.3.3. Gene Expression Profiling of MerTK+ Monocytes 92

2.3.4. Intracellular Cytokine Staining of Monocytes in ACLF 93

2.3.5. Monocyte Phagocytosis: Cell-IQ® Live Cell Imaging 95

2.3.6. Clinical Associations of TAM Receptors..... 97

2.4. Discussion 99

2.5. Conclusion 102

3. The Peritoneal Compartment is an Immunotolerant Environment in Liver Disease Characterised by MerTK^{high} Macrophages 106

3.1. Background and Aims 106

3.2. Material and Methods 108

3.2.1. Patient recruitment..... 108

3.2.2. Clinical Data..... 108

3.2.3. Biological Sample Acquisition..... 109

3.2.4. Acquisition and Storage of Plasma..... 110

3.2.5. Isolation of peripheral blood mononuclear cells, healthy neutrophils and CD14+ monocytes 110

3.2.6. *Ex-vivo* isolation and storage of ascitic cells..... 110

3.2.7. Storage of ascites for cytokine and metabolite analysis and pellet for bacterial DNA analysis 111

3.2.8. Flow cytometry of immune cells for immunophenotyping 111

3.2.9. Multicolour flow cytometry panel design, compensation and analysis 112

3.2.10. Monocyte-derived macrophage *in vitro* culture: M0 Protocol 113

3.2.11. Monocyte-derived Macrophage *in vitro* culture: M1/M2 Protocol 114

3.2.12. *In vitro* culture of healthy peripheral blood mononuclear cells in ascites or plasma 115

3.2.13. *In vitro* culture of healthy PBMCs in cytokines 116

3.2.14. FACS sorting of cells 116

3.2.15. Gene expression analysis 117

3.2.16. Measurement of inflammatory mediator and cytokine concentrations 117

3.2.17. Measurement of Cytokeratin 18 Products 118

3.2.18. Measurement of Gas6 and Galectin-3 Concentrations 118

3.2.19. Differentiation of THP-1 Monocytes to Macrophages 118

3.2.20. Peritoneal Macrophage Efferocytosis of Apoptotic Neutrophils 119

3.2.21. pHrodo™ Phagocytosis Assay for Peritoneal Macrophages 120

3.2.22. Modified *Ex-vivo* Phagoburst™ Oxidative Burst Assay for Ascitic Cells 122

3.2.23. CellROX™ Deep Red Assay for Oxidative Stress Detection 123

3.2.24. Intracellular Cytokine Staining Protocol for TLR Agonists 124

3.2.25. Ascites DNA Extraction and Quantification 124

3.2.26. 16S rRNA Gene qPCR and Sequencing 125

3.2.27. Ascitic and Plasma Metabonomic Profiling 125

3.3. Results 128

3.3.1. Patient Characteristics 128

3.3.2. ACLF Ascites Promotes a MerTK^{high} HLA-DR^{low} Immunosuppressive Phenotype 130

3.3.3. MerTK Expression on Ascites-Conditioned Monocytes Correlates with Ascitic Cell Death Markers and Multiple Inflammatory Cytokines 132

3.3.4. ACLF Ascites Expands the Immunosuppressive M-MDSC-like Cell Population 134

3.3.5. M2c Polarising Cytokines Promote Expression of MerTK, Axl and CD163 136

3.3.6. TAM Receptor Expression in THP-1 Macrophages is Enhanced by ACLF Ascites 137

3.3.7. *Ex-vivo* Phenotype of Peritoneal Macrophages in Decompensated Cirrhosis Reveals a MerTK^{high} Axl$_{low}$ CD16^{high} Predominance 137

3.3.8. Clinical Associations with Peritoneal Macrophage *Ex-Vivo* Phenotype 138

3.3.9. Decompensated Cirrhotic Peritoneal Macrophages Exhibit Higher MerTK and Lower HLA-DR Expression than Ovarian Cancer Ascites and Healthy Monocyte-Derived Macrophages 143

3.3.10. *Ex-vivo* MerTK Expression on Peritoneal Macrophages in Ascites is Significantly Greater than Circulating Monocytes in the Same Patients 145

3.3.11. *Ex-Vivo* Peritoneal Monocytic Myeloid-Derived Suppressor-Like Cells (M-MDSCs) Demonstrate Increased MerTK Expression in AD and ACLF 145

3.3.12. Concentration of M30 and M65 is Increased in Ascites and in ACLF Compared to Plasma and Cirrhosis Without Organ Failure 146

3.3.13. Peritoneal Macrophages in Cirrhotic Ascites Display Greater Efferocytic Capacity than Healthy Circulating Monocytes with Associated Upregulation of MerTK and Axl 149

3.3.14. Peritoneal Macrophages from Cirrhotic Ascites have Attenuated Pro-inflammatory Cytokine Responses to Lipopolysaccharide 151

3.3.15. Peritoneal Macrophages Demonstrate Preserved Bacterial Phagocytosis 153

3.3.16. Peritoneal Macrophages from Patients with Cirrhosis have Impaired Oxidative Burst 156

3.3.17. Analysis of Secreted Factors in Ascites of Patients with ACLF Demonstrated Increased Pro-Inflammatory Cytokines TNF-α and IL-1β but no changes to TAM Ligands Compared to Patients with Cirrhosis without Organ Failure 159

3.3.18. Gene Expression Profiles of MerTK+ FACS Sorted Ascitic Cells Reveals an Immunotolerant Profile in Steady-State 162

3.3.19. LPS-Stimulated Transcriptomic Profile of Peritoneal Macrophages in Cirrhosis in Comparison with Monocyte-Derived Macrophages 164

3.3.20. Ascites 16S Bacterial DNA was not Associated with Poor Clinical Outcomes or TAM Receptor Expression 166

3.3.21. Metabonomic Analysis of Ascites Reveals Switch to Anaerobic Metabolism in ACLF 169

3.3.22. Clinical Associations of Immunological and Soluble Mediator Parameters 171

3.4. Discussion 177

3.4.1. Ascitic Macrophage Phenotype, Cytokines, Mediators and Bacterial DNA 177

3.4.2. Functional Characteristics of Peritoneal Macrophages in Cirrhosis 183

3.5. Conclusion 187

4. Hepatic Macrophage Phenotype and Function in Advanced Liver Cirrhosis 192

4.1. Background and Aims 192

4.2. Materials and Methods 194

4.2.1. Patient Recruitment 194

4.2.2. Isolation of Hepatic Mononuclear Cells 194

4.2.3. Flow cytometry of hepatic mononuclear cells for immunophenotyping 195

4.2.4. Measurement of LPS-Stimulated Liver Macrophage TNF-α Production 196

4.2.5. pHrodo™ Phagocytosis Assay for Liver Macrophages 196

4.2.6. Flow Cytometric Analysis 196

4.3. Results 197

4.3.1. Characteristics of explanted liver 197

4.3.2. Clinical and Biochemical Correlations with Immunophenotype 198

4.3.3. Flow Cytometry Gating and Minimisation of Autofluorescence 199

4.3.4. Immunophenotype of Hepatic Macrophages in Advanced Cirrhosis 200

4.3.5. Comparison of MerTK Expression Between Tissue Compartments 204

4.3.6. Antimicrobial Responses of Hepatic Macrophages 204

4.4. Discussion 206

4.5. Conclusion 210

5. Monocyte Transendothelial Migration 214

5.1. Background and Aims 214

5.2. Material and Methods 216

5.2.1. Hepatic Sinusoidal Endothelial Cell Culture 216

5.2.2. PBMC Isolation and CD14 Magnetic Bead Selection 216

5.2.3. Bidirectional *In Vitro* Transendothelial Monocyte Migration Assay 217

5.2.4. Immunophenotyping of Monocytes 218

5.2.5. Intracellular Cytokine Staining and pHrodo™ Phagocytosis Assays 218

5.2.6. Flow Cytometric and Statistical Analysis 218

5.2.7. Migration Flow Assay 219

5.3. Results 220

5.3.1. Transendothelial Monocyte Migration.....220

5.3.2. Flow Based Adhesion Assay.....223

5.4. Discussion.....225

5.5. Conclusion.....228

6. Inhibition of Mer Tyrosine Kinase Signalling.....232

6.1. Background and Aims.....232

6.2. Materials and Methods.....234

6.2.1. Reconstitution of UNC2025.....234

6.2.2. UNC2025 Titration Experiments.....234

6.2.3. Measurement of Pro-inflammatory Cytokines and Apoptosis Markers by ELISA.....236

6.2.4. Effect of UNC2025 on Efferocytosis of Apoptotic Neutrophils.....236

6.2.5. Proinflammatory Cytokine Production of PBMCs Conditioned in Ascites +/- Antagonists 236

6.2.6. Reconstitution and Concentrations of MerTK Signalling Antagonists.....237

6.3. Results.....238

6.3.1. UNC2025 Concentrations Above 500nM Reduce Ascitic Cell Survival and Impair LPS-stimulated Pro-Inflammatory Cytokine Production.....238

6.3.2. LXR-α Antagonist GSK2033 Enhances LPS-Stimulated TNF-α Production in PBMCs Conditioned in 50% Ascites from Patients with ACLF.....240

6.4. Discussion.....243

6.5. Conclusion.....246

7. General Discussion.....250

7.1. Introduction.....250

7.2. Synthesis of Findings.....251

7.2.1. Circulation 251

7.2.2. Peritoneum 253

7.2.3. Liver 256

7.2.4. Transendothelial Migration 256

7.2.5. Inhibition of MerTK Signalling Pathways 257

7.2.6. Re-circulation Hypothesis: MerTK+ Monocytes/Macrophages Promote Immuneparesis in Compartments in ACLF 259

7.3. Limitations 260

7.4. Future Directions 262

CHAPTER 8 263

8. References 264

9. Appendix 293

Table of Figures

Figure 1.1 Cirrhosis-associated Immune Dysfunction 47

Figure 1.2 Schematic of TAM Receptor and Ligand structure 66

Figure 1.3 Schematic of TAM signalling pathway in innate immune cells 68

Figure 2.1 TAM receptor Immunophenotype of Circulating Monocytes 90

Figure 2.2 Immunophenotype of TAM+ vs. TAM- receptors on monocytes in ACLF 91

Figure 2.3 Gene expression profile of MerTK+ vs. MerTK- monocytes 93

Figure 2.4 Intracellular Cytokine Production of Circulating Monocytes 95

Figure 2.5 Live Cell Kinetic Imaging of *E. coli* BioParticle™ Monocyte Phagocytosis 96

Figure 2.6 Clinical Outcomes and Correlations of Recruited Patients 98

Figure 3.1 Ascites from Patients with ACLF Compared with Cirrhosis without Organ Failure Increases MerTK Expression on Monocytes and Correlates with Clinical Parameters, Cytokines and Outcome 133

Figure 3.2 Effect of the ascitic microenvironment in cirrhosis without organ failure and ACLF on monocyte phenotype and frequency of *in vitro* M-MDSCs 135

Figure 3.3 Effect of Cytokines on CD33+ CD14+ Surface Expression on MerTK, Axl & CD163 136

Figure 3.4 *Ex-vivo* phenotype of peritoneal macrophages from patients with cirrhosis and ascites. 140

Figure 3.5 Percentage of *ex-vivo* MerTK+ peritoneal macrophages correlates with fibrosis surrogate marker Mean Platelet Volume and CD14++ CD16++ MerTK+ macrophages are expanded in AD-ACLF 142

Figure 3.6 Cirrhotic peritoneal macrophage phenotype compared with *in vitro* monocyte-derived macrophage and ovarian cancer ascitic macrophage phenotype 143

Figure 3.7 Comparison of the MerTK expression in matched circulating monocytes and peritoneal macrophages and in peritoneal M-MDSCs 145

Figure 3.8 Cell death marker M30 & M65 concentration in plasma and ascites of patients with cirrhosis without organ failure and ACLF compared with healthy plasma and ovarian cancer ascites 147

Figure 3.9 Efferocytosis of apoptotic neutrophils by peritoneal macrophages from cirrhotic ascites compared with healthy monocytes from PBMCs 149

Figure 3.10 Attenuated LPS-stimulated TNF-α and IL-6 production of peritoneal macrophages from ascites of patients with cirrhosis 151

Figure 3.11 pHrodo™ optimization for peritoneal macrophage phagocytosis assay 153

Figure 3.12 Phagocytosis of *E. coli* BioParticles™ is preserved in ascitic peritoneal macrophages compared with healthy monocytes and *in vitro* monocyte-derived macrophages 154

Figure 3.13 Peritoneal macrophage oxidative burst in patients with cirrhosis and ascites 157

Figure 3.14 Ascites cytokine profile comparing cirrhosis without failure, ACLF and ovarian cancer patients 160

Figure 3.15 Gas6 and Galectin-3 Concentration in Plasma and Ascites 161

Figure 3.16 Gene expression pattern of MerTK+ vs. MerTK- ascitic cells in steady state 163

Figure 3.17 Gene expression profile of peritoneal macrophages and monocyte-derived macrophages sorted according to MerTK status and exposure to LPS 165

Figure 3.18 Ascites bacterial DNA according to outcome and relevant clinical parameters 167

Figure 3.19 Score Scatter and Permutation Plots in a Valid OPLS-DA Model for Ascites CPMG 169

Figure 3.20 Ascites Metabonomic Analysis Reveals Switch to Anaerobic Metabolism in ACLF Compared to Cirrhosis without Organ Failure 170

Figure 3.21 Correlation Matrix of Ascites Metabolites Revealing Metabolically-Stressed Peritoneal Compartment in ACLF 171

Figure 4.1 Liver explant aetiology 197

Figure 4.2 Liver mononuclear cell flow cytometry gating 200

Figure 4.3 Immunophenotype of liver macrophages 202

Figure 4.4 Hepatic macrophage surface marker expression according to CD16 subset 203

Figure 4.5 MerTK-expressing Monocyte/Macrophage Subsets in Tissue Compartments in Cirrhosis 204

Figure 4.6 Phagocytosis and LPS-Stimulated TNF-α Production of Liver Macrophages..... 205

Figure 5.1 Transendothelial Migration Assay to Recapitulate Monocyte Entry into Tissue and Associated Phenotypic and Functional Attributes..... 222

Figure 5.2 Images from Flow-Based Monocyte Adhesion Assay..... 224

Figure 6.1 Effect of MerTK Signalling Inhibitor UNC2025 Concentration on LPS-Stimulated Cytokine Production, Cell Survival and Efferocytosis 239

Figure 6.2 Effect of MerTK antagonists on LPS-Stimulated TNF-α Production, and HLA-DR and MerTK Expression in PBMCs Exposed to 50% Ascites from Patients with ACLF..... 241

Figure 7.1 Schematic Diagram Proposing the Evolution of MerTK+ Monocytes / Macrophages in Compartments in Liver Injury..... 259

List of Tables

Table 1.1 Definition of organ failures in patients with cirrhosis. 33

Table 1.2 Biological and physiological features of M1/M2 macrophages in humans 63

Table 2.1 Summary of clinical, physiological and biochemical parameters of recruited patients for circulation studies 87

Table 3.1 Clinical and Physiological Characteristics of Recruited Patients with Cirrhosis and Ascites without Organ Failure and Patients with Acute-on-Chronic Liver Failure 129

Table 3.2 Characteristics of Patients with Ovarian Cancer and Malignant Ascites 130

Table 3.3 Immunometabolic Variables in Ascites of Patients with Cirrhosis without Organ Failure compared with ACLF 173

Table 3.4 Clinical and Immunometabolic variables Comparing Survivors and Non-survivors at 90 days 174

Table 3.5 Univariate analysis for clinical and immunometabolic variables for development of SBP 176

Table 4.1 Summary of clinical and biochemical characteristics of patients recruited for phenotyping of liver explant specimens, just prior to liver transplant. 199

CHAPTER 1

1. INTRODUCTION

1.1. Liver Failure Syndromes

1.1.1. Liver Cirrhosis: Definition

Chronic liver injury from persistent or repeated insult leads to recurrent inflammation, perpetuation of the normal wound-healing response, and progressive fibrosis, where the injured liver is gradually replaced by increasing amounts of collagenous scar tissue. The rate of liver fibrosis progression depends upon several factors including nature of the insult, host and environmental factors (Schuppan & Afdhal, 2008). Liver cirrhosis is an advanced stage of fibrosis, and is defined histologically by development of regenerative nodules surrounded by dense fibrous septa, accompanied by liver vasculature distortion. The latter leads to increased intrahepatic resistance to blood flow, portal hypertension, and potentially shunting of portal venous blood directly to the hepatic venous outflow via collateral vessels (porto-systemic shunting). Normal functioning of the liver requires exchanges between healthy hepatocytes and hepatic sinusoids, which are vascular spaces lined by fenestrated endothelial cells resting on permeable connective tissue, across the space of Disse (Abdel-Misih & Bloomston, 2010). In cirrhosis, diminished hepatocyte number and function, fibrogenesis from multiple mechanisms including activation of stellate cells in the space of Disse, endothelial cell dysfunction and loss of fenestrations, lead to impaired liver synthetic function and eventually to end-stage liver cirrhosis, providing a substrate for development of hepatocellular carcinoma (HCC) (Pinzani & Macias-Barragan, 2010).

1.1.2. Liver Cirrhosis: Epidemiology and Aetiology

Cirrhosis is a global health problem, accounting for 1.16 million deaths per year. With the additional 788,000 deaths per annum from liver cancer, liver-related deaths account for 3.5% of all deaths worldwide and its burden predicted to increase (Asrani *et al.*, 2019). In contrast to France and Italy, mortality from liver disease in the UK is climbing, having increased four times since 1970 and representing the third most common cause of premature death (Williams & Horton, 2013). In the United

States, deaths from cirrhosis from 1999 to 2016 increased by 65% and mortality due to sepsis increased annually by 7.1% (Tapper & Parikh, 2018). The most common causes for liver cirrhosis in the West include alcoholic liver disease, non-alcoholic fatty liver disease (NAFLD) and hepatitis C, whilst chronic hepatitis B is the leading cause in the Far East and sub-Saharan Africa (Williams & Horton, 2013). The severity and prognosis of cirrhosis can be predicted by using scoring tools, such as the Child-Turcotte-Pugh (CTP) and Model for End-Stage Liver Disease (MELD) scores (Pugh *et al.*, 1973; Wiesner *et al.*, 2003).

1.1.3. Decompensation of Liver Cirrhosis

Cirrhosis may be clinically silent for many years, often being incidentally detected when blood tests or radiology suggests liver disease. In this phase, cirrhosis is referred to as compensated. Symptoms usually develop when liver cirrhosis is complicated by an episode of decompensation. Acute decompensation (AD) of liver cirrhosis refers to a state whereby the residual function of the liver is insufficient, due to parenchymal extinction, leading to ascites (the pathological accumulation of fluid in the peritoneal cavity), bleeding from oesophago-gastric varices (swollen or enlarged veins), hepatic encephalopathy, hepatorenal dysfunction or bacterial infection. Progressive portal hypertension, in which there is an increased hepatic venous pressure gradient (HVPG) due to increased intrahepatic vascular resistance and endothelial dysfunction, is a main factor in decompensation (Berzigotti *et al.*, 2013). Once decompensated, survival reduces to 50% at one year and mortality may be as high as 85% over 5 years in the absence of liver transplantation, evaluation for which is recommended if there are no contraindications (D'Amico *et al.*, 2018).

1.1.4. Acute-on-chronic Liver Failure (ACLF)

Acute-on-chronic liver failure (ACLF) is recognized as a distinct entity characterized by the unexpected and abrupt deterioration of liver function triggered by a precipitating illness (although unidentifiable in 40-50%) in a patient with pre-existing liver disease, associated with extrahepatic organ injury and a high short-term mortality (Bernal *et al.*, 2015). In the landmark Chronic liver failure/Acute-on-Chronic

Liver Failure in Cirrhosis (CANONIC) study, this mortality was 30% at 28-days (Moreau *et al.*, 2013). The increased risk of mortality is comparable to acute liver failure (ALF) and vastly higher than would be expected for the natural progression of chronically decompensated cirrhosis, which is less than 5% at 28-days (Asrani, Simonetto & Kamath, 2015). The economic burden of ACLF is also high, with one US study quoting a cost of $1.7 billion for 32,000 ACLF hospitalizations, the cost of which were 3.5-fold higher per hospitalization than cirrhosis without ACLF (Allen *et al.*, 2016).

1.1.5. Acute Liver Failure

Acute liver failure is a rapid-onset severe liver injury, often with massive hepatic necrosis, associated with diminished hepatic function, defined as coagulopathy (international normalized ratio [INR] > 1.5) and any grade of encephalopathy in a patient without pre-existing liver disease (Polson & Lee, 2005). In severe cases, multi-organ failure may ensue, often necessitating intensive care management. In patients where there is a failure of the liver to regenerate or residual functional liver mass is insufficient to meet demands, liver transplantation is a treatment option (Adam *et al.*, 2012). In the UK, the King's College Hospital criteria is widely used to predict poor survival in the absence of transplant (O'Grady *et al.*, 1989).

1.2. Acute-On-Chronic Liver Failure

1.2.1. Definition

The precise definition of ACLF remains debated globally; the criteria for the European Association of Study of the Liver (EASL) and American Association for the Study of Liver Diseases (AASLD) includes only patients with pre-existing cirrhosis whereas the Asian Pacific Association for the Study of the Liver (APASL) specifies that ACLF occurs in patients with non-cirrhotic chronic liver disease (Duseja & Singh, 2017). The EASL definition is based on the landmark CANONIC study, a prospective observational multicentre European study, conducted by the Chronic Liver Failure-Consortium (CLIF-C). Here, Moreau and colleagues stated the diagnostic criteria of ACLF as having three

components: (1) the presence of acute decompensation of cirrhosis (as described above), (2) organ failure (at least one), as defined by a modified sequential organ failure assessment (SOFA) scale called CLIF-SOFA (**Table 1.1**) and (3) a transplant-free mortality rate greater than 15% at 28 days (Moreau *et al.*, 2013). It should be noted that, irrespective of the precise definition, even the concept of ACLF as a distinct entity is debated by some (O'Grady, 2017).

Table 1.1 Definition of organ failures in patients with cirrhosis.

	The CLIF-SOFA scale				
Organ/system	0	1	2	3	4
Liver Bilirubin (mg/dl)	<1.2	≥1.2-<1.9	≥2-<5.9	≥6-<12	≥12
Kidney Creatinine (mg/dl)	<1.2	≥1.2-<1.9	≥2-<3.5	≥3.5-<5	≥5
Cerebral (HE grade)	No HE	1	2	3	4
Coagulation	INR <1.1	INR 1.1-1.25	INR 1.26-1.5	INR 1.51-2.5	INR >2.5 or platelets ≤20x10^3/µl
Circulation MAP (mmHg)	≥70	<70	Dopamine ≤5 or dobutamine or terlipressin	Dopamine >5-≤15 or epinephrine ≤0.1 or norepinephrine ≤0.1	Dopamine >15 or epinephrine >0.1 or norepinephrine >0.1
Lungs PaO_2/FiO_2 or SpO_2/FiO_2	>400 >512	≤400 >357-≤512	≤300 >214-≤357	≤200 >89-≤214	≤100 ≤89

ACLF grade	**Definition**
No	• No organ failure • Single organ failure (liver, coagulation, circulation, lungs) + creatinine <1.5 mg/dl + no hepatic encephalopathy • Single cerebral failure + creatinine <1.5 mg/dl
1	• Single kidney failure • Single organ failure (liver, coagulation, circulation, lungs) + creatinine 1.5-≤1.9 mg/dl and/or grade 1-2 hepatic encephalopathy • Single cerebral failure + creatinine 1.5-≤1.9 mg/dl
2	• 2 organ failures
3	• 3 organ failures or more

CLIF-SOFA score to determine severity of organ failure. Sub-scores from 0-4 for six organ systems (liver, kidney, cerebral, coagulation, circulation and lungs). Composite score 0-24. Doses of catecholamine vasopressors or inotropes are µg/kg/min. Yellow highlighted areas represent diagnostic criteria for organ failure. Lower table is CLIF-organ failure (OF) score which determined ACLF grade. Abbreviations: HE, hepatic encephalopathy; INR, international normalised ratio; MAP, mean arterial pressure; PaO_2, partial pressure of arterial oxygen; FiO_2, fraction of inspired oxygen; SpO_2, pulse oximetric saturation. Taken from Jalan *et al.* (2014).

1.2.2. Prevalence and Prognosis

Analysis of the 1343 patients with decompensated liver cirrhosis in the CANONIC database suggested a 30.9% prevalence of ACLF either at enrolment or during the 28-day follow-up period. Other studies

confirm ACLF is common, reporting a range of 10-40% of hospitalized patients with cirrhosis (Hernaez *et al.*, 2017). The prognosis was very poor in the CANONIC study, with an overall 28-day mortality of 32.8% and 90-day mortality 51.2% (Moreau *et al.*, 2013). However, mortality in ACLF is independent of the precipitating event but related more to the number of organ failures and the early clinical course of ACLF, highlighting the importance of the host response to injury rather than the nature of the precipitant (Moreau, Jalan & Arroyo, 2015). Indeed, the CANONIC study demonstrated that ACLF is a dynamic syndrome, with 50% improving, 30% with a steady or fluctuating course and 20% worsening over the follow-up period. In the 20% that deteriorated, the mortality was over 50%. Those with three organ failures (deemed ACLF grade 3) had the lowest chances of resolution, with a 74.5% 28-day mortality (Gustot *et al.*, 2015). Survival is less likely with increasing organ failure (Bajaj *et al.*, 2014). Almost half of patients with ACLF either had no preceding decompensations of cirrhosis or developed their first AD within the previous 3 months, suggesting ACLF is not merely at one extreme in the spectrum of severity of decompensated cirrhosis. In fact, 28-day mortality was higher from ACLF in the group without prior decompensation (42% vs. 29%) (Moreau *et al.*, 2013; Moreau, Jalan & Arroyo, 2015).

1.2.3. Pathophysiology and Systemic Inflammation

The pathophysiology of ACLF is commonly described in terms of the predisposition, injury, response and organ (PIRO) framework that was previously used to classify severe sepsis (Jalan *et al.*, 2012). The predisposition refers to any aetiology of chronic liver disease; however, in the CANONIC study, ACLF developed most frequently in patients with acute decompensated cirrhosis who were younger and with an alcohol aetiology. In contrast, those with cirrhosis due to hepatitis C were least likely to develop ACLF. Regardless, once ACLF developed, the outcome was dependent on the severity of the syndrome rather than the predisposing cause (Moreau *et al.*, 2013; Bernal *et al.*, 2015). Lower baseline mean arterial pressure (MAP), presence of ascites, higher MELD score and lower baseline haemoglobin were all found to independent predictors for the development of ACLF at one year (Piano *et al.*, 2017). Part of the predisposition also relates to the pathophysiology of cirrhosis, in which there is felt to be

underlying low grade systemic inflammation. Here, liver tissue injury from the cause of liver disease generates damage-associated molecular patterns (DAMPs) which triggers the immune system and additionally, there is pathological bacterial translocation from the intestine to the systemic circulation, resulting in pathogen associated molecular patterns (PAMPs) further stimulating host immunity (Wiest, Lawson & Geuking, 2014). Systemic circulatory dysfunction also occurs in cirrhosis; any further insult could lead to exacerbation of these underlying processes (Ho & Huang, 2015).

Injury refers to the precipitating event which, 40% of the time, cannot be identified. Where it can, infections are the most common precipitant and bacterial infections are at least twice more common in patients with cirrhosis, who are 2-4 times more like to die from sepsis than non-cirrhotic patients (Foreman, Mannino & Moss, 2003; Arvaniti *et al.*, 2010). Other precipitants include variceal bleeding (especially in patients with Child Pugh C cirrhosis), an alcohol binge or acute alcoholic hepatitis, hepatotoxic drugs, hypoxic hepatitis or viral hepatitis; reactivation of hepatitis B is the commonest cause for ACLF in the Asia-pacific region (Blasco-Algora *et al.*, 2015).

The response in ACLF is typified by the systemic inflammatory response syndrome (SIRS) and is crucial in determining severity and prognosis. In the CANONIC study, the admission white cell count (WCC) and plasma C-reactive protein (CRP) were both higher in the ACLF group compared with the non-ACLF group, irrespective of the presence or absence of bacterial infection or a diagnosis of alcoholic hepatitis (Clària *et al.*, 2016b; Laleman *et al.*, 2018). As seen in sepsis, acute alcoholic hepatitis and acute liver failure (ALF), the presence of the systemic inflammatory response syndrome (SIRS) in ACLF (as defined by two or more of: temperature > 38°C and <36°C, heart rate > 90 beats per minute, respiratory rate > 20 or $PaCO_2$ < 32mmHg, and WCC <4,000/mm^3 or >12,000/mm^3 or > 10% immature forms) predicts a poorer prognosis and in the CANONIC study, mortality correlated with increasing admission WCC (Verbeke, Nevens & Laleman, 2011; Cazzaniga *et al.*, 2009; Michelena *et al.*, 2015; Mehta *et al.*, 2015). Additionally, the number of failing organs positively correlated with the WCC and CRP, suggesting the intensity of the host inflammatory response closely relates to organ failures (Moreau, Jalan & Arroyo, 2015). Whilst there may be a range of elevated pro-inflammatory cytokines in ACLF, a compensatory anti-inflammatory response syndrome (CARS) is concurrently initiated, its persistence leading to immuneparesis (or immune paralysis) in which there

is an increased risk of sepsis and mortality (Wasmuth *et al.*, 2005; Selvapatt *et al.*, 2014; Clària *et al.*, 2016b). Immuneparesis in ACLF including CARS is discussed in greater depth subsequently.

Organ injury may be the most predictive of outcome. Non-survivors in the CANONIC study had significantly higher requirement for renal support, vasopressors/inotropes and mechanical ventilation. Higher scores on scoring systems for organ failure at baseline, the sequential organ failure assessment (SOFA) and Acute Physiology and Chronic Health Evaluation (APACHE) II scores, predicted the mortality risk in ACLF, more so than Child-Turcotte-Pugh and MELD scores (Jalan *et al.*, 2012). The pathogenesis and progression of organ failure in ACLF is incompletely understood, but exacerbation of the predisposing systemic inflammation and circulatory dysfunction in cirrhosis, over-exuberant inflammatory responses and cell death may all contribute (Asrani, Simonetto & Kamath, 2015; Macdonald *et al.*, 2018).

1.2.4. Scoring Systems in ACLF

Several scoring systems for patients with ACLF that are admitted to ITU exist. These include liver-based scores (e.g. MELD, MELD-Na and Child-Turcotte-Pugh), ITU scores that account for organ failure (e.g. SOFA and APACHE II) and recently, more specific scores for ACLF. The CLIF-SOFA, CLIF-OF and CLIF-C ACLF scores were all derived and validated from the original CANONIC study, and include measures of hepatic and extrahepatic organ dysfunction (Moreau *et al.*, 2013; Jalan *et al.*, 2014b). The latter also includes age and WCC as a marker of SIRS. The CLIF-C ACLF score has proven to have the best prognostic value for 28- and 90-day mortality when compared with APACHE II and CTP (Karvellas *et al.*, 2018). However, there was no statistical difference between CLIF-C ACLF and MELD scores. Moreover, CLIF-C ACLF is a more complicated score with twelve variables, whereas MELD has only four (Rajaram & Subramanian, 2018). Nevertheless, its inclusion of extrahepatic organ dysfunction, its specificity for the ACLF ITU population, and the fact it can be used in a dynamic way, particularly on days 3-7 after decompensation to determine response to treatment or futility, makes the CLIF-C ACLF a good choice (Gustot *et al.*, 2015)

1.2.5. Management of ACLF

Currently there are no specific treatments for patients with ACLF and therefore general principles of early recognition and appropriate institution of organ support are the mainstay. This is often in a critical care environment with the rapid identification and treatment of the precipitant, delivery of optimum organ-specific supportive care to stabilize haemodynamic and metabolic derangements and nutritional support (Bernal *et al.*, 2015). Prompt administration of antimicrobial therapy, intravenous fluids and vasopressors in those refractory to fluids, correction of electrolyte imbalances, endotracheal intubation and mechanical ventilation in obtunded patients, renal replacement therapy where there is marked acute kidney injury and individualized correction of coagulation defects according to dynamic functional assays such as thromboelastography (TEG) will optimize outcomes (Blasi *et al.*, 2018; Olson, 2019). Extracorporeal liver support devices have been evaluated in ACLF and none proven to improve survival, though they may function as a bridge to transplant in sub-populations of the ACLF cohort (Struecker, Raschzok & Sauer, 2014). Liver transplantation in ACLF is controversial, with conflicting data on outcomes for the sickest patients (ACLF-3); recent studies have suggested it is a feasible option in selected patients, provided the decision to transplant and the procedure is undertaken rapidly after diagnosis (Artru *et al.*, 2017; Putignano & Gustot, 2017; Fernández & Saliba, 2018). The mechanism for such rapid transplantation does not currently exist in the UK.

1.3. Infections in Cirrhosis

1.3.1. Prevalence, Incidence and Outcomes of Infections in Cirrhosis

Patients with liver cirrhosis have an increased susceptibility to infection. They may be present at admission or develop during hospitalization in 25-35% of patients with cirrhosis, occurring 4-5 times more commonly when compared with the general population (Fernandez *et al.*, 2002; Jalan *et al.*, 2014a). They develop in a third of patients with decompensated cirrhosis over a one year period. (Borzio *et al.*, 2001). In addition to increasing hospital length of stay and healthcare resource burden, infections in liver cirrhosis increase mortality, with a meta-analysis evaluating 178 studies suggesting a 3.75 times greater pooled odds ratio for mortality in cirrhosis than those without infection (Arvaniti

et al., 2010). In patients listed for transplant, 42% of those who are admitted with infection will either be de-listed or die at 6-month follow-up (Reddy *et al.*, 2015).

1.3.2. Second Infections in Hospitalized Cirrhotic Patients

Recurrent infection is also a major problem in liver cirrhosis. Bajaj *et al.*, as part of the North American Consortium for End-Stage Liver Disease (NACSELD), evaluated second infections in 207 cirrhotic patients in a multi-centre prospective study. These were nosocomial infections defined as "an infection separate from and following the first infection during the same hospitalization" (Bajaj *et al.*, 2012). First infections were considered either (a) community acquired if they were diagnosed within 48 hours of admission in patients who had no prior hospitalization over the preceding 6 months, (b) healthcare-associated if they were diagnosed within 48 hours of admission in patients with a hospitalization of at least 2 days in the 6 months prior, or (c) nosocomial if the infection developed after 48 hours of the admission. The authors found that second infections were common, occurring in 24.1% in the cohort, and profoundly increased mortality (49% vs. 16%, $p<0.0001$), independent of the liver disease severity. Second infections were more common in those who required instrumentation related to ITU admission, such as central venous catheter placement and mechanical ventilation.

1.3.3. Characteristics of Infections and Multi-Drug Resistance in Cirrhosis

The most common primary infections in cirrhosis are spontaneous bacterial peritonitis (SBP) and urinary tract infections (UTI), then followed by pneumonia, skin and soft tissue infections and spontaneous bacteraemia (Piano *et al.*, 2018). In a multicentre prospective intercontinental study of 1302 hospitalized patients with cirrhosis and bacterial or fungal infection, whilst only 57% of patients with first infections had positive microbiological culture, where they were positive Gram-negative bacteria predominated (59%), compared to Gram-positive (38%) and fungi (4%). The most frequently isolated bacteria were *Enterobacteriaceae* such as *Escherichia coli* (28%) and *Klebsiella pneumoniae* (15%). Multi-drug resistant (MDR) infection occurs when organisms at resistant to at least three or more of the main antibiotic families (which includes β-lactams) (Magiorakos *et al.*, 2012). Globally,

the prevalence of multi-drug resistant (MDR) bacteria was 34%, highest in India (73%), where possible reasons include over-the-counter community access to antibiotics and widespread use of antibiotics in farming. MDR infections tended to be hospital-acquired, occurred more commonly in patients who had invasive procedures in the previous month or received antibiotics for at least five days in the previous 3 months. The most common MDR organisms were extended-spectrum β-lactamase producing *Enterobacteriaceae.* Infection with MDR was associated with poorer microbiological efficacy of empirical antibiotic treatment and greater in-hospital mortality (Piano *et al.*, 2019). The emergence of resistant organisms potentiates the need for alternative non-antibiotic strategies to overcome infection.

1.3.4. Clinical Risk Factors for Infection in Cirrhosis

Established risks factors for infection include worse liver function, variceal haemorrhage, older age, use of proton pump inhibitors (PPI), previous hospitalizations and in SBP, low ascitic fluid protein concentration and prior episodes of SBP (O'Leary *et al.*, 2015). The use of antibiotic prophylaxis as a cause for infection, particularly MDR, has conflicting data and its utility in a population at high risk of infection remains unclear (Fernandez *et al.*, 2015).

1.3.5. Bacterial Infection as a Precipitant for ACLF

Bacterial infection is the most common precipitant for the development of ACLF in Western countries, occurring in 24-41% of cases (Moreau *et al.*, 2013; Sargenti *et al.*, 2015; Mücke *et al.*, 2017). A study by Bajaj *et al.* using the NACSELD database, identified that in decompensated cirrhotic patients with infection, 37% developed one organ failure, 10% two organ failures, 10% three organ failures and 4% four organ failures during the hospital episode (Bajaj *et al.*, 2014). The prevalence of MDR infection is higher in ACLF at diagnosis than AD (Fernandez *et al.*, 2017). In a German retrospective study, the commonest infections triggering ACLF were SBP (32.4%) and pneumonia (25.4%); infection as the precipitating event in ACLF, was independently and strongly associated with higher 30- and 90-day

mortality in comparison with non-infectious triggers, especially SBP with odds ratios of 4.54 and 4.29 respectively (Mücke *et al.*, 2017).

1.3.6. Development of Infection in ACLF

Data from our group previously described a higher rate of secondary infection in ACLF compared with AD (34% vs. 11.1%) (Bernsmeier *et al.*, 2015). Furthermore, a recent retrospective study of infection in ACLF confirmed a higher incidence of primary bacterial infection in patients with ACLF not triggered by infection during 4-week follow-up compared with patients with AD (46 vs. 18%, $p<0.001$), confirming that ACLF is associated with an increased susceptibility to infection (Fernandez *et al.*, 2017). An even higher incidence of 65.9% during follow-up was reported by other authors (Shalimar *et al.*, 2018). In the Fernandez *et al.* study, all types of bacterial infection were more frequent in ACLF vs. AD, including SBP (8.6% vs. 3.4, $p=0.03$) and pneumonia, but not *Clostridium difficile* infection Risk factors for the development of infection in ACLF included higher grade of SIRS at diagnosis, higher WCC and CRP, greater number of organ failures, and higher CLIF-C ACLF score. Patients with ACLF that developed *de novo* bacterial infection also had a poorer clinical course and higher 90-day mortality. The impact of infection was more pronounced in lower grades of ACLF (ACLF-1 and ACLF-2) (Fernandez *et al.*, 2017). Overall, infection in ACLF, either as a trigger or developing in non-infection triggered ACLF patient, was independently associated with increased 90-day mortality (Fernandez *et al.*, 2017; Shalimar *et al.*, 2018).

1.4. Spontaneous Bacterial Peritonitis

1.4.1. Diagnosis and Sequelae of SBP

Spontaneous bacterial peritonitis (SBP) refers to the infection of ascites, the pathological accumulation of peritoneal fluid, in patients with liver cirrhosis. It is defined by the presence of greater than 250 polymorphonuclear (PMN) cells/mm^3 in ascites in the absence of an intra-abdominal source of sepsis or malignancy (Curry, McCallum & Guth, 1974; Pinzello *et al.*, 1983). SBP may present with the clinical features of peritonitis, including abdominal pain, rebound tenderness and fever, but may also

be asymptomatic. SBP is a common infection in patients with liver cirrhosis, with an incidence of 7-30% in hospitalized patients with cirrhosis and ascites (Marciano *et al.*, 2019). It recurs frequently (70% at 1 year in absence of antibiotic prophylaxis) and is associated with a substantial increase in mortality, with one series reporting a 50-day mortality of 43% after the first episode (Titó *et al.*, 1988; Bal, Daman & Bhatia, 2016). Patients with SBP are especially prone to developing renal dysfunction, which usually occurs in patients with SIRS and with severe circulatory dysfunction during the episode (Ruiz-del-Arbol *et al.*, 2003). Short-term in-hospital mortality from SBP is associated with acute kidney injury, septic shock and liver disease severity (Bal, Daman & Bhatia, 2016). Like most spontaneous infections in cirrhosis, gram-negative *Enterobacteriaceae* and gram-positive *Streptococcal* species are the most common causative organisms. Accordingly, β-lactam and quinolone antibiotics have been the mainstay of treatment (Jalan *et al.*, 2014a).

Bacterascites is defined by a PMN count of less than 250/mm^3 and a positive ascitic fluid culture. It is distinct from SBP, has a prevalence of 8-11% in patients with cirrhosis and ascites, and may represent either an early phase of SBP, spontaneously resolving infection or secondary colonization from extraperitoneal sources of infection (Oey *et al.*, 2018). Patients with bacterascites are similar in liver disease severity and prognosis to those with SBP, and failure to treat could lead to persistence or progression to SBP. Current European guidelines recommend treatment of bacterascites where there are symptoms or signs of infection or systemic inflammation (Angeli *et al.*, 2018).

1.4.2. Risk Factors for Development of SBP

Several studies have investigated risk factors for the development of the first episode of SBP. Clinical factors include advanced cirrhosis (CTP>9), prior variceal haemorrhage and use of proton pump inhibitors (Min *et al.*, 2014; Dever & Sheikh, 2015). Biochemical factors include low ascitic fluid protein concentration of <10g/L (related to reduced ascitic fluid opsonic activity), particularly when combined with: CTP>9, elevated serum bilirubin concentrations (>51μmol/L), renal dysfunction (creatinine > 106μmol/L) or hyponatraemia (Na<130mM) (Angeli *et al.*, 2018). Additional biochemical

factors include low plasma complement C3 and C4, low ascitic C3 (due to activation of the classical complement pathway), and low 25-OH vitamin D levels (Runyon, 1986, 1988; Bird *et al.*, 1992; Andreu *et al.*, 1993; Anty *et al.*, 2014). Genetic variants for toll-like receptor 2 (*TLR2*), nucleotide-binding oligomerisation domain 2 (*NOD2*), monocyte chemotactic protein-1 (*MCP-1*) and tumour necrosis factor receptor-associated factor 6 (*TRAF6*) have evidence for their predisposition to SBP (Gäbele *et al.*, 2009; Bruns *et al.*, 2012; Harputluoglu *et al.*, 2016; Mai *et al.*, 2017). A previous episode of SBP predicts a risk for subsequent SBP episodes (70% cumulative at 1-year) and decreased survival (30-50% at 1-year) (Rimola *et al.*, 2000). Non-selective beta-blockers have previously been found to be protective for SBP in patients with low to moderate severity (Child Pugh A/B), though the benefit of beta-blockers in advanced cirrhotic patients remains controversial (Senzolo *et al.*, 2009; Krag *et al.*, 2012; Mandorfer *et al.*, 2014).

Further controversy exists regarding other risk factors. Some authors provide contravening evidence: PPI therapy does not increase risk of SBP and ascitic fluid protein concentration is not predictive of SBP development (Terg *et al.*, 2015; Bruns *et al.*, 2015). Given the latter, the conventional assumption that the only peritoneal compartmental defect predisposing to SBP was reduced opsonic activity should be now be re-evaluated, with grounds to investigate other local and systemic factors that might predispose to SBP.

1.4.3. Empirical and Prophylactic Antibiotic Treatment for SBP

Recent European guidelines suggest third-generation cephalosporins as first line antibiotics in community-acquired SBP, in countries with low resistance patterns; where there are high rates of resistance or with hospital-acquired SBP, piperacillin/tazobactam or a carbapenem is recommended depending on local resistance patterns. The recommended duration of treatment is 5-7 days (Angeli *et al.*, 2018). Treatment with intravenous albumin is also suggested in patients with baseline bilirubin > 68μmol/L or serum creatinine >88μmol/L to reduce renal dysfunction associated with SBP and lower mortality.

Antibiotic prophylaxis in patients at high risk of SBP is recommended by guidelines. These include patients with cirrhosis and low protein ascites (<10g/L) and/or high serum bilirubin (primary prophylaxis) and in patients with prior SBP (Wiest, Krag & Gerbes, 2011). Ciprofloxacin primary prophylaxis reduces the risk of SBP and improves survival though the benefit is greatest at three months and maybe lost by 12 months (Krag, Wiest & Gluud, 2010). Norfloxacin is recommended for secondary prophylaxis (Gines *et al.*, 1990). The issue of SBP prophylaxis is currently one of substantial debate since there are concerns of the emergence of quinolone-resistance, adverse effects of quinolones (such as tendon rupture) and whether alternative antibiotics such as trimethoprim-sulphamethoxazole or rifaximin might be better or safer alternatives (Rostkowska, Szymanek-Pasternak & Simon, 2018; Lombardi *et al.*, 2019; Facciorusso *et al.*, 2019). Again, since antibiotic prophylaxis has potentially deleterious effects, the prospect of augmenting the immune system to alter susceptibility to SBP should be considered.

1.5. Pathogenesis of Bacterial Infections in Cirrhosis

The current most widely-accepted hypothesis for the development of infection in cirrhosis is pathological intestinal bacterial translocation (BT) along the gut-liver axis. Whilst bacterial translocation itself is a physiological phenomenon that occurs in health, in the pathological BT model there are synergistic aberrations at multiple levels including altered gut microbiota, increased intestinal permeability, increased BT, and regional and systemic immuneparesis (Wiest, Lawson & Geuking, 2014). This model is considered to underlie to pathogenesis of SBP, in which there is enhanced passage of bacteria from the gut through the portal vein and regional lymphatics, into the circulation and permissively spreading to distant sites, such as the peritoneum (Selvapatt *et al.*, 2014).

1.5.1. Alterations to the Gut Microbiome

The gut contains 100 trillion micro-organisms, most of which cannot be cultured; our understanding of the composition of the gut microbiome in health and disease has come from 16S ribosomal RNA, and lately from metagenomic, sequencing (Shreiner, Kao & Young, 2015). We now know that the gut microbiome plays a complex role in shaping local and systemic innate and adaptive immune responses, bile salt and glucose metabolism, liberation of short-chain fatty acids (SCFAs) and vitamin biosynthesis. The composition is influenced by diet (including alcohol), obesity, age and co-morbidities (Shreiner, Kao & Young, 2015). There is a multifarious interaction between bacterial species, bile acids (BAs) from the liver, conversion of BA from primary to secondary by bacterial bile salt hydrolases, SCFAs and other factors that maintain homeostasis and gut barrier integrity. Even in the pre-cirrhotic stage, dysbiosis occurs where is a change in the composition and function of the microbiome, and small intestinal bacterial overgrowth (SIBO), in which there is increased quantity of bacteria (Acharya & Bajaj, 2019). There is a relative decline in beneficial autochthonous bacteria (e.g. *Lachnospiriceae* / *Ruminococcus*) and a relative overgrowth of virulent taxa (e.g. *Staphylococcaceae, Enterobacteriaceae* and *Enterococcaceae*), which has been associated with the liver disease severity and the development of endotoxaemia and multi-organ dysfunction (Woodhouse *et al.*, 2017). Changes to BA composition, reduction of SCFAs and antimicrobial peptides may contribute to dysbiosis.

1.5.2. Intestinal Barrier Dysfunction

Even within the intestinal barrier, multiple alterations are noted in cirrhosis and contributes to pathological bacterial translocation. Tight junctions, that regulate enterocyte paracellular permeability, are loosened in cirrhosis, with downregulation of associated proteins in more advanced cirrhosis, increasing the passage of bacterial products into free spaces (Assimakopoulos *et al.*, 2012). The transcellular route is acknowledged to be of greater importance in translocation of whole bacteria; epithelial cells under stress have reduced resistance to commensal bacterial transcytosis, but data in cirrhosis is lacking (Wiest, Lawson & Geuking, 2014).

1.5.3. Gut-Associated Lymphoid Tissue and Mesenteric Lymph Nodes

Wiest *et al*. also propose that intestinal tolerance exists in cirrhosis, in which there is inability to mount a suitable immune response to the greater bacterial load; this is evidenced by a study in rats with CCl_4-induced cirrhosis and ascites in which gut BT, as determined by culture of mesenteric lymph nodes (MLNs), was associated with lamina propria $CD103^+$ dendritic cells (DCs) that displayed absence of an activated phenotype, attenuated TNF-α production to LPS, impaired phagocytosis and migration, when compared to rats without gut BT (Muñoz *et al.*, 2012). Other changes to the gut-associated lymphoid tissue (GALT) includes increased recruitment of monocytes, DCs and T lymphocytes into the intestinal mucosa and MLNs as a result of increased release of intestinal epithelial cell chemokines, deficiency in antimicrobial peptides and IgA, and impaired microbial killing by Paneth cells (Jalan *et al.*, 2014a; Tsiaoussis, 2015). Unexplored alterations in innate and adaptive immunity in MLNs is presumed to permit the spread of bacteria systemically and to distant tissue sites in the model of pathological BT (Wiest, Lawson & Geuking, 2014).

1.6. Cirrhosis-Associated Immune Dysfunction

Part of the pathological BT hypothesis, with the observation of increased rates of infection in patients with cirrhosis, is the existence of systemic immune dysfunction, termed cirrhosis-associated immune dysfunction (CAID). Two main facets are described: i) immunodeficiency, with impaired pathogen-responses to pathogens at multiple levels of the immune system and ii) systemic inflammation, due to the persistent low-grade stimulation of immune cells (that may be seen in chronic pathological BT). One of the two phenotypes of CAID may dominate at different stages of the disease and under different circumstances. In addition to increasing susceptibility to infection, CAID is also attributable to poor response to vaccination, endothelial activation and haemodynamic dysregulation seen in cirrhosis (Albillos, Lario & Alvarez-Mon, 2014).

1.6.1. Inflammation: Basic Concepts

Immune cells frequently recognise pathogens by pattern recognition receptors (PRRs); they can be located on: the cell surface membrane, e.g. toll-like receptor 4 (TLR4); the endolysosome (e.g. TLR9); the cytosol (e.g. nucleotide-binding oligomerization domain 1, NOD1). They recognise highly conserved structural components, which on pathogens are called pathogen-associated molecular patterns (PAMPs) or on dying host cells are referred to as damage-associated molecular patterns (DAMPs) (Triantafyllou *et al.*, 2018b). Interaction of receptor and ligand leads to activation of intracellular signalling pathways, in which transcription factors and adaptor molecules induce changes to gene expression which in turn encode for inflammatory effector molecules. These inflammatory molecules may include cytokines which act in complex ways to alter the behaviour of cells, sometimes other cells (paracrine) or the cell from which they were produced (autocrine). They may also act synergistically or antagonistically with other cytokines. Their actions may be concentration, tissue and context specific. Archetypal pro-inflammatory cytokines include TNF-α, IL-6, IL-1, IL-17 and type I-III interferons (IFN). Classic anti-inflammatory cytokines are IL-10 and IL-12. A subfamily of cytokines are chemokines, smaller molecules that primarily function as chemotactic agents, recruiting immune cells, but they also have homeostatic and housekeeping roles (Turner *et al.*, 2014). The PAMP-activated inflammatory response is a pivotal host immune process in the antimicrobial response to invading pathogens. Chronic or over-exuberant responses can lead to collateral tissue injury (immunopathology) (Bernardi *et al.*, 2015). TLRs also recognise DAMPs, which are endogenous ligands including high mobility group box 1 (HMGB1), extracellular matrix components, oxidized low-density lipoproteins (LDLs), oxidized phospholipids and many more. These stimulate inflammation and tissue repair processes.

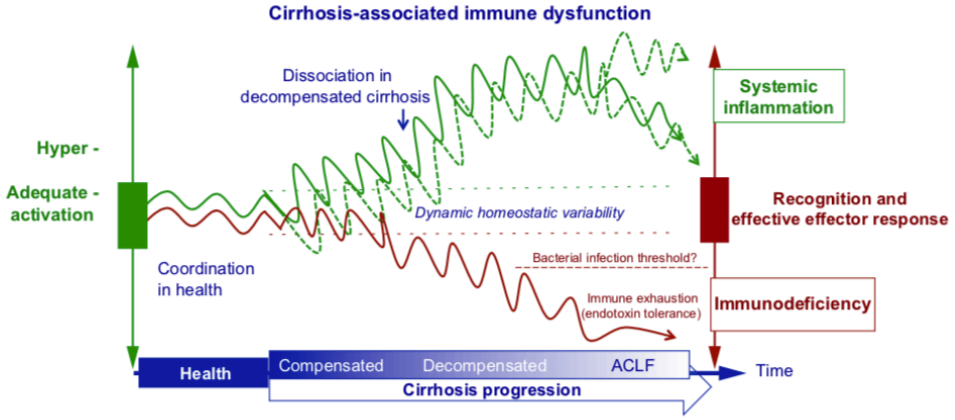
In conjunction with the pro-inflammatory responses, counter-regulatory anti-inflammatory responses may also occur, usually with a lag, to keep the immune system in check, preventing over-exuberant responses and working in the background to ultimately achieve immune homeostasis once the pathogen or tissue injury has been cleared. These responses may be part of the resolution of inflammation, a

process to return damaged tissue and the immune system back to normal. Indeed, in immunopathology, a compensatory anti-inflammatory response syndrome (CARS) may become marked leading to an immunosuppressive state and increased risk of secondary infections and associated mortality (Bernardi *et al.*, 2015). This is seen in severe sepsis, in patients who survive a pronounced initial pro-inflammatory response, but succumb to recurrent infection in the delayed immunosuppression phase (Hotchkiss *et al.*, 2009; Hotchkiss, Monneret & Payen, 2013).

1.6.2. Concepts of Inflammation in Cirrhosis and ACLF

1.6.2.1. Systemic Inflammation in Cirrhosis and ACLF

In CAID, there is a dynamic co-existence of systemic inflammation (SI) and acquired immunodeficiency (**Figure 1.1**) (Albillos, Lario & Alvarez-Mon, 2014).



Predominant CAID phenotypes

Immune characteristic	Pro-inflammatory	Immunodeficient
Pro-inflammatory cytokines (e.g., TNF-α, IL-6, IL-1β)	↑↑	↑
Anti-inflammatory cytokines (e.g., IL-10, TGFβ)	↑	↑↑
Phagocytosis (e.g., dendritic cells)	↑	↓
HLA-DR/co-stimulatory molecules expression on monocytes/macrophages	↑	↓
Expression of negative regulators (e.g., IRAK-M)	↓	↑

Figure 1.1 Cirrhosis-associated Immune Dysfunction

In healthy individuals immune cell activation (green) and antigen recognition (red) function in co-operation to mount an adequate immune response to pathogens. With the progression of liver disease from compensated to decompensated cirrhosis to ACLF, worsening hepatic function, enhanced bacterial translocation and subsequent PAMP- and DAMP-driven stimulation leads to impairment of the normal recognition and effector response. In the compensated stage, necrotic hepatocytes from ongoing liver injury, e.g. from alcohol or hepatitis viruses, still lead to sterile systemic inflammation. In decompensated cirrhosis, pathological BT ensures persistent exposure

to bacterial products, e.g. endotoxin, activating the immune system further with a pro-inflammatory CAID phenotype. However, different mechanisms such as loss of liver surveillance functions also cause progressive immunodeficiency. At end-stage liver disease, under persistent PAMP pressure, immune cells become endotoxin tolerant and functionally exhausted, and the predominant CAID phenotype becomes immunodeficient, with impaired innate and adaptive immune responses and an increased susceptibility to infection. (taken from Albillos *et al*., 2014; permission from Elsevier granted – see Appendix U).

The evidence to support the systemic inflammation (SI) hypothesis includes

i. increased concentrations of pro-inflammatory cytokines including TNF-α, IL-6 and IL-8 in AD, which are even greater in ACLF (correlating with grade), compared to healthy controls, (Clària *et al.*, 2016a)
ii. Circulating soluble CD163 levels, a marker of macrophage activation, are increased in cirrhosis, correlate with HVPG and are an independent risk factor for variceal bleeding and death (Waidmann *et al.*, 2013).
iii. WCC and CRP are significantly increased in ACLF and moderately so in AD without organ failure; in the former, this is comparable to patients with severe sepsis (Moreau *et al.*, 2013). In ACLF, these markers correlate with number of organ failures and prognosis.
iv. SIRS is regarded as a quintessential component of ACLF and associates with poorer outcomes (Mehta *et al.*, 2015; Michelena *et al.*, 2015).

Systemic inflammation is driven by pathological BT, in which PAMPs (bacterial products) are permitted into the systemic circulation due to the aforementioned mechanisms (1.5). In earlier stages of cirrhosis, low-grade BT may reach GALT or MLNs; as cirrhosis progresses, pathological BT also progresses and may overwhelm regional gut immunity permitting entry to the liver, where a pro-inflammatory response may occur. Ongoing hepatocyte necrosis from liver injury also generates DAMPs contributing to SI. In ACLF, it is proposed that there is exacerbation of the low-grade SI already present in cirrhosis. The trigger for ACLF may determine the profile of pro-inflammatory cytokines: IL-8 in alcohol-induced, and TNF-α, IL-6 and IL-1β for sepsis-triggered (Clària *et al.*, 2016a). IL-8 is a neutrophil chemokine, whilst IL-6 shapes Th17 responses, contributing to neutrophil

generation and activation. Recruited neutrophils promote immunopathology due to reactive oxygen species and proteolytic enzyme release (Martin-Mateos, Alvarez-Mon & Albillos, 2019).

1.6.2.2. Immuneparesis in Cirrhosis and ACLF

Despite evidence of SI, patients with decompensated cirrhosis, and especially ACLF, have a paradoxical immuneparesis predisposing to infection. This was confirmed in the CANONIC study in which rates of bacterial infection at diagnosis were significantly higher in ACLF (32.6%) than without (21.8%), and increased with ACLF grade, with 29.9% in ACLF-1 to 44.7% in ACLF-3 (Moreau *et al.*, 2013). An excessive CARS with functionally exhausted immune cells is the pathogenic basis, and has been described in other disorders with high grade SI including severe sepsis, trauma and burns (Taylor, Gordon & Polk, 2000; Ward, Casserly & Ayala, 2008; Hotchkiss, Monneret & Payen, 2013). The insufficient immune cellular response to pathogens affects innate and adaptive immunity.

1.6.2.3. Monocyte Dysfunction in ACLF

Circulating monocytes in ACLF display reduction in the antigen presentation capacity with downregulated HLA-DR expression and reduced LPS-stimulated TNF-α release, which is associated with lower survival in critically ill cirrhotic patients (Wasmuth *et al.*, 2005; Berry *et al.*, 2010a). Detailed descriptions of monocyte dysfunction are given later (1.8.2).

1.6.2.4. Myeloid-Derived Suppressor Cells in ACLF

Myeloid-derived suppressor cells (MDSCs) are part of the myeloid cell population with two subsets, monocytic-MDSCs (M-MDSCs) and polymorphonuclear-MDSCs (PMN-MDSCs). These cells have potent immunosuppressive activity and function to protect the host from tissue damage in the setting of an uncontrolled immune response from unresolved or chronic inflammation or infection (as may be the case with pathological BT) (Bronte *et al.*, 2016). These cells are distinct, cannot be derived from their mature counterparts and have high arginase and inducible nitric oxide synthetase (iNOS) activity, persistently high levels of reactive oxygen species (ROS) and can suppress T-cell proliferative and

anti-tumour responses (Gabrilovich, 2017). M-MDSCs are identified as CD33+ CD11b+ CD14+ CD15- HLA-DR- (Dorhoi & Du Plessis, 2017). Recently, an expansion of circulating M-MDSCs was observed in ACLF with impaired antimicrobial responses, and associated with secondary infection, disease severity and outcome (Bernsmeier *et al.*, 2018).

1.6.2.5. Neutrophil Dysfunction in Cirrhosis and ACLF

Neutrophils have reduced bactericidal capacity due to impaired phagocytosis, oxidative burst in response to microbial ligands and chemotaxis (Panasiuk *et al.*, 2005a). Interestingly, in patients with stable cirrhosis, neutrophil dysfunction occurs despite a higher resting oxidative burst and a higher concentrations of pro-inflammatory cytokines, suggesting persistent *in vivo* stimulation (Tritto *et al.*, 2011). In acute alcoholic hepatitis-related ACLF, neutrophils with high CXCR1/CXCR2 expression promote early apoptosis and necrosis of hepatocytes, and exhibit reduced phagocytic capacity, associated with higher rates of bacterial infection, organ failures and mortality (Khanam *et al.*, 2017).

1.6.2.6. Adaptive Immune Defects in Cirrhosis and ACLF

Both T helper (Th) and cytotoxic T cells (Tc) are depleted in cirrhosis, particularly naïve rather than memory, from its incipience and irrespective of aetiology. Zou *et al.* identified numerical reductions in CD4+ and CD8+ T-cells in cirrhosis and ACLF in comparison to healthy controls and chronic hepatitis B patients (Zou *et al.*, 2009). The mechanisms are manifold and include defective thymopoiesis, hepatic and splenic pooling, and activation-induced apoptosis caused by pathological BT (Lario *et al.*, 2013). In acute alcoholic hepatitis, T-cells upregulate immunoregulatory receptors PD-1 and Tim-3, associated with reduced interferon-gamma (IFN-γ) production, impairing antimicrobial responses (Markwick *et al.*, 2015). B-cell lymphopenia has been reported in alcohol and HCV-related cirrhosis. In particular, there is loss of CD27+ memory B-cells, replaced by functionally exhausted peripheral CD27- CD21- B cells, which show attenuated proliferative responses to CD40/TLR9 activation and impaired IgG production (Doi, Tanoue & Kaplan, 2014).

1.6.2.7. Mechanisms of Immuneparesis in CAID and ACLF

The mechanisms contributing to CARS are not fully understood and represent an area of unmet need. It is seen as a homeostatic process to salvage an excessive inflammation state. IL-10 has been observed to be a key anti-inflammatory cytokine involved in the process, with increased circulating concentrations predictive of poor outcome in ACLF patients (Berry *et al.*, 2010b). IL-10, produced largely by monocytes, regulates NF-κB activity, with subsequent decline in TNF-α, IL-6, IL-8 and IL-12 monocyte production (Saraiva & O'Garra, 2010). A murine model of liver fibrosis suggested a possible mechanism for this in which gut microbial translocation induced tonic type I IFN responses in the liver, resulting in higher myeloid IL-10 production after bacterial infection, resulting in failure to control infection and increased mortality; antibody-mediated blockade of IFN- and IL-10-receptor signalling restored antibacterial responses (Hackstein *et al.*, 2017). The role of monocytes in CAID / immuneparesis is described in greater detail later.

Persistent and exacerbated PAMP and BT in ACLF from a 'leaky gut', and increase DAMP load from hepatocyte injury, may cause a relentless but low-grade stimulation of the immune system leading to a tolerant and exhausted immune state predisposing to acute or chronic infections (von Baehr *et al.*, 2000). Whilst gut decontamination with antibiotics restores LPS-stimulated TNF-α secretion and phagocytosis in a cirrhotic rat model, the evidence in humans is currently lacking (Muñoz *et al.*, 2012). Limited but dated studies in ALF (using oral colistin, tobramycin and amphotericin B) and pre-operatively in patients undergoing elective liver transplant (oral norfloxacin) did not demonstrate a benefit on the risk of infection (Rolando *et al.*, 1996; Zwaveling *et al.*, 2002).

1.6.2.8. Metabolic and Neuroendocrine Factors

Other metabolic and neuroendocrine factors in advanced cirrhosis may contribute to immuneparesis. O'Brien *et al.* (2014) observed an increase in prostaglandin E2 (PGE_2) in patients with end-stage cirrhosis and with AD, where PGE_2 antagonism by indomethacin and by albumin-binding reversed the immunosuppressive effects (O'Brien *et al.*, 2014). Indeed, a serum albumin of less than 30g/L has been

linked to increased risk of infection, and infusion of 20% human albumin solution to achieve a value greater than this can reverse immuneparesis by inactivation of PGE_2 (China *et al.*, 2018). As a possible mechanism, PGE_2 has been demonstrated to inhibit alveolar macrophage phagocytosis associated with increased intracellular cyclic AMP production (Aronoff, Canetti & Peters-Golden, 2004). The synergism of hyponatraemia and hyperammonaemia, seen in hepatic encephalopathy, is noted to cause neutrophil swelling, impaired phagocytosis and increased spontaneous burst in a rat model, reversed by modulation of the p38 mitogen-activated protein kinase (MAPK) signalling pathway (Shawcross *et al.*, 2008). Finally, the tryptophan-kynurenine pathway was noted to be activated in cirrhosis, with the highest kynurenine level noted in immunosuppressed ACLF patients, predicting the development of nosocomial infection and mortality. Elevated kynurenine has been observed in other conditions with chronic SI, where it promotes systemic circulatory dysfunction by enhanced nitric oxide production, oxidative stress and apoptosis of endothelial cells mediated by the expression of indoleamine 2,3-dioxygenase (IDO). IDO is also immunosuppressive by increasing IL-10 levels, thus suggesting it may have a role in the immuneparesis of ACLF (Clària *et al.*, 2019).

1.7. Tissue Compartmental Immune Dysfunction in Cirrhosis

Most of the work carried out to date in the field of immuneparesis in liver disease has concentrated on *ex-vivo* analysis of circulating immune cells. This is important since these cells may be recruited to sites of infection where they exert an innate immune response. However, under conditions of high velocity blood flow seen in the systemic circulation, it is recognized that leucocytes cannot recognize, attract or engulf bacteria (Minasyan, 2016). Hence, where bacteraemia and subsequent seeding of pathogens at tissue sites occurs, tissue-specific immunity may be more relevant. There is also the recognition that many organs can participate in a systemic inflammatory response, with cytokines produced in organs distant to the original site of infection and perhaps part of the pathogenesis of multi-organ failure (Cavaillon & Annane, 2016). The liver is one of the major immunological organs of the body, which functions to provide surveillance and initiate the immune response. Liver resident macrophages (Kupffer cells), representing 80% of the total body macrophage population and located in the slow flow

sinusoids, are therefore of crucial importance in the clearance of bacteria from the circulation. Likewise, in patients with cirrhosis and ascites, as previously mentioned, SBP represents a common and serious infection in the peritoneal compartment; local peritoneal immune dysfunction may be crucial in permitting infection and warrants further exploration.

1.7.1. Role of the Liver in Cirrhosis-Associated Immune Dysfunction

1.7.1.1. Immune Functions of the Liver in Steady-State

The liver is an organ rich in immune cells and comprised of an extensive vascular network of liver sinusoids. There is a mixed arterio-venous perfusion with 20% of blood supplied from the hepatic artery and 80% from the portal vein, the latter containing large quantities of harmless antigens from the diet and commensal microbes from the gastrointestinal tract (Heymann & Tacke, 2016). The antimicrobial surveillance function of the liver is exerted through mixed populations of resident antigen presenting cells (APCs) and lymphocytes. The former includes Kupffer cells and hepatic sinusoidal endothelial cells (HSEC) – which comprise the reticuloendothelial cells of the liver – and DCs. Kupffer cells reside in fixed positions within the lumen of the sinusoidal vascular spaces, where under slow flow conditions, can capture bacteria, dying erythrocytes and eliminate insoluble waste by phagocytosis from the portal and systemic circulation (Ikarashi *et al.*, 2013). In this way, Kupffer cells have an anti-inflammatory role at the interface, by limiting the movement of immunoreactive gut-derived substances entering via the portal vein beyond the hepatic sinusoids. Whilst tissue-resident Kupffer cells may take up microbes, they may also orchestrate recruitment of infiltrating myeloid cells to facilitate killing (Gregory & Wing, 1998). Bone-marrow derived circulating monocytes may infiltrate the liver, either as part of their patrolling function or in direct response to pathogenic and chemotactic signals. There they may differentiate into monocyte-derived macrophages (MoMFs), where they are morphologically distinct from Kupffer cells with few cytoplasmic projections and a more rounded appearance. If recruited after TLR signalling or liver injury, MoMFs increase chemokine CCL2 and CXCL1 levels in murine models to further recruit monocytes, and participate in the response to injury and regeneration, which may also include repopulation of the liver macrophage pool (Guillot & Tacke, 2019)

HSEC have fenestrated endothelium and function to remove soluble macromolecular waste material. They are immunologically active and in conjunction with Kupffer cells, they constitutively express major histocompatibility class (MHC) I and II for antigen presentation, in addition to co-stimulatory molecules (CD80 and CD86). HSEC can present antigen directly to liver resident and circulating T-cells. DCs in the liver have weak T-cell immunostimulatory properties due to the immature status and high IL-10:IL-12 ratio of the hepatic microenvironment (Pillarisetty *et al.*, 2004). Other immune cells scattered in the parenchyma and portal tracts include T and B lymphocytes, natural killer (NK) cells, natural killer T (NKT) cells and γδ T cells which all have a role in innate and adaptive responses.

The liver, being exposed to potential pathogens but also self-antigens, must regulate the balance between immunity and tolerance – immune homeostasis. Mechanisms to achieve tolerance include high IL-10 production by reticuloendothelial cells, low abundance of MHC expression by resident liver cells, and unrestricted exposure of APCs to naïve CD8+ T-cells without CD4+ T-cell activation (Jenne & Kubes, 2013; Albillos, Lario & Alvarez-Mon, 2014; Doherty, 2015)

1.7.1.2. Role of the Liver in the Systemic Immune Response

Molecular alarm signals generated by tissue injury (DAMPs) or microbial invasion (PAMPs) are recognized by antigen-presenting cells (APCs) in the liver. Engagement of DAMPs and PAMPs with PRRs expressed by leucocytes, such as the toll-like receptors (TLRs), result in generation of pro-inflammatory cytokines (e.g. TNF-α, IL-1β, CCL2 and CCL5) (Soehnlein & Lindbom, 2010). These act to recruit other inflammatory cells (e.g. circulating neutrophils and monocytes) and initiate protective apoptotic pathways in hepatocytes. The hepatic macrophage pool itself is substantially expanded early in the inflammatory process, and there is debate as to whether this originates locally from the Kupffer cell population or from infiltrating monocytes that subsequently differentiate (either to inflammatory macrophages or DCs). Hepatic macrophages and recruited neutrophils form the primary components of the mononuclear phagocyte system (MPS), exhibiting high degrees of phagocytic activity. The former, in addition to infiltrating monocytes, are the main initiators of the

inflammatory response, which serves to both destroy invading pathogens or damaged cells, and recruit other professional phagocytic cells such as neutrophils. This signalling, in addition to the action of proteases released by dead cells on extracellular components, may promote an acute phase reaction. This is characterized by an increase in plasma proteins termed acute-phase proteins, many of which are produced by hepatocytes (Pearlman, 1999). These include complement components, which have a wide range of regulatory and effector functions. The complement system has an important role in pathogenic defence. For example, C3b has a role in opsonisation (the molecular mechanism in which microbes or apoptotic cells are chemically modified to increase the attraction to host phagocytic receptors), where it binds target cells (e.g. bacteria), facilitating antibody-binding and subsequent Fcγ-mediated phagocytosis (Merle *et al.*, 2015). The anaphylatoxins C3a and C5a contribute to liver regeneration. Complement is also involved in the priming of Kupffer cells and infiltrating neutrophils for reactive oxygen species generation, important in the bactericidal oxidative burst process. Furthermore, complement activation is involved in the hepatic accumulation of PMNs during infection, and facilitates leucocyte adhesion to the endothelium (Merle *et al.*, 2015). The liver is similarly the major source of soluble PRRs, including C-reactive protein (CRP), LPS-binding protein (LBP) and soluble CD14 which can promote opsonisation and regulate immune function. Liver cells also constitutively express membrane-bound PRRs such as the TLRs and cytoplasmic NOD-like receptors (NLRs). Receptor-ligand engagement leads to downstream signals, such as nuclear factor kappa B (NFκB) for bacterial ligands, generating pro- and anti-inflammatory cytokines. Due to constant low-grade exposure to LPS (a TLR4 agonist) from the gut (normal bacterial translocation), liver cells become refractory to stimulation by TLR4, a phenomenon known as 'endotoxin tolerance', which contributes to liver homeostatic tolerance (von Baehr *et al.*, 2000). Under such conditions, Kupffer cells produce less pro-inflammatory and more anti-inflammatory cytokines, such as interleukin-10 (IL-10) (Jenne & Kubes, 2013; Heymann & Tacke, 2016).

1.7.1.3. Impaired Liver Immune Function in Cirrhosis

In chronic liver injury, the hepatic macrophage pool is expanded. The intermediate subset of monocytes (CD14++ CD16+) are recruited from the circulation in a fractalkine ligand CX3CL1-mediated manner (Heymann & Tacke, 2016). These intermediate monocytes are highly phagocytic, produce pro-inflammatory cytokines (TNF-α, IL-6, IL-1β and IL-8) and activate fibrogenic hepatic stellate cells. Cirrhosis leads to sinusoidal and septal fibrosis, Kupffer cell damage or loss, and porto-systemic shunting, all of which compromise the reticulo-endothelial system, permitting more endotoxin to reach the systemic circulation and resulting in persistent stimulation of the immune system. In some cases, failure to clear bacteria can lead to bacteraemia and infection. Diminished functional liver tissue also results in hampered synthesis of complement (e.g. C3, C4 and CH50) and soluble PRRs, resulting in diminished bactericidal activity and increasing the risk of infection (Albillos, Lario & Alvarez-Mon, 2014; Heymann & Tacke, 2016).

1.7.2. Peritoneal Immunity in Cirrhosis-associated Immune Dysfunction

1.7.2.1. The Peritoneal Cavity

The peritoneum is the mesothelial membrane that lines the abdominal cavity consisting of a mesothelial cell monolayer and loose connective tissue. These cells are characterised by apical microvilli, fragility and high turnover. Two layers of peritoneum exist: parietal peritoneum which lines the abdominal wall and visceral peritoneum lining the abdominal organs. A transudative peritoneal fluid is constitutively produced by mesothelial cells, and reabsorbed by the peritoneal membrane. Under physiological conditions, the volume of fluid in the peritoneal cavity is around 5-20 ml (van Baal *et al.*, 2017). This fluid, in equilibrium with plasma but not containing macromolecules, functions to allow frictionless movement of abdominal organs, exchange nutrients, clear pathogens and enable tissue repair (Capobianco *et al.*, 2017). Pathological accumulation of peritoneal fluid is referred to as ascites, and occurs as a result of imbalance of production and removal, or mechanical forces governing fluid shifts.

1.7.2.2. Characterisation of Peritoneal Macrophages & Ontogeny

Peritoneal macrophages comprise 50-90% of the peritoneal leucocyte pool, the remainder being T- and B-cell subsets and mast cells. The ontogeny of peritoneal macrophages has been historically debated, once considered bone marrow in origin. However, recent murine fate mapping studies suggested peritoneal F4/80^{hi} macrophages independently exist from circulating monocyte input, originating in the fetal yolk-sac, but can self-renew and be replenished by bone marrow derived cells (Yona *et al.*, 2013). Murine data on peritoneal macrophages has suggested two populations: the large peritoneal macrophages (LPM) and the small peritoneal macrophages (SPM), though the dichotomous characterisation has since been demonstrated to be overly simplified (Ghosn *et al.*, 2010; Bain & Jenkins, 2018). In humans, little data exists on peritoneal macrophage populations and their ontogeny – the current knowledge comes from peritoneal fluid obtained from abdominal washouts in gynaecological or biliary surgery, or peritoneal dialysis in patients with renal failure, and hence never truly physiological states. However, peritoneal macrophages express classic macrophage markers CD11b, CD14, CD64, MerTK, CD49F and VSIG4 (CRIg), and exhibit potent phagocytic activity (Kubicka *et al.*, 1996; Irvine *et al.*, 2016; Liao *et al.*, 2017). Ruiz-Alcaraz *et al.* described, in the peritoneal fluid of 51 women who underwent laparotomy, that peritoneal macrophages were a heterogenous group based on morphology and expression of CD14/CD16. Three populations were identified: CD14++ CD16- (18 ± 1.3%), CD14++ CD16+ (49 ± 2.0%) and CD14^{high}CD16^{high} (33 ± 2.4%). The latter group were more mature cells, with larger size and granularity, and higher expression of CD206 and HLA-DR. Expression of CD11c, CD40, CD80, CD206 and Slan were greater in peritoneal macrophages compared with blood monocytes, with an overall expression profile resembling alternatively-activate M2 macrophages (see 1.8.3) (Ruiz-Alcaraz *et al.*, 2018).

The traditional dogma that tissue-resident peritoneal macrophages remain stationary, like Kupffer cells, has recently been disproven. Elegant murine studies performed by Wang *et al.* (2016) using GFP+ reporters identified that in a liver injury model, F4/80^{high} peritoneal macrophages selectively expressing transcription factor GATA6 were, within 4 hours, able to be infiltrate the injured liver via a non-vascular

route using CD44 and danger-signal adenosine triphosphate (ATP), adopt an alternatively-activated phenotype and contribute to tissue repair (Wang & Kubes, 2016). The study nicely demonstrated that bone-marrow derived monocytes infiltrating into sites of tissue injury were not the only source of macrophages, but in fact they might also be rapidly recruited from other organs systems or cavities. A very interesting recent study suggested *Staphylococcus aureus* captured by Kupffer cells escaped across the mesothelium and immediately infected GATA6+ peritoneal cavity macrophages, delaying neutrophil response by 48 hours compared to mice deficient in GATA6+ peritoneal macrophages. Intravenous antibiotics did not prevent dissemination but peritoneal vancomycin administration reduced kidney infection and mortality (Jorch *et al.*, 2019). GATA6 was expressed highly in human peritoneal macrophages (83%), with expression correlating with CD16 expression and more mature cell types (Ruiz-Alcaraz *et al.*, 2018).

1.7.2.3. Peritoneal Macrophage Function at Steady-State

The high expression of phagocytic receptors (e.g. Tim4, MerTK and CD36) suggests that steady-state peritoneal macrophages are primed for performing clearance of apoptotic and senescent cells, a process called efferocytosis. However, in addition to these homeostatic functions, F4/80^{hi} murine macrophages act as innate immune system sentinels, responding to microbial stimulation by recruiting other immune effector cells. Recruited cells include Ly6C^{hi} monocytes, which are more pro-inflammatory and differentiate into T-cell activating F4/80^{lo} macrophages, and neutrophils (Bain & Jenkins, 2018). In humans, Ruiz-Alcaraz *et al*. found that CD16+ peritoneal macrophages had greater phagocytic capacity than CD16-. An oxidative burst assay revealed high resting burst activity, lowest in CD14^{high}CD16^{high} subpopulations, with little incrementation after Phorbol 12-myristate13-acetate (PMA) stimulation, a known inducer of oxidative burst. In terms of intracellular cytokine content, at steady-state, expression was very low for TNF-α (6.3%), IL-6 (14.9%) and IL-10 (4%), implying they are tolerogenic (Ruiz-Alcaraz *et al.*, 2018).

1.7.2.4. Peritoneal Immunity in Cirrhosis

SBP is one of the commonest and most serious infections in decompensated cirrhosis. Limited literature is available on human peritoneal macrophage immunity in decompensated liver cirrhosis. Ahmed *et al.* found in 30 Child-Pugh C cirrhotic patients with ascites that peritoneal macrophages had impaired phagocytosis but a robust oxidative burst capacity, when compared with the macrophages isolated from washouts of healthy women undergoing elective laparoscopic Fallopian tube ligation (Ahmed *et al.*, 2011). Nieto *et al.* found that peritoneal macrophages in culture-positive SBP have reduction in HLA-DR, CD11b, CD16, CD206 and CD86, surface markers suggestive of impaired innate immune function and antigen-presentation capabilities. Of note, both culture-negative and positive SBP demonstrated an enhanced population of $CD14^{low}$ macrophages, whilst CD14 expression strongly correlated with phagocytosis and inversely correlated with IL-6 expression (Nieto *et al.*, 2015). In a comprehensive study of patients with cirrhosis and ascites, Irvine *et al*. (2016) described two human CD14+ populations that were high or low expressers of the CRIg receptor. Compared with $CRIg^{lo}$ cells, $CRIg^{hi}$ peritoneal macrophages were larger in size, higher in autofluorescence, CCR2- and had higher expression of surface markers CD16, CD169 and CD163, and increased gene expression of macrophage markers *VSIG4* (encoding CRIg), *SIGLEC-1, CD163, FCGR1A*, and efferocytosis-related receptors *TIMD4* and *MERTK*. The authors likened these to $F4/80^{hi}$ self-renewing tissue resident macrophages in the mouse. $CRIg^{hi}$ macrophages had enhanced phagocytic, antimicrobial activity and an anti-inflammatory IL-4 activation gene signature, resembling alternatively-activated macrophages (see 1.8.3). Whilst the proportion of $CRIg^{hi}$ macrophages varied between patients and in the same patient over time, an increased proportion of $CRIg^{hi}$ macrophages correlated with a lower MELD score (Irvine *et al.*, 2016). A Spanish study identified that healthy neutrophils cultured in the ascites of patients with SBP, when compared with sterile ascites, exhibited lower oxidative burst and neutrophil extracellular trap (NET) formation (both part of the neutrophil antimicrobial armamentarium). Both were associated with higher ascitic resistin concentration, a product of myeloid cells, which is also shown to directly reduce the inflammatory phenotype of monocytes and their TNF-α production (through blocking LPS-TLR4 interaction) (Jang *et al.*, 2017; Nieto *et al.*, 2018).

1.7.2.5. Dysregulated Ascitic Microenvironment

Alterations to the microenvironment may also reflect immune dysregulation and influence clinical outcomes. In a study comparing the concentrations of inflammatory cytokines (e.g. IL-6) and microbial richness of ascites in decompensated cirrhosis to the corresponding blood compartment, the peritoneal compartment appeared to have greater levels for both, though there was no relationship to systemic inflammation for either. The higher cytokine and microbial richness are interesting given the cell count of ascites is markedly lower than blood. The authors concluded that their study suggests dysregulated compartmental myeloid function in cirrhosis (Alvarez-Silva *et al.*, 2019). Even in non-neutrocytic / culture negative ascites, bacterial DNA levels are important, and in one study high levels were associated with reduced peritoneal macrophage HLA-DR expression and poor 6-month clinical outcomes (readmission and death), highlighting that the bacterial DNA burden in the ascitic microenvironment may modulate innate immune function (Fagan *et al.*, 2015). The relationship of bacterial DNA and reduced survival was supported by another study (Engelmann *et al.*, 2016b). There are differences in the methods of detecting bacterial DNA however, with another study not detecting bacterial DNA in non-neutrocytic ascites (Sersté *et al.*, 2011).

1.8. Monocyte and Macrophage Dysfunction in Liver Disease

1.8.1. Monocytes in Health

Blood monocytes comprise 10% of the circulating leucocyte population and form a crucial part of the innate immune system. Equipped with chemokines and adhesion receptors, they circulate for days and can then emigrate from blood vessels in response to inflammatory or metabolic cues to enter tissue where they can give rise to macrophages, as well as specialized antigen presenting cells called dendritic cells (DCs), making vital contributions to host defence, tissue remodelling and repair. They have the capacity to take up toxic molecules and produce inflammatory cytokines. They originate from bone

marrow common myeloid progenitors, and in the circulation monocytes vary in size, granularity and morphology with heterogenous phenotypes and functions (Kapellos *et al.*, 2019).

1.8.1.1. Monocyte Classification

Monocytes are divided into three subsets depending on their expression levels of CD14 and CD16: classical CD14++ CD16-, intermediate CD14++ CD16+ and non-classical CD14+/^{low} CD16++ (Ingersoll *et al.*, 2010; Xue *et al.*, 2014). Monocytes ubiquitously express CD11b and HLA-DR. The latter is often used to distinguish CD16-expressing monocytes and CD16-expressing NK cells (Abeles *et al.*, 2012). HLA-DR, a MHC class II surface receptor, is regarded as an activation marker, with a role in antigen presentation, with higher expression in CD16+ monocytes. There is also differential chemokine receptor expression: CD14+ CD16+ monocytes express CCR5, whilst CD14+ CD16- monocytes express CCR2. Expression of adhesion markers and production of cytokines also differs between subsets (Gordon & Taylor, 2005; Wong *et al.*, 2012). Non-classical monocyte subsets are patrolling monocytes, which express the fractalkine chemokine receptor CX_3CR1 and function to actively patrol vasculature; they are thought to rapidly respond to tissue injury, participating in the resolution response (Thomas *et al.*, 2015). In contrast, classical and intermediate monocytes have proinflammatory roles.

1.8.1.2. Monocyte Recruitment to Sites of Injury or Infection

In steady state, monocytes function to replenish tissue macrophages and DCs. However, when a tissue site is injured or infected, monocytes are rapidly recruited to mediate direct antimicrobial activity and orchestrate the host immune response. Recruitment involves rolling, adhesion and transmigration across vessel walls. Once migrated, monocytes may become macrophages or DCs, producing cytokines (e.g. TNF-α) and chemokines, and killing invading pathogens by phagocytosis and respiratory burst mechanisms. Inflammatory DCs may home to lymph nodes where antigen presentation engages the adaptive immune system (Shi & Pamer, 2011).

1.8.2. Monocyte Dysfunction in Cirrhosis and ACLF

Monocyte dysfunction in cirrhosis and ACLF is well described. A monocytosis is frequently observed in cirrhosis, with reports of an expansion of the pro-inflammatory intermediate subset (CD14++ CD16+) in the diseased liver (Berry *et al.*, 2010a; Liaskou *et al.*, 2012). Circulating monocytes display reduced HLA-DR expression and cytokine production in response to microbial challenge. Additionally, some authors report impaired monocyte bacterial killing and phagocytosis in cirrhosis (Bonnel, Bunchorntavakul & Reddy, 2011). In alcohol-related liver disease, abstinent patients with cirrhosis demonstrate preserved monocyte oxidative burst (MOB), but actively drinking cirrhotics and those with severe alcoholic hepatitis (SAH) have defective MOB due to reduced NAPDH oxidase expression (Vergis *et al.*, 2016). Sargenti *et al.* found increased circulating myeloid cell resting and *E. coli*-stimulated oxidative burst in ambulatory cirrhotic patients without evidence of AD compared to healthy controls. Increased stimulated burst independently predicted subsequent occurrence of severe sepsis and ACLF. Phagocytosis was only significantly impaired in neutrophils but there was also a tendency towards reduction with monocytes (Sargenti *et al.*, 2016). In both studies, where defective myeloid bacterial uptake or killing exists, this predicted subsequent infection and mortality. O'Brien *et al*. demonstrated that increased circulating concentrations of prostaglandin E_2 (PGE_2) observed in patients with cirrhosis and AD was associated with suppression of monocyte/macrophage LPS-stimulated proinflammatory cytokine secretion and impaired bacterial killing. Immune competence could be restored with human albumin solution infusions which lowered circulating PGE_2 levels (O'Brien *et al.*, 2014). In ACLF, data from Bernsmeier *et al*. reported impaired monocyte pro-inflammatory cytokine signalling associated with an expansion of circulating MerTK+ monocytes (see 1.9.8.2) (Bernsmeier *et al.*, 2015). A subsequent study by Korf *et al*. confirmed monocytes from patients with ACLF had reduced HLA-DR expression, increased IL-10-producing cells, impaired phagocytosis and oxidative burst capacity. Pharmacological inhibition of glutamine synthetase restored monocyte phagocytic and inflammatory capacity in ACLF, highlighting the prospect of metabolic reprogramming as a potential immunotherapeutic modality (Korf *et al.*, 2019).

1.8.3. Macrophage Biology

Macrophages were first identified in the late 19th century by Elie Metchnikoff who outlined their phagocytic activity (Tauber, 2003). Most tissues of the body contain tissue-resident macrophages, which originate from either embryological yolk sac or fetal liver, or from bone marrow-derived monocytes (Yona *et al.*, 2013). These macrophages show substantial heterogeneity, due to their tissue-specific functions and unique microenvironments. Their primary functions are as immune sentinels, where they act as the first line of defence against invading pathogens or tissue injury. They may subsequently orchestrate tissue repair and the resolution of inflammation, to achieve homeostasis (Davies *et al.*, 2013). Traditionally, macrophages were considered to be dichotomously polarised, with either classically-activated M1 or alternatively activated M2. Classically-activated macrophages are shaped by Th1 lymphocytes, LPS and IFN-γ; they primarily orchestrate host bacterial defence, with production of pro-inflammatory cytokines (e.g. IL-1 and TNF-α), produce chemokines (e.g. CCL5, CCL3), have professional phagocytic activity including oxidative burst and nitric oxide generation, and antigen presentation to T-cells with high MHC class II expression. Alternatively-activated M2 macrophages are shaped by Th2 lymphocytes, IL-4, IL-13 and IL-10. M2 macrophages have an anti-inflammatory cytokine profile, producing IL-10 and TGF-β, with sub-categorisations as below (**Table 1.2**) (Shapouri-Moghaddam *et al.*, 2018). They function in the resolution of inflammation, clearance of apoptotic cells and debris, angiogenesis, extracellular matrix digestion and deposition, and tissue repair and remodelling (Sica, Invernizzi & Mantovani, 2013).

Table 1.2 Biological and physiological features of M1/M2 macrophages in humans

Phenotype	Stimuli	Cell Markers	Secreted mediators	Functions
M1	IFN-γ, TNF-α, LPS	CD80, CD86, CD68, MHC II, TLR4, iNOS	TNF-α, IL-1β, IL-6, IL-12, IL-23, IL-27	Pro-inflammatory; Th1 response
M2a	IL-4, IL-13	CD206	IL-10, TGF-β, CCL17, CCL18, CCL22, CCL2	Anti-inflammatory, tissue remodelling
M2b	TLR ligands, IL-1β	IL-10 high, IL-12 low, CD86	TNF-α, IL-1β, IL-6, IL-10	Th2 activation, immunoregulation
M2c	IL-10, TGF-β, steroids	CD206, TLR-1, TLR-8	IL-10, TGF-β, CCL16, CCL18, CXCL13	Phagocytosis of apoptotic cells
M2d	TLR and adenosine receptor ligands	VEGF, IL-10 high, TNF-α low	IL-10, VEGF	Angiogenesis, tumour progression

However, extensive transcriptomic analyses of human MoMFs cultured with various stimuli (e.g. LPS, cytokines, fatty acids), revealed a broad spectrum of macrophage activation states not adequately described by the M1/M2 dichotomy; only a few gene signatures are common to human macrophages that distinguish them from DCs and blood monocytes, including *CD14, FCGR2A* (CD32)*, MERTK, FCGR1A* (CD64) and *CD13* (Xue *et al.*, 2014). However, the signals received by macrophages in their microenvironment are wide-ranging and dynamic, both temporally and spatially (Ginhoux *et al.*, 2016). Macrophages can respond with diverse phenotypes but reversibly switch from one type to another (Sica & Mantovani, 2012). A proposed new way of describing macrophages is to consider a multidimensional model including the source of macrophages, collection of expressed macrophage markers and their specific local microenvironmental mediators (Triantafyllou *et al.*, 2018b).

1.8.4. Resolution Responses and the Role of Macrophages

In order to prevent persistent and over-exuberant pro-inflammatory responses, counter-regulatory anti-inflammatory processes commence at the same time. When an infectious insult subsides, to restore tissue and immune homeostasis, the balance between these two processes must shift towards resolution responses. Central to the resolution of inflammation is the termination of neutrophil influx and the clearance of neutrophils, which become apoptotic even after they have phagocytosed small quantities of pathogenic material, bacterial endotoxin or cytokines (Ortega-Gómez, Perretti & Soehnlein, 2013). Their survival however, is governed by microenvironmental cues. For example, hepatic macrophages can secrete high concentrations of death receptor ligands, such as Fas ligand, TNF and tumour necrosis factor-related apoptosis-inducing ligand (TRAIL), promoting neutrophil apoptosis. Other mediators such as resolvins, reactive oxygen species, lactoferrin and Annexin A1 are also pro-apoptotic (Soehnlein & Lindbom, 2010). A blend of pro-survival and pro-apoptotic signals may exist in the same microenvironment, the relative potency of each influencing the nature of the resolution response.

Apoptotic cells display “eat me” signals, which mark them for phagocytic clearance, or efferocytosis. The most common of these is exposure of phosphatidylserine (PtdSer) on the outer leaflet membrane

of the cell (Nagata *et al.*, 2016). Clearance by tissue macrophages is either direct by cell-to-cell contact or via bridging molecules. Successful internalisation of the apoptotic cell leads to a multitude of mechanisms dampening the immune system. These include lipids in apoptotic cells inducing the activation of transcription factors peroxisome proliferator-activated receptor-delta (PPAR-δ) and liver X receptor (LXR), inhibition of ROS and IL-1β production, inhibition of the TLRs and NF-κB. Finally, there is switch to a resolution-phase M2-like phenotype, with increased production of anti-inflammatory cytokines (IL-10 and TGF-β) rendering macrophages and DCs refractory to further stimulation, enhancing efferocytotic capacity and promoting a tendency to migrate to lymph nodes (Ortega-Gómez, Perretti & Soehnlein, 2013). Failure to clear apoptotic cells and debris prevents a restoration of tissue homeostasis and can also lead to further tissue damage, as lysed neutrophils leak destructive enzymes and ROS. Additionally, unregulated release of immunogenic self-antigens into the microenvironment can result in autoimmunity (Nguyen *et al.*, 2013).

1.9. TAM Receptors

1.9.1. Immunobiology of TAM Receptors

Receptor tyrosine kinases (RTKs) are surface transmembrane receptors, with inherent protein tyrosine kinase activity within the cytoplasmic domain, which when activated results in receptor dimerization, autophosphorylation and a signal transduction cascade with influence over a wide range of cellular processes (Lemke & Rothlin, 2008). The TAM family of receptor kinases consists of Mer tyrosine kinase (MerTK), along with Tyro3 and Axl (Rothlin *et al.*, 2015). The primary functions of TAM signalling pathways include (a) negative regulation in immune homeostasis by inhibition of the inflammatory response of macrophages and DCs to pathogens and (b) phagocytic elimination of apoptotic cells or debris (efferocytosis) in the resolution of inflammation and in tissue homeostasis and renewal (c) Stabilisation of platelet aggregates after vascular injury (Rothlin *et al.*, 2007; Dransfield *et al.*, 2015).

1.9.2. TAM Receptor Structure and Expression

The structure of the receptor consists of a tandem arrangement of two N-terminal immunoglobulin-like binding domains and two fibronectin type III repeats (FNIII), followed by a single pass transmembrane domain and then a cytoplasmic RTK (**Figure 1.2**). The TAM receptors all signal as dimers. The transmembrane domain Pro^{485} between the FNIII domains makes MerTK susceptible to cleavage by metalloproteinase ADAM17 (Thorp *et al.*, 2011). Activation of PRR with LPS or PolyI:C have been demonstrated to induce ADAM17-dependent MerTK cleavage, shedding the extracellular domain, and similar findings have been described with Axl (Orme *et al.*, 2016). TAM receptors are expressed on macrophages and DCs, and MerTK on immature NK cells, Sertoli cells of the testes and retinal pigment epithelial cells of the eye, amongst others. There is no MerTK expression on neutrophils at steady-state or non-malignant lymphocytes (Williams *et al.*, 2009). Ligand binding leads to autophosphorylation, with three tyrosine sites identified (Tyr^{749}, Tyr^{753} and Tyr^{754}) present in the three TAM receptors (Ling, Templeton & Kung, 1996).

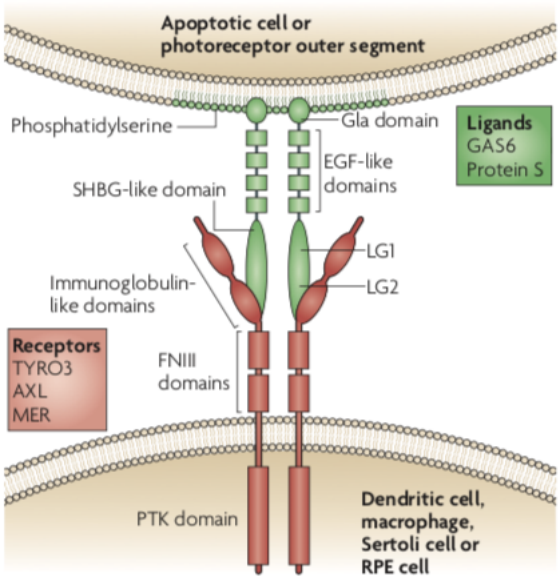


Figure 1.2 Schematic of TAM Receptor and Ligand structure

TAM receptors consist of a tandem of two PTK domains, two FNIII domains, and two immunoglobulin-like domains. Their ligands, e.g. Gas6 and Protein S, consist of two laminin G domains, related to sex hormone binding globulin, two EGF-like repeats and N-terminal GLA domains, the latter binding to exposed PtdSer on apoptotic

cells. Abbreviations: EGF, epidermal growth factor; FNIII, fibronectin type III; PTK, protein tyrosine kinase; TAM, Tyro3, Axl, MerTK; SHBG, sex hormone-binding globulin; LG, laminin G; RPE, retinal pigment epithelial; PtdSer, phosphatidylserine (taken from Lemke *et al.* [2008]; permission from Springer Nature).

1.9.3. TAM Receptor Ligands

The ligands for the TAM receptors are growth arrest-specific-6 (Gas6), protein S (Pros1), galectin-3, tubby and tubby-like protein 1 (Tulp1). Gas6 and Pros1 are the main ligands and share an approximately 40% amino acid sequence homology. Both have a ~60 amino acid Gla domain at the N-terminus, rich in gamma-carboxylated glutamic acid residues. These domains bind phosphatidylserine (PtdSer) "eat me" signals on the outer membrane of apoptotic cells, acting as bridging molecules between TAM receptors and dying cells (Lemke & Rothlin, 2008; Rothlin *et al.*, 2015). Pros1 has an independent role in the coagulation cascade as a natural anticoagulant, which is not affected by Gas6. The affinity of the ligands for the individual receptors is known – Gas6 can bind all three receptors, with highest affinity Axl > Tyro3 >> MerTK, whereas Pros1 binds Tyro3 and MerTK in cells where they are co-expressed, but not Axl (Graham *et al.*, 2014). Gas6 and Pros1 Vitamin-K-dependent co-carboxylation is needed for full activation of the TAMs.

1.9.4. Signal Transduction of the TAM Receptors in Immune Regulation

Much of the understanding of the signalling pathway has come from murine experiments with TAM receptor murine knockouts models (Camenisch *et al.*, 1999; Rothlin *et al.*, 2007). Binding of ligand (e.g. Gas6) to the extracellular domain of the TAM receptor leads to dimerization of the Gas6-TAM complex. Autophosphorylation of the aforementioned tyrosine residues leads to binding with subunits of phosphoinositide 3-kinase (PI3K), phospholipase C (PLC) and growth-factor-receptor bound protein (Grb2). PI3K binding leads to the activation of the PI3K/AKT pathway, and Grb2 binding the MEK pathway. Both have roles in cell proliferation and survival and therefore important in the ectopic expression of MerTK and Axl in tumours (Cummings *et al.*, 2013). In inflammation, TAM signalling has an inhibitory effect on TLR and Janus kinase (JAK)-STAT pathways. Inhibition occurs with TLR3, TLR4 and TLR9 activation and occurs at multiple points in their signalling cascade, including inhibition

of activation of p38 MAPK, extracellular-signal regulated kinase 1 (ERK1)/ERK2, NF-κB, TNF-receptor associated factor 3 (TRAF3) and TRAF6 (Lemke & Rothlin, 2008). This has the effect of inhibiting production of TNF-α, IL-6, IL-12 and type I IFNs (Lee *et al.*, 2012a). The inhibition is part of a dynamic feedback loop that is activated after TLR signalling and generation of STAT1. New gene expression is required for this inhibition, most notably TAM-downstream induction of suppressor of cytokine signalling 1 (SOCS1) and SOCS3 proteins, which act as E3 ubiquitin ligases and are also dependent on co-activation of the type I IFN receptor (IFNAR) and STAT1 transcription factor (Rothlin *et al.*, 2007). SOCS1 and 3 also inhibits the Janus-activated kinase (JAK)-STAT pathway, the principal signalling pathway for the generation of several cytokines involved in sepsis (**Figure 1.3**) (Cai *et al.*, 2015; Wang *et al.*, 2018). Whilst these are the typical pathways for TAM-induced inhibition of inflammation, many other permutations exist, including MerTK-induced PI3K/Akt and SOCS3 co-operation in negative regulation of lipoteichoic-acid-induced inflammation (Zhang *et al.*, 2016).

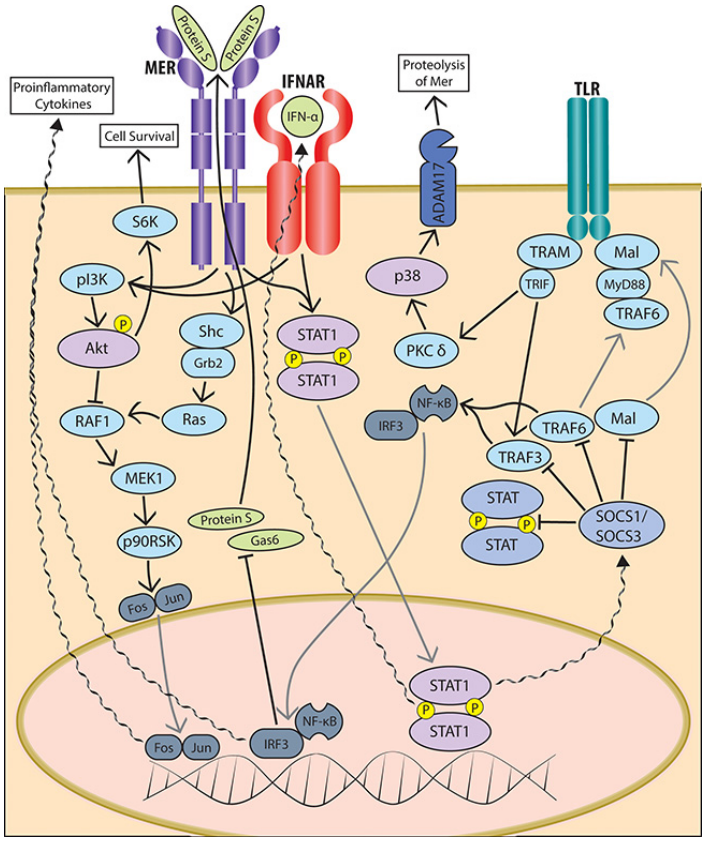


Figure 1.3 Schematic of TAM signalling pathway in innate immune cells

Schematic diagram displaying relevant signalling cascades on ligation of TAM receptor MerTK with one of its ligands Pros1. Taken from Wang *et al.* (2018) (see Appendix U).

TAM signalling in macrophages also modulates the cytokine profile to promote wound healing and resolution of inflammation after uptake of apoptotic cells. Again, much of our understanding of this role for the receptor comes from knockout mouse models. For example, after injection of mice with dexamethasone to induce thymocyte death, MerTK$^{-/-}$ knockout mice have a 7.4 fold increase in apoptotic thymocytes compared to wild type (Scott *et al.*, 2001). In fact, Dransfield *et al.*, also by studying glucocorticoid-treated apoptotic thymocytes, recently identified a dual role of MerTK in tethering and internalizing apoptotic cells (Dransfield *et al.*, 2015). MerTK-mediated efferocytosis yields IL-4, IL-10 and TGF-β, by inhibition of NF-κB and activation of PI3K pathways (Sen *et al.*, 2007). Efferocytosis itself generates signals to promote MerTK signalling; cholesterol and lipoproteins from the cell wall of apoptotic cells in the phagolysosome activate LXR, which activates the MerTK promoter (A-Gonzalez *et al.*, 2009a). IL-10 generated acts in an autocrine fashion to further upregulate MerTK expression and skew the macrophage phenotype towards M2c (Zizzo *et al.*, 2012). TAM signalling is auto-amplified by macrophage and DC secretion of Gas6 and Pros1 in response to MerTK and Axl activation (Rothlin *et al.*, 2007). Efferocytosis leads to induction of engulfment signals involving Src-mediated generation of p130CAS/CRKII/Dock 180 complex, leading to Rac1 activation, and also generates hepatocyte growth factor (HGF) through a Rho-A dependent pathway (Singh *et al.*, 2007; Park *et al.*, 2012). TAM receptors appear to have no role in the phagocytosis of pathogens (Zhang *et al.*, 2019).

1.9.4.1. Differential Expression of TAM Receptors

Zagorska *et al.* identified the differential expression of TAM receptors, with MerTK predominantly expressed in murine macrophages and Axl more abundant in DCs. Induction of the mRNA was also differential, with LPS and poly I:C increasing Axl expression whilst MerTK signalling was more responsive to uptake of apoptotic cells and IL-10, suggesting Axl signalling functioned in inflammatory setting in antigen presenting cells, whilst MerTK has a greater role in tissue homeostasis (Zagórska *et al.*, 2014). Other authors confirm the dependence of Axl and Tyro3 in murine DC efferocytosis, whilst

MerTK is crucial for macrophage activity in retinal homeostasis and clearance of apoptotic thymocytes, though likely that all three TAM receptors co-operate (Seitz *et al.*, 2007).

1.9.5. TAM Receptors and Autoimmunity

Persistence of apoptotic cell debris is an abundant supply of autoantigens, which if not cleared can lead to autoimmunity. Autoimmune diseases such as systemic lupus erythematosus (SLE) are linked with apoptotic cell accumulation (Rothlin & Lemke, 2010). Indeed, delayed efferocytosis of apoptotic cells seen in TAM triple negative knockout (TKO) mice resulted in higher levels of circulating autoantibodies, development of lupus-like autoimmunity, unregulated B and T-cell proliferation and lymphocyte accumulation in secondary lymphoid organs (Rothlin & Lemke, 2010). Human studies link SLE to MerTK including one demonstrating genetic polymorphisms in MERTK as a risk factor for leukopenia in SLE patients (Cheong *et al.*, 2007). Deficiencies in the TAM ligand Pros1 have been detected in SLE patients, suggesting impaired TAM signalling may be part of the pathogenesis (Song, Park & Kim, 2000). Finally, a recent study revealed a novel immunotolerance mechanism in which murine T-cells produce Pros1 which bind to autologous PtdSer and engages with TAM signalling pathways in DCs to restrain immune responses (Carrera Silva *et al.*, 2013).

1.9.6. TAM Receptors in Viral Infection

TAM receptors confer susceptibility to viral infections including Lassa, Dengue, Ebola, West Nile and Marburg viruses (Rothlin *et al.*, 2015). These viruses evade immune capture by apoptotic mimicry, whereby exposing PtdSer on their surfaces and employing TAM bridging molecules Gas6 and Pros1can facilitate endocytic entry into target cells in a TAM-mediated process. Indeed, in haemorrhagic fever with renal syndrome caused by the enveloped Hantaan virus, monocyte Tyro3 was increased compared to healthy controls and Gas6 levels were shown to correlate with disease severity, suggesting the Gas6-Tyro3 axis may facilitate disease progression (Zhang *et al.*, 2017). Enveloped viruses can even potentiate TAM receptor phosphorylation to facilitate their uptake (Shimojima, Ikeda & Kawaoka,

2007; Meertens *et al.*, 2012). *In vitro*, the addition of TAM inhibitors to cell cultures can reduce TAM receptor-facilitated uptake of viral infections (Meertens *et al.*, 2012).

1.9.7. TAM Receptors in Cancer Immunopathology

TAM receptors are aberrantly and ectopically expressed in a variety of tumours, promoting oncogenic phenotypes and cancer escape mechanisms, conferring resistance to chemotherapy. These malignancies are: haematological (acute myeloid leukaemia, acute lymphoblastic leukaemia, chronic lymphocytic leukaemia and multiple myeloma); dermatological (e.g. malignant melanoma); neurological (e.g. glioblastoma multiforme), lung (e.g. non-small cell lung cancer) and metastatic breast to name a few (Graham, 2006; Holland *et al.*, 2010; Wang *et al.*, 2013; Schlegel *et al.*, 2013; Lee-Sherick *et al.*, 2013; Xie *et al.*, 2015). Here, TAM receptors are either overexpressed in tumour cells or in tumour-associated immune cells, where they exert an anti-apoptotic and pro-survival effect, and are negative regulators of DC and T-cell activation that favour malignant cell evasion of host anti-tumour defences. Disabling TAM signalling has been evaluated for its potential in cancer immunotherapy and early phase translation trials are in progress (Kariolis *et al.*, 2016; Sufit *et al.*, 2016; Huey *et al.*, 2016; Akalu, Rothlin & Ghosh, 2017; Deryckere *et al.*, 2017).

1.9.8. TAM Receptors in Liver Disease

1.9.8.1. Steady State

TAM receptors maintain immune tolerance in the liver by clearance of dead cells and thereby auto-antigens. In steady state, murine livers demonstrate MerTK expression in Kupffer cells and HSECs but not hepatocytes. Axl, on the other hand, is also expressed on hepatocytes whilst Tyro3 is only seen on resident macrophages. Murine experiments with triple TAM receptor knockouts demonstrated that at 6 months, the mice spontaneously developed autoimmune hepatitis, characterised by transaminitis, auto-antibody (anti-nuclear and anti-smooth muscle) development and infiltration of autoreactive circulating CD4+ T cells. This autoimmune phenotype was prevented when TAM knockout mice

receive a bone marrow transplant of wild-type stem cells, presumably resulting in restoration of TAM-mediated clearance of apoptotic cells (Qi *et al.*, 2013; Mukherjee, Wilhelm & Antoniades, 2016).

1.9.8.2. Acute and Chronic Liver Injury

In murine acute liver injury, TAM receptors may be protective; hepatic arterial ligation and ischaemia led to raised serum Gas6 levels soon after and homogenized liver extracts showed selective increases in phosphorylated MerTK and Axl. Gas6 knockout mice however showed higher mRNA expression for pro-inflammatory cytokines and were more prone to fulminant liver failure, with restoration of protection from fulminant disease with administration of recombinant Gas6 (Llacuna *et al.*, 2010). In humans, Bernsmeier *et al.* demonstrated an expansion of MerTK+ circulating monocytes in patients with ACLF, and to a lesser extent in acute decompensated cirrhotic patients, when compared with healthy controls. Heightened plasma concentrations of Gas6, Pros1 and galectin-3, in addition to phosphorylation of MerTK demonstrated on Western Blot, suggested activated MerTK signalling. The phenotype was recapitulated when healthy monocytes were exposed to ACLF plasma. And in keeping with previously described immunobiology, MerTK+ monocytes exhibited dampened LPS-evoked TNF-α production. Expansion of this immunosuppressive MerTK+ subset correlated with hepatic and extrahepatic disease scores (MELD, CLIF-SOFA, SIRS) and was implicated in a higher risk of nosocomial infection and death (Bernsmeier *et al.*, 2015). This may be a SIRS-related phenomenon since MerTK+ myeloid cell expansion was also reported in severe sepsis (Guignant *et al.*, 2013). Recently, Triantafyllou *et al.* demonstrated the expansion of a pro-restorative $MerTK^{+/high}$ $HLA\text{-}DR^{+/high}$ monocyte/macrophage subset in the circulation and liver in the resolution phase in murine and human acute liver failure. Secretory leucocyte protease inhibitor (SLPI) reprogrammed myeloid cells towards this phenotype, promoting neutrophil apoptosis and their clearance (Triantafyllou *et al.*, 2018a).

Murine carbon tetrachloride models of chronic liver injury suggest activation of hepatic stellate cells, that are pivotal in the pathogenesis of hepatic fibrogenesis and cirrhosis, depends upon Gas6-mediated Axl activation (Bárcena *et al.*, 2015). Soluble Axl has been proven in humans to be an accurate

biomarker for cirrhosis and development of hepatocellular carcinoma (HCC), highlighting receptor shedding may also play a role in pathogenesis (Dengler *et al.*, 2017).

1.10. Summary and Aims

Decompensated cirrhosis and ACLF are increasingly common conditions with high healthcare resource utilisation, morbidity and mortality. The triggers for decompensation and ACLF in patients with cirrhosis is most frequently bacterial infection, for which they seem predisposed. Once AD or ACLF are established, irrespective of the precipitant, there is a higher risk of infection and death. SBP is common and linked to poor outcomes. Sepsis-induced ACLF has a particularly poor prognosis and many patients die despite potent antibiotic therapy. In part, this may be due to the emergence of multi-drug resistant bacterial species, but a dysfunctional immune system, or immuneparesis, is a major contributor to this susceptibility to infection. A greater understanding has been achieved over the last decade, with the recognition that dysfunctional monocytes and macrophages may be a key factor in immuneparesis, but the mechanisms leading to impaired antimicrobial responses are incompletely understood. Moreover, whilst most research to date has focused on circulating cells, little is understood about the function of immune cells at tissue compartments, such as the peritoneum and liver, where infections may disseminate. Recently, observations were made of upregulation of TAM receptor MerTK on the cell surface of circulating monocytes in severe sepsis and in ACLF. The primary functions of TAM (Tyro3, Axl and MerTK) receptors are mediating clearance of apoptotic cells and debris and inhibition of pro-inflammatory innate immune responses. The conjecture therefore was that enhanced MerTK signalling on monocytes in these inflammatory diseases may ultimately lead to attenuated antimicrobial responses and increased susceptibility to infection. With all this in mind, several questions remain unanswered. In liver disease, both in decompensated cirrhosis and ACLF, what is the expression of all the TAM receptors in different tissue compartments? What factors may influence their expression? How do the TAM receptors correlate with innate immune function? Given the dismal prognosis of patients with infections in advanced liver disease including ACLF, could

modulation of TAM receptor signalling represent a potential immunotherapeutic target to reduce susceptibility to infection and improve outcomes?

The aims of research in this thesis accordingly are to:

1) determine the expression levels and functional role of TAM receptors on monocytes and macrophages in different compartments including the circulation, peritoneum and liver.

2) identify local microenvironmental factors in the ascites that may influence the immune composition of the peritoneum in liver disease.

3) explore the modulation of the MerTK signalling pathway as a potential immunotherapeutic target to reduce the susceptibility to infection in decompensated cirrhosis and ACLF.

CHAPTER 2

2. PHENOTYPE AND FUNCTION OF CIRCULATING MONOCYTES IN ACUTE-ON-CHRONIC LIVER FAILURE

2.1. Background and Aims

The development of bacterial infections in cirrhosis is frequent and increases mortality four-fold (Arvaniti *et al.*, 2010; Jalan *et al.*, 2014a). They can trigger the development of organ failure, acute-on-chronic liver failure (ACLF), underpinned by a systemic inflammatory response syndrome (SIRS), which portends an even worse outcome (Moreau *et al.*, 2013). Even where ACLF is not sepsis-triggered, there is a higher risk of recurrent infections and subsequently an even poorer outcome (Bajaj *et al.*, 2012; Fernandez *et al.*, 2018). In some cases, these infections may be multi-drug resistant (Piano *et al.*, 2018). Underlying this propensity to infections is a dysfunctional immune system, termed immuneparesis or cirrhosis-associated immune dysfunction (Wasmuth *et al.*, 2005; Selvapatt *et al.*, 2014; Albillos, Lario & Alvarez-Mon, 2014). Circulating monocyte dysfunction is a pivotal component of this immunopathology, and has also been described in other systemic inflammatory diseases with higher risks of secondary infection including trauma, acute pancreatitis and severe sepsis (Taylor, Gordon & Polk, 2000; Hotchkiss, Monneret & Payen, 2013; Pan *et al.*, 2017). Reduced monocyte HLA-DR expression in cirrhosis has previously been found to predict outcome (Berry *et al.*, 2010a). Recently, functionally-impaired monocytes in ACLF, with attenuated pro-inflammatory cytokine responses to microbial challenge, were correlated to increased numbers of MerTK+ monocytes (Bernsmeier *et al.*, 2015). The main role of MerTK, primarily expressed by tissue macrophages, like the other TAM receptors Axl and Tyro3, is the clearance of apoptotic cells and debris after acute tissue injury, but this is biologically coupled with a dampening of innate immune responses (Lemke & Rothlin, 2008; Rothlin *et al.*, 2015). In acute liver failure, resolution-like MerTK+ HLA-DR^{high} circulating monocytes and hepatic macrophages are expanded, showing suppressed innate but enhanced phagocytic/efferocytic responses (Triantafyllou *et al.*, 2018a).

Hypothesis and aims:

Given the historical and recent findings on circulating monocytes and hepatic macrophages, it was hypothesised that the other TAM receptors, Axl and Tyro3, may be similarly expanded in the circulatory compartment of patients with ACLF, associated with attenuated pro-inflammatory responses and could also predict outcome. Additionally, given the role of MerTK as a mediator of apoptotic cell phagocytosis and the observation MerTK+ monocytes are expanded in ACLF, it was also hypothesised that monocytes in ACLF display enhanced phagocytosis in ACLF compared to healthy monocytes. In this chapter therefore, the aims were to:

- Examine the immunophenotype and functional profile of circulating monocytes obtained from advanced cirrhotic and ACLF patients in comparison with healthy controls.
- Determine the gene expression profile of MerTK+ monocytes.
- Investigate the phagocytic capacity of monocytes in ACLF.

2.2. Materials and Methods

2.2.1. Patient recruitment

For the circulatory component of the work, patients with acute-on-chronic liver failure (ACLF, n=18) and cirrhosis without organ failure (OF) (n=30) were recruited from two sites, King's College Hospital (London, UK, n=30) and St. Mary's Hospital (London, UK, n=18), between 2015 and 2018. The ACLF patients were recruited into the study within 24 hours following admission to the Intensive Care Units at these institutions. Patients with cirrhosis without OF were either stable (n=11), recruited on the wards at King's College Hospital as transplant assessments or on the ambulatory unit at St. Mary's Hospital, or acute decompensated (n=19), admitted via Accident and Emergency (**Table 2.1**). Healthy volunteers (n=29) were recruited as controls. Data was recorded in accordance with Good Medical Practice and General Data Protection Regulation (GDPR) guidelines. The diagnosis of cirrhosis was confirmed by review of clinical, radiological and histological data. ACLF was defined according to the CLIF Sequential Organ Failure Assessment (CLIF-SOFA) criteria (Moreau *et al.*, 2013). Exclusion criteria for the study were age <18 years old, evidence of disseminated malignancy, human immunodeficiency virus or receipt of high-dose immunosuppressive therapy (excluding steroids) up to one month prior to study entry. The study was approved by the NRES Health Research Authority (Research Ethics Committee [REC] reference: 12/LO/0167). In the event of patient incapacity, assent was obtained from the patients' nominated next of kin. If the patient regained capacity, informed consent was obtained. Haematological and biochemical parameters were determined using automated analysers at King's College Hospital (Siemens Advia 2120, Berks, UK) and St. Mary's Hospital (Sysmex XE-2100, Japan).

2.2.2. Clinical Data

Clinical data for all recruited patients was acquired with their consent as above and stored pseudo-anonymised in a computerised password-protected database. Datasets included hospital episode characteristics (date of admission, sampling date, hospital length of stay, location of sampling, episode

mortality), demographics (date of birth, age, gender, ethnicity), aetiology, current or prior complications of liver disease (variceal haemorrhage, hepatic encephalopathy and renal dysfunction), co-morbidities, concurrent medications, physiological observations and outcome data (28- and 90-day mortality, liver transplantation and subsequent sepsis). For those on critical care, organ support requirements (vasopressors, ventilator settings, haemofiltration) were noted. Laboratory parameters included full blood count (FBC), urea and electrolytes (U&Es), coagulation screen, liver function tests (LFTs) and C-reactive protein (CRP). Hepatic disease severity scores were calculated including original MELD, Child-Pugh-Turcotte score and where relevant, CLIF-SOFA, CLIF-C AD and CLIF-C ACLF scores.

2.2.3. Isolation of Peripheral Blood Mononuclear Cells

Whole blood was collected from each recruited subject by venepuncture, or via central venous or arterial catheter, into lithium heparin vacutainers in order to isolate peripheral blood mononuclear cells (PBMCs). Blood was combined, diluted with phosphate buffered saline (PBS, Life Technologies, UK) at a 1:1 ratio and layered on Ficoll-Paque Plus (GE Healthcare, UK). After centrifugation at 450*g* for 20 minutes without brake to obtain a density gradient separation, the buffy coat was aspirated carefully with a Pasteur pipette to obtain PBMCs. Cells were washed and counted using trypan blue to identify dead cells, a haemocytometer (Neubauer, Germany) and light microscope. Where required, cells were frozen using a freezing mixture (10% DMSO 90% FBS), placed into a graduated cooling device (CoolCell®, Biocision, USA) and stored in -80°C freezer.

2.2.4. Isolation of CD14+ Monocytes by Magnetic Bead Separation

A protocol using a CD14+ monocyte bead-based isolation kit (Miltenyi Biotec, UK) was used. Healthy PBMCs were obtained as above. A buffer solution containing PBS, pH 7.2 0.5% bovine serum albumin (BSA) and 2mM EDTA was prepared by diluting MACS BSA stock solution 1:20 with autoMACS® Rinsing solution, which was kept at 2-8°C. The PBMC pellet was resuspended in 10ml of buffer in a 15ml Falcon tube, and the volume was passed through a 30μm nylon mesh (MACS Pre-Separation Filter) to obtain a single-cell suspension. After centrifugation and resuspension of the pellet with buffer,

cells were counted with a haemocytometer and trypan blue to determine the proportion of dead cells. The cells were pelleted and subsequently resuspended in 20µl of Miltenyi CD14+ magnetic microbeads and 80µl of buffer for every 10^7 cells, then vortexed and the mixture kept at 4°C for 15 minutes. After this time, the volume was made up to 15mls with buffer, solution centrifuged and the supernatant discarded to generate a dry cell pellet. This pellet was resuspended in 500µl buffer and then passed through a MACS LS column in a magnetic field, achieved by attaching the column to a MACS separator, resulting in magnetically-labelled CD14+ cells to be retained within the column. The column was washed with buffer (3 x 3mls) with CD14- cells collected in a 15ml Falcon tube. The column was then removed from the MACS separator, placed on to a new 15ml Falcon tube. Five ml of buffer was pipetted into the column and CD14+ cells immediately flushed by pushing a plunger into the column. The purity of the CD14+ positive selection was enhanced by attaching another MACS LS column to the MACS separator and repeating the aforementioned process. CD14+ cells were washed and counted. Purity was assessed by flow cytometry using monoclonal antibodies against CD14 (BD Biosciences, UK).

2.2.5. Isolation of Healthy Neutrophils by Density-Gradient Separation

For efferocytosis assays, healthy neutrophils were required in order to render them apoptotic. Blood collected from healthy volunteers (REC: 12/LO/0167) in lithium heparinized vacutainer tubes was layered in equal volumes (1:1) using a serological pipette on to Polymorphprep™ (Abbott Diagnostic Technologies AS, Oslo, Norway), a cell separation media containing sodium diatrizoate 13.8% (w/v) and polysaccharide 8.0% (w/v), in a 50ml Falcon tube. After density-gradient separation by centrifugation at 400*g* for 35 minutes without brake, neutrophils appeared in a distinct band below PBMCs. Neutrophils were careful extracted from this layer with a pipette, and combined in a separate Falcon tube. After resuspending in PBS and subsequent centrifugation, the neutrophil pellet was resuspended in 1ml complete media (10% FBS 1% penicillin / streptomycin 89% RPMI) and neutrophils manually counted using trypan blue to identify dead cells using a C-Chip haemocytometer (NanoEnTek, China), in order to determine the concentration of neutrophils in solution. Neutrophils

required immediate use and their purity was assessed by monoclonal antibodies against CD66b (BD Biosciences, UK).

2.2.6. Immunophenotyping of Monocytes by Flow Cytometry

For immunophenotyping, human PBMCs that were previously thawed in a 37°C water bath for 1 minute were incubated with mouse anti-human monoclonal antibodies including: CD14 PE-Cy7, CD16 APC-H7, CD163 PE, CCR2 AF647, CCR7 PE (BD Biosciences, UK); HLA-DR PerCP Cy5.5 (Life Technologies, UK); MerTK APC, Axl AF488, Tyro3 PE (R&D Systems, UK); CCR5 BV421, CD11b BV421, CD206 BV421 (BioLegend, UK). The panel layout is described in Appendix A. Incubation was for 30 minutes at 4°C in the dark, followed by assessment by flow cytometry (BD Fortessa at St. Mary's Hospital; BD Canto II at King's College Hospital, BD Biosciences, UK) for surface marker expression. Flow cytometric data analysis was conducted using FlowJo v10.4.2 software (FlowJo LLC, USA), with isotype or fluorescence minus one (FMO) controls used to establish the gates for positive expression. Due to differences in FACS machines and calibration between these sites (as above), in order to combine the datasets, surface marker expression was given as percentage of monocytes expressing the marker, rather than median fluorescence intensity (MFI) which varies depending on the flow cytometry. Where MFI is reported, the site of the sample cohort was specified.

2.2.7. Intracellular Cytokine Staining of PBMCs

Intracellular cytokine staining (ICCS) is a flow cytometry-based assay which measures the production of cytokines in response to a triggering agent, such as a PAMP like LPS, a component of gram-negative bacterial cell walls. Cells are stimulated *in vitro* by LPS, which interacts with toll-like receptor 4 (TLR4) on the macrophage and monocyte cell surface, for a fixed duration with addition of a reagent to prevent cytokine cellular export, followed by permeabilization of the cell membrane to allow multi-colour monoclonal antibody intracellular staining. To determine the LPS-stimulated monocyte production of TNF-α and IL-6, an ICCS kit was used (BD Biosciences, UK). Initially, PBMCs were thawed in a water bath, washed in pre-warmed RPMI, centrifuged and cells in the pellet counted with trypan blue and a

haemocytometer after resuspension in 1ml of complete media. PBMCs were resuspended at one million per ml density in complete medium (89% RPMI, 10% heat-inactivated fetal bovine serum [FBS], 1% penicillin/streptomycin) and aliquoted to wells of a 24-well plate (Corning, UK). Subsequently, LPS 100ng/ml (LPS *E. coli* K12, InvivoGen, France) was added. The cell plate was incubated at 37°C (5% CO_2) for 1 hour, after which time 0.5µl BD GolgiStop™ containing monensin (BD Biosciences, UK) was added to each well to halt export of cytokines from the cells. For wells in which supernatants were to be collected for subsequent ELISA determination of cytokine concentration, GolgiStop™ was not added to permit extracellular secretion. The cell plate was returned to the incubator for a further 4 hours such that total TLR agonist exposure was 5 hours. Cells were cultivated after this time and transferred to polystyrene tubes, stained with a fixable viability dye and subsequently an antibody mixture to stain for cell surface markers including CD14 Pe-Cy7 and CD16 APC-H7 (BD Biosciences, UK), HLA-DR PerCP Cy5.5 (Life Technologies, UK), MerTK APC and Axl AF488 (R&D Systems, UK). Cells were subsequently permeabilized with BD Cytofix/Cytoperm (BD Biosciences, UK) and washed with 1:50 diluted (dH_2O) BD Perm/Wash buffer. Permeabilized cells were then stained in Perm/Wash buffer with an intracellular antibody mixture containing TNF-α PE (BD Biosciences, UK) and IL-6 BV421 (BioLegend, UK) with subsequent acquisition on the flow cytometer. Fluorescence minus one (FMO) controls were used for MerTK and Axl extracellular stains and isotype controls used for intracellular stains. In a small cohort, stimulation of PBMCs with TLR2 agonist Pam_3CSK_4 (Sigma Aldrich) at 5µg/ml and with negative control (PBS) was also performed for comparison. Thawed PBMCs from a total of 57 subjects underwent ICCS: healthy control (n=23), cirrhosis without OF (n=17) and ACLF (n=17), either at King's College Hospital (n=19) or Imperial College London (n=38).

2.2.8. Fluorescence Activated Cell Sorting of Live Cells

Fluorescence activated cell sorting (FACS) enables the physical separation of cells labelled with monoclonal antibodies to isolate purer populations for subsequent experimental work. The sorting process was conducted in the Imperial College London St. Mary's Campus Flow Cytometry Sorting facility using a FACS Aria II, with the assistance of the Flow Cytometry Core Facility Manager

Yanping Guo. In the tissue culture laboratory, enough cryovials to obtain 20-30 million PBMCs were thawed in a water bath set at 37°C, contents centrifuged in pre-warmed RPMI and combined. CD3 magnetic bead isolation was performed to exclude T-cells. In short, cells were diluted in separation buffer, flushed through a 30μm pre-separation filter (Miltenyi Biotech, UK) and centrifuged to obtain a single-cell pellet. CD3 magnetic beads were added with separation buffer according to the cell count, incubated at 4°C and washed. The cell solution was passed through a pre-wet LS column and the effluent (negative fraction) centrifuged to acquire a CD3 negative pellet. These cells were then exposed to fixed viability dye and an antibody mixture (Appendix B) sequentially. The volume of antibody used was upscaled depending on the number of cells. Ultra-Comp eBeads™ compensation beads, ArC™ amine reactive compensation bead kit (ThermoFisher Scientific, UK) and FMOs were prepared for controls.

2.2.9. Gene Expression Analysis

Gene expression analysis (transcriptomic profiling) was performed using the Nanostring nCounter® XT GX Human Immunology V2 assay (Nanostring Technologies, Seattle, WA) with the myeloid code set, in which 594 related genes are interrogated. FACS-sorted monocytes (MerTK+ and MerTK- separation) were pelleted by centrifugation at 16,000*g* for 10 minutes, lysed in RLT lysis buffer (Qiagen, Germany) at a concentration of maximum 50,000 cells per 2μl and stored at -80°C. Cell lysates were incubated overnight with reporter and capture probes with subsequent immobilisation on a cartridge using the nCounter® Prep Station (Nanostring Technologies, Seattle, WA). The cartridge was then scanned on the nCounter® Digital Analyser at 600 fields of view at the UCL Nanostring Facility (University College London, UK). Differential gene expression was analysed and plotted as heat maps using the nSolver™ Analysis software 4.0 with advanced analysis module (Nanostring Technologies, Seattle, WA, USA). Results were only considered relevant if there was a 1.5x higher or lower fold change and the difference was statistically significant ($p<0.05$), though non-significant but theoretically relevant genes are also displayed. Functional gene clustering was performed using gene set enrichment analysis (GSEA)

through the nSolver™ Advanced Analysis module and using online GSEA programme WebGestalt (Subramanian *et al.*, 2005; Wang *et al.*, 2017).

2.2.10. Phagocytosis Imaging of Monocytes Conditioned in ACLF Plasma by Cell-IQ®

Monocytes were isolated from healthy control PBMCs (n=1) by CD14 magnetic bead separation as per manufacturers' protocol. Half a million monocytes were added per well of a 24-well plate in 500µl of complete media and 25% plasma from healthy controls (n=2) and ACLF (n=2), and left incubated for 24 hours at 37°C. An additional well contained cells in complete media alone to be used as a control. Purity of CD14+ cells was confirmed as >90% by flow cytometry. After 24 hours, conditioned CD14+ cells were collected from the wells, washed with PBS and resuspended in a new 24-well plate in complete media supplemented with 10% human AB serum (to provide opsonins) to a volume of 500µl per well. 10µl of reconstituted *Escherichia coli* (*E. coli*) Green BioParticles™ (Life Technologies, UK) were added to each well, except the control well in which 10µl PBS was added. The 24-well plate was secured and transferred to the Cell IQ® (CM Technologies, Finland) for live cell kinetic imaging, recording the duration and intensity of pH-dependent fluorescent emission after BioParticle™ phagocytosis. The linked Imagen™ and Analyser™ software were used for data processing and automated analysis of fluorescence images.

In a separate experiment to evaluate the efferocytic capacity of ACLF monocytes, healthy control PBMCs underwent CD14+ magnetic bead isolation and were conditioned in 25% HC and ACLF plasma for 24 hours. As previously described, healthy neutrophils were obtained by Polymorphprep™ density gradient separation. Neutrophils were stained with 5µM Cell Tracker Green CMFDA (ThermoFisher Scientific, UK) and after washing, resuspended in complete media and incubated for >20 hours at 37°C to render them apoptotic as per previously published methods (Zigmond *et al.*, 2014). After this time, conditioned monocytes and neutrophils were mixed together in a 4:1 neutrophil: monocyte ratio and imaged using the Cell-IQ® system.

2.2.11. Statistical Analysis

Analysis and graphical representation of data was generated using GraphPad Prism v8.2 (GraphPad Software, La Jolla California, USA). Statistical significance was assessed with non-parametric testing on the assumption that data was not normally distributed, unless otherwise specified in the figure legends. Results are presented as median with interquartile range unless otherwise specified. Correlations with clinical or biochemical parameters was conducted with SPSS v23 (IBM Corporation, USA).

2.3. Results

2.3.1. Clinical Summary of Recruited Patients

The clinical and biochemical characteristics of the whole cohort are summarised in Table 2.1. Patients with ACLF had a significantly higher WCC, total bilirubin, creatinine and INR. Disease severity scores were significantly higher in the ACLF group including MELD (33 vs. 18, $p<0.0001$) and CLIF-C AD score (69 vs. 54, $p<0.0001$). As expected, both 28- and 90-day mortality was higher in the ACLF group. A portion of the whole cohort was used for immunophenotyping (healthy, n=15; cirrhosis, n=19 and ACLF, n=12) and intracellular cytokine staining experiments (healthy, n=23; cirrhosis, n=17 and ACLF, n=17).

Table 2.1 Summary of clinical, physiological and biochemical parameters of recruited patients for circulation studies

Variable	Cirrhosis w/o OF	ACLF	Healthy	p-value
Number of patients	30	18	29	n/a
Age, *y*	56 [26-74]	52 [36-64]	34 [24-54]	0.752[a]
Sex, male:female	20:10	11:7	12:17	0.697[b]
Aetiology				
Alcohol	24	14	-	
Non-alcoholic fatty liver (NAFLD)	5	1	-	
Viral (HBV/HCV)	0	2	-	
Autoimmune (AIH/PBC/PSC)	1	1	-	
Mixed/other	0	0	-	
White cell count, x10^9/L	7.0 [4.0-21.6]	12.8 [4.3-28.7]	-	<0.0001[c]
Neutrophil	5.0 [2.8-19.0]	10.8 [3.8-26.9]	-	<0.0001[c]
Monocyte	0.48 [0.22-0.70]	0.76 [0.20-2.51]	-	0.209[c]
Platelets, x10^9/L	113 [84-204]	63 [36-140]	-	0.09[c]
Total Bilirubin, µmol/L	181 [17-424]	102 [21-527]	-	0.011[c]
Albumin, g/L	25 [18-34]	30 [14-36]	-	0.492[c]
Sodium, mmol/L	135 [133-138]	139 [127-154]	-	<0.189[c]
Creatinine, µmol/L	98 [62-115]	174 [52-426]	-	<0.0001[c]
INR	1.79 [1.47-3.01]	2.06 [1.40-3.75]	-	<0.01[c]
MELD Score at Time of Sampling	18 [10-31]	33 [16-47]	-	<0.0001[c]
CLIF-C AD Score	54 [31-72]	69 [48-89]	-	<0.0001[c]
CLIF SOFA	n/a	14 [8-17]	-	n/a
CLIF-C ACLF Score	n/a	64 [39-73]	-	n/a
28-day Mortality	3 (10.3%)	11 (61.1%)	-	<0.001[b]
90-day Mortality	4 (13.8%)	13 (72.2%)	-	<0.0001[b]

Statistical tests: [a] Student t-test [b] Chi-Square test [c] Mann-Whitney U test. All values are displayed as median with ranges in brackets below.

2.3.2. Immunophenotype of Circulating Monocytes

Monocytes were selected by the gating strategy previously described by Abeles *et al.*, in which neutrophils and NK cells are reliably excluded by gating using only CD14, CD16 and HLA-DR, without the need for specific markers (i.e. CD56 and CD66b) (Abeles *et al.*, 2012) (**Figure 2.1A**). This strategy is subsequently referred to as the HLA-DR gating strategy. Results from samples that were fixed with fixation buffer (BD Biosciences, UK) were excluded from the analysis since these had notably diminished expression of MerTK (healthy, n=4, cirrhosis, n=6 and ACLF, n=4). Evaluation of the MerTK monocyte expression revealed a significant expansion of MerTK expressing-monocytes in ACLF, by both percentage and MFI, in ACLF when compared to healthy controls (median %: 29.6 vs. 5.2, $p<0.0001$; MFI: 250 vs. 126, $p=0.0002$) and patients with cirrhosis without organ failure (OF) (median %: 29.6 vs. 13.1, $p=0.0039$; MFI: 250 vs. 141.5, $p=0.0021$). No significant differences were detected between healthy controls and cirrhotic patients without OF. The patients used in the analysis were distinct from those in the Bernsmeier *et al*. paper, and internally validated these findings (Bernsmeier *et al.*, 2015). Axl percentage expression however did not demonstrate significant differences (Kruskal Wallis $p=0.08$), and was generally less than 5%, with the highest median value in cirrhosis without OF at 1.19%. The range of Axl percentage was substantial (0.48-39.6%), but even with exclusion of the highest outlier (39.6%), differences were not significant. On the contrary, Axl MFI showed a significant increase in ACLF compared to healthy control. Tyro3 percentage expression (%) did not demonstrate significant differences between groups, though Tyro3 MFI expression was increased in patients with ACLF and cirrhosis without OF when compared with healthy controls (**Figure 2.1B**). Taken together, these data demonstrated that all TAM receptor expression was increased in ACLF by MFI of the monocyte population, but the most discriminatory marker appeared to be MerTK%. In ACLF, of the Axl- monocytes, most were MerTK-, but in Axl+ monocytes, over 75% were MerTK+ (**Figure 2.1C**). The TAM receptor triple positive (MerTK+ Axl+ Tyro3+) circulating monocyte percentage was significantly expanded in ACLF compared to healthy control, but remained only 0.5-1.0% of the total monocyte population, due to the low occurrence of Axl+ monocytes (**Figure**

2.1D). As previously described, HLA-DR+ monocyte percentage is diminished in ACLF (Berry *et al.*, 2010a) (**Figure 2.1E**).

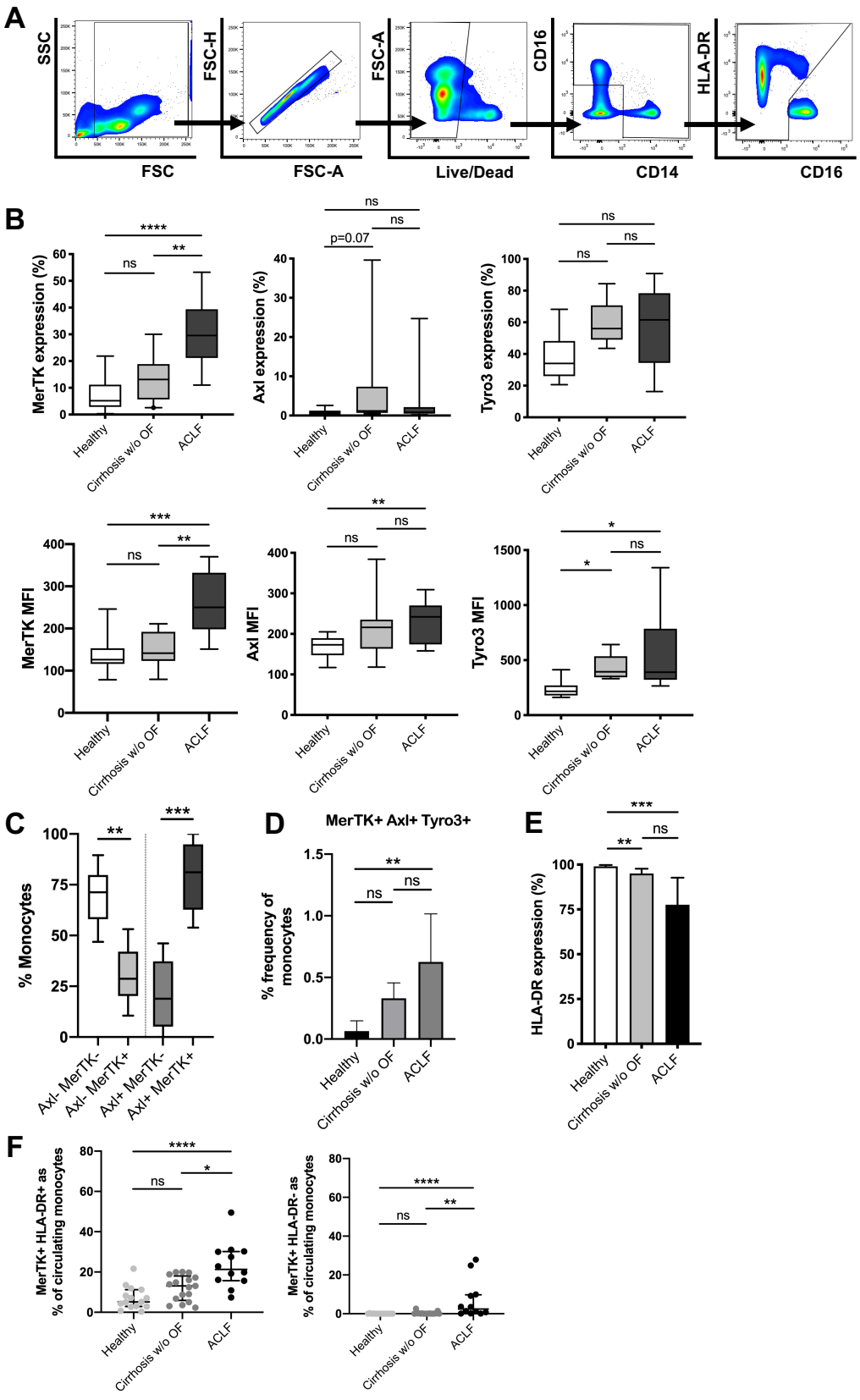


Figure 2.1 TAM receptor Immunophenotype of Circulating Monocytes

Peripheral blood mononuclear cells (PBMCs) were thawed from frozen and immunophenotyped. (A) Gating strategy employed to select monocytes (B) Monocyte TAM receptor (MerTK / Axl / Tyro3) expression by

percentage (top row) or median fluorescence intensity (MFI) (bottom row) according to groups healthy control (HC, n=15), cirrhosis without organ failure (w/o OF) (n=17) and acute-on-chronic liver failure (ACLF) (n=11). (C) Double TAM receptor (MerTK+/- and Axl+/-) percentage expression in ACLF (n=11). (D) Triple TAM receptor percentage co-expression (MerTK+ Axl+ Tyro3+) in difference disease groups: healthy (n=8), cirrhosis w/o OF (n=5) and ACLF (n=8). (E) Monocyte HLA-DR percentage expression in disease groups: HC (n=15), cirrhosis w/o OF (n=17), ACLF (n=12). (F) MerTK+ HLA-DR+ and MerTK+ HLA-DR- as a percentage of circulating monocytes in disease groups. Data presented with median and interquartile range. Statistical analysis included Kruskal Wallis with Dunn's multiple comparison for more than two groups, or Wilcoxon ranked test for paired samples (C). *p<0.05, **p<0.01, ***p<0.001, p<0.0001.

Both MerTK+ HLA-DR+ and MerTK+ HLA-DR- monocytes are significantly expanded in ACLF (Kruskal Wallis p=0.0002 and p<0.0001 respectively) as a percentage of circulating monocytes, though there was no significant difference between healthy control subjects and patients with cirrhosis without organ failure (**Figure 2.1F**).

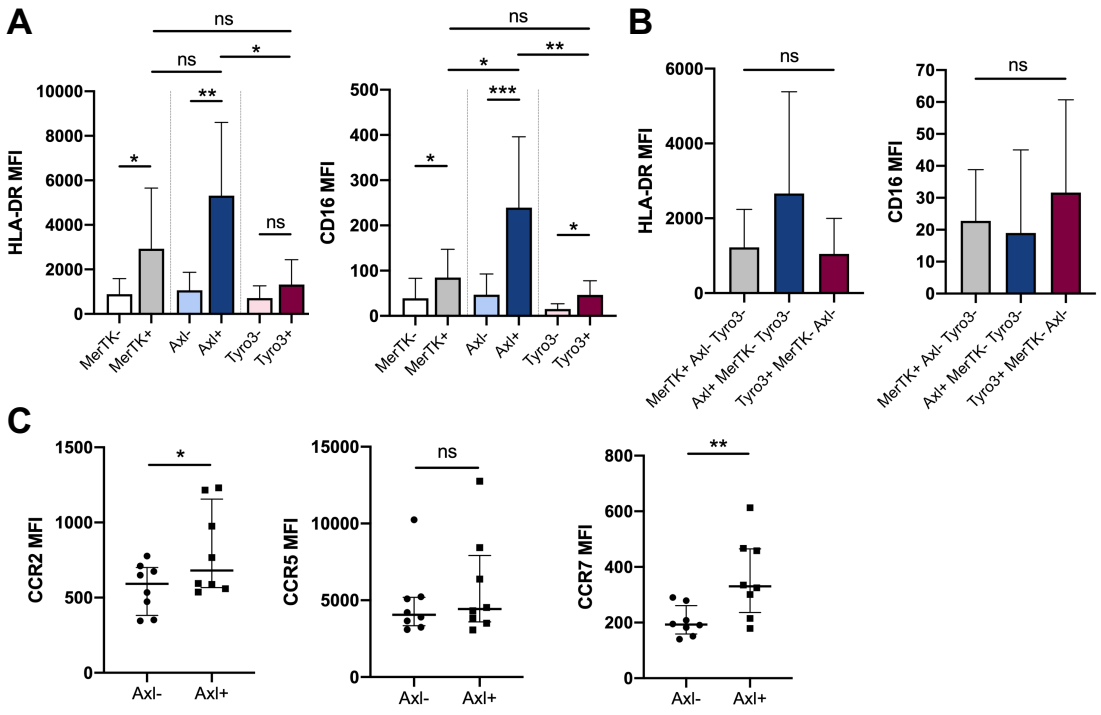


Figure 2.2 Immunophenotype of TAM+ vs. TAM- receptors on monocytes in ACLF

(A) Comparison of monocyte HLA-DR and CD16 MFI expression between Axl+/-, MerTK+/- and Tyro+/- when these markers are considered in isolation. (B) HLA-DR and CD16 MFI monocyte expression with combinations of TAM receptor expression (with one positive and other two negative). (C) Monocyte MFI expression of homing markers CCR2, CCR5 and CCR7 according to Axl+/- status. Data is presented as median with interquartile range. Statistical analysis was by Wilcoxon paired rank (A), Kruskal Wallis (B) or Mann Whitney U (C). *p<0.05, **p<0.01, ***p<0.001, p<0.0001.

Axl+ monocytes in ACLF appeared to be CD16^{high} HLA-DR^{high} CCR2^{high} CCR7^{high}, similar to MerTK+ monocytes as published in the Bernsmeier *et al.* paper, with higher CD16 MFI compared to MerTK+ and Tyro3+ monocytes (**Figure 2.2A&C**). However, since most Axl+ monocytes are also MerTK+, this may be primary phenotypic contributor. Indeed, by gating for one positive TAM receptor and two negatives in combination (i.e. MerTK+ Axl- Tyro3-, Axl+ MerTK- Tyro3- and Tyro3+ MerTK- Axl-), there was no significant difference in HLA-DR and CD16 MFI expression in ACLF between the TAM receptors, though only a small cohort was stained for all three TAM receptors (n=8) (**Figure 2.2B**).

2.3.3. Gene Expression Profiling of MerTK+ Monocytes

PBMCs from patients with cirrhosis due to alcohol-related liver disease were FACS sorted to isolate monocytes and separate them into MerTK+ and MerTK- subsets (**Figure 2.3A**). Since MerTK+ monocytes do not comprise a distinct population, but rather the receptor is expressed across a spectrum, the negative population was selected according to the FMO control whilst the positive population selected by the highest MerTK-expressing monocytes in the population. Transcriptomic profiling of the cell lysates revealed upregulation of the *C1q* (A-C) cluster of genes (**Figure 2.3B**) with >20-fold increase in MerTK+ monocytes compared with MerTK-. The *LIPA* gene encoding lipase A, a lysosomal enzyme crucial for hydrolysis of internalized cholesteryl esters and triglycerides, was also significantly upregulated ($p<0.001$). Other significantly upregulated genes included those for phagocytosis (e.g. *FCGR3A, FPR3*), antigen presentation (e.g. *HLA-DRA, HLA-DMA, HLA-DPA1, HLA-DPB1*), cellular cytokinesis (e.g. *CTTNPB2, RHOC*) and regulation of apoptosis (e.g. *BCL2* and *CASP5*). Genes for monocyte or neutrophil chemotaxis were upregulated (e.g. *CCR5* and *LGALS3*) and downregulated (e.g. *FPR2* and *CXCL1*) in MerTK+ monocytes. Pattern recognition receptors were also both upregulated (e.g. *NOD1*) and downregulated (e.g. *TLR4*) (**Figure 2.3B&C**). There was no significant change in *SOCS1*, *SOCS3* and *STAT1* gene expression. *AXL* and *TYRO3* genes were not measured in this particular code set.

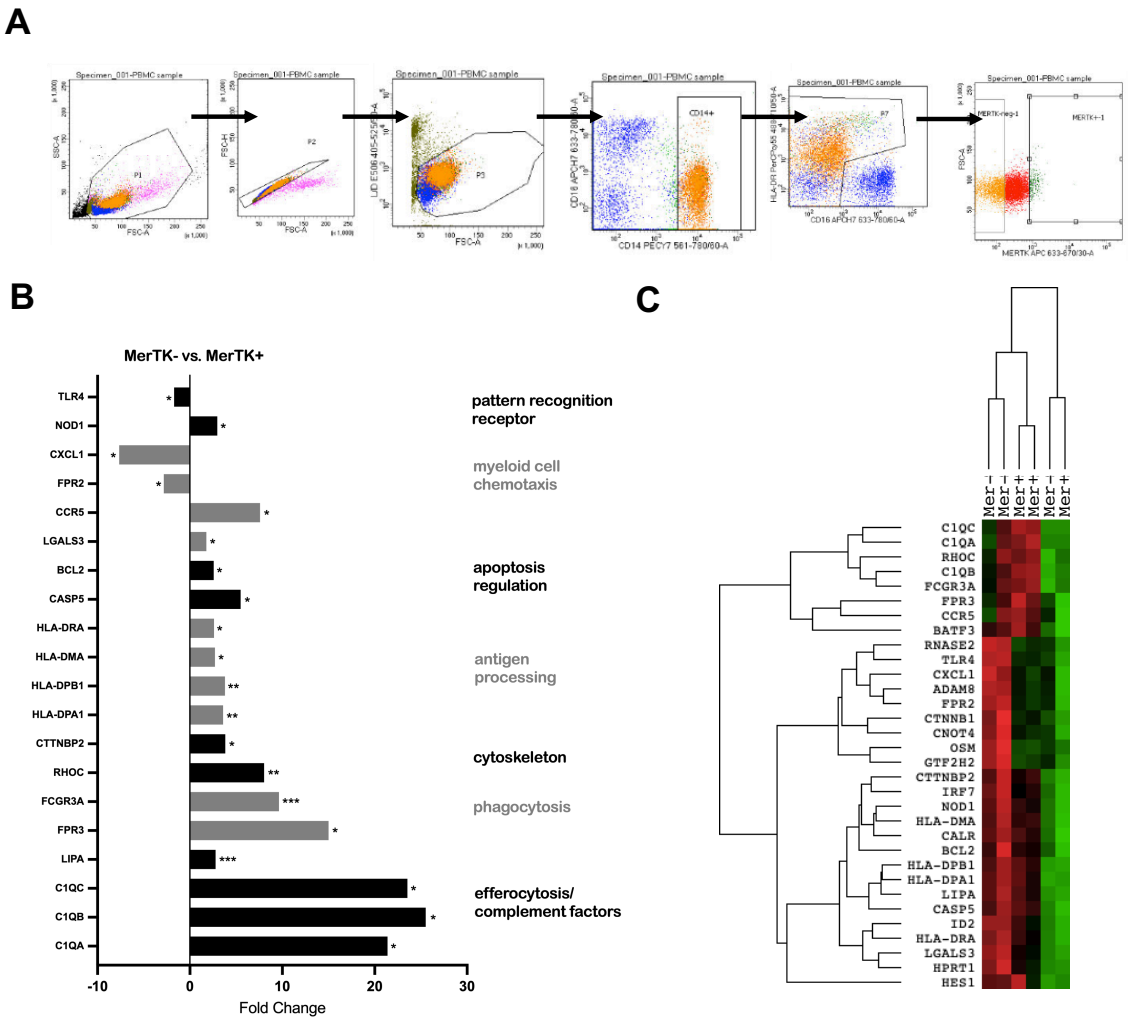


Figure 2.3 Gene expression profile of MerTK+ vs. MerTK- monocytes

(A) PBMCs from patients with decompensated alcohol-related liver cirrhosis (n=3) were FACS cell-sorted using the displayed gating strategy and separated according to MerTK+ and MerTK- using an FMO MerTK control. (B) Quantitative microarray gene expression (fold-change) of MerTK+ monocytes vs. MerTK- (baseline) and categorised according to function, measured by nCounter GX Human Immunology V2 kit (Nanostring Technologies, USA). (C) Gene expression by agglomerative hierarchical cluster (heatmap, z-score; green=min and red=max magnitude of expression). *p<0.05, **p<0.01, ***p<0.001.

2.3.4. Intracellular Cytokine Staining of Monocytes in ACLF

Gating of the flow cytometry plots was conducted as previously described (**Figure 2.1A**). LPS stimulation of monocytes resulted in an expected loss of CD14 receptor and therefore the appearance of two clouds in the FACS plots (Thaler *et al.*, 2016) (**Figure 2.4A**). Both clouds were included in the CD14+ gate since even monocytes that have lost CD14 may have produced cytokines. TNF-α and IL-6

production on LPS stimulation, as a percentage of CD14+ monocytes, declined markedly in patients with ACLF ($p<0.0001$) and in cirrhosis without organ failure ($p<0.05$) compared with healthy control (**Figure 2.4B**). Analysis of the production of TNF-α from subpopulations of CD14+ monocytes according to MerTK and Axl positive/negative status interestingly suggested that the greatest yield came from MerTK- Axl+ monocytes in healthy and cirrhosis groups but MerTK+ Axl+ in ACLF. This was only significant in the ACLF group, where there were significant differences between MerTK- Axl- and MerTK- Axl+ ($p<0.05$), and MerTK- Axl- and MerTK+ Axl+, populations ($p<0.01$) (**Figure 2.4C**). LPS-stimulated TNF-α and IL-6 production were not significantly different between Tyro3+ and Tyro3- monocytes when the results were pooled between disease groups ($n=4$, $p=0.88$; data not displayed).

Complicating the interpretation of these results was the observation that LPS-stimulation of monocytes resulted in reduction of MerTK% surface expression after 5 hours. To further investigate, a small group of samples was tested with PBS (negative control, $n=9$) and Pam_3CSK_4 (TLR2 agonist, $n=3$) to compare with LPS. There was a significant reduction in MerTK% with LPS compared with PBS (15.0 vs. 27.5%, $p<0.05$, Wilcoxon test) (**Figure 2.4D**).

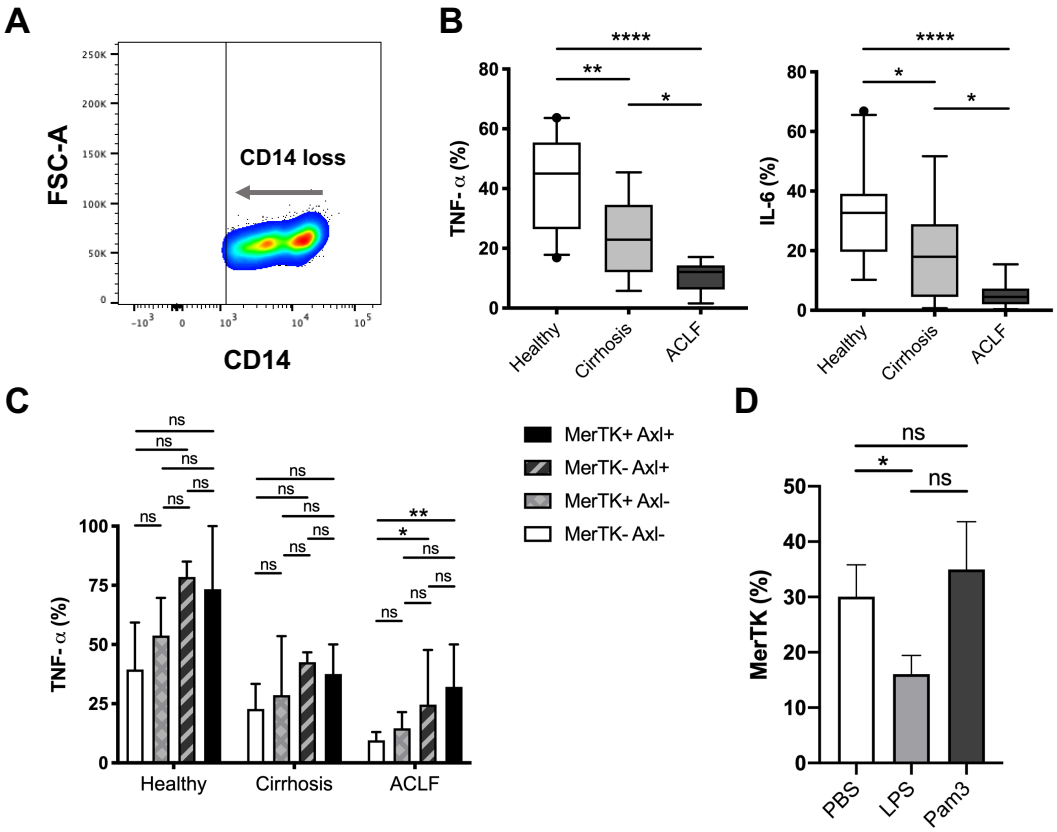


Figure 2.4 Intracellular Cytokine Production of Circulating Monocytes

PBMCs from three groups (healthy control, n=23; cirrhosis without organ failure, n=17; ACLF, n=17) were stimulated with 100ng/ml LPS for 5hrs. (A) Loss of CD14 receptor was seen on flow cytometry plots (B) TNF-α and IL-6 production (displayed as % of CD14+ cells) in healthy, cirrhotic and ACLF patients. (C) TNF-α production in these groups according to monocyte-expressing MerTK+/- Axl+/- combination. (D) Change in MerTK% monocyte surface expression with PBS, LPS and Pam_3CSK_4 after 5hrs. Statistical analysis was performed by non-parametric Kruskal-Wallis testing with Dunn's multiple comparison (B-C), or Wilcoxon test for paired non-parametric analysis. *p<0.05, **p<0.01.

2.3.5. Monocyte Phagocytosis: Cell-IQ® Live Cell Imaging

Using the Cell-IQ® live cell imaging and data processing system, phagocytosis of monocytes conditioned in healthy vs. ACLF plasma was visualised. Peak phagocytosis of *E. coli* BioParticles™ occurred at 1 hour 57 minutes (**Figure 2.5B**), at which point ACLF plasma-conditioned cells showed impaired particle uptake compared to healthy ($p<0.01$). By 15 hours, there was no difference in the cell fluorescence, though the number of living cells in healthy vs. ACLF was not compared at this time point.

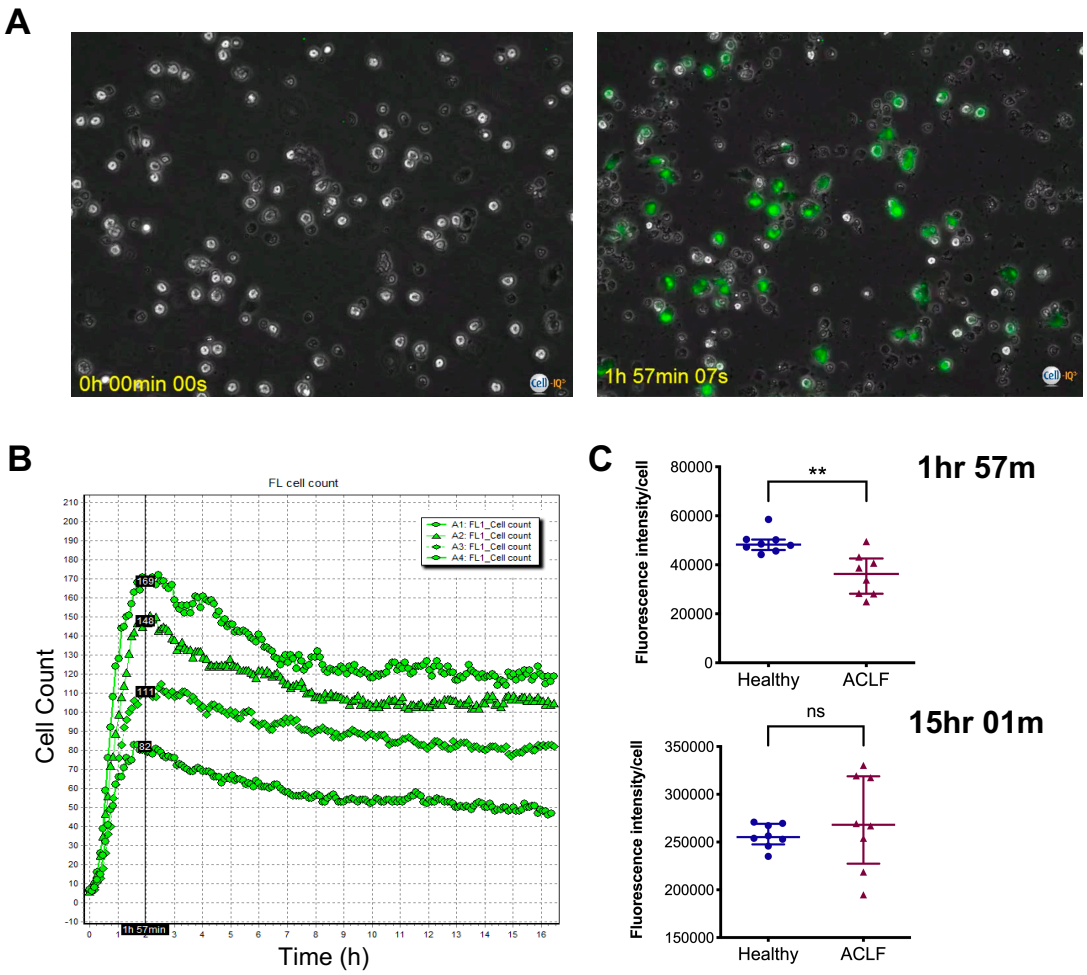


Figure 2.5 Live Cell Kinetic Imaging of *E. coli* BioParticle™ Monocyte Phagocytosis

Monocytes conditioned in 25% plasma of healthy control vs. ACLF (n=2) were exposed to green-fluorescent *E. coli* BioParticles™ and imaged using the Cell-IQ® integrated cell culture and analysis system with automated quantitative analysis of fluorescence images. (A) Difference in cell uptake of fluorescent particles at t=0 and t= 1hr 57mins (B) Peak fluorescence at 1hr 57mins (top two A1&2 – healthy control; bottom two A3&4 – ACLF) (C) Difference in fluorescence intensity per cell at 1hr 57m and 15hr 1m between monocytes conditioned in healthy and ACLF plasma. Graphs are expressed as median with interquartile range. Statistical analysis by Mann Whitney U. **p<0.01.

The Cell-IQ® efferocytosis experiment unfortunately did not work as planned, with no uptake of apoptotic neutrophils. Flow cytometry of neutrophils in a control well revealed >95% apoptosis using Annexin V FITC and CD66b PE monoclonal antibodies. Hence, this experiment requires repeating with further evaluation of the contributing factors.

2.3.6. Clinical Associations of TAM Receptors

Survival analysis of the dataset using Kaplan-Meier identified a significant difference in survival (log rank, p=0.01) between ACLF (mean survival 37 days) and cirrhosis without OF (203 days) (**Figure 2.6A**). Only MerTK% was significantly increased in patients who died within 90 days of admission ($p<0.05$) when compared with Axl (p=0.382) and Tyro3 (p=0.731) (**Figure 2.6B**). The correlation matrix did not identify any statistically significant correlation of TNF-α or IL-6 with any TAM receptor % monocyte expression. MerTK% did correlate with disease severity scores MELD and CLIF-AD ($p<0.05$). Axl% negatively correlated with serum sodium and creatinine ($p<0.01$) and Tyro3% negatively with INR (**Figure 2.6C**).

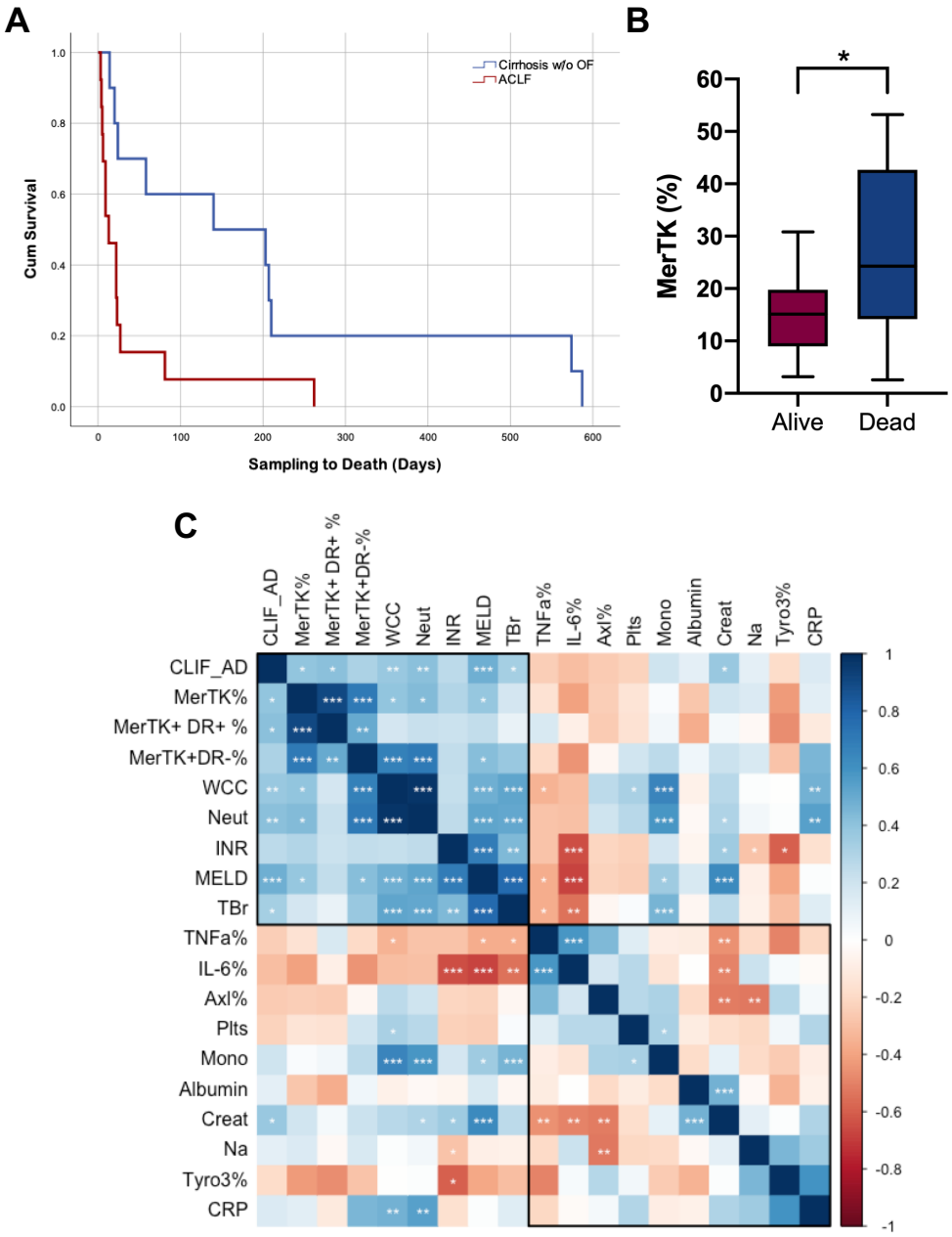


Figure 2.6 Clinical Outcomes and Correlations of Recruited Patients

(A) Kaplan-Meier survival curve comparing sampling to death (days) in patients with cirrhosis without organ failure and patients with ACLF. (B) Difference in MerTK% in patients who survived within 90 days of admission and those of died. (C) Correlogram with hierarchical clustering of clinical, biochemical and immunological readouts. Correlation with Spearman Rank test. Mann Whitney used for non-parametric differences between two groups. *p<0.05, **p<0.01, ***p<0.001.

2.4. Discussion

Key findings in this chapter included the confirmation of an expansion of MerTK+ monocytes in ACLF compared to healthy and cirrhosis without organ failure, validating the results obtained in the Bernsmeier *et al.* paper., and confirmation of a reduction HLA-DR. Both pro-resolution MerTK+ HLA-DR+ and immunosuppressive MerTK+ HLA-DR- subsets were expanded in ACLF as seen in ALF (Triantafyllou *et al.*, 2018a). Both are known to demonstrate impaired pro-inflammatory cytokine responses, but the former has enhanced efferocytic capabilities and peak at admission whereas the latter has poor efferocytic capacity and can persist at higher levels after admission. Liver tissue necrosis in ACLF may drive the expansion of MerTK+ HLA-DR+ subsets, which in ALF were seen to form ring-like structures around necrotic areas.

Refuting the hypothesis, Axl% monocyte expression was low (6%) and not significantly different between disease groups. Similarly, Tyro3 demonstrated variable and non-significant expression in ACLF. A recent study confirmed low Axl and Tyro3 monocyte expression in healthy volunteers (Barth *et al.*, 2018). That said, considering expression by MFI, all TAM receptors showed a significant increase in ACLF compared with healthy. Furthermore, whilst absolute numbers were low, the percentage frequency of MerTK+ Axl+ Tyro3+ (triple-expressing) monocytes was expanded in ACLF vs. healthy, supporting the hypothesis. Axl+ monocytes were MerTK^{high} HLA-DR^{high} CD16^{high} with significantly higher expression of monocyte chemotaxis marker CCR2 and lymph node homing marker CCR7. However, when combinations of the three TAM receptors were considered together rather than in isolation, no significant differences in CD16 and HLA-DR expression were found. This highlights their similarities and a tendency for co-expression in ACLF, but clearly the change in MerTK% had the greatest discriminant value in identifying ACLF. Zagórska *et al.* report that MerTK expression is inducted by tolerogenic stimuli whilst Axl expression is driven by inflammatory signals, such as poly I:C and LPS (TLR3 and TLR4 agonists respectively) (Zagórska *et al.*, 2014). The MerTK+ Axl- monocyte subset is expanded in ACLF and indicates an immunotolerant circulatory compartment.

Gene expression profiling demonstrated that MerTK+ monocytes have upregulated genes involved in efferocytosis (*C1Q*) and intracellular lipid regulation (*LIPA*), the latter crucial to cell

homeostasis since monocytes/macrophages accumulate substantial amounts of cholesterol after ingesting apoptotic cells (Liu *et al.*, 2006; Viaud *et al.*, 2018). C1q is a complement molecule that regulates a variety of cellular processes independent of complement activation including mediation of a multitude of immunoregulatory functions (Thielens *et al.*, 2017). Indeed, C1q is reported to elicit MerTK expression, limit pro-inflammatory immune responses and generate macrophage-DC like-hybrids (Galvan *et al.*, 2012; Ghebrehiwet, Hosszu & Peerschke, 2017). C1q deficiency and associated impaired clearance of apoptotic cells, is known to be a factor in the development of SLE, as was also seen in TAM receptor knockout mice (Lemke & Rothlin, 2008; Muñoz *et al.*, 2010). In a spectrum between autoimmunity and tolerance, the latter may be promoted by overexpression of *C1q* and MerTK, thus leading to increase susceptibility to infection. In keeping with the macrophage-DC hybrid theory, phagocytic receptors and antigen presentation genes were also upregulated, including genes for CD16 and HLA-DR respectively, in line with phenotypic data.

Of course, the transcriptomic profiling performed in this chapter was for advanced alcohol-related cirrhotic patients and not ACLF. This was due to insufficient cells available from ACLF patients. Further work should look to establish the gene profile MerTK+ vs. MerTK- monocytes in ACLF although the recent paper from Korf *et al.* comprehensively confirms an immunosuppressive transcriptomic profile in ACLF (Korf *et al.*, 2019).

Intracellular cytokine staining experiments confirmed dampened TNF-α and IL-6 production in ACLF, corroborating Bernsmeier *et al.* MerTK and Axl monoclonal antibodies were included in the extracellular stain to identify which subpopulations produced most cytokines. Results suggested that in ACLF, Axl+ cells produced most TNF-α, with a significant increase observed in MerTK+ Axl+ and MerTK- Axl+ monocytes compared with MerTK- Axl-. However, on reflection, interpretation of the TAM receptor subpopulation cytokine results is not straightforward. This is because the proportion of MerTK+ monocytes drastically lowers during the ICCS experiments. This reduction is due to a combination of cell fixation using the BD permeabilization/fixation solution (which was also seen in the immunophenotyping experiments), and exposure to LPS itself, which is known to promote cleavage of the extracellular domain of the MerTK transmembrane receptor, and increase in extracellular soluble

MerTK, via the metalloproteinase complex ADAM17 (Thorp *et al.*, 2011; Lee *et al.*, 2012b; Choi *et al.*, 2013). The latter is also known to mediate cleavage of membrane-bound Axl, resulting in increased extracellular soluble Axl concentrations, though LPS is also known to increase Axl mRNA expression (Zagórska *et al.*, 2014; Orme *et al.*, 2016). Consequently, since both MerTK and Axl expression may change during the ICCS experiment, determining the cytokine production of subpopulations is flawed. Correlation between membrane-bound TAM receptors and TNF-α/IL-6 was not significant. Future experiments to cell sort according TAM receptor positive or negative expression, LPS stimulation and subsequent measurement of cytokine concentration by ELISA may provide better clarification.

The existence of soluble MerTK and Axl complicates the picture more generally. Soluble MerTK has been detected in healthy human plasma and is therefore postulated to have a physiological role. Both soluble forms act antagonistically to their respective TAM receptors, as decoy receptors, sequestering their ligands, including Gas6, and thereby preventing its action on the membrane-bound receptors, and regulating Gas6-mediated apoptotic cell engulfment (Sather *et al.*, 2007). Whilst LPS was primarily used in these ICCS experiments, it is also unclear the impact of other TLR agonists on TAM receptor cleavage. Pam_3CSK_4 is a synthetic triacylated lipopeptide, TLR2/1 agonist, that mimics bacterial lipopeptide and activates NF-κB. However, it has been shown to promote monocyte-differentiation into immunosuppressive macrophages, though did not seem to impact on MerTK expression in our dataset (Bayik *et al.*, 2017). In advanced cirrhosis and ACLF, there is hypothesised to be pathological bacterial translocation, where there is low-grade persistence of LPS, bacterial DNA and other bacterial cellular components. Viral and fungal products may also circulate. These may differentially promote TAM membrane-bound receptor shedding and therefore influence the overall balance between inflammation and resolution. Further work should explore the effect of other TLR agonists of TAM receptor expression, function and shedding. Of particular interest would be an investigation into the effects of TLR9 agonists (e.g. unmethylated cytosine phosphate guanine [CpG] oligonucleotides), a surrogate for bacterial DNA.

Finally, the Cell-IQ® experiment rebutted the hypothesis that monocyte phagocytosis was enhanced in ACLF; bacterial uptake was diminished though efferocytosis requires testing. MerTK is not known to influence bacterial phagocytosis so further work is required to establish the contributory factors including co-staining for TAM receptors in repeat Cell-IQ® experiments (Zhang *et al.*, 2019).

2.5. Conclusion

Data presented here demonstrated that MerTK was the prominent, discriminatory and predictive TAM receptor in ACLF as compared to Axl and Tyro3. MerTK+ cells have increased expression of genes related to efferocytosis, phagocytosis, antigen presentation and cell motility, though bacterial phagocytosis in ACLF was shown to be impaired. Further work is needed to establish the role of Axl and Tyro3 monocyte expression in ACLF, and identify potential immunotherapeutic targets.

In summary, key findings from this chapter include:

- Patients with ACLF were found to have increased WCC, MELD score and 28- and 90-day mortality compared with AD, supporting existing literature.
- MerTK+ monocytes were expanded in ACLF compared with healthy controls and cirrhosis without organ failure, in association with reduced HLA-DR expression, validating previously published data.
- Baseline MerTK % was increased in non-survivors at 90 days with ACLF, and correlated with disease severity scores (e.g. MELD and CLIF-AD).
- Monocyte Axl % expression was low and Tyro3 % variable in ACLF.
- All TAM receptor expression by median fluorescence intensity was increased in monocytes in ACLF compared to healthy control, but only MerTK percentage was significantly elevated suggesting MerTK was most relevant or discriminatory.
- Transcriptomic profiling suggested an upregulation of efferocytosis and lipid metabolism genes (*C1q, LIPA, APOE*) in MerTK+ vs. MerTK- monocytes.

- LPS-stimulated TNF-α and IL-6 production was attenuated in ACLF compared to healthy control; the production of MerTK+ or Axl+ monocyte subpopulations could not be accurately determined by flow cytometry due to LPS-induced ADAM17-mediated cleavage of both receptors, and reduction of MerTK expression with BD™ fixation buffer.
- Monocytes conditioned in ACLF plasma had impaired phagocytosis of *E.* coli BioParticles™ at 2 hours (peak uptake) compared to healthy control, seen using cell kinetic imaging.
- With the knowledge of the biological role of MerTK in dampening innate immune cytokine responses to microbial challenge, the observation of increased MerTK monocyte expression in ACLF represents the most promising translational aspect of the data, with MerTK a potential immunotherapeutic target in altering the susceptibility to infection.
- Areas for future research should concentrate on:
    a) Gene expression profiling in ACLF monocytes, and the inter-relationship of *MERTK*, *C1q*, *LIPA* and *APOE* pathways
    b) Evaluating soluble Mer and Axl in ACLF
    c) The effect of TLR9 agonists (bacterial DNA analogues) on TAM receptor expression, shedding and function in view of pathological bacterial translocation described in cirrhosis.

CHAPTER 3

3. THE PERITONEAL COMPARTMENT IS AN IMMUNOTOLERANT ENVIRONMENT IN LIVER DISEASE CHARACTERISED BY MERTK^{HIGH} MACROPHAGES

3.1. Background and Aims

Patients with liver cirrhosis who decompensate with ascites, the pathological accumulation of fluid within the peritoneal compartment, have a markedly worse prognosis compared to patients with compensated cirrhosis (D'Amico, Garcia-Tsao & Pagliaro, 2006). These patients are at risk of developing bacterial infection of the ascitic fluid, named spontaneous bacterial peritonitis (SBP), which portends an even higher mortality (Caly & Strauss, 1993). Historically, low ascitic fluid protein was attributed to increased risk of infection but recent studies have cast doubt (Bruns *et al.*, 2015). There is a paucity of published data evaluating peritoneal immune cells in cirrhotic ascites and its contribution to susceptibility to infection. The most substantial study by Irvine *et al.* identified that peritoneal macrophages that highly expressed the complement receptor of the immunoglobulin superfamily (CRIg^{high}) had a high phagocytic capacity and anti-inflammatory activation signature compared with CRIg^{lo} populations (Irvine *et al.*, 2016). Reduction in CRIg^{high} populations was associated with increased liver disease severity. Fagan *et al.* suggested a higher ascites bacterial burden, measured by quantitative PCR and 16S rRNA gene sequencing, was associated with reduced peritoneal macrophage HLA-DR expression and poor clinical outcomes in patients with decompensated cirrhosis (Fagan *et al.*, 2015). Some investigators have evaluated the immune cell composition during SBP, including reduction phenotypic markers (CD16, HLA-DR, CD11b and CD206) on peritoneal macrophages and impaired oxidative burst of ascitic neutrophils due to bacterial-induced resistin in comparison to uninfected controls (Nieto *et al.*, 2015, 2018). Whilst useful in charting the dynamic evolution of the immune response to SBP, they do not fully explore the susceptibility to SBP and therefore miss immunotherapeutic potential. No studies explore the risk of SBP in patients with established ACLF.

Given the previously identified expansion of MerTK+ monocytes in the circulation of ACLF patients, and its association with impaired antimicrobial responses, it is logical to study the phenotype and function of peritoneal macrophages focusing on role of MerTK and the other TAM receptors, and the corresponding contribution of the ascitic microenvironment in decompensated cirrhosis and ACLF (Bernsmeier *et al.*, 2015).

Hypothesis and aims:

Accordingly, it was hypothesised that the MerTK+ macrophage subsets may be also expanded in the peritoneum, especially in ACLF, promoting an immunotolerant microenvironment by attenuating inflammatory responses to microbial challenge and thereby increasing the risk of SBP.

Hence, in this chapter, the aim was to:

- Determine the effect of ascites from patients with cirrhosis and ACLF on the immunophenotype of healthy cells conditioned *in vitro.*
- Explore the inflammatory cues within the ascitic microenvironment by measuring: concentrations of inflammatory cytokines, ligands facilitating TAM receptor-mediated efferocytosis; markers of cell death; the metabonomic profile; bacterial DNA quantification and species diversity.
- Assess the phenotypic, transcriptomic and functional profile of peritoneal macrophages from ascites, with particular regard to MerTK.

3.2. Material and Methods

3.2.1. Patient recruitment

Fifty-two patients (n=52) with ascites were recruited into the study across two sites, King's College Hospital (London, UK) and St. Mary's Hospital (London, UK), which included patients with decompensated cirrhosis without organ failure (n=43) and patients with acute-on-chronic liver failure (ACLF, n=9), as detailed in Table 3.1. Healthy control volunteers (HC, n=32 over study period) were recruited as a control group for experimental work. Some cirrhotic patients with ascites (n=5) were sampled more than once, on subsequent hospital episodes, in order to generate sufficient ascitic cells for experimental work. Details of the study ethics, inclusion and exclusion criteria are provided in 2.2.1. Most patients at King's College Hospital were co-recruited under the Gut-Liver-Axis (GLA) study (REC 12/LO/1417) in which there was a bidirectional material transfer agreement allowing biological samples to transfer between the two institutions as above. The GLA study had similar exclusion criteria and recruitment policies.

Patients with ovarian cancer and malignant ascites (n=7) provided a pathological control group for experimental work and samples (cell suspensions and acellular ascites) were kindly provided by the Imperial College Healthcare Tissue Bank (HTA Licence 12275, REC: 17/WA/0161) courtesy of Professor McNeish (McNeish Ovarian Tissue Sub-collection: ONC_IN_18_012) at the Hammersmith Hospital (London, UK), collected with local REC approval and patient consent (**Table 3.2**).

3.2.2. Clinical Data

Clinical data for all recruited patients was acquired as per section 2.2.2, with additional outcome data including incidence of subsequent SBP following sampling. In addition to blood tests, ascites WCC, total protein, albumin, and positive blood or fluid cultures were recorded. Stable cirrhotic patients were classed as those having interval abdominal paracentesis in an ambulatory day case unit, acute

decompensated those admitted to hospital with an episode of decompensated liver disease and ACLF, an acute decompensation with organ failure as per EASL CLIF definitions (1.2.4). One ACLF patient recruited was subsequently identified as having concurrent spontaneous bacterial peritonitis (SBP), defined as > 250/mm^3 PMNs or > 500/mm^3 white cells in ascites; this case was excluded from the whole clinical cohort summary characteristics (Table 3.1) and is considered separately from the experimental data obtained.

3.2.3. Biological Sample Acquisition

Ascites was obtained from drainage bags of all patients soon after therapeutic abdominal paracentesis. This procedure was performed, when clinically indicated, for the relief of abdominal distention in patients with moderate to large volume ascites. In short, patients were consented for the procedure by a member of the clinical team. The presence of ascites, and ideal anatomical position, was confirmed by clinical examination and bedside ultrasound with the patient lying supine or semi-recumbent. Skin was sterilised using a solution of 2% chlorhexidine gluconate and 70% isopropyl-alcohol (ChloraPrep^{TM}, BD, USA). Local anaesthetic (1-2% lidocaine chloride) was infiltrated into the skin, subcutaneous tissues and parietal peritoneum. A 20ml sample of ascites was aspirated using a syringe and 21G needle to confirm position and for NHS laboratory diagnostic analysis. Subsequently, a small scapel incision was made to the skin and a Bonanno^{TM} catheter (BD, USA) inserted, with removal of the metal trocar such that a pigtail plastic catheter tube remained in the peritoneal cavity. The other end of the catheter was attached to a 2L collection bag with drainage of peritoneal fluid by gravity. Ascites sample processing is described in section 3.2.6 and 3.2.7. Patients routinely received 20% human albumin solution intravenously during the paracentesis to reduce the risk of post-paracentesis circulatory dysfunction. Some patients also received prior to the procedure, on a case-by-case basis, intravenous fresh frozen plasma (FFP) or vitamin K, in light of an elevated international normalised ratio (INR) result (usually >1.5) which was traditionally regarded as representative of an increased bleeding risk.

In some patients with ascites, concurrent whole blood sampling was performed by peripheral vein venepuncture, or in patients on the intensive care unit, by sampling from arterial or central venous access devices using sterile technique.

Patients' blood or ascitic clinical haematological parameters were determined using automated analysers at King's College Hospital (Siemens Advia 2120, Berks, UK) and St. Mary's Hospital (Sysmex XE-2100, Japan).

3.2.4. Acquisition and Storage of Plasma

Whole blood obtained in lithium heparin Vacutainer^{TM} (BD, USA) was centrifuged at 400*g* for 10 minutes. The acellular plasma supernatant was aspirated, aliquoted to labelled 2ml eppendorfs and snap frozen in a -80°C freezer.

3.2.5. Isolation of peripheral blood mononuclear cells, healthy neutrophils and CD14+ monocytes

After removal of plasma, whole blood in lithium heparin tubes was diluted in Phosphate-Buffered Saline (PBS) and combined into one 50ml Falcon tube. PBMCs were isolated using Ficoll-Paque Plus (GE Healthcare, UK) and washed in PBS (Life Technologies, UK) as per previous protocol (2.2.3). Cell viability was > 95% determined by trypan blue staining. Where required, healthy neutrophils (2.2.5) and CD14+ monocytes (2.2.4) were obtained as per previously described methods.

3.2.6. *Ex-vivo* isolation and storage of ascitic cells

After therapeutic paracentesis, a volume of ascites (500-2000ml) in a clamped drainage bag was taken, split between multiple 50ml Falcon tubes under a tissue culture hood and centrifuged at 425*g* for 10 minutes. The ascitic supernatant was discarded, 1ml sterile PBS added to the pellet in each tube, resuspended and combined into one 50ml Falcon tube. This was topped up with PBS and centrifuged again leaving a cell pellet. Five ml of red cell ACK lysis buffer (Life Technologies, UK) was added to

1ml of cell suspension in, left for 5 minutes and washed with PBS, resulting in a cell pellet without red cells. Cell counting was performed using trypan blue and a C-Chip haemocytometer (NanoEnTek, China). Ascitic cells were then allocated for *ex-vivo* assays (phenotyping or Phagoburst) and any excess frozen at -80°C in cryovials using pre-prepared freezing media (10% DMSO 90% FBS), with a maximum of 10^6 cells/ml per cryovial. A polycarbonate freezing container (Thermo Scientific, UK) was used to provide graduated cooling at -1°C/min.

3.2.7. Storage of ascites for cytokine and metabolite analysis and pellet for bacterial DNA analysis

One 50ml Falcon tube containing ascites was centrifuged at 10000*g* for 10 minutes. The supernatant was removed using a Pasteur pipette, aliquoted to microcentrifuge tubes and frozen immediately at -80°C for future use with *in vitro* culture experiments and cytokine analysis. Any excess ascites supernatant was discarded leaving behind a pellet to which was added 500µl of sterile PBS. This was resuspended, aliquoted to a 600µl Eppendorf tube and frozen immediately at -80°C for storage for subsequent total DNA and 16S bacterial DNA quantification, and 16S sequencing.

3.2.8. Flow cytometry of immune cells for immunophenotyping

For identification of monocytes and macrophages, human PBMCs and ascitic cells (ACs) were incubated with a monoclonal antibody mixture in which the common backbone used for all samples consisted of mouse anti-human CD14 PE-Cy7, CD16 APC-H7 (BD Biosciences, UK), HLA-DR PerCP Cy5.5 (eBioscience, UK) and MerTK APC (R&D Systems, UK). Additionally, combinations of other monoclonal antibodies were used in compatible panels including: CD163 PE, CD11b PE, CCR2 Alexa Fluor (AF)-647, CCR5 FITC, CCR7 FITC, PD-1 FITC (BD Biosciences, UK); Axl AF488, Tyro3 PE (R&D Systems, UK); CX_3CR1 PE (eBiosciences, UK); CD206 Brilliant Violet (BV)-421 and CD64 BV421 (BioLegend, UK). Other compatible antibody combinations were used; a full list of all monoclonal antibodies used is listed in Appendix C. Antibody mixtures were added to a set concentration of cells in a flow cytometry staining buffer, typically containing PBS and 1%

heat-inactivated fetal bovine serum (FBS), for 30 minutes in the dark at 4°C, washed, re-suspended and then analysed by flow cytometry for surface marker expression. Fluorescence minus one (FMO) controls were routinely performed for HLA-DR and the TAM receptors (Tyro3, Axl and MerTK). The FACS Canto II (BD Biosciences, UK) was used for analysis at King's College Hospital and FACS Fortessa (BD Biosciences, UK) at St. Mary's Hospital.

For *ex-vivo* phenotypic analysis, ascitic cells were isolated as per 3.2.6 and a proportion stained immediately. If matched whole blood was taken, this was also phenotyped straight away, following pre-treatment with Cal-Lyse red cell lysis buffer (Thermo Fisher, UK).

Since ovarian cancer ascites single cell suspensions were only available frozen, phenotyping these cells and their comparator cirrhotic ascitic cells, was conducted after thawing the cell suspension for 1 minute in a 37°C water bath and washing twice in Roswell Park Memorial Institute (RPMI) media. A fixed viability dye conjugated to the eFluor506 fluorochrome (Life Technologies, UK) was used whenever a freeze/thaw cycle was involved. (Appendix D for flow cytometry panel).

3.2.9. Multicolour flow cytometry panel design, compensation and analysis

Anti-human monoclonal antibodies were selected based on their compatibility with the flow cytometer and optical setup, brightness corresponding to target antigen expression, and cost. Multicolour antibody panels were designed to minimize spectral overlap between fluorochromes. Each antibody was titrated using peritoneal mononuclear cells and calculation of the flow cytometry stain index to optimize the antibody concentration (Johansson *et al.*, 2014). The FACS instruments were calibrated weekly using cytometer, setup and tracking (CS&T) beads kit in conjunction with the BD FACS Diva^{TM} software (BD Biosciences, UK). Experimental controls included corresponding isotype monoclonal antibody (ISO) controls to setup the cytometer for the cell population. Every sample included an FMO for the TAM receptors, when included in the panel, for improved identification of positive populations. Compensation for fluorochrome spectral overlap involved the use of compensation beads, either

OneComp (FACS Canto II) or UltraComp (FACS Fortessa) eBeads (ThermoFisher Scientific, UK). In short, one drop of the compensation bead solution was added to 100µl of flow cytometry staining buffer (Life Technologies, UK) in a polystyrene tube for each of the fluorochromes used in the phenotyping experiment, with subsequent addition of the volume of antibody used in the phenotyping panel. This was vortexed, left at 4°C for 30 minutes protected from light, washed and resuspended in 200µl flow cytometry buffer ready for acquisition. For compensation for fixed viability dyes (FVD), an amine reactive compensation (ArC^{TM}) bead kit (ThermoFisher Scientific, UK) was used. Here, one drop of the ArC beads reagent A was left in a 5ml polystyrene tube at room temperature (RT) for 5 minutes after which 1µl of the FVD was added, vortexed and left light-protected for 30 minutes at RT. This was then washed twice in 3mls of PBS and resuspended in 500µl of reagent B. After acquisition of each of the fluorochrome-labelled compensation beads, the FACS Diva software (BD Biosciences, UK) automatically generated and applied a compensation matrix to the acquired data. Flow cytometric data analysis was conducted using FlowJo v10.4.2 software (FlowJo LLC, USA). Gating was conducted using a validated HLA-DR gating strategy to select macrophages from the peritoneal mononuclear cells (Abeles *et al.*, 2012). Macrophage surface receptor expression was displayed as percentage (%) or MFI. Statistical and graphical analysis was performed using GraphPad Prism v6.0-8.0 (GraphPad Software Inc, USA).

3.2.10. Monocyte-derived macrophage *in vitro* culture: M0 Protocol

Monocyte-derived macrophages were generated as a comparator group to peritoneal macrophages by culture *in vitro* of healthy monocytes using a 7-day protocol kindly supplied by Dr Alaistair O'Brien (UCL, UK) (O'Brien *et al.*, 2014). The macrophages obtained from this protocol are not exposed to strong polarising signals and are deemed "M0" macrophages. On day 1, 100mls of whole blood from a healthy donor was collected in EDTA vacutainer collection tubes, and divided between 50ml Falcon tubes. RosettaSep (StemCell Technologies, UK), a monocyte enrichment cocktail, was added to each tube and left on an orbital shaker for 20 minutes. After this time, the volume of each Falcon tube was made up to 50ml with media containing PBS, 2% FBS and 1mM EDTA. This was then layered on to

15mls Ficoll (GE Healthcare, UK) and centrifuged at 1000*g* for 30 minutes without brake for density gradient separation of monocyte-enriched mononuclear cells. The buffy coat was collected and washed in Hank's Balanced Salt Solution (HBSS, Life Technologies, UK). ACK lysing buffer was used to remove red cells from the cell pellet and washed. The cell pellet in HBSS was passed through a 35µm cell strainer, washed and resuspended in culture media containing X-Vivo 15 (Lonzo, UK), 10% human AB serum (Sigma Aldrich, UK), 1% penicillin/streptomycin and 1% (200mM) L-glutamine. Cells were added to a 6-well polystyrene plate (Corning, UK) with 4 million cells in 3ml media per well. Media was aspirated and replaced after one hour to remove cells that had not adhered to the plate, followed by the addition of M-CSF to each well at a concentration of 20ng/ml per well. On day 4, wells were examined under the microscope to verify growth and absence of infection; media was then replaced and further supplemented with 20ng/ml M-CSF. This was repeated on day 6. Finally, on day 7, media was aspirated completely from each well. To detach macrophages from the well base, 1ml of separation buffer containing PBS, 10mM EDTA (Sigma Aldrich, UK) and 4mg/ml lidocaine hydrochloride (Sigma Aldrich, UK) was added and left at room temperature for 20 minutes. A cell scraper (Fisher Brand, UK) was then used to gently mechanically detach macrophages. Wells were examined under the microscope to ensure adequate detachment and the separation process repeated if required. Phenotyping was then performed as described in section 3.2.8.

3.2.11. Monocyte-derived Macrophage *in vitro* culture: M1/M2 Protocol

Prior to acquisition of the M0 protocol, another monocyte-derived macrophage protocol was used in which polarising cytokines were used to generate both M1 and M2 macrophages *in vitro*. Here, on day 0, monocytes were obtained from healthy PBMCs by CD14+ magnetic bead isolation as per 2.2.4. CD14+ cells were plated in complete media (RPMI, 10% FBS, 1% penicillin/streptomycin, 1% L-glutamine) in a 24-well plate at 500,000 cells/well in 500µl volume. For M1 differentiation, to each assigned well was added complementary media consisting of 490µl complete media and 10µl of 5µg/ml stock premium GM-CSF (Miltenyi Biotec, UK), yielding a final concentration of 50ng/ml. For M2 differentiation, 490µl complete media and 10µl of 10µg/ml stock M-CSF (Miltenyi Biotec, UK),

yielding a final concentration of 100ng/ml, was added. The plate was left in an incubator at 37°C (5% CO_2). On day 2, 500µl media was aspirated from each well and replaced with fresh media containing GM-CSF for M1 and M-CSF for M2 as described. On day 5, again 500µl of media was aspirated from each well. However, this time for M1 differentiation, this was replaced in each well by 489µl media, 10µl GM-CSF, 1µl of 1mg/ml LPS (final concentration 1µg/ml, Sigma Aldrich, UK) and 0.3µl of 100µg/ml stock interferon-γ1b (final concentration 30ng/ml, premium grade, Miltenyi Biotec, UK). For M2 differentiation, the aspirated media was replaced by fresh 490µl media, 10µl M-CSF and 0.5µl of stock 100µg/ml stock IL-10 (final concentration 50ng/ml, research grade, Miltenyi Biotec, UK). On day 7, cells were collected by washing each well with ice-cold PBS, adding 1ml 2mM EDTA /PBS to each well and leaving in the incubator for 15 minutes, and finally pipette aspirating. This method of macrophage detachment achieved greatest yield for this particular protocol. Cells were resuspended in complete media and counted, ready for subsequent use in functional assays.

3.2.12. *In vitro* culture of healthy peripheral blood mononuclear cells in ascites or plasma

To determine the effect of ascites on the phenotype of monocytes, PBMCs were obtained from healthy donors (n=3) as per the method described in 3.2.5. Red cells were lysed by adding 5ml of ACK Lysing Buffer (ThermoFisher, UK) to the cell pellet, resuspended in 1ml PBS for 5 minutes and followed by centrifugation 300*g* for 10 minutes. Cell count was determined using a C-Chip disposable haemocytometer (NanoEnTek, China) and 500,000 PBMCs were added per well of a 24-well plate (Corning, USA) in complete media to a total volume of 250µl. To this was added 250µl of sterile ascites per well (50% of total volume) obtained from patients undergoing abdominal paracentesis with cirrhosis without organ dysfunction (n=13) and patients with cirrhosis and organ dysfunction (acute-on-chronic liver failure, ACLF) (n=7) recruited from King's College and St. Mary's Hospitals. Controls included ovarian cancer ascites (n=7) obtained from patients at Hammersmith Hospital as pathological control, healthy control plasma (n=9) and complete media only (n=4). These cells were cultured for 48 hours in an incubator set at 37°C 5% CO_2 (per protocol Wu *et al.*, 2017; the authors established 50% ascites and 48-hour culture as optimum conditions for generation of MDSCs). After this time, cells were collected

from 24-well plates by washing with cold PBS, and subsequently stained for antibodies for phenotypic analysis (CD14, HLA-DR and MerTK expression by % and MFI; M-MDSC frequency as % of CD33+ cells). M-MDSCs were identified as CD33+ CD11b+ CD15- CD14+ HLA-DR- cells, using fluorescence minus one (FMOs) to set the gates (Bronte *et al.*, 2016). A total of three independent experiments were performed, each with a different healthy donor; the latter experiment also evaluated the surface expression on CD14+ cells of TAM receptor Axl, Fc-gamma receptor CD16 and M2 marker CD163 when exposed to culture-negative ascites (n=4), SBP ascites (n=1), ovarian cancer ascites (n=1) and healthy plasma (n=3).

3.2.13. *In vitro* culture of healthy PBMCs in cytokines

To investigate the effect of inflammatory cytokines on phenotype, healthy control PBMCs were cultured for 48 hours at 37°C (5% CO_2) in complete media supplemented with the following: a) premium-grade GM-CSF (Miltenyi Biotec, UK) 10 ng/ml; b) GM-CSF 10 ng/ml plus IL-6 10 ng/ml (Peprotech, US) as per protocol by Lechner *et al.*; and c) interferon gamma (IFN-γ) 10ng/ml (Miltenyi Biotec, UK); d) IL-4 20ng/ml (Peprotech, US); e) premium grade IL-10 50ng/ml (Miltenyi Biotec, UK); f) IL-17 100ng/ml (Peprotech, US) as per protocol by Zizzo *et al.* (Lechner, Liebertz & Epstein, 2010; Zizzo & Cohen, 2013). Complete media alone, without additional cytokines, acted as a control. Surface monocyte expression of HLA-DR, MerTK, Axl and CD163 were assessed by flow cytometry.

3.2.14. FACS sorting of cells

Enough cryovials to obtain 20-30 million ascitic cells were thawed in a 37°C water bath. Preparation for FACS sorting was conducted as per 2.2.8, including CD3 exclusion by magnetic bead separation.

3.2.15. Gene expression analysis

In the first experiment, the transcriptomic profile of FACS-sorted (MerTK+ and MerTK- separation, as per section 3.2.14) ACs and matched PBMCs (n=3, ALD cirrhosis) was analysed as per the method described in 2.2.9. Absolute numbers of MerTK+ and MerTK- cells are listed in Appendix E.

In the second experiment, after FACS sorting of ACs (n=3) for MerTK+ and MerTK- subsets, an identical number of cells were plated on to wells of a 24- or 48-well culture plate and exposed to 100 ng/ml LPS or PBS to investigate the effect of TLR4 agonism on AC gene expression. As a comparator, healthy monocyte-derived macrophages (MDMs, n=3), obtained and stored as per 3.2.10, were also FACS sorted and exposed to LPS vs. PBS.

3.2.16. Measurement of inflammatory mediator and cytokine concentrations

Enzyme-linked immunosorbent assays (ELISAs) were used to measure IL-6 concentration (pg/ml) (Thermo Fisher Scientific, UK) in ascites, with a 10-20x dilution required to bring the concentration into the assay detection range (0-500pg/ml), and AC culture supernatants following 6h LPS (100 ng/ml) stimulation (Sigma-Aldrich, UK). Similarly, a human TNF-α enzyme-amplified sensitivity immunoassay (EASIA) (Thermo Fisher Scientific, UK) was performed to assess TNF-α concentrations in ascitic cell and PBMC culture supernatants after LPS exposure, with a 4-10x dilution to bring the concentration into the detection range (0-1500pg/ml). Finally, an MSD® Human Proinflammatory 10-plex cytokine multi-spot assay (Meso Scale Discovery, USA) was additionally used to assess concentrations of IFN-γ, IL-1β, IL-2, IL-4, IL-6, IL-8, IL-10, IL-12p70, IL-13 and TNF-α (pg/ml) in ascites and cell culture supernatants. All experiments were performed in duplicates and according to the manufacturer's instructions. ELISA microplates were read at 450nm using a Multiskan Go plate reader (Thermo Scientific, USA) and SkanIt software (Thermo Fisher, USA). MSD® plates were analysed using the Sector Imager 2400 (Gaithersburg, MD). For IL-6 ELISAs, standard curves were plotted using a 4-parameter logarithmic (4-PL) scale on GraphPad Prism 7.0 software (GraphPad Software, La Jolla California, USA) as per manufacturer's recommendations. For the TNF-α EASIA,

a linear regression standard curve was formulated as recommended, with interpolation of absorbance values to obtain TNF-α concentration.

3.2.17. Measurement of Cytokeratin 18 Products

Human ELISAs for cytokeratin 18 products M30, marker of apoptosis, and M65, marker of cell death, were performed on ascites and matched plasma (Bioaxxess, UK). After absorbance reading at 450nm, standards were fit with a third order polynomial (cubic) curve with interpolation of values.

3.2.18. Measurement of Gas6 and Galectin-3 Concentrations

ELISAs were used to measure ascites and matched plasma concentrations of TAM receptor ligands Growth arrest-specific 6 (Gas6) protein (Elabscience, USA) and Galectin-3 (R&D Systems, UK), with healthy plasma as a control. All experiments were performed in duplicates and according to the manufacturer's instructions. As recommended, ELISA plates were read at 450nm with subtraction from 540nm as a wavelength correction and standard curves were analysed using a log/log 4-PL sigmoidal curve fit on GraphPad Prism 7.0 software.

3.2.19. Differentiation of THP-1 Monocytes to Macrophages

To investigate the effect of ascites on macrophages, THP-1 monocytes from an acute monocytic leukaemic cell line (ATCC, UK) were differentiated using a protocol as described by Starr *et al.* (2018). THP-1 monocytes were cultured over several days in upright T75 flasks (Corning, UK) in media (10% FCS 90% RPMI) at 37°C 5% CO_2. Subculture was undertaken when cell density was greater than $8x10^5$ cells/ml, by removing half the volume and replacing with fresh pre-warmed media. Subsequently, THP-1 monocytes were seeded into wells of a 24-well plate at a density of 500,000 cells per well in 500µl of medium (90% RPMI 10% FBS). Phorbol 12-myristate13-acetate (PMA) at a concentration of 100ng/ml was added to the wells and left for 72 hours at 37°C 5% CO_2. Control wells with no PMA added were included. After incubation, media was aspirated and cells washed with PBS. To detach the

cells, 5mM EDTA / PBS was added for 2 minutes in an incubator at 37°C 5% CO_2 followed by gentle mechanical detachment using a disposable cell scraper (FisherBrand, UK).

To identify the effect of ascites on the phenotype of THP-1 macrophages, media was aspirated after 72 hours and replaced with 50% ascites from patients with cirrhosis without organ failure (n=2) and from patients with ACLF (n=2) with controls as media only and THP-1 monocytes (not exposed to PMA). This was left for 24 hours and cells were then detached as above. Phenotyping was performed as previously described with surface marker expression assessed by flow cytometry (see Appendix F for panel).

3.2.20. Peritoneal Macrophage Efferocytosis of Apoptotic Neutrophils

To assess the capacity of peritoneal macrophages in the ascites of patients with cirrhosis to phagocytose apoptotic cells (efferocytosis), an assay was performed using apoptotic neutrophils and thawed ascitic mononuclear cells with subsequent analysis by flow cytometry (Zizzo *et al.*, 2012). Healthy neutrophils were obtained as per 2.2.5, and after cell counting, neutrophils were washed to obtain a pellet. To track neutrophils, the pellet was resuspended in 2ml 5μM Cell Tracker Violet BMQC (Thermo Fisher Scientific, USA) and pre-warmed in an incubator at 37°C 5% CO_2. The mixture was left at 37°C 5% CO_2 for 30 minutes, washed in PBS and the pellet resuspended in complete media. The BMQC fluorescent dye has an excitation/emission maximum of 415/516nm respectively with the violet laser of the flow cytometer and is retained in the cell for > 72 hours with low cytotoxicity. The BMQC-stained neutrophil solution was aliquoted to wells of a 24-well plate at a concentration of one million neutrophils per millilitre per well. Neutrophils were left for 20 hours at 37°C 5% CO_2 to render the majority apoptotic. The degree of apoptosis was verified for every assay performed by staining neutrophils from a designated well with CD66b PE-Cy7 (BioLegend, UK) and Annexin V FITC (BioLegend, UK) with flow cytometric analysis (apoptotic neutrophils were CD66b+ BMQC+ Annexin V+).

One hour prior to the end of the 20-hour incubation, ACs were thawed using a water bath, washed twice with RPMI, counted, resuspended in complete media and left in an incubator at 37°C to rest. Neutrophils in the 24-well plate were retrieved by pipette, combined into a single 15ml Falcon tube, washed with PBS and resuspended in complete media at 1 million cells/ml. In a new 24-well plate, ACs and neutrophils were then co-cultured in a 1:2 ratio, with total well volume of 1ml, for four hours in an incubator. Extra wells were prepared for FMO controls. After four hours, well contents were washed in ice cold PBS, transferred to polystyrene tubes, centrifuged and then stained with fixable viability dye eFluor780 (Life Technologies, UK) at 4°C for 30 minutes. After washing with staining buffer, cells were then stained with CD14 PE-Cy7 (BD Biosciences, UK), CD16 BV785 (BioLegend, UK), HLA-DR PerCP Cy5.5 (Life Technologies, UK), MerTK APC and Axl Alexa Fluor 488 (R&D Systems, UK) for 30 minutes, washed and acquired on the flow cytometer (Appendix H). Healthy PBMCs were used as a comparator cohort for ACs. Optimisation experiments are included in Appendix H; it was decided not to use CD66b magnetic bead selection since this spuriously enhanced efferocytosis in the assay, and purity by flow cytometric analysis of the unselected population was >70%.

3.2.21. pHrodo™ Phagocytosis Assay for Peritoneal Macrophages

In order to assess the capacity of ACs to phagocytose bacteria, the pHrodo™ BioParticles Phagocytosis assay (Life Technologies, UK) for flow cytometry was used, though modified from the whole blood protocol suggested by the manufacturer. The BioParticles™ are inactivated unopsonized *E. coli* fluorogenic particles, which increase their fluorescence as their surrounding environment becomes more acidic, as is the case when they are ingested into a phagosome, with peak fluorescence at pH 4. The pHrodo™ Green BioParticles™ were used for the assay to determine peritoneal macrophage phagocytic capacity, excited by 488nm argon-ion laser and with an emission maximum of 533nm (FITC channel). To prepare the BioParticles™ solution, lyophilised particles were mixed with 2.2ml of Buffer B (provided in the kit), vortexed and sonicated using a water-bath sonicator.

For each sample, polystyrene tubes were labelled for: 1) negative control (PBS only; no particles) 2) *E. coli* BioParticles™ positive 3) FMO controls for HLA-DR, MerTK and Axl for each of BioParticles™ negative and positive. Conditions for each tube for the assay included a total volume of 250µl containing 500,000 ACs and 10% AB serum (Sigma Aldrich, UK) to provide relatively constant quantity of opsonins to facilitate phagocytosis. After thawing ACs from frozen in the water bath, cells were washed in pre-warmed RPMI and the cell pellet resuspended in 1ml to count and establish the volume required for 500,000 ACs. Further RPMI and the AB serum were added to make up the conditions aforementioned. To the negative tubes was added 10µl PBS and to the positive tubes, 10µl of pre-cooled *E. coli* BioParticles™ (40µg/ml concentration). Tubes were vortexed, and incubated at 37°C 5% CO_2 for 60 minutes. Tubes were subsequently placed on ice for 2-3 minutes to stop the reaction, washed with staining buffer and stained with Zombie Violet fixable viability dye (BioLegend, UK) at room temperature for 20 minutes. After washing again in staining buffer, cells were stained with an antibody mixture including CD14 PE-Cy7, CD16 APC-H7, HLA-DR V500 (BD Biosciences, UK), MerTK APC and Axl PerCP (R&D Systems, UK) (see Appendix I for panel), at 4°C for 20 minutes in the dark. Cells were subsequently washed in staining buffer and acquired on the flow cytometer. Compensation beads (Life Technologies, UK) to account for fluorochrome spectral overlap and Amine Reactive Compensation Beads (Life Technologies, UK) for the fixed viability dye were used in flow cytometric experimental calibration. Healthy control thawed PBMCs, and thawed M1 & M2 *in vitro* monocyte-derived macrophages, obtained as per 3.2.5 and 3.2.11 respectively, were used as comparators to peritoneal macrophages / ACs from patients with cirrhosis.

In an initial set of limited experiments at King's College Hospital, optimal conditions for peritoneal macrophage phagocytosis were determined by evaluating variables such as BioParticle™ concentration, incubation time and whether autologous ascites, autologous serum or donor AB serum, in comparison to whole blood, influenced phagocytosis. Here, the aforementioned protocol varied: *E. coli* Red BioParticles™ were used; no fixable viability dye was used since the assay was performed on *ex-vivo* ACs; the antibody panel was different – CD14 APC-H7, CD16 PerCP Cy5.5 (BD Biosciences,

UK), HLA-DR APC (Life Technologies, UK) – but otherwise the protocol remained the same with 250µl total volume and 500,000 cells.

For flow cytometric analysis, after identification of the macrophage population using the validated HLA-DR gating strategy (**Figure 3.4A**), the negative control sample was used to set the gate and applied to the positive sample to identify the percentage change in phagocytosis with the addition of BioParticles™ in the particular sample and BioParticle™ MFI of the total macrophage population. FMOs were used as controls for the various surface markers, e.g. MerTK and Axl, in both the presence and absence of BioParticles™.

3.2.22. Modified *Ex-vivo* Phagoburst™ Oxidative Burst Assay for Ascitic Cells

To quantitatively determine the oxidative burst activity of ascitic leucocytes, the Phagoburst™ assay (Glycotope Biotechnology, Germany) was performed on freshly isolated ACs (as per 3.2.6), modified from the whole blood protocol provided by the manufacturer. Briefly, this assay involved exposing ACs to unlabelled opsonised *E. coli* bacteria followed by the addition of fluorogenic substrate, dihydrorhodamine (DHR) 123, which is oxidised to rhodamine (R123) in the presence of reactive oxygen species (ROS), e.g. superoxide anions or hydrogen peroxide, and emits on the green (FITC) fluorescence channel when excited by 488nm laser, with subsequent flow cytometric analysis. A sample without stimulus served as negative background control. Specifically, *ex-vivo* ACs were resuspended in 1ml of pre-warmed RPMI and counted using a C-Chip haemocytometer. To each of two 5ml polystyrene tubes was added a volume of cell suspension corresponding to 500,000 cells, sterile filtered 10% human AB serum (Sigma Aldrich, UK) to provide additional opsonins for phagocytosis, and supplemental RPMI to achieve a final volume of 100µl. One tube was labelled "rest" (as control, with no stimulant) and the other "burst". Both tubes were pre-cooled on ice for 10 minutes. Afterwards, 20µl burst wash buffer was added to the "rest" tube and 20µl *E. coli* to the "burst" tube in quick succession. The tubes were then placed in an incubator at 37°C for 20 minutes. After exactly this time, 20µl DHR123 was added to each tube and returned to the incubator precisely for a further 15 minutes. Then,

1ml of Phagoburst™ lyse buffer was added (which effectively stopped the reaction) to each tube and left at room temperature in the dark for 10 minutes. The cells were washed with 2ml wash buffer, centrifuged and resuspended in 100µl staining buffer. An antibody staining mix was added to each tube: CD14 PE-Cy7 and CD16 APC-H7 (BD Biosciences, UK), HLA-DR PerCP Cy5.5 (Life Technologies, UK) and MerTK APC (R&D Systems, UK). For comparison, the oxidative burst of healthy monocytes from *ex-vivo* PBMCs was measured by the same method. Additional comparators included monocyte and neutrophil burst in anticoagulated (lithium heparinised) whole blood, from healthy control subjects and patients with decompensated cirrhosis without organ failure. The whole blood Phagoburst™ assay was followed as per manufacturer's protocol, which is similar to the aforementioned protocol but differs in that 100µl of whole blood is used without specified cell counts nor supplemental serum. Neutrophil detection by flow cytometry was achieved by using anti-human CD66b PE-Cy7 (BioLegend, UK) and CD177 Alexa Fluor 647 (BD Biosciences, UK). Since dead cells may generate ROS, the manufacturers recommend use of samples with high viability and therefore the assay was performed *ex-vivo* only. Optimization experiments are described in the Appendix J.

Results were expressed as percentage of CD14+ cells producing ROS, MFI as an indicator of ROS cellular activity and oxidative index, the ratio of stimulated and unstimulated mean fluorescence intensity of the CD14+ population.

3.2.23. CellROX™ Deep Red Assay for Oxidative Stress Detection

CellROX™ Deep Red reagent is a fluorogenic probe for measuring oxidative stress, non-fluorescent in the reduced state but generating bright fluorescence when oxidised by ROS, with absorption/emission maxima at ~644/665nm. An *ex-vivo* ascitic cell suspension was obtained at a concentration of 500,000 cells / ml of RPMI in a polystyrene tube. To one tube 20µl of *E. coli* particles was added and to the other 20µl of PBS served as negative control. The cell suspension was incubated at 37°C for 40 minutes in the dark. After this time, 500nM of CellROX™ Deep Red Reagent was added and the cells incubated for a further 30 minutes. Cells were subsequently washed with PBS. Thereafter, cells were exposed to

an antibody mixture for 20 minutes containing CD14 Pe-Cy7, CD16 APC-H7, HLA-DR PerCP Cy5.5, Axl AF488 and MerTK PE. Cells were washed again, stained with 1µl 10X dilute Sytox Blue live/dead stain for 15 minutes, and analysed by flow cytometry without further washing steps.

3.2.24. Intracellular Cytokine Staining Protocol for TLR Agonists

Initially, ACs were thawed in a water bath, washed in pre-warmed RPMI, centrifuged and the cell viability determined by 0.4% trypan blue staining. The same protocol as per 2.2.7 was followed. Compensation beads and CS&T beads were used to calibrate the flow cytometer as previously described. Experiments were performed in batches, initially at King's College Hospital and latterly at Imperial College London. Comparator groups included healthy control PBMCs, which were run simultaneously to ACs using the same method, and ovarian cancer ACs. The HLA-DR gating strategy, as previously described, was employed to select monocytes and macrophages for flow cytometric analysis. To corroborate the ICCS data, the TNF-α concentrations in supernatants generated from LPS stimulations of ACs were measured using a TNF-α EASIA as outlined in 3.2.16.

3.2.25. Ascites DNA Extraction and Quantification

Ascitic total DNA was extracted and measured, in order to determine dilutions required for subsequent bacterial DNA quantification, using samples stored as per 3.2.7, with assistance by Dr Rocio Castro Seoane from the Professor Marchesi laboratory group at Imperial College London. DNA was extracted from pellets (n=23) using the PowerLyzer DNA Isolation Kit (Mo Bio, Carlsbad, California). In short, this involved addition of a Power Bead Solution to each pellet, transfer to PowerBead tubes and incubation at 65°C for 10 minutes. Samples were lysed by bead beating for 3 minutes at speed 8 using a Bullet Blender Storm machine (Chembio Ltd., St Albans, UK). Bead Tubes were centrifuged at 10,000*g* for 30 seconds and DNA aliquoted and frozen at -80°C until required. DNA concentration (ng/µl) was determined using 5µl of unfrozen sample with Qubit™ dsDNA BR Assay Kit (Thermo Fisher Scientific, UK) and the Qubit™ 2.0 Fluorometer (McDonald *et al.*, 2018).

3.2.26. 16S rRNA Gene qPCR and Sequencing

To quantify the biomass present in each sample, 16S rRNA gene qPCR was performed using DNA extracted from ascites, following a previously published protocol based on stool DNA extraction (Liu *et al.*, 2012). Guidance through the protocol and analytic assistance was provided by Jesús Miguéns Blanco from the Marchesi Laboratory. For each reaction, a total of 20µl was made up, consisting of the following: 1x Platinum Supermix with ROX (Life Technologies, Carlsbad, USA), 1.8 µM BactQUANT forward primer (5'-CCTACGGGAGGCAGCA-3'), 1.8 µM BactQUANT reverse primer (5'-GGACTACCGGGTATCTAATC-3'), 225nM probe ((6FAM) 5'-CAGCAGCCGCGGTA-3' (MGBNFQ)), PCR grade water (Roche, Penzberg, Germany), and 5µl DNA. An *E. coli* DNA (Sigma-Aldrich, UK) standard curve was included, consisting of 3-300,000 copies per reaction in 10-fold serial dilutions, and a 'no template' negative control. All samples, standards, and controls were performed in triplicate. Extracted DNA samples were diluted to ensure they fit within the standard curve. One SBP case was used as a positive control. The Applied Biosystems StepOnePlus Real-Time PCR System (Applied Biosystems, Waltham, Massachusetts) was used for amplification and real-time fluorescence detections using the following PCR cycling conditions: 50°C for 3 min, 95°C for 10 min, and 40 cycles of 95°C for 15 sec and 60°C for 1 min (McDonald *et al.*, 2018). 16S DNA is expressed as mean from triplicate data (copies/µg DNA). The 16S gene sequencing pre-processing and analysis were performed exclusively by the Marchesi lab according to the protocol set out in McDonald *et al.* (2018), with calculation of the Shannon Diversity Index as a measure of species diversity.

3.2.27. Ascitic and Plasma Metabonomic Profiling

Ascites from patients with cirrhosis (n=39; ACLF n=7), matched plasma (n=26; ACLF n=6), unmatched plasma from cirrhotic patients (n=15; ACLF n=11) and healthy control plasma (n=8) were analysed to evaluate their metabonomic profile according to ^{1}H-nuclear magnetic resonance (NMR) spectroscopy using the Carr-Purcell-Meiboom-Gill (CPMG) and 2D/3D Nuclear Overhauser Enhancement Spectroscopy (NOESY) sequences. The former pulse sequence reduces signal from larger molecules for better quantification; the latter reduces signal to noise (Tognarelli *et al.*, 2015). The

experiment involved (i) sample preparation, (ii) experiment execution and data acquisition, (iii) data pre-processing and multivariate analysis. The whole process was supervised by Dr Mark McPhail based at King's College London, with specific assistance with buffer preparation given by Dr Rabiya Zia (McPhail Laboratory) for (i), Dr Andrew Atkinson at the Guy's Campus NMR Facility for (ii) and analysis completed for (iii) by David Erminelli (McPhail Laboratory) using programs TopSpin (Bruker Corporation, MA, USA), Simca (Sartorius Stedim Biotech, Sweden) and Matlab (Mathworks, MA, USA).

For plasma samples, NMR NaH_2PO_4 buffer was constituted by mixing 0.2g trimethylsilylpropanoic acid (TSP), 2.66g of NaH_2PO_4, 0.1g NaN_3 (sodium azide), 50ml deuterated water (D_2O) and 180ml water (H_2O). TSP provides a reference peak at zero. The pH was measured and 1M NaOH added until pH 7.4 obtained. For ascites samples, an NMR KH_2PO_4 buffer was made up by combining 100mg TSP, 20.4g KH_2PO_4, 13mg NaN_3 and 80ml D_2O with sonication to facilitate mixing. The buffer was pH adjusted by addition of KOH pellets. Buffer purity was checked by ^1H NMR.

Ascites and plasma samples were thawed and 600µl transferred to Eppendorfs. These were centrifuged at 12,000*g* at 4°C for 5 minutes and 540µl of the supernatant combined with 60µl of appropriate buffer into new 600µl Eppendorfs. These were vortexed and the mixture manually added to 5mm SampleJet NMR tubes (Sigma Aldrich, UK), with care to avoid bubbles in the tube. Tubes were transferred to a 96-well plate and inverted to mix (Dona *et al.*, 2014). Six quality controls (2 ascites, 2 cirrhotic plasma and 2 healthy control plasma) were used in which pooled samples from each cohort were used in combination with buffer. Samples were kept at 4°C overnight and analysed the following day. Two samples from patients with hepatitis C were excluded after sample preparation due to limitations of the NMR facility in using infected biofluids.

A data matrix of samples vs. detected features and corresponding intensity values was generated with multivariate analysis. Principle component analysis (PCA) was performed to visualise clustering and

identify outliers. To maximise differences in class and minimize variability unrelated to class, orthogonal projection to latent structures discriminant analysis (OPLS-DA) was performed. The R^2 value was calculated as a measure of goodness-of-fit and cross-validated Q^2 statistic calculated to quantitively measure predictability of the model for the Y-variable (McPhail *et al.*, 2016).

3.3. Results

3.3.1. Patient Characteristics

The clinical characteristics of the patients with ascites recruited to the study are described in Table 3.1, separated into two groups: cirrhosis without organ failure (OF) and ACLF. The latter were a significantly younger group, and as expected had a much higher mortality at 90-days (77.7% vs. 13.9%, $p<0.001$). Similarly, patients with ACLF showed significantly higher biochemical indices of liver injury, including international normalized ratio (INR), creatinine, bilirubin and AST, in addition to disease severity scores (e.g. MELD and Child Pugh) in comparison with patients with cirrhosis without OF. Alcohol-related liver disease was the most abundant aetiology (69%). In the whole cohort, 8/52 (15.4%) developed subsequent SBP after the sampling episode and 9/52 had previous SBP (17.3%).

In the whole cohort, univariate analysis revealed potential predictors for developing SBP after the sampling episode as proton pump inhibitor therapy ($p=0.076$) and MELD score at time of paracentesis ($p=0.053$) but not ascitic protein ($p=0.538$), ascitic WCC ($p=0.341$), rifaximin ($p=0.283$), non-selective beta-blockers ($p=0.322$) nor previous SBP ($p=0.422$).

Table 3.1 Clinical and Physiological Characteristics of Recruited Patients with Cirrhosis and Ascites without Organ Failure and Patients with Acute-on-Chronic Liver Failure

Variable	Cirrhosis w/o OF	ACLF	Healthy	p-value
Number of patients	43	9	27	n/a
Age, *years*	58 [29-84]	50 [36-65]	33 [25-48]	<0.05[a]
Sex, male:female	28:15	1:8	13:14	0.16[b]
Aetiology				
Alcohol	31	5	-	
Non-alcoholic fatty liver (NAFLD)	7	1	-	
Viral (HBV/HCV)	2	1	-	
Autoimmune (AIH/PBC/PSC)	3	0	-	
Mixed/other	0	2	-	
White cell count, x10^9/L	6.2 [2.5-22.8]	10.6 [2.2-8.6]	-	0.261[c]
Neutrophil	4.2 [1.6-20.9]	8.5 [1.5-16.0]	-	0.113[c]
Monocyte	0.60 [0.18-2.50]	0.60 [0.20-0.94]	-	0.674[c]
Platelets, x10^9/L	117 [46-347]	85 [34-172]	-	0.079[c]
Mean Platelet Volume, fL	9.2 [6.7-13.9]	9.8 [7.3-12.2]	-	0.239[c]
Total Bilirubin, μmol/L	43 [10-350]	293.0 [126-527]	-	<0.001[c]
AST, IU/mL	52 [16-225]	99.0 [71-415]	-	<0.01[c]
Albumin, g/L	28 [18-47]	28 [22-36]	-	0.865[c]
Sodium, mmol/L	134 [126-141]	138 [132-143]	-	<0.05[c]
Creatinine, μmol/L	93 [26-182]	239 [84-274]	-	<0.01[c]
INR	1.45 [1.10-4.53]	2.08 [1.53-3.56]	-	<0.01[c]
Child Pugh Score	9 [7-13]	12 [10-15]	-	<0.01[c]
MELD Score at Time of Paracentesis	16 [7-34]	33 [25-45]	-	<0.001[c]
CLIF-C AD Score	54 [42-78]	64 [45-71]	-	0.103[c]
CLIF SOFA	n/a	13 [9-16]	-	n/a
CLIF-C ACLF Score	n/a	62 [35-68]	-	n/a
28-day Mortality	0	6 (66.7%)	-	<0.001[c]
90-day Mortality	6 (13.9%)	7 (77.7%)	-	<0.001[c]

Abbreviations: HBV, hepatitis B virus; HCV, hepatitis C virus; AIH, autoimmune hepatitis; PBC, primary biliary cholangitis; PSC, primary sclerosing cholangitis; AST, aspartate transaminase; INR, international normalised ratio; MELD, model for end-stage liver disease; OF, organ failure; ACLF, acute-on-chronic liver failure. Statistical tests: [a] Student t-test [b] Chi-Square test [c] Mann-Whitney U test. All values are displayed as median with ranges in brackets below.

Ovarian cancer patients with malignant ascites (n=7) were used as a pathological control group for aspects of the experimental work (**Table 3.2**).

Table 3.2 Characteristics of Patients with Ovarian Cancer and Malignant Ascites

Sample No.	Histology	Grade	Stage	Presentation
1	Serous Adenocarcinoma	High	3C	Relapse
2	Serous Adenocarcinoma	High	3C	Relapse
3	Serous Adenocarcinoma	High	4B	Relapse
4	Serous Adenocarcinoma	High	4A	Relapse
5	Serous Adenocarcinoma	High	3C	Relapse
6	Serous Adenocarcinoma	High	3C	Newly diagnosed
7	Serous Adenocarcinoma	High	3C	Relapse

3.3.2. ACLF Ascites Promotes a MerTK^{high} HLA-DR^{low} Immunosuppressive Phenotype

To investigate the effect of ascitic soluble mediators on healthy cells, the monocyte immunophenotype following culture in ascites derived from the patient groups listed in 3.2.12 was evaluated using flow cytometry, looking at surface marker expression and frequency of monocytic –myeloid suppressor cells (M-MDSC) (section 3.3.4). In a smaller sample of patients, the effect of ascites on CD14+ cell expression of Axl and CD163 was also examined. The gating process (**Figure 3.1A**) involved exclusion of doublets and dead cells, then selection of myeloid cells (CD33+) and monocytes (CD14+). Monocyte (CD14+) MerTK% expression was > 94% when exposed to healthy plasma or patient ascites at 50% volume for 48 hours from any group compared with complete media alone (median 32.8%), reflecting

the maturation of these cells in culture and the fact that MerTK% could not be used to discriminate phenotype in this assay. MerTK expression on CD33+ CD14+ cells by MFI when compared with healthy plasma (median: 3497) was greater but not significant in cirrhotic ascites (6028, $p>0.99$, Kruskal Wallis), significant in ACLF ascites (10747, $p=0.03$) and not significant in ovarian cancer ascites (9555, $p=0.09$) (**Figure 3.1B**). No significant differences were detected in monocyte MerTK MFI between those exposed to ascites from cirrhosis without OF, ACLF and ovarian cancer patients. In comparison to complete media, MerTK MFI was significantly increased in ACLF and ovarian cancer ascites ($p<0.01$, Kruskal Wallis).

Monocyte HLA-DR MFI expression was significantly diminished in CD14+ PBMCs exposed to ACLF ascites (median: 7834) compared with complete media (34268, $p<0.01$), and in ovarian cancer ascites (8677, $p<0.05$) though no significant differences were seen in comparison between healthy, cirrhosis, ACLF and ovarian cancer ascites groups (**Figure 3.1C**). There were similar findings with MerTK+ monocyte HLA-DR MFI expression with the addition of a significant decline in cirrhotic ascites compared with complete media (**Figure 3.1D**).

The percentage of CD14+ MerTK+ cells that were HLA-DR-, a previously described immunosuppressive subset, was increased in ACLF ascites (25.8%) vs. complete media (0.33%, $p<0.01$), though not significant when compared with healthy plasma (3.8%, $p=0.12$) (Triantafyllou *et al.*, 2018a). A similar percentage was seen in ovarian cancer ascites (28.7%). Both groups had a higher percentage than cirrhotic without OF but was not significant (**Figure 3.1E**).

When pooled together, CD14+ cells exposed to 50% ascites from patients with cirrhosis without OF and in those with ACLF that died within 28 days from ascites sampling had significantly higher MerTK MFI ($p<0.001$) and MerTK+ HLA-DR- % ($p<0.05$) and lower HLA-DR MFI ($p<0.05$) than those that were alive (**Figure 3.1F**). This only held true for MerTK MFI when 90-day mortality was considered ($p<0.01$) (**Figure 3.1G**). The analysis of the MerTK MFI expression in the cirrhosis without OF group alone did not demonstrate a significance differences in the 28- and 90-day mortality.

A subset of ascites-exposed PBMCs was further analysed for their expression of TAM receptor Axl and scavenger receptor CD163 (%/MFI). Percentage of CD14+ Axl+ cells was seen to fall in PBMCs exposed to ascites from patients with cirrhosis without OF (n=4, median 5.07%) compared to healthy plasma (n=3, 64.6%, p=0.057). The proportion of CD14+ cells expressing Axl in ovarian cancer ascites was 20.2% though the sample size was too small for meaningful comparisons (n=1). A similar pattern was seen with Axl MFI expression (**Figure 3.1H**). CD163 expression did not demonstrate any significant differences (**Figure 3.1I**). In the only patient with culture-positive SBP, Axl % (1.89%), Axl MFI (297), CD163 MFI (286) and MerTK MFI (199) were all reduced when compared to healthy control but the SBP sample size was insufficient for reliable conclusions. The effect of ascites on THP-1 macrophage phenotype is shown in Appendix G.

3.3.3. MerTK Expression on Ascites-Conditioned Monocytes Correlates with Ascitic Cell Death Markers and Multiple Inflammatory Cytokines

Correlation matrices were generated to explore the relationship between CD33+ CD14+ MerTK and HLA-DR surface expression in ascites-conditioned PBMCs and ascitic cytokines, cell death markers and clinical parameters using Spearman's co-efficient. This revealed that MerTK MFI positively correlated with bacterial DNA quantity ($r = 0.821$, $p<0.05$, n=7, not shown), M65 concentration in ascites ($r = 0.539$, $p<0.05$) and multiple inflammatory ascitic cytokines including IL-1β ($r = 0.636$, $p<0.05$), IL-12p70 ($r = 0.815$, $p<0.001$), IL-2 ($r = 0.879$, $p<0.001$), IL-4 ($r = 0.749$, $p<0.01$), IL-6 ($r = 0.758$, $p<0.01$) and TNF-α ($r = 0.701$, $p<0.01$). There was no significant correlation with the immunoregulatory cytokine IL-10 ($r = 0.292$, $p=0.311$). HLA-DR MFI expression significantly inversely correlated with the aforementioned inflammatory cytokines (**Figure 3.1J**).

Correlation of clinical biochemical parameters within the ascites groups (cirrhosis without OF and ACLF groups together) revealed significant correlation between MerTK MFI and creatinine ($r = 0.573$, $p<0.01$) (**Figure 3.1K**), as to be expected given creatinine is elevated, by definition, in the ACLF group.

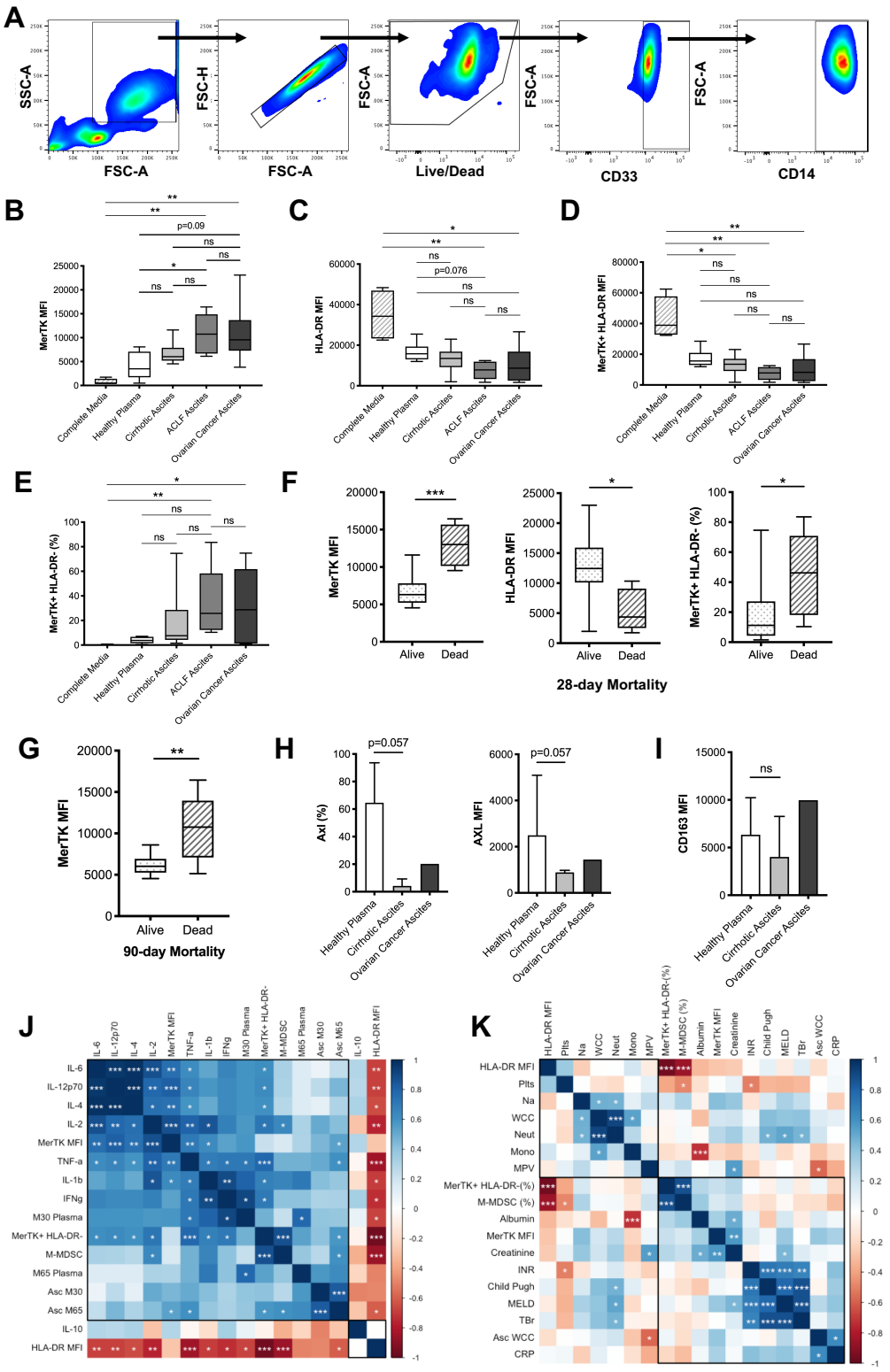


Figure 3.1 Ascites from Patients with ACLF Compared with Cirrhosis without Organ Failure Increases MerTK Expression on Monocytes and Correlates with Clinical Parameters, Cytokines and Outcome

Healthy PBMCs exposed to 50% ascites for 48hrs from patients with ACLF (n=7), cirrhosis without organ failure (OF) (n=13), ovarian cancer (n=7), HC plasma (n=9) and complete media alone without ascites, were phenotypically characterised by flow cytometry. **(A)** Representative flow cytometry gating strategy to determine MerTK and HLA-DR expression in CD33+ CD14+ monocytes. **(B)** Monocyte MerTK expression by MFI in different study groups. **(C)** Monocyte HLA-DR MFI expression. **(D)** MerTK+ HLA-DR- MFI expression **(E)** MerTK+ HLA-DR- % expression. **(F)** Difference between MerTK MFI, HLA-DR MFI and MerTK+ HLA-DR- % according to 28-day mortality. **(G)** Difference in MerTK MFI according to 90-day mortality. **(H)** Effect of 50% HC plasma (n=3), cirrhosis without OF ascites (n=4) and ovarian cancer ascites (n=1) on TAM receptor Axl % and MFI. **(I)** Effect on M2c marker CD163 MFI expression. **(J)** Correlation of phenotypic markers with M-MDSC, cytokines and cytokeratin-18 markers (M30 and M65). **(K)** Correlation with clinical laboratory parameters (Spearman's coefficient). Data presented as box and whisker plots (5-95th percentile) or column graphs as median values with interquartile range (IQR). Non-parametric (Mann-Whitney for two groups and Kruskal Wallis with Dunn's multiple correction for more than two groups) statistical analysis was used. * $p<0.05$, ** $p<0.01$, *** $p<0.001$. SSC-A: side scatter area, FSC-A: forward scatter area, MFI: median fluorescence intensity, M-MDSC: monocytic myeloid-derived suppressor cell, plts: platelets, Na: serum sodium, WCC: white cell count, neut: neutrophil count, mono: monocyte count, MPV: mean platelet volume, Creat: creatinine, INR: international normalized ratio, MELD: model for end-stage liver disease score, TBr: total bilirubin, Asc WCC: ascites white cell count, CRP: C-reactive protein.

3.3.4. ACLF Ascites Expands the Immunosuppressive M-MDSC-like Cell Population

Monocytic myeloid-derived suppressor cells (M-MDSCs) were identified as CD33+ CD11b+ CD15- CD14+ HLA-DR- (**Figure 3.2A**) using a previously established gating strategy (Bronte *et al.*, 2016; Bernsmeier *et al.*, 2017). A higher frequency of M-MDSC-like cells (as a % of CD33+ cells) was seen with exposure to ACLF ascites compared to complete media (median 9.49 vs. 0.02%, p=0.02) though this was not significant for cirrhotic ascites (6.51%, p=0.12). No significant differences were identified between healthy control and cirrhosis or ACLF. The median M-MDSC percentage was highest for ovarian cancer ascites (23.1%) but wide range (0.97-65.9%) meant differences were not significant (**Figure 3.2B**). There was no significant difference in MerTK expression (MFI) between M-MDSCs in cirrhotic ascites and ACLF ascites, unlike monocytes where ACLF MerTK expression was significantly greater ($p<0.05$) (**Figure 3.2C**)**.** Since >94% of the CD14+ cells exposed to ascites were MerTK+ by percentage after 48 hours, the value of MerTK+ HLA-DR- % change in ascites is questionable and rather reflects the reduction in HLA-DR%. As such, M-MDSC% strongly positively correlates with MerTK+ HLA-DR- %, but also with ascitic cell death marker M65 ($r = 0.608$, $p<0.05$) and cytokine IL-2 ($r= 0.648$, $p<0.05$, **Figure 3.1J&K**).

Wu *et al*. suggest that, in ovarian cancer ascites, exposure of PBMCs to IL-6 results in an expansion of the M-MDSC population (Wu *et al.*, 2017). Condamine *et al*. proposed that GM-CSF, especially in combination with IL-6, could drive *ex-vivo* expansion of MDSCs (Condamine *et al.*, 2011). Exposure to GM-CSF and GM-CSF+IL-6 (as per section 3.2.13) suggested the greatest increase of M-MDSC frequency with GM-CSF+IL-6 treatment (Appendix K), however the sample size (n=3) was prohibitively small to generate reliable conclusions. No significant differences were observed in IL-6 concentration of ascites between groups: cirrhosis without OF (n=10), ACLF (n=7) and ovarian cancer ascites (n=5). There was no significant correlation between IL-6 and M-MDSC % in any group, nor M-MDSCs and MerTK MFI or MELD score at the time of paracentesis.

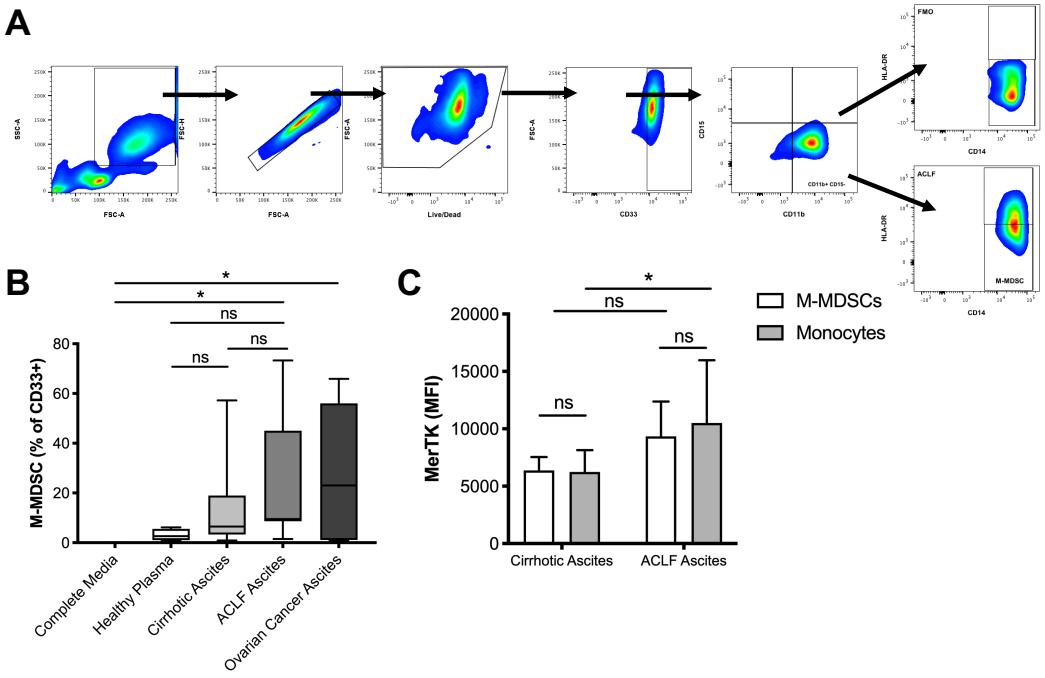


Figure 3.2 Effect of the ascitic microenvironment in cirrhosis without organ failure and ACLF on monocyte phenotype and frequency of *in vitro* M-MDSCs.

PBMCs were isolated from healthy donors (n=3) and cultured for 48hrs in 50% complete media alone (n=3), plasma from healthy subjects (n=6), or ascites obtained from patients with cirrhosis without OF (n=10), ACLF (n=7) or ovarian cancer ascites (n=6), with subsequent phenotypic characterisation using flow cytometry. **(A)** Representative flow cytometry gating and analysis to determine frequency (%) of M-MDSCs (CD33+ CD11b+ CD15- CD14+ HLA-DR-). **(B)** Frequency of M-MDSCs (as % of CD33+ cells) in different groups. **(C)** MerTK expression in M-MDSC vs. monocytes between cirrhosis without organ failure and ACLF groups. Non-parametric (Mann Whitney for two groups; Kruskal Wallis with Dunn's multiple correction for multiple groups) statistical analysis was used. Data is presented as median values with interquartile range. *p<0.05 ** p<0.01. FSC-A: forward scatter area FSC-H: forward scatter height, SSC-A: side scatter area.

3.3.5. M2c Polarising Cytokines Promote Expression of MerTK, Axl and CD163

Zizzo *et al*. (2013) report that IFN-γ promotes an M1 macrophage polarisation, IL-4 an M2a phenotype and IL-10, especially in synergism with IL-17, an M2c phenotype (Zizzo & Cohen, 2013). Whilst it is appreciated that there is a spectrum of macrophage phenotype expression, it can be useful to categorise them as belonging to M1/M2a/M2c in some instances to give a general picture. To verify the effect of these cytokines on the surface monocyte expression of MerTK, Axl and archetypal M2 surface marker CD163, PBMCs were cultured in complete media were supplemented with these cytokines, at concentrations as previously specified (section 3.2.13), for 48 hours. In comparison to the M1 polarising effect of IFN-γ, the combination of IL-10 and IL-17 enhanced the MFI expression of MerTK ($p=0.06$), Axl ($p<0.05$) and CD163 ($p<0.03$). There was also a significant reduction in HLA-DR MFI with this cytokine combination when comparing with complete media alone ($p<0.05$) (**Figure 3.3**). GM-CSF alone, and in combination with IL-6, appeared to reduce MerTK expression in CD33+ CD14+ cells but the sample size (n=3) was insufficient to draw conclusions (Appendix K).

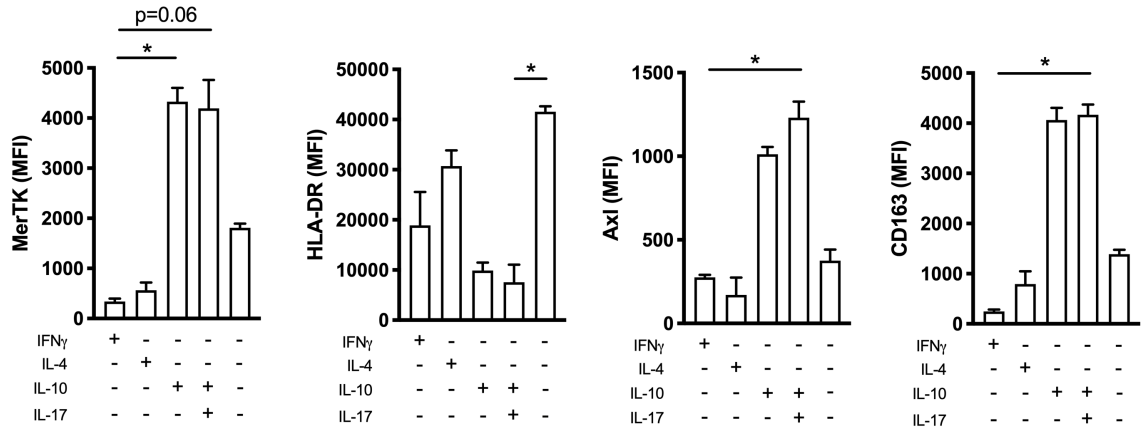


Figure 3.3 Effect of Cytokines on CD33+ CD14+ Surface Expression on MerTK, Axl & CD163

Peripheral blood mononuclear cells isolated from same healthy donor and in triplicate cultured in complete media supplemented with IFN-γ, IL-4, IL-10 or combination IL-10+IL-17 for 48 hours. Subsequent measurement of MerTK, Axl and CD163 monocyte surface expression by MFI using flow cytometry. Data presented as median with interquartile range. Unpaired non-parametric statistical analysis using Kruskal Wallis with Dunn's multiple comparisons test was used. *$p<0.05$. Where unspecified, differences are non-significant.

3.3.6. TAM Receptor Expression in THP-1 Macrophages is Enhanced by ACLF Ascites

To provide proof of principle that MerTK expression is increased in macrophages exposed to ACLF ascites, and not just monocytes in PBMCs, THP-1 monocytes were cultured, differentiated into macrophages with PMA and exposed to ascites as per 3.2.19. A progressive increase in % and MFI expression was seen for all TAM receptors on THP-1 macrophages in complete media only, 50% cirrhotic ascites and 50% ACLF (Appendix G), reaffirming that ACLF ascites promotes greater TAM expression in macrophages compared with ascites from cirrhotic patients without OF.

3.3.7. *Ex-vivo* Phenotype of Peritoneal Macrophages in Decompensated Cirrhosis Reveals a MerTK^{high} Axl$_{low}$ CD16^{high} Predominance

Peritoneal mononuclear cells were isolated after therapeutic paracentesis as per protocol (section 3.2.6) and immediately immunophenotyped *ex-vivo* (section 3.2.8). The validated HLA-DR gating strategy was used to identify the total macrophage population (**Figure 3.4A**) (Triantafyllou *et al.*, 2018a). The peritoneal macrophage population in patients with cirrhosis and ascites was highly MerTK positive (median positive 80.15%, $p<0.0001$, n=28) with low Axl expression (median positive 2.35%, $p<0.0001$, n=18). There was no significant difference between the macrophage Tyro3 positive and negative percentage (median 47.5% vs. 52.6%, p=0.28, n=14) (**Figure 3.4B**). Phenotype characterisation of the macrophage MerTK negative and positive subtypes revealed that MerTK positive cells had increased percentage expression of a) activation markers: HLA-DR (79.7 vs. 98.3, $p<0.0001$), CD86 (20.6 vs. 86.1%, $p<0.01$) and CD11b (94.7 vs. 99.9%, p=0.056) b) Fc-gamma receptor CD16 (43.8 vs. 91.8%, $p<0.0001$) c) tissue and lymph node homing markers CCR5 (10.0 vs. 56.4%, $p<0.05$) and CCR7 (0.46 vs. 8.89%, $p<0.05$) respectively d) immunoregulatory markers: PD-1 (28.6 vs. 83.6%, $p<0.05$), CD206 (8.96vs. 65.4%, p=0.057) and CD163 (5.62 vs. 70.9%, $p<0.0001$). Of note, MerTK positive macrophages have a higher expression of Axl (0.10 vs. 2.61%, $p<0.0001$) and Tyro3 (8.32 vs. 54.6%, p=0.0501), reaffirming co-expression of the TAM receptors (**Figure 3.4C**). The CD14$_{low}$ CD16+ (non-classical) subset seen in circulating monocytes is negligible in the peritoneal macrophage compartment. This is supported by the previous observation of Ruiz-Alcaraz *et al.*, who in addition also

describe the presence of a more complex and granular CD14++ CD16++ subpopulation in peritoneal macrophages, not seen in the blood compartment, representing 33% of the total macrophage population (Ruiz-Alcaraz *et al.*, 2016). The other subsets are CD14+ CD16- (classical) and CD14++ CD16+ (intermediate). In our cohort, the CD14++ CD16++ population was similarly the dominant (39%) population (**Figure 3.4D**). Further analysis of the subsets highlighted significantly increased percentage expression of MerTK ($p<0.0001$) and Axl ($p<0.0001$), though not significant for Tyro3, in this CD14++ CD16++ population when compared with the classical subset (**Figure 3.4E**). Moreover, the CD14++ CD16++ population demonstrated significantly increased expression of CD163, CD206, CX_3CR1, CCR5 and CCR7 (**Figure 3.4F&G**). Taken together, the phenotype of MerTK+ peritoneal macrophages in cirrhotic ascites highlights their plasticity, and suggests they are primed for Fcγ-receptor-mediated phagocytosis (CD16, CD64), tissue homeostasis and immune tolerance (CD163, CD206, PD-1), antigen presentation (HLA-DR), tissue (CCR5) and lymph node (CCR7) homing. The latter may suggest circulation of these cells through tissue compartments, but it remains unclear as to whether they represent tissue resident macrophages or infiltrating monocytes.

3.3.8. Clinical Associations with Peritoneal Macrophage *Ex-Vivo* Phenotype

In contrast to what is observed in the systemic circulation by Bernsmeier *et al.*, there was no statistical difference in MerTK expression (%) of peritoneal macrophages between patients with stable cirrhosis, AD and ACLF ($p= 0.394$, Kruskal Wallis), though the ACLF group for *ex-vivo* phenotyping in this study was underpowered (n=3) (Bernsmeier *et al.*, 2015). There was no significant correlation of MerTK+ % with hepatic disease severity scores, nor biochemical parameters, except for gamma-glutamyl transpeptidase (GGT, $r= 0.602$, $p<0.01$, Spearman's correlation), GGT to platelet ratio (GPR, $r=-0.482$, $p<0.05$) and mean platelet volume (MPV, $r = 0.512$, $p<0.01$) (**Figure 3.5A**). Both MPV and GPR have been previously been reported to be associated with liver fibrosis in the chronic hepatitis B population; this aetiology was not represented here and this correlation warrants further exploration (Ceylan *et al.*, 2013) (Lemoine *et al.*, 2016). Peritoneal macrophage surface CD163% expression was significantly inversely correlated with MELD score ($r = -0.781$, $p<0.01$, n=13) but there was no

significant difference between CD163% in survivors and non-survivors at 90-days (data not shown). Axl% expression was strongly inversely correlated with immunosuppressive subset MerTK+ HLA-DR-% ($r = -0.732$, $p=0.001$). There was a trend towards higher peritoneal macrophage MerTK% in non-survivors at 90 days ($p=0.076$, Mann Whitney) but not 28-days. When considering *ex-vivo* peritoneal macrophage expression of MerTK MFI (King's and St. Mary's data separated for all MFI data), MerTK+ HLA-DR- (%), HLA-DR (%/MFI), Axl (%/MFI), Tyro3 (%/MFI) and CD163 (%) there was no significant difference between stable cirrhosis, AD and ACLF groups (data not shown). In stable cirrhosis, most macrophages were CD14+ CD16++. In AD, the CD14+ CD16++ subset significantly declined in comparison to stable cirrhosis with CD14++ CD16++ significantly expanded. In ACLF, the most dominant subset was CD14++ CD16++ but there were no significant differences between subsets (**Figure 3.5B**).

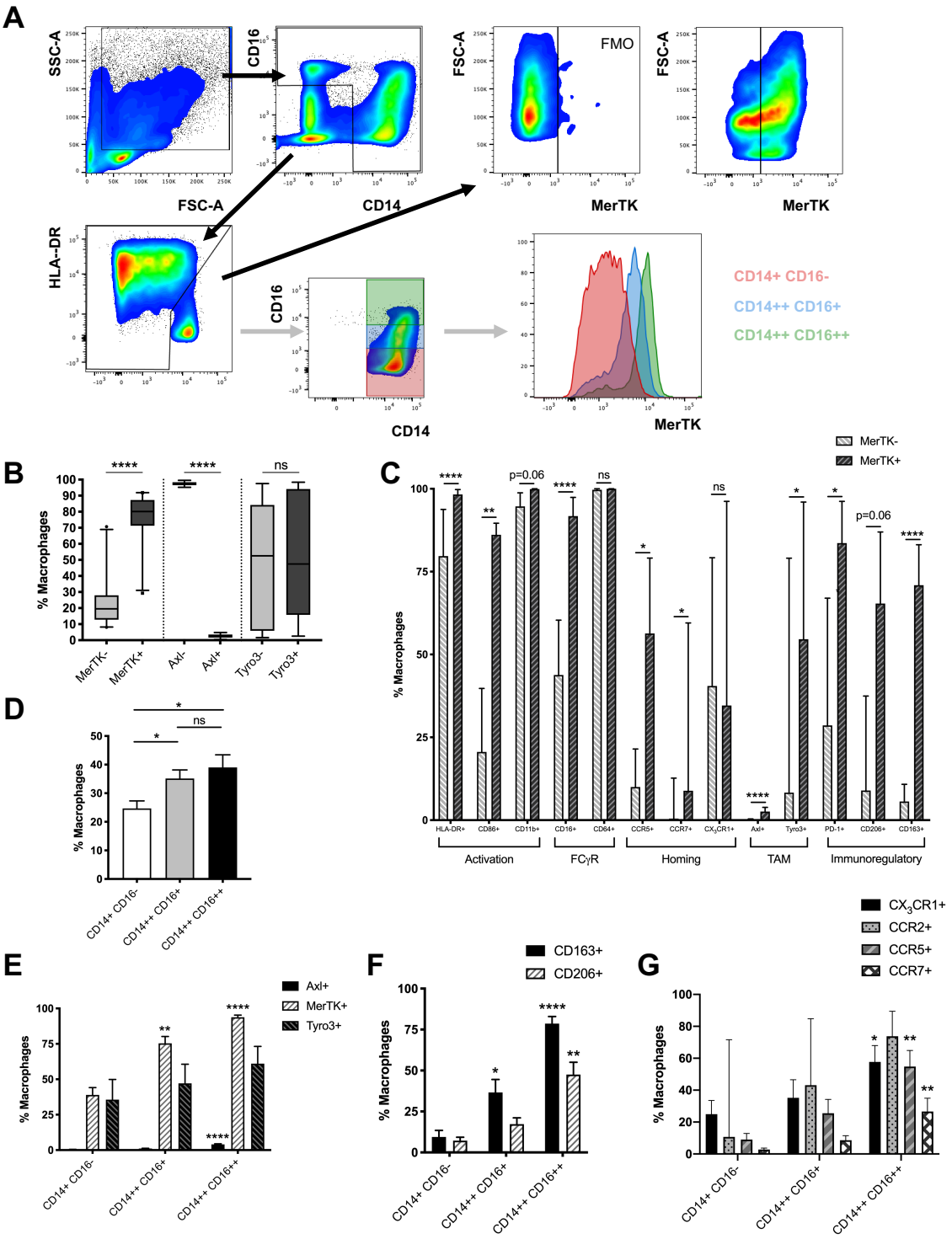


Figure 3.4 ***Ex-vivo*** **phenotype of peritoneal macrophages from patients with cirrhosis and ascites.**

Cells isolated from ascites obtained from patients with cirrhosis undergoing paracentesis were phenotyped *ex-vivo* by flow cytometry (n=30). (A) Representative FACS plots demonstrating HLA-DR+ gating strategy (Abeles *et al.*, 2016) and gating strategy used to identify CD14+ CD16 subpopulations (CD14+ CD16-, CD14++ CD16+, CD14++ CD16++) using FMO CD16 and position of neutrophil cloud ($CD14^{low}$ CD16++) (Ruiz-Alcaraz *et al.*, 2016); histograms normalized to mode demonstrating increase in MerTK% expression in different CD16 subsets;

FMO MerTK used for each patient sample. (B) TAM receptor % expression in peritoneal macrophages for MerTK (n=28), Axl (n=18) and Tyro3 (n=14). (C) Phenotypic expression of surface markers according to MerTK status (negative vs. positive): HLA-DR (n=28), CD86 (n=5), CD11b (n=5), CD16 (n=20), CD64 (n=21), CCR5 (n=4), CCR7 (n=9), CX3CR1 (n=7), Axl (n=19), Tyro3 (n=13), PD-1 (n=7), CD206 (n=4) and CD163 (n=15). (D) CD16 subpopulation as percentage of total macrophage population (E) Percentage expression of MerTK (n=22), Axl (n=12) and Tyro3 (n=8) according to CD16 subpopulation (F) Percentage expression of M2 markers CD163 (n=12) and CD206 (n=5) according to CD16 subpopulation (G) Homing marker percentage expression according to CD16 subset: CX3CR1 (n=12), CCR2 (n=5), CCR5 (n=9) and CCR7 (n=8). Data expressed at mean with standard error of mean (SEM) except (C) expressed as median with interquartile range (IQR). Non-parametric (Mann-Whitney and Kruskal Wallis with Dunn's Correction) statistical analysis was used; control set as CD14+ CD16- in (D)-(G). Data is presented as median values with interquartile range. *$p<0.05$ ** $p<0.01$, ****$p<0.0001$. FSC-A: forward scatter area FSC-H: forward scatter height, SSC-A: side scatter area.

With AD and ACLF groups combined (AD-ACLF), the CD14++ CD16++ subpopulation was significantly elevated when compared with stable cirrhotic patients ($p<0.01$, Mann Whitney), with reciprocal reduction in CD14+ CD16- macrophages. The frequency of macrophages that were CD14++ CD16++ MerTK+ (as % of the total macrophage population) was significantly higher in the AD-ACLF group (**Figure 3.5C**). Crucially, neither total macrophage MerTK% nor CD14++ CD16++ MerTK% demonstrated any significant difference in patients who had previous or subsequent SBP (data not shown), suggesting it cannot be used to predict its development.

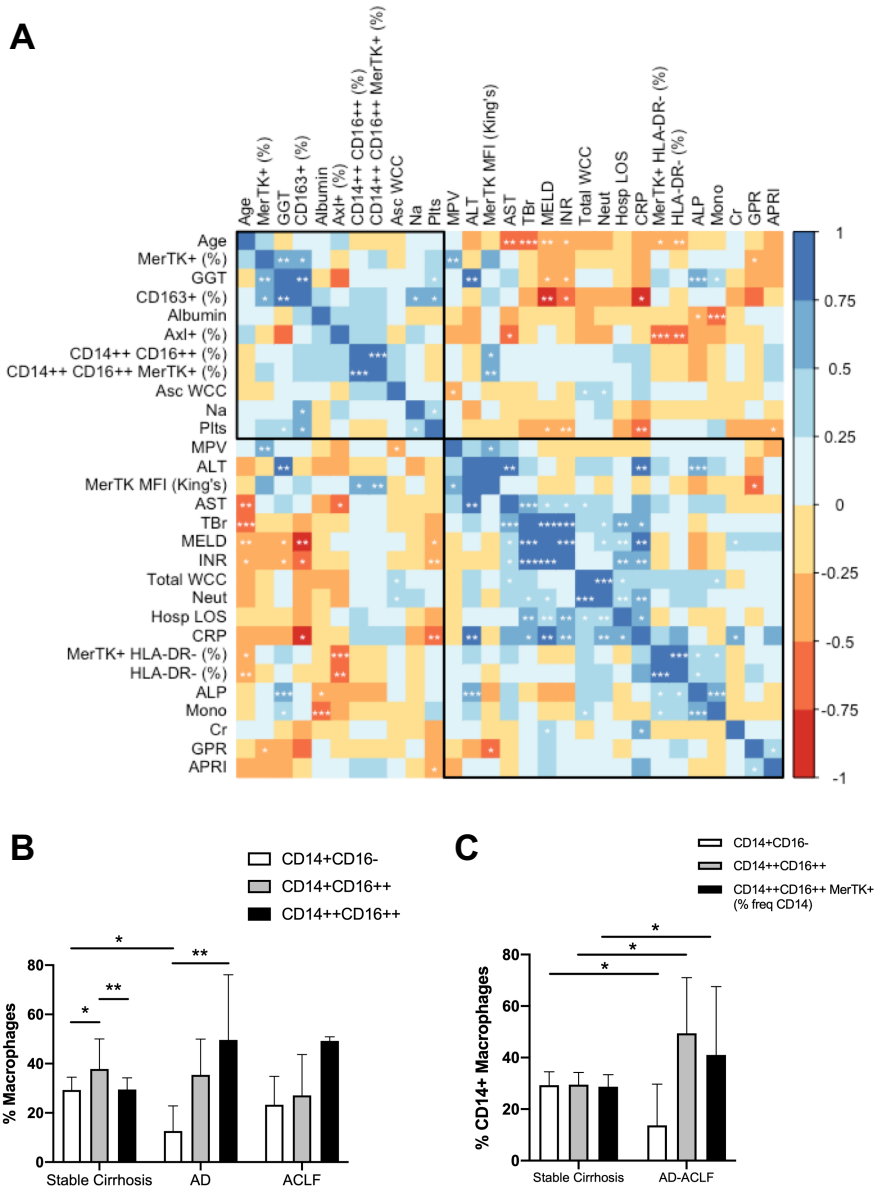


Figure 3.5 Percentage of *ex-vivo* MerTK+ peritoneal macrophages correlates with fibrosis surrogate marker Mean Platelet Volume and CD14++ CD16++ MerTK+ macrophages are expanded in AD-ACLF

(A) Correlation of *ex-vivo* phenotype with clinical parameters in a correlogram using hierarchical clustering. (B) Expression of macrophage subsets as percentage of total macrophage population in stable cirrhotic (SC, n=10), acute decompensated (AD, n=9) and ACLF (n=3) patients. Differences in CD16 subpopulations and CD14++ CD16++ MerTK (as % frequency of total CD14+ population) between SC and AD-ACLF (groups combined). Spearman's correlation with *p<0.05, **p<0.01, ***p<0.001. Data in graphs expressed as median with IQR and non-parametric analysis by Kruskal Wallis. Where not specified, differences between groups were not significant.

3.3.9. Decompensated Cirrhotic Peritoneal Macrophages Exhibit Higher MerTK and Lower HLA-DR Expression than Ovarian Cancer Ascites and Healthy Monocyte-Derived Macrophages

Since ascites in cirrhosis has no healthy control equivalent, comparator groups for phenotypic analysis included *in vitro* healthy monocyte-derived macrophages (MDMs), and ovarian cancer ascites macrophages. MDMs were derived as per 3.2.10 from healthy volunteers (n=4) on separate weeks and compared with *ex-vivo* cirrhotic ascites macrophage phenotype, whilst ovarian cancer ascites was obtained as frozen single cell suspensions (3.2.8) and compared with frozen ascitic cells in order to standardize conditions.

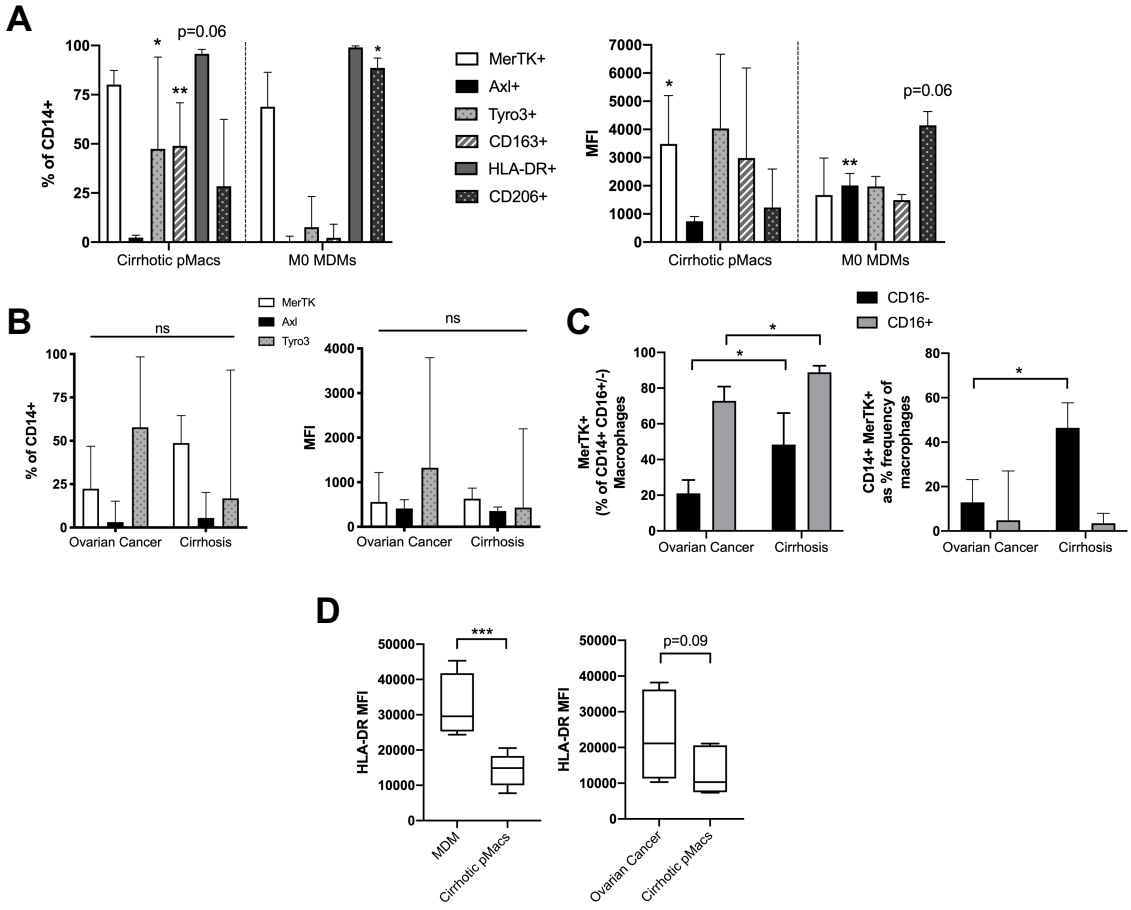


Figure 3.6 Cirrhotic peritoneal macrophage phenotype compared with *in vitro* monocyte-derived macrophage and ovarian cancer ascitic macrophage phenotype

(A) *Ex-vivo* phenotype of peritoneal macrophages determined by flow cytometry in patients with cirrhosis without OF for percentage expression of MerTK (n=28), Axl (n=17), Tyro3 (n=14), CD163 (n=14), HLA-DR (n=28) and CD206 (n=8), in comparison with non-polarised monocyte-derived macrophages (M0 MDM, n=4). Expression by MFI was restricted to the cohort analysed at St. Mary's Hospital using FACS Fortessa for comparability, for MerTK (n=14), Axl (n=13), Tyro3 (n=13), CD163 (n=4), CD206 (n=4) compared with MDM (n=4). (B) TAM

receptor expression by percentage and MFI of thawed ovarian cancer ascitic vs. cirrhosis without organ failure ascitic peritoneal macrophages (both n=5). (C) MerTK% expression as proportion of CD14+ CD16-/+ and total % frequency of CD14+ MerTK+ CD16-/+ cells in both groups. (D) HLA-DR MFI expression of *ex-vivo* cirrhotic peritoneal macrophages vs. *in vitro* MDM (left) and thawed ovarian cancer ascites vs. thawed cirrhotic peritoneal macrophages (right). Data expressed as medial with IQR and non-parametric analysis by Mann Whitney test. *p<0.05, **p<0.01, ***p<0.001.

Compared with MDMs, peritoneal macrophages from patients with cirrhosis without OF demonstrated a significantly higher percentage expression of Tyro3 and CD163, significantly lower expression of CD206 and a trend towards lower HLA-DR expression (p=0.057) (**Figure 3.6A**). MerTK% expression was not significantly higher in the cirrhotic group (p=0.45); Axl% was <5% in both groups with no significant differences observed between groups. According to MFI, MerTK expression was significantly higher in the cirrhotic group (p<0.05) whereas Axl was significantly lower (p=0.0036) compared to the MDM group. Comparing the cirrhotic and ovarian cancer ascites groups, there were no significant differences between TAM receptor expression both by percentage and MFI, but there was a trend towards higher MerTK expression in the cirrhotic group (22.4 vs. 48.7%, p=0.15) (**Figure 3.6B**). When CD14+ cells were subcategorized by CD16 expression (+/-), the proportion of these macrophages expressing MerTK (%) was significantly higher in the cirrhotic group in both subsets (**Figure 3.6C**). However, by percentage of the whole macrophage population, only CD14+ CD16- MerTK+ macrophages were significantly elevated in the cirrhosis group, suggesting that there are differences in the thawed cell phenotype compared to *ex-vivo*, with a reduction in CD16+ absolute numbers. Notably, the percentage expression of MerTK on peritoneal macrophages in cirrhotic patients without OF was less in the thawed cells (40-50%) compared to *ex-vivo* macrophages (70-80%), suggesting the freeze/thaw process may have impacted on phenotypic expression. HLA-DR expression on peritoneal macrophages in cirrhosis is significantly less than MDM (p<0.001) and less than in ovarian cancer ascites macrophages (p=0.09). Taken together, peritoneal macrophages from the ascites of patients with cirrhosis without organ failure show higher MerTK and lower HLA-DR expression compared to *in vitro* MDMs and ovarian cancer ascites macrophages, which is phenotypically consistent with a more immunotolerant state, and supported by work from our group describing this phenotype in other immunosuppressive states such as acute liver failure (Triantafyllou *et al.*, 2018a).

3.3.10. *Ex-vivo* MerTK Expression on Peritoneal Macrophages in Ascites is Significantly Greater than Circulating Monocytes in the Same Patients

Whole blood was obtained concurrently with ascites in order to compare the *ex-vivo* MerTK expression in circulating monocytes and peritoneal macrophages simultaneously in the same patient, as per protocol (3.2.8). The aforementioned HLA-DR gating strategy was used to identity the monocyte / macrophage population. Expression of MerTK % on peritoneal macrophages was significantly greater than matched whole blood monocytes (3.2 vs. 74.3%, $p<0.01$, Mann Whitey U), as was MerTK MFI in these cells (188 vs. 4604, $p<0.05$, Mann Whitney) (**Figure 3.7A**). The ratio of matched MerTK % and MFI expression did not demonstrate any significant correlations to clinical or biochemical parameters.

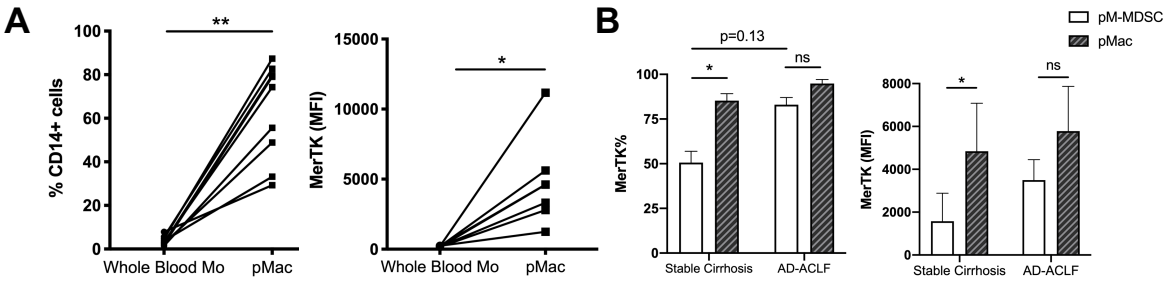


Figure 3.7 Comparison of the MerTK expression in matched circulating monocytes and peritoneal macrophages and in peritoneal M-MDSCs

(A) Matched whole blood monocyte (Mo) and peritoneal macrophage (pMac) MerTK expression by % and MFI in the same patients (n=9, King's cohort) (B). MerTK % and MFI (St. Mary's) expression in peritoneal M-MDSCs (pM-MDSC) compared with matched peritoneal macrophages in stable cirrhosis (n=4) and AD-ACLF (n=2). Data expressed as median with IQR and non-parametric analysis by Mann Whitney test. *$p<0.05$, **$p<0.01$, ***$p<0.001$. Where not specified, difference between groups is not significant.

3.3.11. *Ex-Vivo* Peritoneal Monocytic Myeloid-Derived Suppressor-Like Cells (M-MDSCs) Demonstrate Increased MerTK Expression in AD and ACLF

Ex-vivo ascitic mononuclear cells (n=6) were assessed for the expression of M-MDSC markers (CD33+ CD11b+ CD15- CD14+ HLA-DR$^{neg/low}$) by flow cytometry as per the gating strategy in **Figure 3.2A**. No fixable viability stain was used since the cells were analysed immediately after isolation. Overall, the mean M-MDSCs frequency as a percentage of CD33+ cells was 29.4%. The MerTK percentage and

MFI expression was significantly less in stable cirrhotic M-MDSC than compared with monocytes ($p<0.05$) (**Figure 3.7B**). There was a trend for the same in AD-ACLF. In the latter, the expansion of MerTK % expression was mainly in M-MDSCs, but failed to reach significance compared to stable cirrhotic patients ($p=0.13$). Whilst the sample size requires substantial increment to make valid conclusions, taken together this would suggest that the development of AD or ACLF results in increased MerTK expression in HLA-DR- cells, including M-MDSC-like cells, in the peritoneum.

3.3.12. Concentration of M30 and M65 is Increased in Ascites and in ACLF Compared to Plasma and Cirrhosis Without Organ Failure

The concentration of cytokeratin-18 cleavage products M30 (apoptosis marker) and M65 (cell death marker) were measured using ELISA in plasma and ascites. When patients with liver disease (cirrhosis without OF and ACLF) were considered together, the concentration of cell death markers was greater in ascites (M30 median 1020 U/L; M65 median 2790 U/L) than plasma (M30 median 615.9 U/L, $p=0.0696$; M65 median 484.6 U/L, $p<0.0001$) (**Figure 3.8A**). When the cirrhosis without OF group was subclassified into stable cirrhosis and acute decompensated, significant differences were identified between ascitic M30 concentration in stable cirrhosis vs. ACLF ($p<0.01$) and for ascitic M65 between stable cirrhosis and ACLF ($p<0.05$) and AD and ACLF ($p<0.05$) (**Figure 3.8B**). ACLF had significantly higher M30 and M65 concentrations in plasma and ascites compared with cirrhosis without OF (**Figure 3.8C**). Of note, whilst in cirrhosis without OF, the plasma M30 concentration is less than ascites (median 485.1 U/L vs. 781.1, $p=0.07$), this is reversed in ACLF with M30 plasma concentration exceeding ascites (2173 U/L vs. 760.1, $p=0.2$). The M30 and M65 concentrations were not significantly different in ovarian cancer ascites compared with ACLF. Healthy plasma M30 and M65 are significantly less than cirrhosis without OF and ACLF plasma and ascites ($p<0.01$).

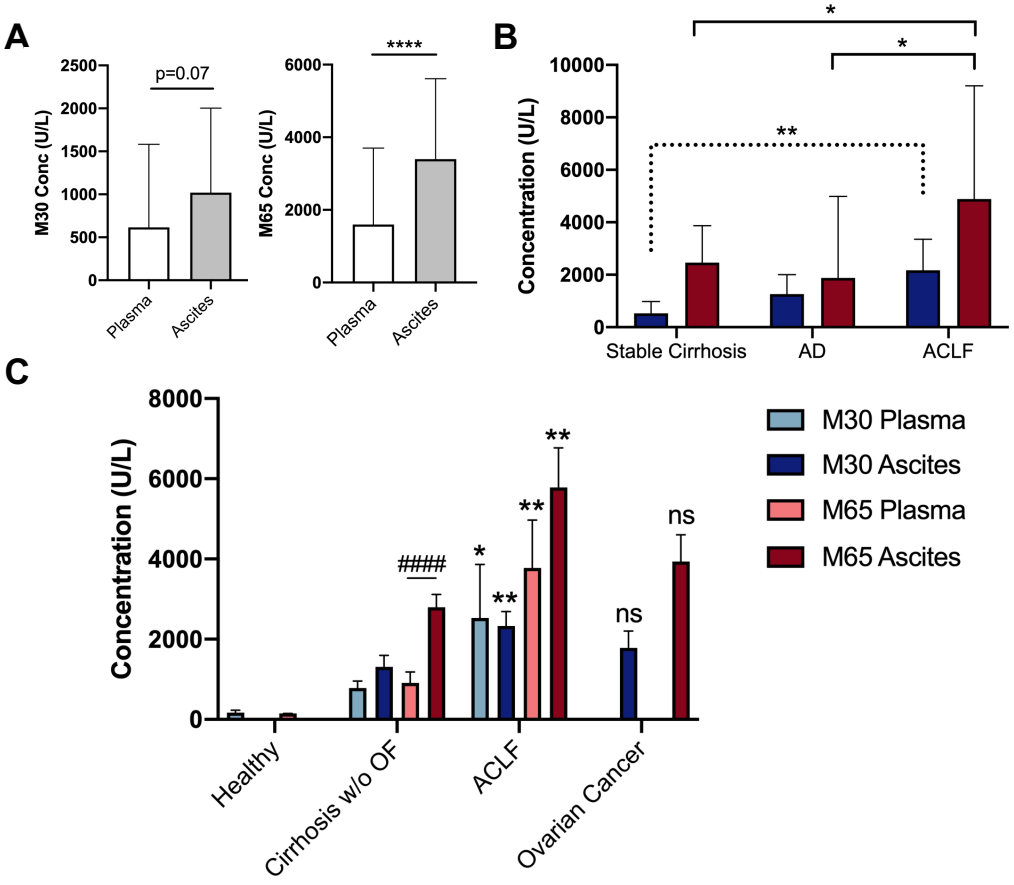


Figure 3.8 Cell death marker M30 & M65 concentration in plasma and ascites of patients with cirrhosis without organ failure and ACLF compared with healthy plasma and ovarian cancer ascites

(A) Concentration of M30 (U/L) in plasma (n=25) compared with ascites (n=32) in liver disease (cirrhosis without OF and ACLF groups combined) and M65 concentration (U/L) in plasma (n=25) and ascites (n=35). (B) Ascitic concentration of M30 and M65 in stable cirrhosis (n=14), acute decompensated cirrhosis (n=13) and ACLF (n=7) (C) Comparison of M30 and M65 concentration in patients with cirrhosis without OF in plasma (n=18 and n=19 respectively) and ascites (n=25 and n=28) with ACLF plasma (n=7 and n=6) and ascites (n=7 for both). Healthy plasma (n=5) and ovarian cancer ascites (n=6 and n=7) were used as controls. Data expressed as median with non-parametric analysis by Mann-Whitney test for differences between two groups and Kruskal-Wallis with Dunn's multiple comparison for more than groups (B and C). For (C) * represents difference between cirrhosis without OF and ACLF groups, and # difference between M65 plasma and ascites in cirrhosis without OF group. *p<0.05, **p<0.01, ****p<0.0001, #### p<0.0001. Where not specified, difference between groups is not significant.

Taken together, M30 and M65 concentrations are higher in ascites compared with plasma, and significantly higher in ACLF compared with cirrhosis without OF. The plasma to ascites M30 concentration gradient seen in cirrhosis without OF is reversed in ACLF with disproportionate increase

in plasma M30, perhaps suggesting cellular apoptosis in organ injury spills over into the circulation. Given that MerTK is integral to apoptotic cell clearance, it could be speculated that its expansion on the surface on circulating monocytes and peritoneal macrophages in ACLF may be driven by cell death.

3.3.13. Peritoneal Macrophages in Cirrhotic Ascites Display Greater Efferocytic Capacity than Healthy Circulating Monocytes with Associated Upregulation of MerTK and Axl

Given the observation of increased cell death markers M30 and M65 in the ascites, the hypothesis that MerTK expression is enhanced by phagocytosis of apoptotic debris (efferocytosis) was tested by the efferocytosis assay described in 3.2.20.

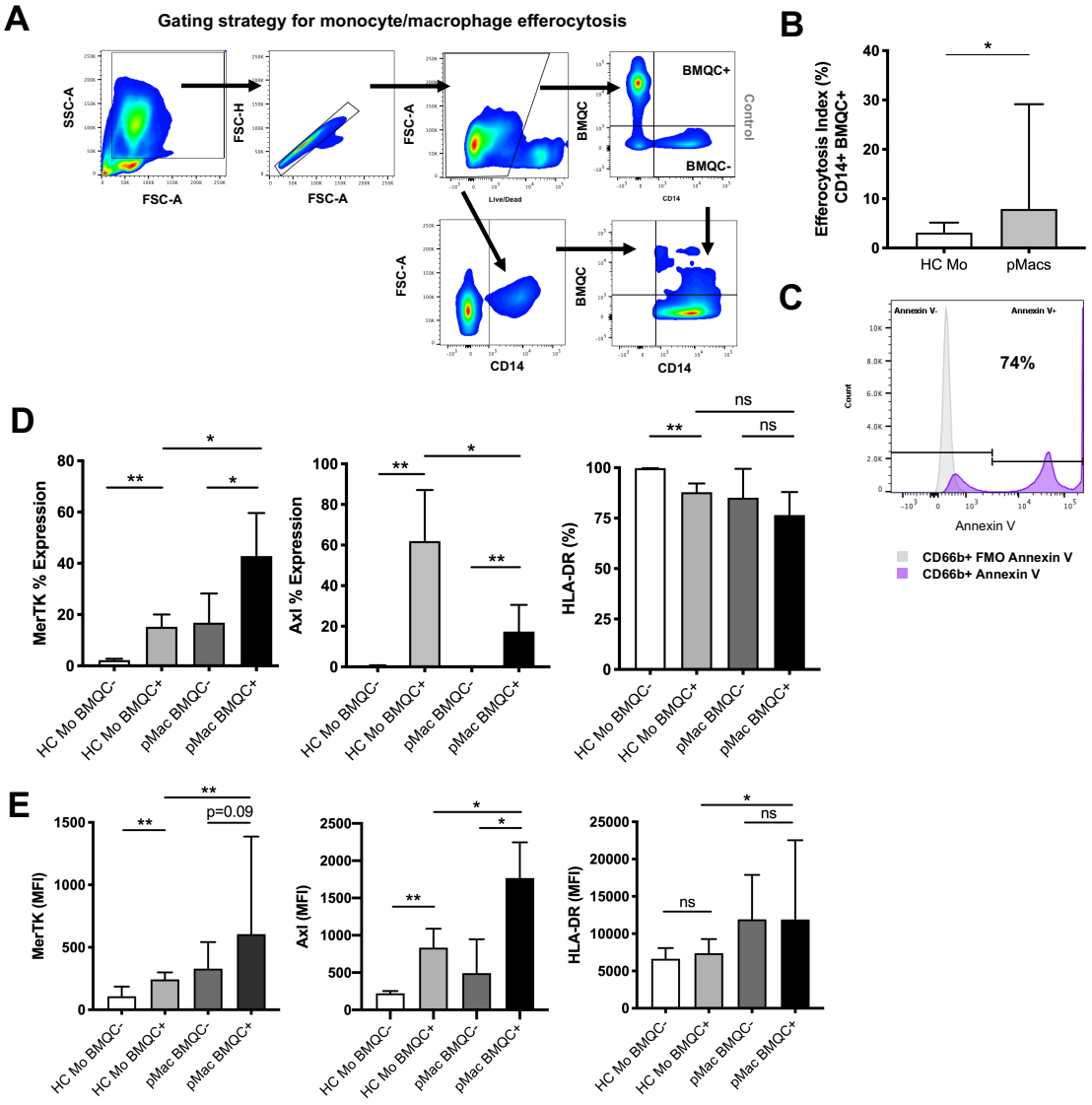


Figure 3.9 Efferocytosis of apoptotic neutrophils by peritoneal macrophages from cirrhotic ascites compared with healthy monocytes from PBMCs

(A) Flow cytometry gating strategy to determine degree of efferocytosis – CD14+ monocytes / macrophages that have phagocytosed labelled BMQC+ apoptotic neutrophils are CD14+ BMQC+ (B) Efferocytosis index – the percentage of CD14+ cells that contain BMQC+ neutrophils – in peritoneal macrophages (pMac, n=6) compared with healthy control (HC) monocytes (Mo) from PBMCs (n=6) (C) Representative histogram plot to demonstrate that the assay based on Zizzo *et al.* (2012) renders >70% neutrophils apoptotic after 20 hours in culture (D)

Percentage expression of MerTK, Axl and HLA-DR of monocytes/macrophages determined by flow cytometry according to the presence (BMQC+) or absence (BMQC-) of apoptotic neutrophils (E) Expression by median fluorescence intensity (MFI) of the same markers. Data expressed as median with IQR with non-parametric analysis by Mann-Whitney test for differences. *p<0.05, **p<0.01.

Healthy neutrophils labelled with Cell Tracker Violet (BMQC) were rendered apoptotic, co-cultured with thawed ascitic mononuclear cells (all from patients with cirrhosis without OF) and healthy PBMCs. Greater than 70% of neutrophils were rendered apoptotic by this method (**Figure 3.9C**). Their uptake by living CD14+ cells (monocytes/macrophages) was measured by flow cytometry, detected as CD14+ BMQC+ cells (**Figure 3.9A**). The efferocytic index, percentage of CD14+ cells containing BMQC+ cells, was significantly higher in peritoneal macrophages than healthy monocytes (3.13 vs. 7.92%, $p<0.05$) (**Figure 3.9B**). The BMQC MFI of CD14+ cells showed a similar pattern, higher in peritoneal macrophages, but was not significant ($p=0.31$; data not shown). In healthy monocytes or peritoneal macrophages, cells that had ingested BMQC+ neutrophils had a significantly higher percentage of MerTK+ and Axl+ cells than BMQC-, though a significant reduction in HLA-DR% was only seen in BMQC+ healthy monocytes (**Figure 3.9D**). Axl% expression of BMQC+ healthy monocytes was significantly higher than BMQC+ peritoneal macrophages, whereas MerTK% was greater in peritoneal macrophages ($p<0.05$). Expression by MFI showed similar trends with increased MerTK expression in BMQC+ healthy monocytes ($p<0.01$) and peritoneal macrophages ($p=0.09$) compared with BMQC- cells and increased Axl in BMQC+ healthy monocytes ($p<0.01$) and peritoneal macrophages ($p<0.05$) but no significant changes with HLA-DR. There was no significant difference in HLA-DR expression in MerTK+ peritoneal macrophages that has ingested apoptotic neutrophils compared to those that had not (data not shown).

Taken together, this data suggested that peritoneal macrophages from cirrhotic ascites have an enhanced efferocytic capacity compared to healthy monocytes, and the expression of MerTK and Axl is upregulated after efferocytosis of apoptotic neutrophils. Although the ascitic cells used in this assay were not from patients with ACLF, this could explain the aforementioned observations of higher

MerTK expression in ACLF ascites-exposed cells and higher concentrations of cell death markers in ACLF ascites.

3.3.14. Peritoneal Macrophages from Cirrhotic Ascites have Attenuated Pro-inflammatory Cytokine Responses to Lipopolysaccharide

Since activation of TAM receptor signalling by efferocytosis is known to be coupled with dampening of pro-inflammatory cytokine responses, the production of archetypal pro-inflammatory cytokines TNF-α and IL-6 were measured by flow cytometry in peritoneal macrophages stimulated with LPS (Lemke & Rothlin, 2008).

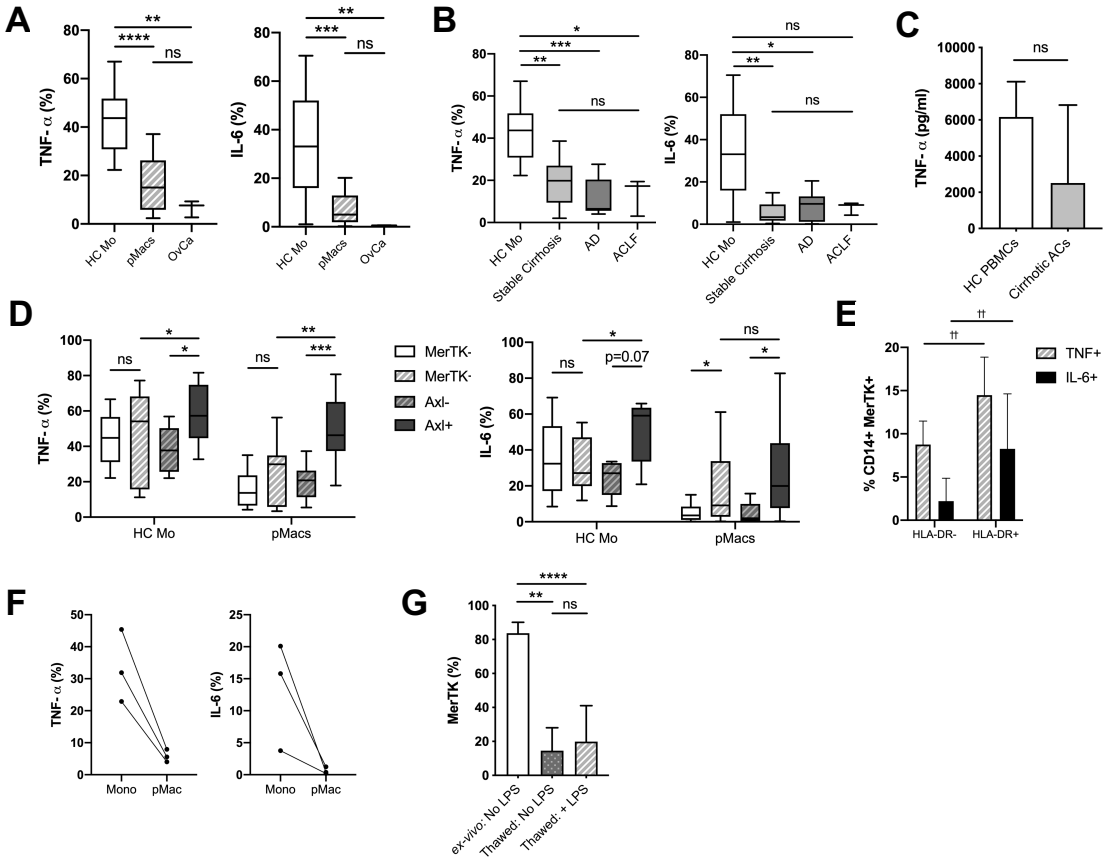


Figure 3.10 Attenuated LPS-stimulated TNF-α and IL-6 production of peritoneal macrophages from ascites of patients with cirrhosis

(A) TNF-α and IL-6 (%) production of healthy control monocytes (HC Mo, n=14), peritoneal macrophages (pMacs) from cirrhotic ascites (n=23) and peritoneal macrophages from ovarian cancer ascites (OvCa, n=3) after 5 hours of LPS (100ng/ml) stimulation. (B) TNF-α and IL-6 (%) production according to disease group: healthy control (n=14), stable cirrhosis (n=12), acute decompensation of cirrhosis (AD, n=8) and ACLF (n=3). (C) TNF-α

concentration (pg/ml) measured in the supernatants of LPS-stimulated healthy control PBMCs (n=4) and cirrhotic ascitic cells (ACs, n=7). (D) Cytokine production (%) in healthy control monocytes and cirrhotic peritoneal macrophages according to MerTK+ or MerTK- (HC Mo n=9; pMac n=17) and Axl+ or Axl- cells (HC Mo n=8; pMac n=9). (E) TNF-α and IL-6 (%) in cirrhotic peritoneal macrophages according to MerTK+ HLA-DR- vs. MerTK+ HLA-DR+ status (n=9) (F) TNF-α and IL-6 (%) in matched circulating monocytes and peritoneal macrophages sampled concurrently from the same patient (n=3) (G) MerTK % peritoneal macrophage expression in *ex-vivo* phenotyping (n=10), compared with expression on freeze/thawed cells (n=3) given PBS only (no LPS) and freeze/thawed cells treated with LPS (n=11) to highlight the change in MerTK% with the freeze/thaw process +/- LPS. Data is expressed as median with IQR with non-parametric analysis by Mann-Whitney for two groups or Kruskal-Wallis and Dunn's multiple comparison for greater than two groups. *p<0.05, **p<0.01 ***p<0.001 **** p<0.0001. (E) was analysed with Wilcoxon matched-pairs signed rank test. ††p<0.01

The data demonstrated a significantly attenuated TNF-α (43.7% vs. 15.0%, p<0.0001) and IL-6 (33.1% vs. 5.02%, p<0.001) production of peritoneal macrophages in cirrhotic ascites in response to LPS stimulation when compared to healthy control monocytes. Ovarian cancer ascitic cells also had impaired cytokine production but was not significant and sample number was low (n=3) (**Figure 3.10A**). When cirrhotic peritoneal macrophages were subcategorised according to stable cirrhosis, AD and ACLF, no significant differences between these groups were noted (**Figure 3.10B**). To corroborate the data, the TNF-α concentration from supernatants from ACs incubated with LPS was measured using an EASIA (3.2.16), which demonstrated a trend towards lower TNF-α production in ACs compared to healthy PBMCs (2508 vs. 6164 pg/ml, p=0.16) (**Figure 3.10C**). Analysis of subpopulations according to MerTK and Axl positivity, unexpectedly found no significant difference in pro-inflammatory cytokine production between MerTK+ and MerTK– cells, whereas Axl+ cells produced significantly more TNF-α and IL-6 compared with Axl- cells and MerTK+ cells, in both healthy monocytes and peritoneal macrophages (**Figure 3.10D**), consistent with the observations on Axl+ circulating monocytes in Chapter 2. The previously described MerTK+ HLA-DR– immunosuppressive subset indeed demonstrated attenuated pro-inflammatory cytokine production in peritoneal macrophages though this subset represented <10% of the MerTK+ population (**Figure 3.10E**). In patients where PBMCs and ACs were collected simultaneously, circulating monocytes were found to produce more TNF-α and IL-6 that matched peritoneal macrophages (n=3, p=0.10) (**Figure 3.10F**). No significant differences in TNF-α and IL-6 MFI expression were identified, but King's and Imperial College cohorts

were separated and therefore each smaller due to analysis with two different flow cytometers. *Ex-vivo* peritoneal macrophage MerTK %/MFI did not correlate significantly with TNF-α or IL-6 MFI, as seen previously with circulating monocytes (Bernsmeier *et al.*, 2015).

3.3.15. Peritoneal Macrophages Demonstrate Preserved Bacterial Phagocytosis

Data thus far has demonstrated enhanced efferocytic capabilities and attenuated LPS-stimulated pro-inflammatory cytokine responses of cirrhotic peritoneal macrophages in comparison to healthy circulating monocytes. To investigate whether bacterial pathogen uptake was deranged in these cells, the pHrodo™ assay was utilized, as described in 3.2.21.

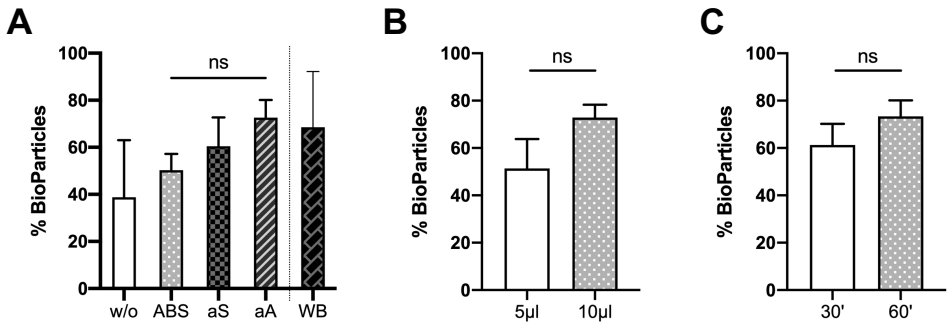


Figure 3.11 pHrodo™ optimization for peritoneal macrophage phagocytosis assay

(A) pHrodo™ assay (60 minutes, 10µl Red BioParticles™) performed with ACs from cirrhotic patients with variation in supplemental opsonins: w/o (without, n=2), 10% ABS (donor AB serum, n=4), 10% aS (autologous serum, n=4), 10% aA (autologous ascites, n=8); WB (whole blood phagocytosis of cirrhotic patients, n=3). (B) Optimum volume of *E. coli* Particles: 5 vs. 10µl) (C) Optimum duration: 30 vs. 60 mins. Data expressed as percentage of total macrophages containing BioParticles™ and median with IQR; statistical analysis by non-parametric paired Wilcoxon signed rank test. Where not specified, differences between groups are not significant.

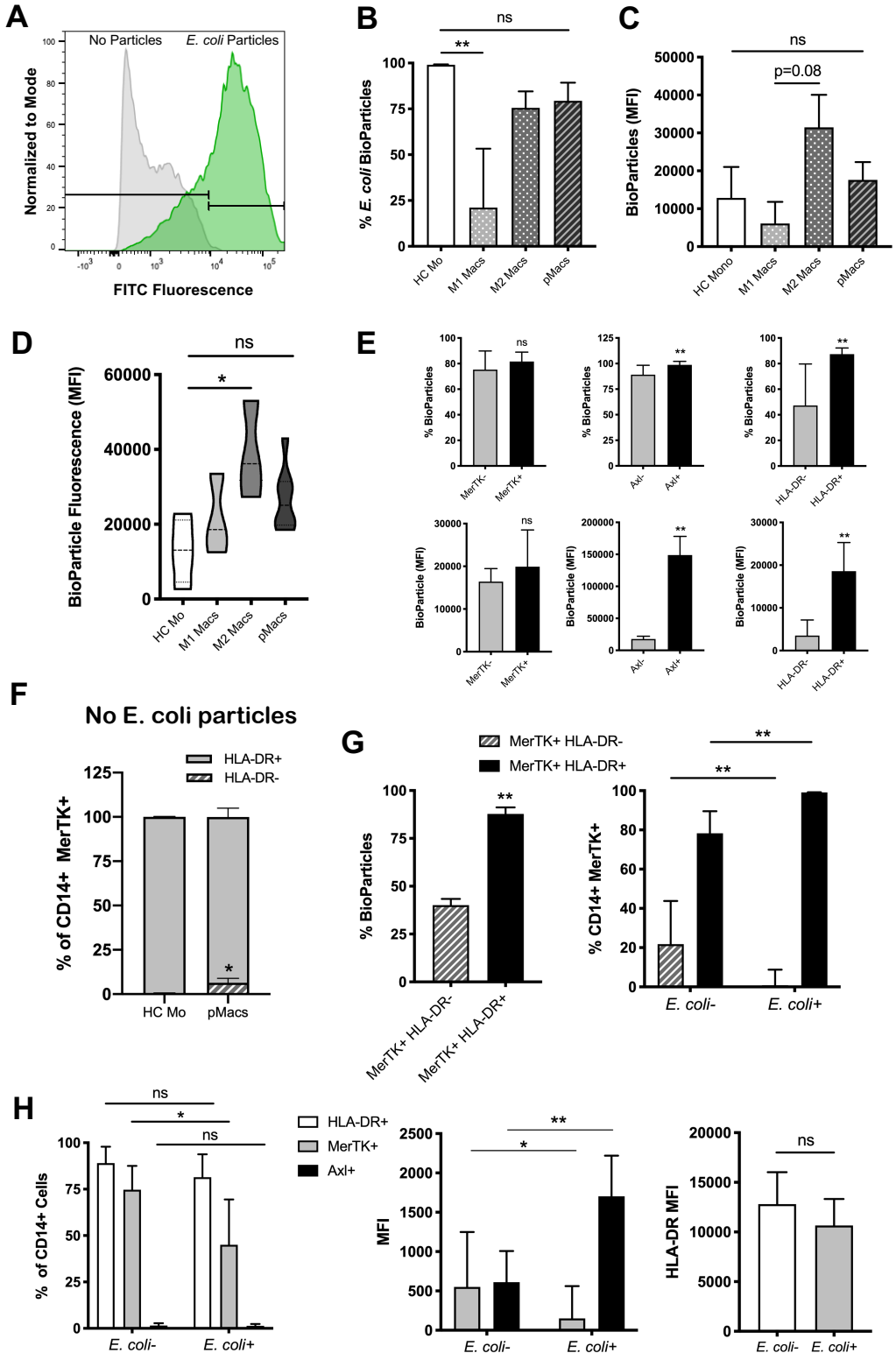


Figure 3.12 Phagocytosis of *E. coli* BioParticles™ is preserved in ascitic peritoneal macrophages compared with healthy monocytes and *in vitro* monocyte-derived macrophages

(A) Representative histogram illustrating shift in green (FITC) fluorescence on peritoneal macrophage stimulation with *E. coli* BioParticles™ (B) Percentage of CD14+ peritoneal macrophages that have phagocytosed

BioParticles™ (n=8) compared with healthy monocytes from PBMCs (n=5), M1 healthy *in vitro* monocyte-derived macrophages (MDM, n=3) and M2 MDM (n=3). (C) MFI of Green BioParticles™ in CD14+ population (D) MFI of BioParticles™ in CD14+ monocytes / macrophages that have specifically taken up particles (E) The % uptake of *E. coli* BioParticles™ by peritoneal macrophages in patients with cirrhosis and ascites and BioParticle™ MFI of CD14+ population according to surface receptor (MerTK, Axl & HLA-DR, n=8 for each) (F) Percentage of CD14+MerTK+ cells that are HLA-DR- vs. HLA-DR+ in healthy monocytes vs. peritoneal macrophages in the absence of *E. coli* particles; (G) % *E. coli* particle uptake by MerTK+ HLA-DR- vs. MerTK+ HLA-DR+ peritoneal macrophages (left) and proportion of CD14+ MerTK+ peritoneal macrophages that are HLA-DR- or HLA-DR+ depending on whether they have taken up *E. coli* particles (right). (H) Difference in phenotype (MerTK, Axl and HLA-DR %; MerTK, Axl and HLA-DR MFI) of peritoneal macrophages exposed to BioParticles™ that have phagocytosed particles compared to those that have not. Data expressed as median with IQR with non-parametric analysis by Mann-Whitney test for differences between two groups and Kruskal Wallis for > 2 groups with Dunn's multiple comparison test between each group. *p<0.05, **p<0.01.

Limited preliminary optimization experiments with ACs determined that the addition of either 10% AB serum (Sigma Aldrich, UK), autologous serum, or autologous ascites enhanced phagocytosis compared to no additions, presumably due to the additional availability of opsonins for Fcγ-mediated phagocytosis (**Figure 3.11A-C**). Of these, 10% autologous ascites provided the best conditions (median 72.5%) for phagocytosis of BioParticles™. However, because the concentration of opsonins inevitably would have varied between the ascites of different patients and therefore impacted on phagocytosis, 10% donor AB serum was used for each sample instead of autologous ascites to assess the phagocytic capacity of the peritoneal macrophages independently of the presence of opsonins. A volume of 10μl of BioParticles™ (**Figure 3.11B**) and 60-minute duration (**Figure 3.11C**) were deemed optimal conditions.

Bacterial phagocytosis, as measured by percentage of peritoneal macrophages containing BioParticles™, was not significantly reduced when compared with healthy control monocytes (median 99.0% vs. 79.4%, p=0.21, Kruskal-Wallis test with Dunn's multiple comparison) (**Figure 3.12B**). Uptake was most similar to M2 macrophages; M1 monocyte-derived macrophages showed significantly impaired uptake compared to healthy monocytes (p<0.01). The differences in phagocytosis of M1 and M2 *in vitro* macrophages may be explained by the kinetics of phagosome maturation which has been demonstrated as delayed in M1 polarised macrophages (Canton, 2014). The intensity of particle uptake of the whole CD14+ population measured by MFI was not significantly increased in peritoneal macrophages compared with healthy monocytes (**Figure 3.12C**). Likewise, in CD14+ cells that had

taken up particles, the MFI was not significantly greater in peritoneal macrophages compared with healthy monocytes and M1 MDM (**Figure 3.12D**). Overall, the data did not demonstrate any significant differences in particle uptake in peritoneal macrophages compared to healthy cells suggesting preserved phagocytic capacity. When phagocytosis was analysed according the surface receptor expression, there was no significant difference in percentage and MFI between MerTK+ and MerTK- peritoneal macrophages (**Figure 3.12E**). However, Axl+ demonstrated a significantly enhanced phagocytic capacity than Axl- (%: 89.1 vs. 100%, $p<0.01$ and MFI: 17758 vs. 148987, $p<0.001$) despite Axl being present at relatively low levels. HLA-DR+ peritoneal macrophages had significantly greater percentage uptake than HLA-DR- (median: 47.3 vs. 87.4%, $p<0.01$) and greater MFI (3518 vs. 18589, $p<0.01$). Moreover, in this assay a higher percentage of CD14+ MerTK+ HLA-DR- peritoneal macrophages were identified in ACs at steady state (in the absence of BioParticles^{TM}) compared to healthy monocytes (median: 0.25 vs. 6.43%, $p<0.05$), confirming the observations from 3.3.2 (**Figure 3.12F**). This subset had impaired phagocytic capacity (median: 40.1 vs. 87.8%, $p<0.01$); CD14+ MerTK+ cells macrophages that had not taken up *E. coli* had a significantly higher percentage of HLA-DR- cells than those that had taken up *E. coli* (**Figure 3.12G**). Phenotypic changes in peritoneal macrophages after *E. coli* particle ingestion demonstrated a significant reduction in MerTK % (median: 69.1 vs. 42.4%, $p<0.05$) and MFI (552 vs. 150.5, $p<0.05$), significant increase in Axl MFI (610.5 vs. 1704, $p<0.01$) but no significant changes in Axl % or HLA-DR (%/MFI) (**Figure 3.12G&H**). No significant differences in phenotype were seen after particle uptake with healthy monocytes or M1/M2 *in vitro* MDMs (data not shown).

3.3.16. Peritoneal Macrophages from Patients with Cirrhosis have Impaired Oxidative Burst

Efficient pathogen killing involves the ability of myeloid cells to generate reactive oxygen species (ROS) after pathogen phagocytosis, also termed oxidative burst (Nüsse, 2011). Several reports suggest impaired circulating myeloid cell oxidative burst in patients with liver cirrhosis compared with healthy subjects (Bruns *et al.*, 2011; Panasiuk, 2005; Satsangi *et al.*, 2018). In order to assess the oxidative burst capacity of peritoneal macrophages from ACs, the Phagoburst^{TM} assay (Glycotope Biotechnology, Germany) was modified from the manufacturer's whole blood protocol (3.2.22).

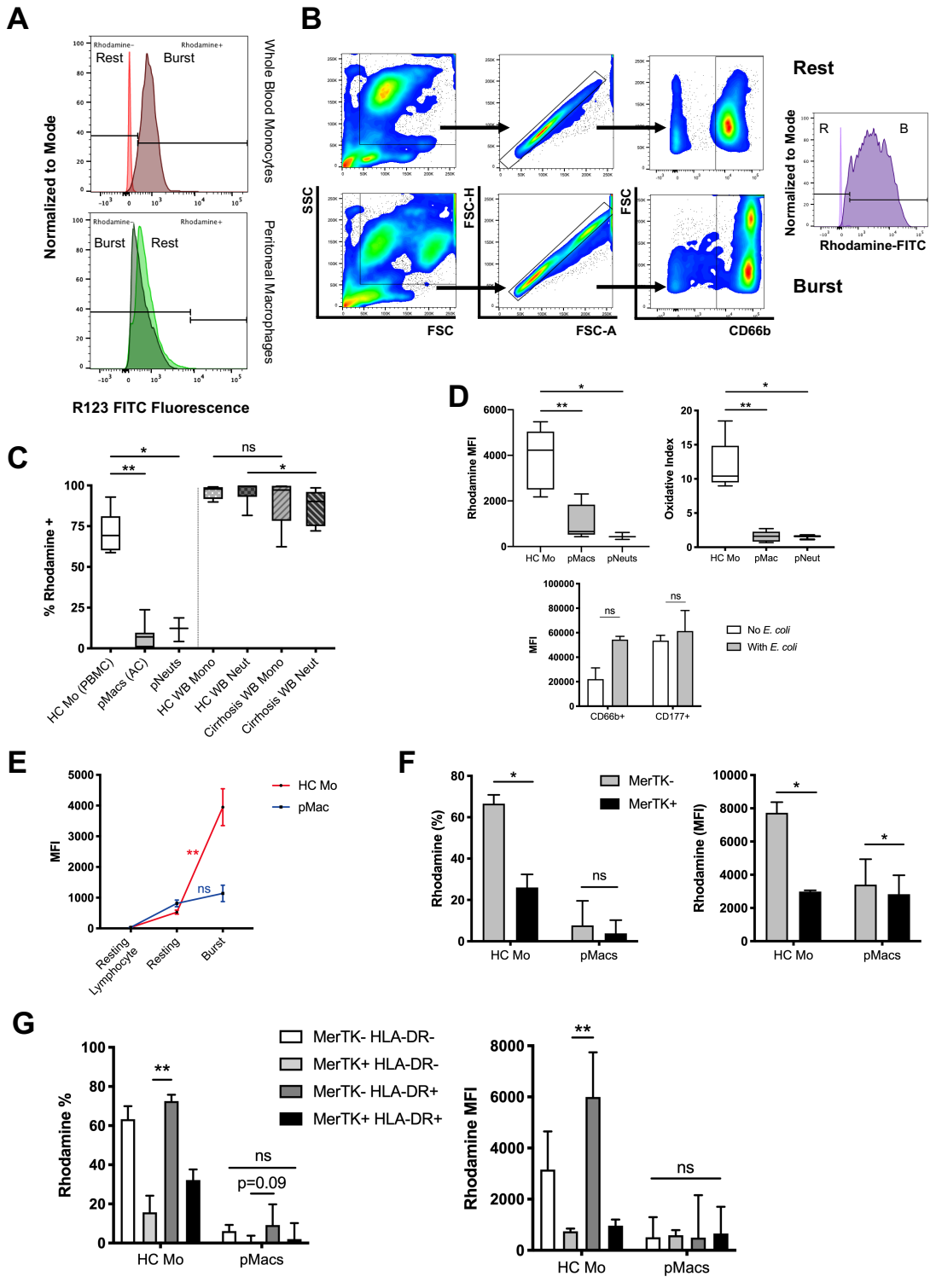


Figure 3.13 Peritoneal macrophage oxidative burst in patients with cirrhosis and ascites

(A) Histograms of rhodamine 123 fluorescence with and without *E. coli* stimulation of monocytes from whole blood (top) and peritoneal macrophages from ACs (bottom). (B) Whole blood neutrophil flow cytometry gating strategy: FSC-A vs. SSC-A to select granulocytes, FSC-H vs. FSC-A to exclude doublets, FSC-A vs. CD66b to select CD66b+ neutrophils and histogram demonstrating rhodamine 123 fluorescence shift on stimulation with *E. coli* (Burst, B vs. Rest, R). (C) Percentage healthy monocytes (from PBMCs, n=5) vs. peritoneal macrophages

(n=8) vs. peritoneal neutrophils (from ACs, n=3) producing ROS (% rhodamine); healthy control (HC) whole blood (WB) monocyte (Mo, n=5) and neutrophil (neut, n=6) and cirrhotic WB monocyte (n=5) and neutrophil (n=5) % rhodamine expression is displayed for comparison. (D) Rhodamine MFI (left) in healthy monocytes (PBMCs, n=5), peritoneal macrophages (n=8) and neutrophils (n=3, ACs) and oxidative index (right; ratio of unstimulated and stimulated mean fluorescence intensity); MFI expression of neutrophil activation markers CD66b and CD177 (n=3, bottom). (E) Comparison of rhodamine MFI in unstimulated (resting) lymphocytes vs. resting burst and *E. coli* stimulated burst in healthy control monocytes and peritoneal macrophages. (F) Association of MerTK expression and rhodamine % and MFI. (G) Association of MerTK+/- HLA-DR+/- with rhodamine % and MFI. Data expressed as median with IQR for column graphs and 5-95% percentile for box and whisker. Non-parametric statistical analysis for two groups with Mann Whitney and >2 groups with Kruskal-Wallis test with Dunn's multiple comparison. *p<0.05, **p<0.01

Whilst whole blood monocytes at rest had a narrow histogram, with clear shift on stimulation with *E. coli* ("burst"), the resting histogram for peritoneal macrophages was wide-based and there was no appreciable shift with stimulation, suggesting impaired oxidative burst (**Figure 3.13A**). Like monocytes, neutrophils from whole blood from a patient with cirrhosis, gated as CD66b+ cells, also demonstrated clear histogram shift on stimulation (**Figure 3.13B**). Evaluation of the percentage of rhodamine (a measure of the percentage of cells producing ROS) revealed peritoneal macrophages had significantly impaired oxidative burst compared with healthy control circulating monocytes (median: 69.3 vs. 7.0%, p<0.01), as did peritoneal neutrophils (69.3 vs. 12.3%, p<0.05) (**Figure 3.13C**). The difference between peritoneal macrophage and neutrophil % rhodamine was not significant (p=0.37). Whilst the whole blood protocol and ascites protocol differed and so results may not be directly comparable, healthy monocyte and neutrophil oxidative burst demonstrated a mean of >98% cells producing rhodamine, 89.0 % for circulating cirrhotic monocytes and 88.6% for cirrhotic neutrophils highlighting markedly improved burst of circulating cells compared to peritoneal macrophages, though the differences between circulating cells were not significant (p=0.48, Kruskal-Wallis). These trends in oxidative burst between healthy monocytes from PBMCs and peritoneal macrophages (same protocol) were mirrored in rhodamine MFI expression and oxidative index (**Figure 3.13D**). Although peritoneal neutrophil burst capacity was attenuated, there was evidence of neutrophil activation with *E. coli*, with increased CD66b and CD177 MFI expression, albeit not significant. Peritoneal macrophage burst activity was elevated at rest when compared with healthy monocytes and peritoneal lymphocytes. Whilst *E. coli* stimulation significantly upregulated rhodamine MFI in healthy monocytes (p<0.01),

there was no significant increase in peritoneal macrophages (**Figure 3.13E**). MerTK+ peritoneal macrophages were associated with significantly reduced rhodamine MFI for healthy monocytes (% and MFI, $p<0.05$) and for peritoneal macrophages (MFI only, $p<0.05$) (**Figure 3.13F**). In healthy monocytes, MerTK+ HLA-DR- cells demonstrated the lowest rhodamine MFI, but this was not observed at significance for peritoneal macrophages (**Figure 3.13G**). The CellROX^{TM} DeepRed assay was attempted as an alternative method to corroborate these findings but was not adequately optimized (Appendix L).

Overall, there was evidence of impaired oxidative burst on challenge with *E. coli* particles in peritoneal macrophages (and neutrophils), which had higher resting burst activity (as previously reported in circulating neutrophils in cirrhosis) compared with healthy monocytes with MerTK+ cells associated with lower burst activity than MerTK- populations (Tritto *et al.*, 2011).

3.3.17. Analysis of Secreted Factors in Ascites of Patients with ACLF Demonstrated Increased Pro-Inflammatory Cytokines TNF-α and IL-1β but no changes to TAM Ligands Compared to Patients with Cirrhosis without Organ Failure

Systemic inflammation associated with CAID is related to an increase in circulating levels of pro-inflammatory cytokines (e.g. IL-6) whilst increased concentrations of anti-inflammatory cytokines (e.g. IL-10) have been observed in cases of advanced disease and linked to immuneparesis (Clària *et al.*, 2016a). Some circulating cytokines have been found to have prognostic value, IL-10 associated with progression to death in ACLF (Fischer *et al.*, 2017). Analysis of acellular ascites with the MSD® Cytokine Multi-array assay was performed to investigate the cytokine profile in ascites of patients with decompensated cirrhosis and ACLF in order explore similar potential relationships. Analysis revealed significantly elevated pro-inflammatory cytokines TNF-α ($p<0.05$) and IL-1β ($p<0.05$) in ACLF ascites compared with cirrhosis without OF (**Figure 3.14**). IL-12p70 was raised in ACLF but not significant ($p=0.08$). There were no significant differences with other cytokines while a reciprocal trend with anti-inflammatory cytokine IL-10 was observed.

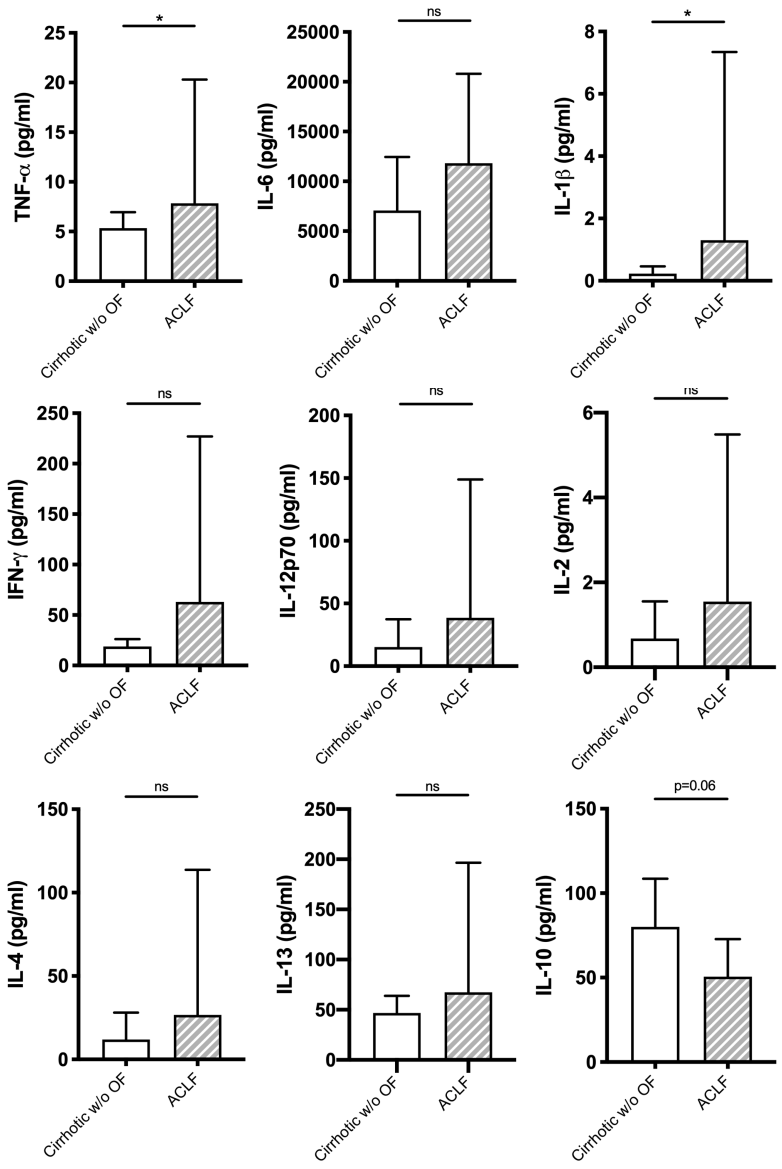


Figure 3.14 Ascites cytokine profile comparing cirrhosis without failure, ACLF and ovarian cancer patients

The acellular ascites from patients with cirrhosis without organ failure (n= 17) and ACLF (n=7) were analysed with a multi-array proinflammatory cytokine assay. Data expressed as median with IQR. Non-parametric statistical analysis for two groups with Mann Whitney. *p<0.05, **p<0.01

The ligands of the TAM receptors include Gas6 and Galectin-3, bridging molecules that facilitate activation of the signalling pathway (Lemke & Rothlin, 2008). Pros1 was not measured.

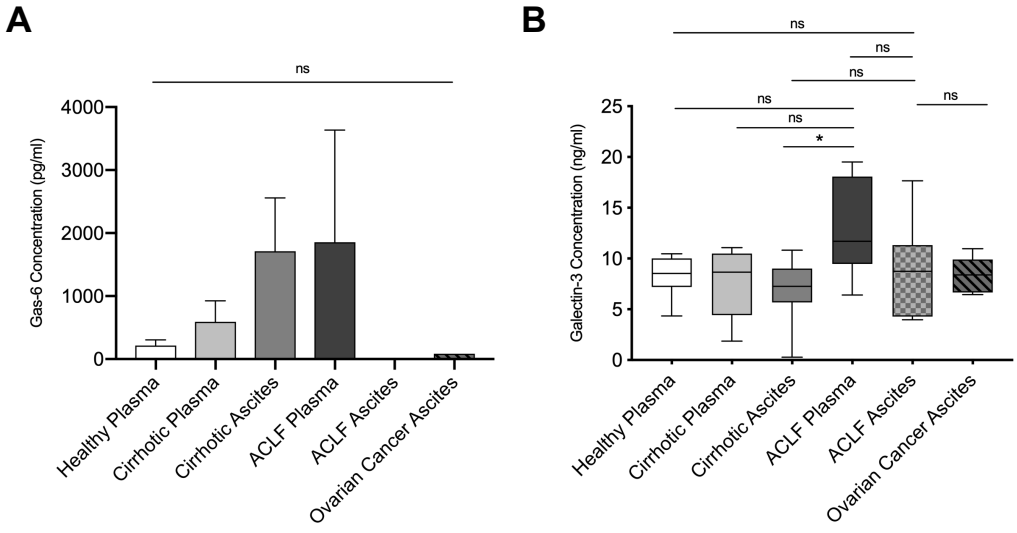


Figure 3.15 Gas6 and Galectin-3 Concentration in Plasma and Ascites

(A) Gas6 concentration (pg/ml) was measured by ELISA in healthy plasma (n=7), plasma of patients with cirrhosis without OF (n=20), ascites in cirrhosis without OF (n=16), ACLF plasma (n=4), ACLF ascites (n=5) and ovarian cancer ascites (n=6). Data is expressed as mean with standard error of mean. ns = not significant. (B) Galectin-3 concentration (ng/ml) was measured in healthy plasma (n=7), cirrhotic plasma (n=9), cirrhotic ascites (n=13), ACLF plasma (n=6), ACLF ascites (n=7) and ovarian cancer ascites (n=5). Data is expressed with box and whisker plots with 5-95% percentiles and median. Differences between groups are expressed with Kruskal Wallis with Dunn's multiple correction non-parametric statistical tests. *p<0.05, **p<0.01

Both have been described as pro-fibrogenic markers, with a progressive increase in their plasma or serum concentration correlating with higher degrees of fibrosis and severity of liver disease (Bellan, Castello & Pirisi, 2018; Gudowska *et al.*, 2015). Here their concentrations in plasma and ascites were measured by ELISA in patients with cirrhosis without organ failure and ACLF, and in healthy volunteer plasma and ovarian cancer ascites. Results from Gas6 analysis showed a higher mean concentration in ACLF plasma (median 107.5 pg/ml) compared to other groups (**Figure 3.15A**) but differences were not significant. Moreover, the range of concentration was 0 to 9954, with multiple results returning as zero within cirrhotic and ACLF plasma and ascites groups. Ascitic Gas6 inversely correlated with ascitic IL-12p70 (r_s = -0.572, p=0.026, n=15). The Galectin-3 results similarly showed highest concentrations in ACLF plasma; this was significantly elevated compared to healthy plasma when considered in

isolation (Mann Whitney, $p<0.05$). But with all groups considered, using the Kruskal-Wallis test and Dunn's multiple comparison, only a significant difference between ACLF plasma galectin-3 and cirrhotic ascites was detected ($p<0.05$) (**Figure 3.15B**). Plasma galectin-3 in the whole cirrhotic cohort (cirrhosis without OF and ACLF) correlated positively with plasma M65 ($r_s = 0.56$, $p=0.049$, $n=13$), MELD score ($r_s = 0.525$, $p=0.045$, $n=15$), CLIF-AD score ($r_s = 0.504$, $p=0.056$, $n=15$) and creatinine ($r_s = 0.629$, $p=0.012$, $n=15$).

3.3.18. Gene Expression Profiles of MerTK+ FACS Sorted Ascitic Cells Reveals an Immunotolerant Profile in Steady-State

Given the observation of a predominance of the MerTK+ subset of peritoneal macrophages compared to MerTK-, further characterisation of these subpopulations was sought by gene expression profiling. Ascitic cells (ACs) were labelled with monoclonal antibodies and FACS sorted as per 3.2.14. The transcriptomic profile of MerTK+ FACS-sorted ACs was compared with a baseline of MerTK- cells (**Figure 3.16A**). Gene set enrichment analysis with functional groupings revealed that in comparison with MerTK–, MerTK+ ascitic macrophages at steady state had multiple downregulated pathogen response genes including those involved in the NOD2-signalling pathway / inflammasome generation (e.g. *NOD2, NLRP3, CASP1, SYK* and *PYCARD*), downregulated neutrophil migration, activation and superoxide anion generation genes (e.g. *FPR1, FPR2, NCF2*), downregulated TLR- and IL-1-signalling genes (e.g. *MYD88, TRAF1, IL1RAP, IKBKE*), and downregulated *CCR2*. Upregulated genes involved the LXRα pathway (e.g. *NR1H3*), lipid metabolism / cholesterol efflux (e.g. *APOE, LIPA*) and C1q complement (e.g. *C1QA, C1QB, C1QC*) (**Figure 3.16B&C**). *APOE* had the highest fold change (41.3, $p=0.014$). There was no difference in the *GATA6*, *SOCS1*, *SOCS3* and *STAT1* gene expression when comparing between MerTK+ and MerTK- peritoneal macrophages.

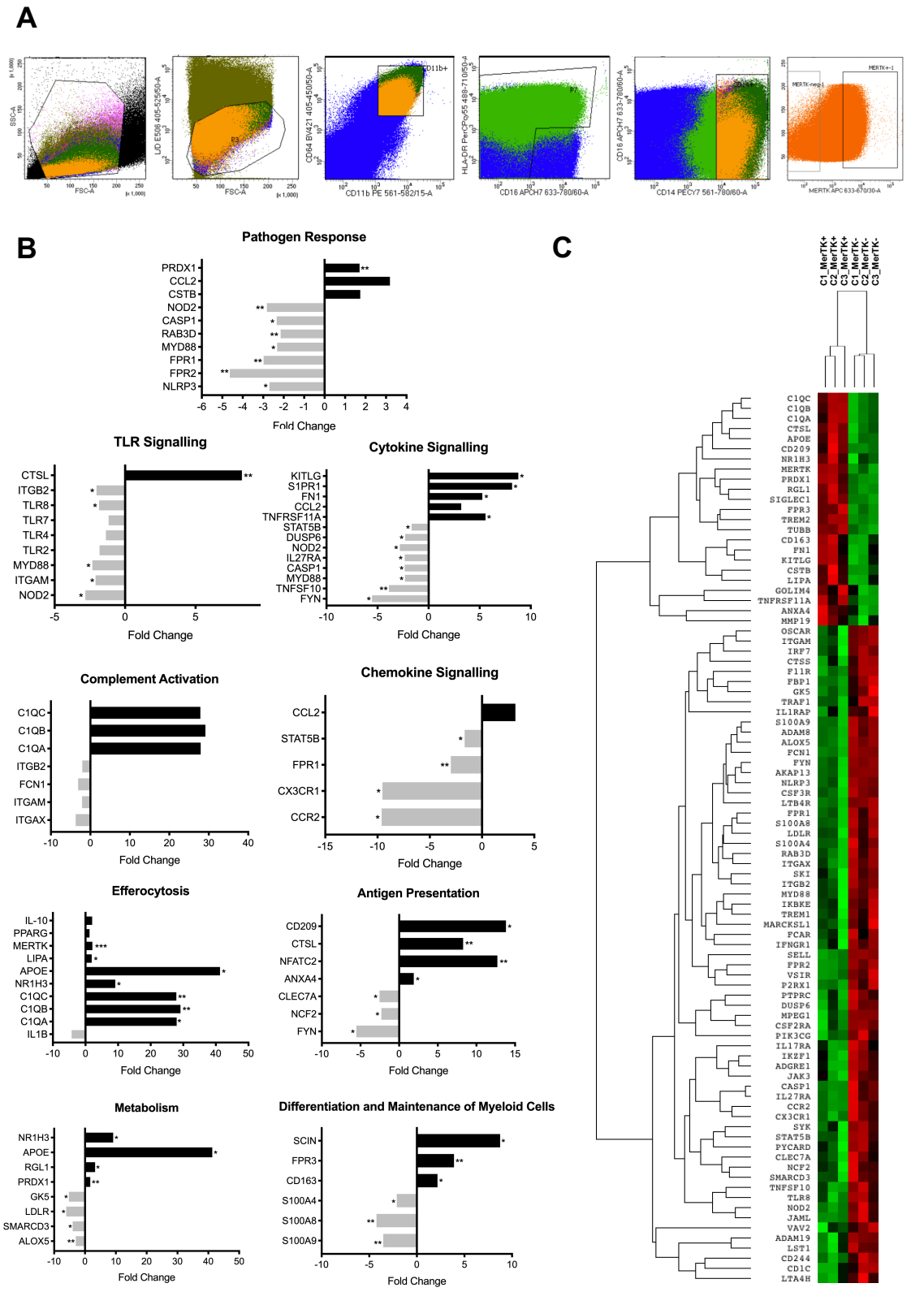


Figure 3.16 Gene expression pattern of MerTK+ vs. MerTK- ascitic cells in steady state

(A) Human MerTK+ and MerTK- macrophages were FACS-sorted in ascitic cells in patients with cirrhosis due to alcoholic liver disease without organ failure (n=3) with gating strategy displayed in representative plots. (B) Pure isolates of ascitic macrophage MerTK+/- subsets were quantitatively analysed by microarray gene

expression analysis and subsequent gene set analysis to group genes by biological function, with MerTK+ cells compared to MerTK- cells (=baseline; black bars indicate fold-increase in MerTK+ subset). Data show fold-change expression and (C) agglomerative cluster (heatmap, z-score; green =min, red=max magnitude of expression). *p<0.05 **p<0.01 ***p<0.001. SSC, side scatter, FSC, forward scatter.

3.3.19. LPS-Stimulated Transcriptomic Profile of Peritoneal Macrophages in Cirrhosis in Comparison with Monocyte-Derived Macrophages

FACS sorted peritoneal macrophages in the ascites of patients with cirrhosis according to MerTK+ or MerTK- were LPS-stimulated or unstimulated (PBS) with subsequent transcriptomic analysis (3.2.15). Pathway expression analysis was performed via online platform WebGestalt (Wang *et al.*, 2017). Genes are expressed as fold change from baseline and only genes with significance level $p<0.1$ were displayed in addition to selection method previously described (3.2.15). MerTK+ cirrhotic peritoneal macrophage gene expression was compared to MerTK- after LPS stimulation, which demonstrated that MerTK+ cells significantly upregulated genes related to the phagolysosome (e.g. cathepsin genes, *LIPA* and *FCGR3A*), cytokine signalling (e.g. *PTX3*) and macrophage polarisation (e.g. *SIGLEC-1* and *TREM-2*) (**Figure 3.17A&B**). Of note, Pentraxin-3 (*PTX3*) has been previously noted to attenuate LPS-induced inflammation in liver macrophages, triggering receptor expressed on myeloid cells-2 (*TREM-2*) to suppress LPS-induced NF-kB activation and Siglec-1, upregulated on endotoxin-tolerant cells, to suppress innate immune responses by TGF-β1 production (Turnbull *et al.*, 2006; Wu *et al.*, 2016; Perea *et al.*, 2017; Rosciszewski *et al.*, 2017). Although not significant, the upregulation of pro-efferocytic and anti-inflammatory genes *APOE* and *C1Q(A-C)* was also maintained in MerTK+ macrophages after LPS-stimulation as per steady-state data (**Figure 3.16B**). When MerTK+ monocyte-derived macrophages (MDMs) were stimulated with LPS, a classical inflammatory response was seen with enhanced TLR4 and NOD1/2 signalling cascades on pathway analysis (**Figure 3.17C**). *IL6* expression was ~200-fold ($p<0.01$), *IL1B* ~40-fold ($p<0.05$) and *TNF* ~10-fold ($p<0.05$). Counter-regulatory genes were also expressed including *SOCS1* ($p<0.05$) and *ACOD1* ($p<0.001$) (Mills *et al.*, 2018). In contrast, MerTK+ peritoneal macrophages stimulated with LPS (compared to PBS) do not display a similar inflammatory profile (**Figure 3.17D&E**). Instead, they upregulate a range of anti-inflammatory,

transcriptional repressor and anti-apoptotic genes to mitigate against LPS-induced cell injury, e.g. *IER3*, with over-representation pathway analysis suggesting binding and uptake of ligands by scavenger receptors (enrichment ratio 26.0, p=0.003) and IL-10 signalling (enrichment ratio 23.2, p=0.003) as the top enriched gene sets (Schott *et al.*, 2014; Wang *et al.*, 2017).

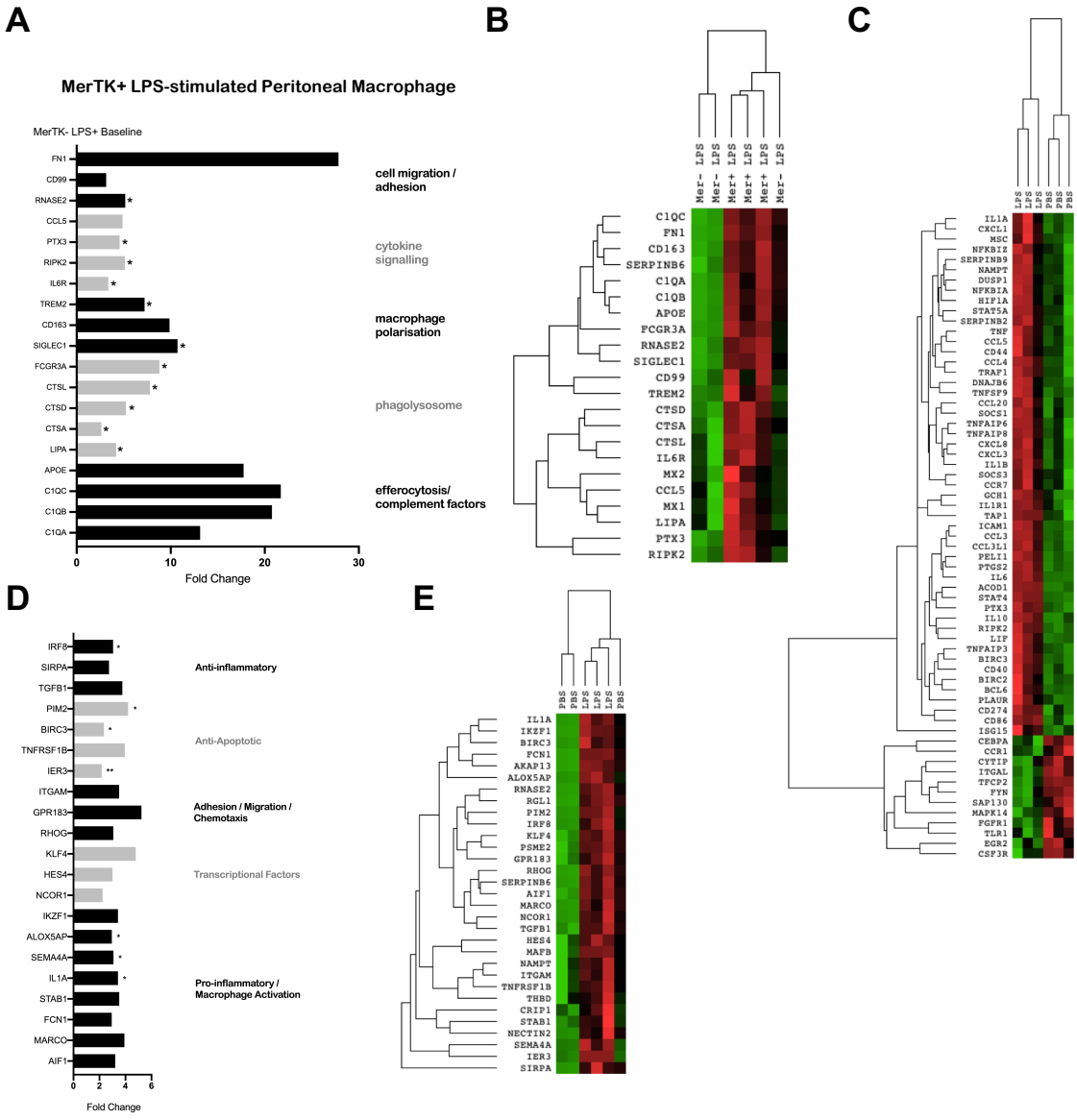


Figure 3.17 Gene expression profile of peritoneal macrophages and monocyte-derived macrophages sorted according to MerTK status and exposure to LPS

(A) LPS-stimulated MerTK+ vs. MerTK- (baseline) peritoneal macrophage gene expression (B) Agglomerative cluster heatmap of LPS-stimulated MerTK + vs. MerTK- peritoneal macrophages (C) Agglomerative cluster heatmap for MerTK+ monocyte-derived macrophages LPS vs. PBS (baseline) (D) Gene expression profile of MerTK+ peritoneal macrophages from patients with cirrhosis and ascites LPS vs. PBS (baseline) (E) Agglomerative cluster heatmap of MerTK+ pMac LPS vs. PBS. Heatmaps: z-score, green=min, red=max magnitude of expression. *p<0.05 **p<0.01

3.3.20. Ascites 16S Bacterial DNA was not Associated with Poor Clinical Outcomes or TAM Receptor Expression

Previous studies have observed an association between the ascites bacterial burden, as measured by quantitative PCR and 16S rRNA gene sequencing, reduction in HLA-DR peritoneal macrophage expression and early death and readmission in patients with decompensated cirrhosis (Fagan *et al.*, 2015). To investigate its relationship with TAM receptors and clinical factors, ascites bacterial DNA was measured (n=19) using 16S rRNA DNA qPCR as described in 3.2.26. All patients (except one for which the data is not shown graphically) did not have SBP or evidence of overt infection. The standard curve and amplification plots are shown in Appendix M. Ascites bacterial DNA showed no significant correlation (Spearman's rank) with *ex-vivo* peritoneal macrophage TAM receptor expression by percentage (MerTK: r= -0.176, p=0.566; Axl: r= -0.220, p=0.471; Tyro3: r= -0.490, p= 0.106) nor MFI (St. Mary's cohort only; MerTK: r= -0.441, p=0.152; Axl: r= -0.441, p=0.152; Tyro3: r= -0.545, p= 0.067). All demonstrated an inverse relationship, such that increasing ascitic bacterial DNA concentrations correlated with lower TAM receptor expression.

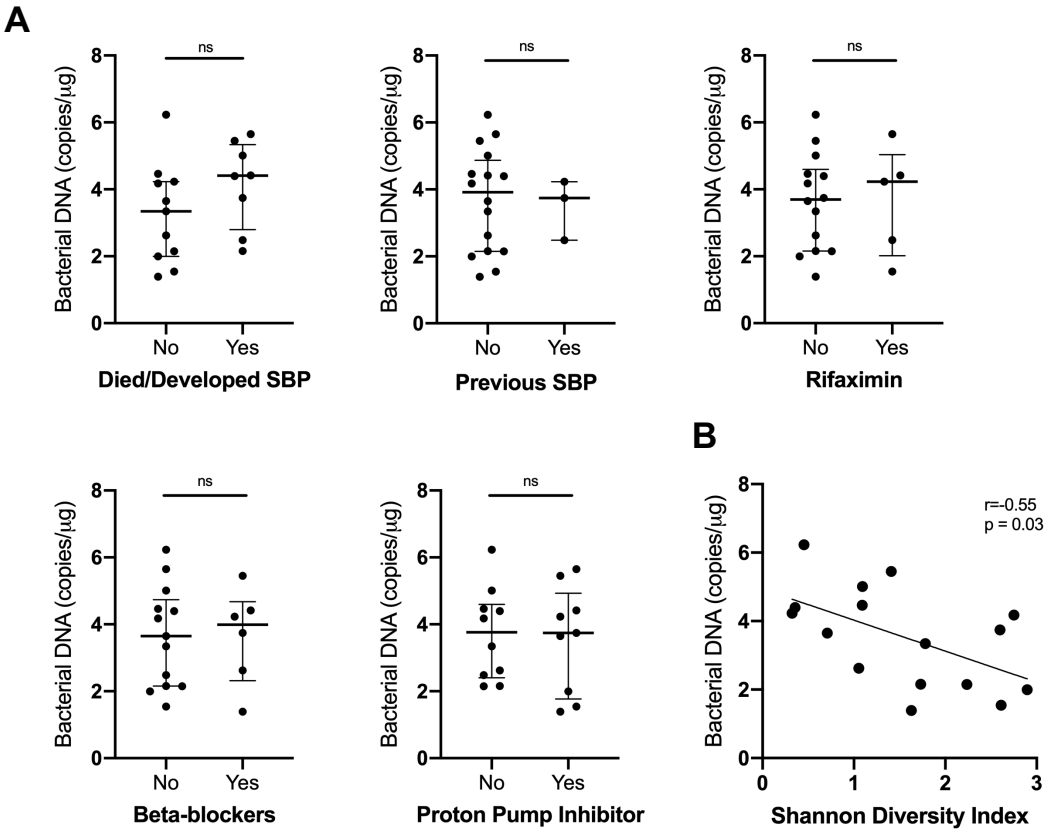


Figure 3.18 Ascites bacterial DNA according to outcome and relevant clinical parameters

(A) Ascites bacterial DNA (n=19, copies/µg) is compared between patients who died within 6 months of sampling or developed SBP, patients who had previous SBP, patients on rifaximin in previous 2 weeks, those on non-selective beta-blockers (propranolol or carvedilol) and proton pump inhibitors (B) Correlation of ascites bacterial DNA and species diversity (n=15) as quantified by the Shannon Diversity Index. Data is expressed as median with IQR, with non-parametric tests using Mann Whitney. Correlation using Spearman's coefficient. *p<0.05, **p<0.01

There was a significant but moderate positive correlation with platelet count (r_s = 0.470, p=0.043), the relevance of which is uncertain. However, there was no significant association with any other clinical, biochemical or immunological parameter including MELD score, ascitic white count, serum WCC (r_s = 0.404, p=0.086) or CRP. No significant differences were seen in ascites bacterial DNA between patients on rifaximin, non-selective beta blockers and proton pump inhibitors and those that were not (**Figure 3.18A**), nor in patients who had previous SBP compared with those that did not. Likewise, ascites bacterial DNA was not significantly different in patients who either died within the next 6-months or developed SBP subsequent to sampling, though there appeared to be a trend towards this

(p=0.13), as described in other reports (Fagan *et al.*, 2015). As species diversity increased, as quantified by the Shannon Diversity Index, the total ascitic bacterial DNA burden declined (**Figure 3.18B**). Shannon Diversity Index demonstrated a positive correlation with Axl MFI expression (r_s = 0.927, p<0.001, n=10) and negative correlation with serum neutrophil count (r_s = -0.450, p=0.053, n=19) of uncertain meaning. Species identified are graphically represented in Appendix N. Only one case had ACLF and so further work is required to establish the ascitic bacterial DNA burden in cirrhosis and organ failure. A patient with ACLF and concurrent SBP was excluded from the dataset which demonstrated a much larger bacterial DNA quantity (219.8 copies/μg DNA) compared to the mean (3.64 copies/μg DNA) and had only two dominant species (*Escherichia/Shigella* and unclassified *Enterobacteriaceae*).

3.3.21. Metabonomic Analysis of Ascites Reveals Switch to Anaerobic Metabolism in ACLF

Analysis of the ascites metabolome in ACLF potentially provides insight into the metabolic niche of the ascitic microenvironment in which immune cells reside. OPLS-DA analysis was able to generate a valid model for plasma CPMG to differentiate healthy control and patients with cirrhosis (both cirrhosis without organ failure and ACLF in same group) (**Figure 3.19A**). A 3-component model was used with $R^2Y=0.744$ and $Q^2Y=0.532$ (CV-ANOVA $p<0.001$). Only lactate ($p<0.05$) and glucose ($p<0.05$) were significantly higher in the cirrhosis group compared with healthy control (data not shown). Similarly, OPLS-DA was able to differentiate patients with ACLF and cirrhosis (without organ failure) in a valid model for both ascites CPMG (2 principle components with a $R^2Y=0.761$ and $Q^2Y=0.475$, CV-ANOVA $p<0.001$) and ascites NOESY (3 principle components with $R^2Y=0.771$ and $Q^2Y=0.381$, CV-ANOVA $p<0.05$) (**Figure 3.19B-C**). The loadings plot identified alanine, acetone and lactate as the key ascitic discriminators in ACLF compared to cirrhosis without organ failure (**Figure 3.19D**)

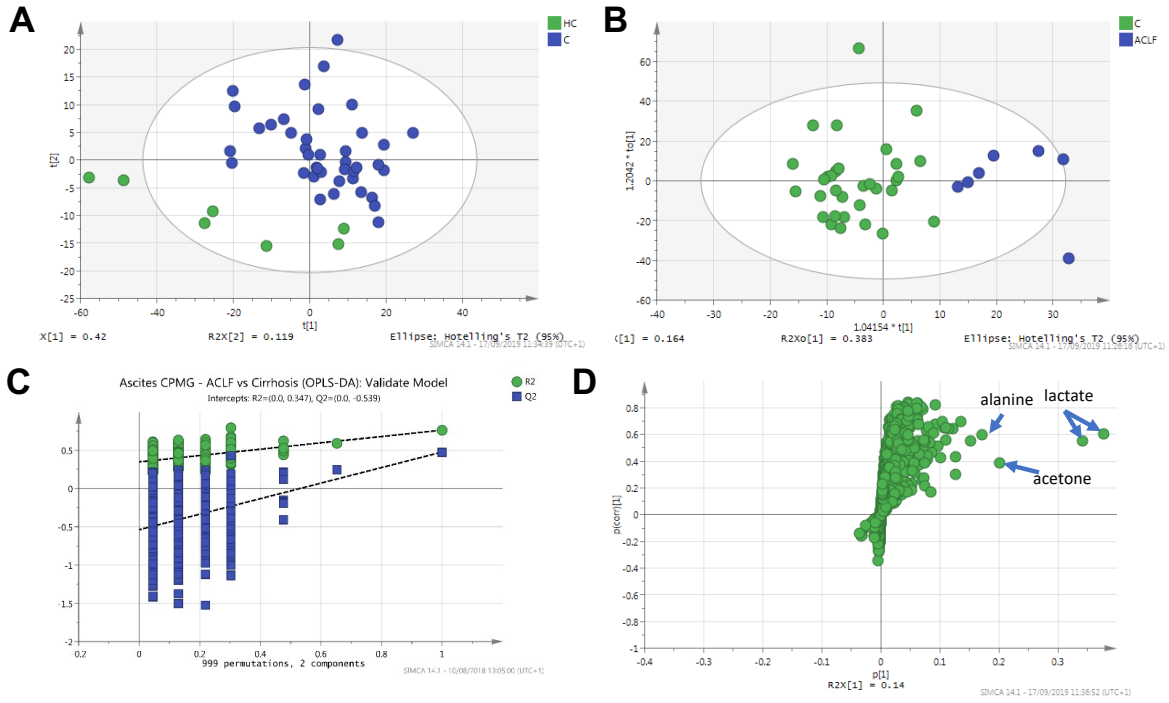


Figure 3.19 Score Scatter and Permutation Plots in a Valid OPLS-DA Model for Ascites CPMG

^{1}H-NMR Ascites Profile Models. (A) Plasma OPLS-DA PCA showing discrimination between healthy control (HC, green) and any cirrhosis (C, combination of cirrhosis without organ failure and ACLF groups, blue) X-axis = first principle component and Y-axis = second principle component. (B) Ascites CPMG OPLS-DA with cirrhosis without organ failure (green, n=32) and ACLF (blue, n=7). (C) Permutation plot for (B) Permutation plot – 999 random generated models; the validated model is on the right whilst on the left the random generated

models with lower correlation (x-axis) values compared to the validated model and lower R^2 and Q^2. (D) S-plot loadings for ascites of cirrhosis vs. ACLF highlighting lactate, alanine and acetone as the most important variables in ACLF.

Analysis of each metabolite revealed that lactate, methionine, N-acetylated glycoproteins, alanine, glutamine, acetone and creatinine were significantly elevated in the ascites of ACLF patients compared with patients with cirrhosis without OF. There was also a trend towards increased ascitic lipids in ACLF (p=0.068) (**Figure 3.20**). Lipids correlated with cell death markers M30 and M65 in ascites (**Figure 3.21**). *Ex-vivo* peritoneal macrophage MerTK (%) expression did not correlate with any metabolite.

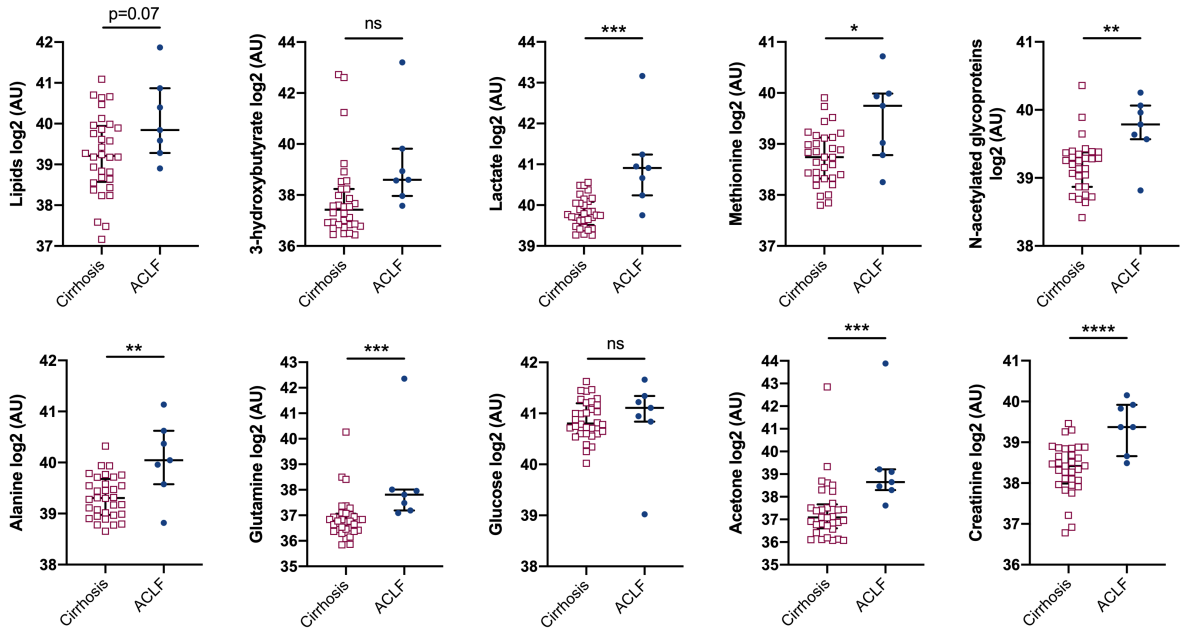


Figure 3.20 Ascites Metabonomic Analysis Reveals Switch to Anaerobic Metabolism in ACLF Compared to Cirrhosis without Organ Failure

Metabonomic analysis of ascites from patients with cirrhosis without organ failure (n=32) and ACLF (n=7) demonstrating differences in selected metabolites expressed as log2 of arbitrary units (AU): lipids (including LDL and VLDL), 3-hydroxybutyrate, lactate, methionine, N-acetylglycoproteins, alanine, glutamine, glucose, acetone and creatinine. Statistical analysis evaluated normality of distributions of each metabolite by the Shapiro-Wilk test. Tests for differences between groups were unpaired Student's t-test for normal distributions (only creatinine and glucose) or Mann-Whitney U for non-parametric analysis (the remainder). *p<0.05, **p<0.01, ***p<0.001, ****p<0.0001.

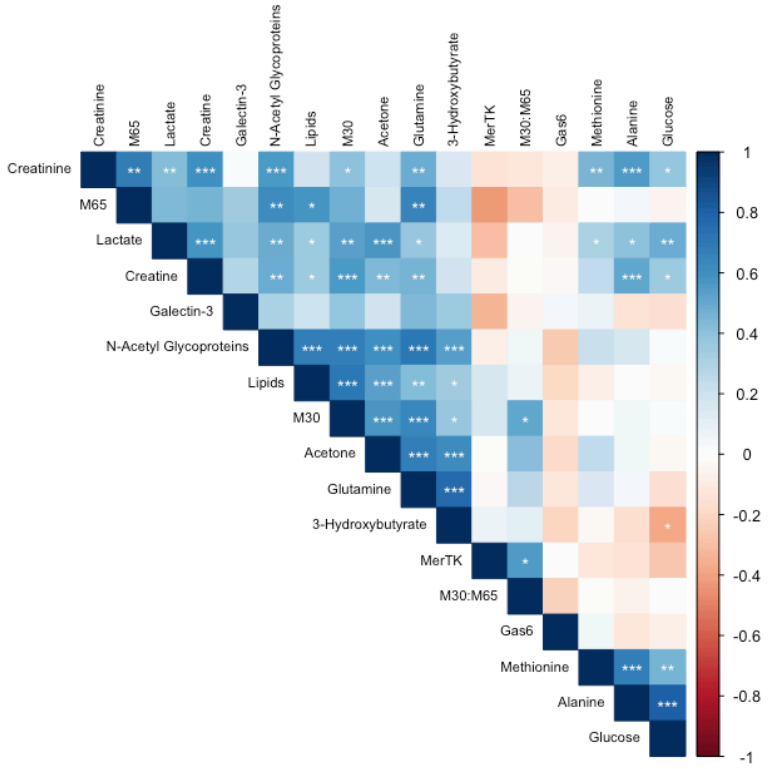


Figure 3.21 Correlation Matrix of Ascites Metabolites Revealing Metabolically-Stressed Peritoneal Compartment in ACLF

Correlation matrix (Spearman's rank) with hierarchical clustering of metabolites measured on ascites CPMG OPLS-DA, cell death markers M30 and M65 (and their ratio M30:M65), percentage of CD14+ peritoneal macrophages expressing MerTK (%), TAM receptor ligands Gas6 and Galectin-3. *p<0.05, **p<0.01, ***p<0.001.

3.3.22. Clinical Associations of Immunological and Soluble Mediator Parameters

No significant difference in peritoneal macrophage *ex-vivo* phenotype was identified in patients with cirrhosis without OF and patients with ACLF (Table 3.3). As previously described, M30, M65, TNF-α and IL-1β were significantly elevated in ACLF ascites. Comparing survivors to non-survivors at 90-days, lower creatinine (likely a surrogate of being on haemofiltration), higher WCC and neutrophil count, higher MELD and CLIF-C AD scores were significant (

Table 3.4). MerTK% was higher in non-survivors but was not significant (p=0.08). Elevated plasma M65, plasma M30 and ascites M30 were also observed in the non-survivor group. Reduction in ascitic IL-2 and increase in IL-1β were seen. Plasma galectin-3 was elevated in non-survivors but this did not

reach significance (p=0.08). Univariate regression analysis was performed to identify predictor variables in patients who subsequently develop SBP after ascitic sampling. Patients who died were excluded; no patients died from SBP in this cohort. The only significant predictor was plasma lymphocyte count (p<0.01) but proton pump inhibitor (PPI) use (p=0.09) and MELD score at paracentesis (p=0.1) demonstrated a trend. Ascitic total protein, ascitic bacterial DNA quantity and previous SBP, described as predictors in the literature, did not show significance (Table 3.5). When the former three variables were assessed by multivariate regression analysis (enter method), lymphocyte count (OR 107, p=0.02) and PPI use (OR 0.26 p=0.05) were statistically significant but in combination with the known risk factors for SBP, no variable was significant. The analysis is limited by small numbers of patients who developed SBP (n=8) so an expanded dataset would be valuable.

Table 3.3 *Immunometabolic Variables in Ascites of Patients with Cirrhosis without Organ Failure compared with ACLF*

Variable	Cirrhosis w/o OF (n=43)	ACLF (n=9)	p-value
pMac *ex-vivo* Phenotype (%)			
CD14++ CD16++	31.4 [12.3-81.0]	49.2 [32.6-50.9]	0.308
MerTK	80.3 [23.3-91.8]	68.6 [55.9-91.9]	0.726
Axl	2.34 [1.00-4.80]	1.36 [0.47-2.24]	0.209
Tyro3	49.1 [8.35-98.4]	-	-
HLA-DR	95.8 [44.4-99.9]	89.2 [72.9-97.2]	0.524
MerTK+ HLA-DR-	1.43 [0.00-48.30]	8.36 [0.07-12.20]	0.923
CD163	56.1 [22.2-90.3]	-	-
pMac *ex-vivo* Phenotype (MFI)			
MerTK (KCH)	3072 [1246-11171]	4343 [1392-5688]	0.734
MerTK (STM)	3452 [2236-6067]	-	-
Axl (STM)	714 [312-1302]	-	-
Tyro3 (STM)	4520 [441-7269]	-	-
HLA-DR (KCH)	16769 [1594-44656]	22614 [1108-44119]	0.154
HLA-DR (STM)	14516 [7782-20569]	-	-
CD16 (STM)	2676 [687-7596]	-	-
CD16 (KCH)	7317 [1002-16769]	5270 [4008-6531]	0.769
M65 Concentration (U/L)			
M65 Plasma	311 [161-4274]	3238 [870-8470]	**0.003**
M65 Ascites	1651 [307-4400]	5432 [2790-9420]	**0.003**
M65 Ascites:plasma ratio	5.15 [0.29-14.79]	1.83 [0.18-3.30]	**0.027**
M30 Concentration (U/L)			
M30 Plasma	485 [123-2222]	2026 [704-10335]	**0.019**
M30 Ascites	502 [313-2017]	2173 [1368-3358]	**0.007**
M30 Ascites:plasma ratio	1.47 [0.14-4.28]	1.45 [0.13-4.42]	0.638
Ascites cytokine concentration (pg/ml)			
TNF-α	10.83 [7.11-14.56]	20.29 [16.02-42.59]	**0.047**
IL-6	1803 [1579-2028]	20811 [8320-21711]	0.166
IL-4	3.54 [3.51-3.57]	113.67 [22.56-155.93]	0.130
IL-2	6.05 [0.243-11.86]	4.25 [1.54-9.22]	0.113
IL-1β	0.47 [0.15-0.80]	3.41 [1.30-11.29]	**0.019**
IL-13	33.23 [22.19-44.27]	196.63 [57.45-277.72]	0.252
IL-12p70	5.19 [4.16-6.23]	148.95 [21.27-171.28]	0.087
IL-10	31.20 [29.34-33.04]	57.28 [13.70-112.20]	0.418
IFN-γ	87.36 [16.45-158.27]	100.21 [25.77-269.15]	0.226
Gas6 / Galectin-3 Concentration			
Ascitic Gas6	64 [0-2056]	0 [0-36]	0.179
Plasma Gas6	190 [27-6305]	107 [0-7199]	0.575
Ascitic Galectin-3	8.11 [1.32-10.45]	8.29 [3.97-17.66]	0.351
Plasma Galectin-3	7.47 [2.59-10.08]	10.79 [6.41-19.50]	**0.026**

Table 3.4 *Clinical and Immunometabolic variables Comparing Survivors and Non-survivors at 90 days*

Variable	Survivors (n=39)	Non-survivors (n=13)	p-value
Clinical Parameters			
Age	58 [29-72]	57 [36-84]	0.664
INR	1.88 [1.41-2.41]	3.01 [1.50-4.53]	0.205
Albumin	31 [22-34]	27 [25-29]	0.727
Total Bilirubin	61 [17-84]	139 [24-253]	0.054
ALT	31 [25-35]	27 [26-28]	0.12
Na	133 [131-136]	133 [132-134]	0.211
Creatinine	116 [45-174]	98.5 [94-103]	**0.003**
Mean Platelet Volume	7.5 [6.9-8.7]	7.9 [7.3-8.4]	0.068
Total white cell count	5.91 [5.37-19.25]	9.10 [7.47-10.73]	**0.029**
Neutrophils	3.86 [2.62-15.36]	7.20 [5.57-8.84]	**0.008**
Monocytes	0.66 [0.38-0.81]	0.41 [0.39-0.43]	0.762
Lymphocytes	1.00 [0.30-2.02]	1.04 [0.40-2.50]	0.719
Platelets	115 [77-149]	95 [80-109]	0.512
C-Reactive Protein	27.4 [11-35]	18.3 [17-20]	0.847
Ascites WCC	130 [42-360]	60 [54-66]	0.838
Ascites total protein	21.5 [18-41]	11.0 [8-14]	0.376
Serum-ascites albumin gradient	17 [14-24]	21.5 [21-22]	0.328
Hepatic Disease Severity Scores			
MELD score at paracentesis	17 [7-31]	29 [13-45]	**0.007**
CLIF-C AD Score	52.6 [42.9-76.4]	59.8 [47.7-78.1]	**0.012**
pMac *ex-vivo* Phenotype (%)			
CD14++ CD16++	31.4 [12.3-81.0]	32.3 [13.9-49.2]	0.720
MerTK	80.5 [64.6-89.5]	90.7 [68.6-91.9]	0.082
Axl	2.44 [1.00-4.80]	1.78 [0.47-2.34]	0.127
Tyro3	49.1 [11.6-98.1]	8.35 [2.55-98.4]	0.456
HLA-DR	96.4 [44.4-99.9]	91.6 [72.9-96.2]	0.390
MerTK+ HLA-DR-	1.15 [0-48.3]	6.48 [2.97-12.2]	0.144
pMac *ex-vivo* Phenotype (MFI)			
MerTK (KCH)	3352 [1246-11171]	2868 [1392-4343]	0.686
MerTK (STM)	3490 [2236-6267]	3483 [3420-5136]	0.885
Axl (STM)	752 [312-1302]	692 [574-1032]	0.937
Tyro3 (STM)	4520 [441-7269]	954 [801-6733]	0.692
CD16 (STM)	2676 [687-7596]	3863 [2837-4150]	0.368
HLA-DR (STM)	15312 [7782-20569]	14151 [10271-16458]	0.659
M65 Concentration (U/L)			
M65 Plasma	311 [161-4274]	2892 [870-8470]	**0.029**
M65 Ascites	1800 [1119-4400]	4888 [2790-9402]	0.131
M65 Ascites : plasma ratio	5.15 [0.29-14.79]	1.76 [0.18-8.18]	**0.047**
M30 Concentration (U/L)			
M30 Plasma	485 [123-2222]	2026 [760-10335]	**0.012**
M30 Ascites	502 [313-2017]	2173 [1000-3358]	**0.022**
M30 Ascites:plasma ratio	1.50 [0.14-4.28]	0.98 [0.13-4.42]	0.257
Ascites cytokine concentration (pg/ml)			
TNF-α	10.83 [7.11-14.56]	20.29 [16.02-42.59]	0.169
IL-6	1803 [1578-2028]	20810 [8320-21711]	0.953
IL-4	3.54 [3.51-3.57]	113.67 [22.56-155.93]	0.726
IL-2	6.05 [0.243-11.86]	4.25 [1.54-9.22]	**0.018**
IL-1β	0.47 [0.15-0.80]	3.41 [1.30-11.29]	**0.005**
IL-13	33.23 [22.19-44.27]	196.63 [57.45-277.72]	0.299
IL-12p70	5.19 [4.16-6.23]	148.95 [21.27-171.27]	0.599
IL-10	31.20 [29.35-33.04]	57.28 [13.70-112.20]	0.411
IFN-γ	87.36 [16.45-158.27]	100.21 [25.78-269.15]	0.864
Gas6 / Galectin-3 Concentration			
Ascitic Gas6	0 [0-2056]	0 [0-35]	0.535
Plasma Gas6	320 [27-7199]	85 [0-130]	0.923
Ascitic Galectin-3	8.84 [1.31-10.45]	7.74 [3.97-17.66]	0.305
Plasma Galectin-3	8.67 [2.59-11.08]	10.50 [6.41-19.50]	0.075

Ascites Bacterial DNA Quantity			
16S Bacterial DNA	3.34 [1.39-6.23]	4.46 [4.40-5.45]	0.307
Shannon Diversity Index	1.73 [0.32-2.90]	1.09 [0.36-1.41]	0.421

Table 3.5 *Univariate analysis for clinical and immunometabolic variables for development of SBP*

Characteristics	Odds ratio	95% CI	p-value
Clinical Parameters			
Age	1.017	0.941-1.098	0.677
INR	0.167	0.014-2.040	0.161
Albumin	0.996	0.893-1.112	0.950
Total Bilirubin	0.978	0.951-1.006	0.120
ALT	0.993	0.961-1.026	0.664
Na	1.063	0.891-1.268	0.495
Creatinine	1.001	0.990-1.013	0.990
Mean Platelet Volume	1.178	0.773-1.795	0.447
Total white cell count	0.953	0.786-1.156	0.626
Neutrophils	0.853	0.616-1.181	0.339
Monocytes	5.764	0.472-70.359	0.170
Lymphocytes	36.618	2.417-554.858	**0.009**
Platelets	1.008	0.996-1.020	0.194
C-Reactive Protein	0.973	0.908-1.043	0.439
Ascites WCC	1.003	0.995-1.012	0.451
Ascites total protein	1.034	0.920-1.162	0.572
Serum-ascites albumin gradient	1.078	0.818-1.420	0.595
Previous SBP	3.73	0.492-28.327	0.203
Medications			
Rifaximin	2.875	0.502-16.477	0.236
Proton pump inhibitors	6.923	0.734-65.259	0.091
Non-selective beta blockers	2.400	0.445-12.939	0.308
Hepatic Disease Severity Scores			
MELD score at paracentesis	0.886	0.767-1.024	0.101
CLIF-C AD Score	0.931	0.836-1.037	0.194
Child Pugh Score	0.758	0.483-1.189	0.227
pMac *ex-vivo* Phenotype (%)			
CD14++ CD16++	0.957	0.887-.032	0.256
MerTK	1.021	0.955-1.090	0.545
Axl	1.089	0.44-4-2.670	0.853
Tyro3	1.002	0.973-1.032	0.878
HLA-DR	0.983	0.930-1.039	0.534
CD163	0.962	0.850-1.090	0.544
pMac *ex-vivo* Phenotype (MFI)			
MerTK (KCH)	1.000	0.999-1.001	0.689
MerTK (STM)	1.000	0.999-1.000	0.315
Axl (STM)	0.999	0.995-1.003	0.708
Tyro3 (STM)	1.000	1.000-1.000	0.877
CD16 (STM)	1.000	0.999-1.000	0.659
HLA-DR (STM)	1.000	0.999-1.000	0.141
M65 Concentration (U/L)			
M65 Plasma	1.000	0.999-1.000	0.307
M65 Ascites	1.000	0.999-1.000	0.461
M65 Ascites : plasma ratio	1.225	0.941-1.594	0.132
M30 Concentration (U/L)			
M30 Plasma	0.999	0.998-1.001	0.300
M30 Ascites	0.999	0.997-1.000	0.134
M30 Ascites:plasma ratio	0.879	0.515-1.498	0.635
Ascites cytokine concentration (pg/ml)			
TNF-α	1.025	0.982-1.071	0.260
IL-6	1.000	1.000-1.000	0.936
IL-4	0.989	0.945-1.035	0.629
IL-2	1.296	0.899-1.86	0.164
IL-1β	0.311	0.014-6.888	0.460
IL-13	0.984	0.915-1.058	0.661
IL-12p70	0.992	0.956-1.028	0.644
IL-10	1.002	0.978-1.026	0.893
IFN-γ	1.000	0.984-1.016	0.980

Gas6 / Galectin-3 Concentration			
Ascitic Gas6	1.000	0.999-1.000	0.520
Plasma Gas6	1.000	1.000-1.001	0.371
Ascitic Galectin-3	0.856	0.633-1.157	0.311
Plasma Galectin-3	0.893	0.675-1.180	0.425
Ascites Bacterial DNA Quantity			
16S Bacterial DNA	1.497	0.684-3.275	0.313
Shannon Diversity Index	1.536	0.430-5.483	0.509

Comparing patients who remained alive from time of sampling who developed subsequent SBP (n=8) and those without subsequent SBP (n=31). Statistical tests: Non=parametric Mann-Whitney U test performed for differences between groups. All values are displayed as median with ranges in brackets. Abbreviations: KCH – King's College Hospital; STM – St. Mary's Hospital; INR – international normalised ratio; SBP – spontaneous bacterial peritonitis.

3.4. Discussion

3.4.1. Ascitic Macrophage Phenotype, Cytokines, Mediators and Bacterial DNA

In this chapter, the hypothesis that the peritoneal compartment in patients with cirrhosis and ascites is an immunotolerant microenvironment, especially in ACLF and is characterised by MerTK+ macrophage expansion, is supported in a multitude of ways. Exposure to ACLF ascites increased monocyte and THP-1 macrophage MerTK MFI expression. Whilst not significant, monocyte HLA-DR expression was diminished and the immunosuppressive MerTK^{high} HLA-DR$_{low}$ and M-MDSC subsets were expanded. Here, MerTK MFI expression was associated with higher 28-day and 90-day mortality. Since MerTK is a macrophage differentiation marker, almost all cells cultured in ascites over 48 hours were MerTK+ and so MerTK % could not be used to quantify expression (Xue *et al.*, 2014). Changing the experimental conditions, e.g. lower % of ascites, may improve discrimination. The observation of a reciprocal reduction in Axl monocyte expression compared with MerTK on exposure to ascites is supported by studies to suggest that tolerogenic stimuli such as dexamethasone increase MerTK mRNA production and inhibit Axl mRNA whereas inflammatory stimuli such as LPS achieves the opposite (Zagórska *et al.*, 2014).

The increase in the MerTK+ HLA-DR- subset seen in PBMCs conditioned in ACLF plasma is relevant because this subset has been previously described as immunosuppressive (Antoniades *et al.*,

2012; Bernsmeier *et al.*, 2015; Triantafyllou *et al.*, 2018a). Moreover, in a second immunosuppressive mechanism, ACLF ascites also promotes a switch towards an M-MDSC-like phenotype; M-MDSCs are known to have immunosuppressive properties and have been identified in variety of disease states including in the circulation of ACLF patients, where they have impaired antimicrobial responses (Bernsmeier *et al.*, 2018). However, M-MDSCs do not have significantly different MerTK expression in comparison to their HLA-DR+ monocyte counterparts. *Ex-vivo* characterisation of peritoneal M-MDSC-like cells suggested lower MerTK expression compared to peritoneal macrophages in stable cirrhosis but no difference in AD-ACLF. Ovarian cancer ascites, used here as a pathological control and previously described as an immunosuppressive environment has similar properties (Giuntoli *et al.*, 2009). The anti-inflammatory M2c phenotype ($MerTK^{high}$ $HLA\text{-}DR_{low}$ $CD163^{high}$) appears to be promoted by cytokines IL-10 in combination with IL-17 though the positive correlation of MerTK MFI and ascitic IL-10 did not reach significance, and ascitic IL-17 was not measured. The significant positive correlation between monocyte MerTK MFI in PBMCs exposed to ascites and cell death marker M65 in the ascites, and between M-MDSC % and M65, suggests that cell death in the peritoneal compartment is enhanced in ACLF, either through cellular turnover or accumulation of cell death products from other sites, and may play a role in promoting an immunotolerant microenvironment. In ACLF, perhaps this is due to hepatocyte injury with leakage of apoptotic/necrotic debris into the adjacent ascites, or reflects the circulatory compartment. Perhaps it reflects inadequate clearance from the peritoneal compartment or maybe even mesothelial cell death in the setting of a stressed metabolic environment. This requires further mechanistic exploration. The positive correlation of M-MDSCs and IL-2 is also intriguing, the latter potentially functioning to downregulate T-cell responses in the setting of persistent exposure to self-antigens (Bachmann & Oxenius, 2007). In these ascites-conditioning experiments, only a switch to an M-MDSC-like phenotype was measured; true determination of M-MDSCs require proof by demonstrating inhibition of proliferation or IFN-γ production by T-cells (Peranzoni *et al.*, 2010; Bronte *et al.*, 2016).

Ex-vivo phenotyping of peritoneal macrophages revealed a $MerTK^{high}$ Axl_{low} profile with co-expression of other immunotolerant surface markers on the MerTK+ subset including CD163, CD206 and PD-1. However, whilst historically regarded as polarised and labelled M1 or M2,

macrophages do in fact exhibit plasticity; MerTK+ peritoneal macrophages likewise also exhibit higher proportions of Fc-gamma receptor CD16, antigen-presenting markers HLA-DR and CD86, and homing markers CCR5 (tissue) and CCR7 (lymph node), suggesting they may be primed for antigen presentation, phagocytosis and some may migrate to lymph nodes (Seki *et al.*, 1998; Gordon, Plueddemann & Estrada, 2014; Hume, 2015). They may represent macrophage-DC hybrids. Tyro3 expression on peritoneal macrophages was highly variable and so its significance is unclear. The MerTK+ subset had higher expression of Axl and Tyro3 suggesting a tendency for co-expression of TAM receptors though the biological relevance of MerTK in this compartment appeared the greatest. MerTK expression was comparatively higher in peritoneal macrophages from cirrhotic ascites than ovarian cancer ascites and higher compared with *in vitro* healthy monocyte-derived macrophages. When compared with circulating monocytes from the same patients, matched MerTK% expression is much higher in peritoneal macrophages. The relevance of positive correlation of MerTK% with MPV and GPR is uncertain; both are measures of fibrosis and limited data (unpublished) suggests MerTK may have a hepatic pro-fibrogenic role (Pastore *et al.*, 2018).

Axl signalling in chronic inflammatory disease is incompletely understood but divergence in the function of MerTK and Axl has been previously recognised, with Axl upregulated in inflammatory environments and MerTK expressed with immunosuppressive stimuli (Zagórska *et al.*, 2014). This may explain why Axl% expression was inversely correlated with immunosuppressive MerTK+ HLA-DR- peritoneal macrophage subsets. Cells that respond to LPS and produce more intracellular TNF-α and IL-6 may correspondingly increase Axl mRNA and surface expression hence their association. That said, Axl expression on peritoneal macrophages in very low (0-10%) and so makes a minor contribution to the overall profile.

Of note, clinical correlations with phenotypic markers revealed a significant inverse correlation of the percentage of peritoneal macrophages expressing surface CD163 and MELD score. The shed receptor, soluble CD163 (sCD163), in the circulation has previously been described as a macrophage activation marker and found to correlate with markers of gut permeability (e.g. endotoxin) and predict short-term mortality particularly in patients with AD and concurrent bacterial infection (Tornai *et al.*,

2016; Rainer *et al.*, 2018). Further work to evaluate sCD163 in ascites may prove interesting, especially to see if it could predict SBP.

To characterise the ascitic microenvironment further, several immunometabolic markers were measured in ascites. Cytokeratin-18 products M30 and M65 are markers of cellular apoptosis and necrosis respectively and their serum concentrations have been previously shown to reflect liver disease severity and predict outcome (Oweira *et al.*, 2018). These cell death markers have never previously been measured in ascites; here, it was demonstrated that both M30 and M65 were elevated in ascites compared with plasma, and in ACLF, the concentration of M30 and M65, in both plasma and ascites was significantly elevated compared with patients with cirrhosis without organ failure. This may be of biological relevance since MerTK is an efferocytic receptor and higher quantities of apoptotic/necrotic material in the circulation and tissue compartments may drive its upregulation and subsequent dampening of innate immune responses (Zizzo *et al.*, 2012; Nishi *et al.*, 2014). In keeping with higher cell death in the peritoneal compartment in ACLF, ascites lipids measured by ^{1}H-NMR was raised (though not significant) compared to ascites of patients with cirrhosis and no organ failure, suggesting cell membrane destruction with release of phospholipids or increased efferocytosis with greater macrophage lipid efflux. Generally, the metabolites identified in ACLF ascites (acetone, lactate, creatinine, 3-hydroxybutyrate and N-acetylated glycoproteins) suggest a switch from aerobic glycolysis towards anaerobic and lipid metabolism. This mirrors that found in the serum of ACLF patients (Amathieu *et al.*, 2014; McPhail *et al.*, 2016).

Cytokine experiments with PBMCs revealed that IL-10 and IL-17 are two key mediators in promoting MerTK expression (Zizzo & Cohen, 2013). Indeed, efferocytosis is known to generate anti-inflammatory cytokines, including IL-10 and TGF-β, and suppress pro-inflammatory signalling (TNF-α, IL-6 and IL-1) (Elliott, Koster & Murphy, 2017). However, multi-array cytokine analysis of ascites did not reveal significantly elevated IL-10 in ACLF as expected, but instead demonstrated significant increases in ascitic TNF-α and IL-1β concentration compared to cirrhotics without OF,

suggesting a Th1 cytokine profile. A similar pro-inflammatory profile has been seen in the circulation of patients with ACLF, a condition regarded to be driven by the systemic inflammatory response syndrome (Laleman *et al.*, 2018). The importance of increased pro-inflammatory cytokines in the ascites is unknown, especially since the time-course for their accumulation and clearance from the compartment is unexplored. It could relate to pathological BT from the gut and chronic engagement of the PAMP-TLR axis. Whilst increased pro-inflammatory cytokines in ACLF plasma has been observed, anti-inflammatory cytokines such as IL-10 also show higher concentrations compared to cirrhotics without organ failure and circulating immune cells still demonstrated dysfunctional attributes irrespective of cytokine concentrations (Wasmuth *et al.*, 2005; Albillos, Lario & Alvarez-Mon, 2014; Bernsmeier *et al.*, 2015; Clària *et al.*, 2016a). Further work is required to identify unmeasured cytokines such as TGF-β, IL-8, IL-17 and IL-1ra and the impact of milieu cytokines on peritoneal macrophage phenotype and function. It must be appreciated that there is a complex interplay between cytokines, some of which can have both pro- and anti-inflammatory actions dependent on the micro-environment, target cells on which they act, timing and concentration (Cavaillon, 2001). The cytokine profile in other ascitic microenvironments, e.g. ovarian cancer ascites and cardiac ascites, should be determined in future work; in these conditions, there is no established risk of spontaneous bacterial peritonitis and so comparisons with cirrhotic ascites would be informative (Bac, de Marie & van Blankenstein, 1996).

Bridging molecules Gas6 and Galectin-3 were measured to identify their abundance as substrates or mediators for the TAM receptor signalling pathways. A higher but non-significant concentration both mediators was seen in ACLF plasma, though ACLF ascites returned several results as zero for Gas6; this may be a reflection on a poor assay rather than a true result so requires repetition with another ELISA or quantification method to make firm conclusions. That said, an inverse correlation of ascitic Gas6 was seen with ascitic IL-12p70. Several studies have reported Gas6 as an anti-inflammatory mediator, including suppression of TLR4-stimulated IL-12p70 production via MerTK & Axl signalling (Wallet *et al.*, 2008; Shibata & Ato, 2017). Gas6 has also been previously shown to diminish TNF-α and IL-1β production in murine macrophages after liver ischaemia-reperfusion injury (Alciato *et al.*,

2010; Llacuna *et al.*, 2010). Galectin-3 was observed in the data presented to have highest concentration in ACLF plasma but was not elevated in ascites (**Figure 3.15**). In 2.3.3, increased gene expression of *LGALS3* (the gene for Galectin-3) was observed in MerTK+ monocytes compared to MerTK- and perhaps this is enhanced in ACLF. Galectin-3 is produced by hepatic macrophages under physiological conditions but in liver injury, it acts as a DAMP and higher plasma concentrations are observed (Sato *et al.*, 2009). Tian *et al.* report in cholestatic liver injury that Galectin-3 promotes NLRP3 inflammasome activation, resulting in IL-1β production and subsequent IL-17 proinflammatory cascades (Tian *et al.*, 2016). As previously demonstrated (**Figure 3.3**), IL-17 acts synergistically with IL-10 to increase MerTK and Axl monocyte surface expression, perhaps part of an immune homeostatic mechanism in the circulation. Of course, Galectin-3 is also a TAM ligand, mediating efferocytosis; this highlights the multitude of autocrine and paracrine effects a single ligand can have. Further work is required to evaluate this pathway and galectin-3 may represent a promising circulatory target to modulate the inflammatory reaction in the evolution of ACLF. From the ascites perspective, neither Gas6 nor Galectin-3 showed increased concentrations; this could signify inactive TAM receptor signalling in this compartment but more likely either the assays were imperfect, their concentration is dynamic and not reflective of TAM receptor signalling, or other bridging molecules, e.g. Pros1, could be involved. The latter requires further work to measure but it should be noted that both Gas6 and Pros1 are vitamin-K dependent mediators; some patients, especially those with alcohol-related or cholestatic cirrhosis, may have had vitamin-K deficiency and some patients received vitamin K prior to therapeutic paracentesis to correct elevated INR (Hafizi & Dahlbäck, 2006).

Given that pathological bacterial translocation may underlie the pathogenesis of SBP, to identify whether bacterial DNA quantity related to peritoneal macrophage TAM receptor expression and predicted outcome, 16S rRNA was measured by PCR in ascites. No significant associations were identified including none with TAM receptor peritoneal macrophage expression, nor with outcome measures such as subsequent SBP development and mortality within 6-months, though a trend towards the latter was observed in line with published work (Fagan *et al.*, 2015). The results would suggest that ascitic bacterial DNA cannot be used to predict death or development of SBP alone, though higher

quantity may result in lower species diversity. The small sample size, unvalidated method of bacterial DNA quantification and single measure of species diversity limits firm conclusions.

Finally, transcriptomic analysis of FACS-sorted MerTK+ macrophages compared to a baseline of MerTK- macrophages revealed these cells at steady-state are primed for efferocytosis, with significant upregulation of genes for *C1q, APOE, NR1H3* (liver X receptor-α) and *LIPA*. All are involved in cholesterol and lipid efflux from the cell, which accumulate in efferocytosis and can cause metabolic inflammation if not appropriately cleared (A-Gonzalez *et al.*, 2009b; Galvan *et al.*, 2012; Levy *et al.*, 2015; Pulanco *et al.*, 2017; Viaud *et al.*, 2018). Studies have identified anti-inflammatory and antioxidant properties of apolipoprotein E including binding of LPS, inhibiting activation TLRs and limiting neutrophil influx to LPS-exposed tissue sites (Madenspacher *et al.*, 2012; Levy *et al.*, 2015). The increased expression of LXRα and C1q has been previously noted in the post-engulfment phase of efferocytosis and both pathways have been linked to enhanced MerTK expression and MerTK-mediated efferocytosis (Galvan *et al.*, 2012; Sarang *et al.*, 2014; Choi *et al.*, 2015; Elliott, Koster & Murphy, 2017; Pulanco *et al.*, 2017). This phase is also associated with increased production of pro-restorative mediators (e.g. Gas6, IL-10, TGF-β) and attenuated TNF-α, IL-6, IL-1, IL-12 and CCR2. Moreover, pro-inflammatory genes were downregulated in MerTK+ peritoneal macrophages, including inflammasome components *CASP1*, *NOD2* and *NLRP3*. To simulate an inflammatory environment, MerTK+ and MerTK- FACS-sorted cirrhotic peritoneal macrophages were LPS-stimulated; *SIGLEC-1*, *TREM-2* and *PTX3* were all upregulated, all of which are associated with immune tolerance.

3.4.2. Functional Characteristics of Peritoneal Macrophages in Cirrhosis

Peritoneal macrophages in the ascites of patients with cirrhosis displayed enhanced efferocytic capacity of labelled apoptotic neutrophils compared with healthy monocytes, and MerTK expression was observed to be upregulated in the post-engulfment phase. Axl expression was also enhanced by efferocytosis but the greatest percentage change was observed in healthy monocytes rather than peritoneal macrophages, perhaps suggesting Axl is of greater importance in the circulation. Likewise,

plasma-exposed PBMCs had much higher expression of Axl than ascites-exposed (3.3.2), perhaps suggesting plasma promotes DC-like phenotypes whilst ascites macrophage-like. Multiple studies highlight the importance of M2c polarisation and MerTK activation in the efficient clearance of apoptotic cells (Zizzo *et al.*, 2012; Dransfield *et al.*, 2015; Zizzo & Cohen, 2018). Perhaps the increased apoptotic and necrotic cells or debris in the peritoneum, as evidenced by higher M30 and M65, results in increased efferocytosis and expanded MerTK+ subsets with higher receptor expression. Unfortunately, there were insufficient ACLF samples available to test efferocytosis in this group.

Significantly attenuated TNF-α and IL-6 cytokine production upon LPS-stimulation was observed in cirrhotic peritoneal macrophages (stable cirrhosis, acute decompensation and ACLF) compared with healthy monocytes, which concurs with gene expression data of peritoneal macrophages compared with MDMs. Although the Axl+ subset demonstrated the greatest pro-inflammatory cytokine production, there was no significant differences between MerTK+ and MerTK- subsets, and likewise no significant inverse correlation between MerTK MFI and TNF-α or IL-6 MFI as described in the circulation (Bernsmeier *et al.*, 2015). However, MerTK+ HLA-DR- macrophages did demonstrate blunted *ex-vivo* TNF-α and IL-6 production. Biologically, MerTK signalling is known to dampen pro-inflammatory cytokine production and previous work by our group has revealed circulating monocyte MerTK+ HLA-DR- subsets as the weakest TNF-α producer (Triantafyllou *et al.*, 2018a; Zhang *et al.*, 2019). The assay has its limitations including the effect of freeze/thaw cycles and LPS on downgrading MerTK expression (**Figure 3.10G**). Further work should evaluate Axl and Tyro3 signalling with LPS stimulation in conjunction with receptor blockade for a better understanding. More samples were also needed for ovarian cancer ascitic macrophages as an effective comparison.

From a bacterial killing standpoint, cirrhotic peritoneal macrophages showed preserved phagocytosis with no difference between MerTK +/- subsets but greater phagocytic capacity in the Axl+ subset. Other authors have previously noted that MerTK does not have a role in bacterial phagocytosis directly (Zhang *et al.*, 2019).With low expression on peritoneal macrophages, the relevance of Axl is doubtful. When

compared to healthy monocytes, a higher proportion of CD14+ peritoneal macrophages that were MerTK+ HLA-DR- at steady state (in the absence of *E. coli* particles) was observed. With the addition of *E. coli* BioParticles^{TM}, this subset was associated with impaired phagocytic capacity. Impaired phagocytosis of the MerTK+ HLA-DR- subset compared to their HLA-DR+ counterparts has been previously demonstrated in circulating monocytes from healthy patients and those with acute liver failure (Triantafyllou *et al.*, 2018a). These MerTK+ HLA-DR- cells may correspond to M-MDSCs which have been similarly demonstrated to have impaired phagocytosis (Bernsmeier *et al.*, 2018). The adapted phagocytosis assay evaluated peritoneal macrophages out of their microenvironment; as the optimization experiments demonstrated, the microenvironment (ascites, serum or donor AB serum) has an impact on phagocytosis. Variations in protein content including complement undoubtedly influence phagocytic capacity (Runyon, 1986, 1986; Bird *et al.*, 1992). Post-engulfment of BioParticles^{TM}, MerTK expression was seen to diminish, supporting the concept that MerTK is suppressed in inflammatory environments (Zagórska *et al.*, 2014). Interestingly, efferocytosis promotes increased MerTK surface expression whilst in bacterial phagocytosis, it is diminished. This may reflect a transition from M2c like macrophage polarisation towards M1, which would be appropriate in response to pathogens, or receptor shedding (Sather *et al.*, 2007). However, in ACLF, where high levels of cell death may result in higher background efferocytosis, one could postulate that higher MerTK expression may promote a pro-restorative immunotolerogenic microenvironment, increasing the susceptibility to infection. At face value, Axl expressing cells appeared to be highly phagocytic and pro-inflammatory. Axl MFI expression increased in both efferocytosis and bacterial phagocytosis, suggesting it is upregulated in the post-phagocytotic state though its percentage expression is minimal. The cause or consequence of Axl in these settings requires exploration.

Further work is required to optimise experimental conditions, establish the efferocytic capacity of ACLF peritoneal macrophages, and use other comparator cohorts such as monocyte-derived macrophages or ovarian cancer ascitic macrophages. Supplementation of the data with apoptotic cell trackers and live cell imaging would be useful to examine efferocytosis in greater detail. Similarly, extra investigation into the impact of efferocytosis on pathogen uptake (by serial exposure of ACs to

apoptotic neutrophils then BioParticles™), phagocytosis of other pathogen types (e.g. Gram-positive bacteria, fungi) and the kinetics of pathogen uptake would be valuable.

The most substantial functional defect was observed with oxidative burst, in which peritoneal macrophages had markedly impaired reactive oxygen species (ROS) generation in response to *E. coli*, compared with healthy monocytes. The MerTK+ subset produced less ROS. Peritoneal neutrophils had marginally better oxidative burst than macrophages but insufficient sample size precluded firm conclusions. The recruitment of circulating neutrophils (and monocytes) that migrate to the peritoneal compartment, which defines SBP, may be mandatory for effective bacterial killing once organisms are already established in an immunotolerant environment. But as our data demonstrates, even circulating neutrophils and monocytes in cirrhosis have impaired burst activity compared with healthy control counterparts. Impaired ascitic neutrophil burst has been similarly observed in other groups, corrected by autologous plasma highlighting the necessity of a circulating mediator (Engelmann *et al.*, 2016a). Impaired circulating monocyte oxidative burst and neutrophil burst have also been observed in other reports though there is conflicting evidence (Panasiuk *et al.*, 2005b; Ahmed *et al.*, 2011; Vergis *et al.*, 2016; Satsangi *et al.*, 2018). Interpretation of the flow cytometry results regarding peritoneal macrophages was complicated by their autofluorescence, particularly on the FITC and PE channels. This was evidenced by the broad-based histogram (**Figure 3.12A**) though heterogeneity in macrophage morphology may have also been responsible for this appearance. Both the pHrodo™ and Phagoburst™ assays used FITC-labelled substrate to detect differences in phagocytosis and oxidative burst respectively. To minimize this effect, strict and consistent gating methods were used but nevertheless, autofluorescence represents a limitation. Repeating the assays with fluorochromes less prone to macrophage autofluorescent interference would be useful.

In addition to the limitations already mentioned, patient recruitment over two sites, at King's College and St. Mary's Hospitals, over the course of 2 years, meant that the cohort sizes for percentage expression of surface markers were greater than those for MFI expression, Given MFIs are unique to the flow cytometer, this data could not be combined. Similarly, initially only MerTK was investigated

but Axl and Tyro3 were evaluated over the course of the research period, resulting in smaller sample sizes for the latter.

3.5. Conclusion

Taken together, the data reveals the peritoneal compartment in patients with cirrhosis and ascites consisted of peritoneal macrophages primed for efferocytosis at steady-stated with a MerTK^{high} Axl$_{low}$ CD16^{high} phenotype and gene expression profile with markedly upregulated *APOE*, *LIPA* and *CQ1A-C*. Ascites contains high concentrations of apoptotic or necrotic cells/debris, especially in ACLF, which requires greater efferocytosis, results in over-stimulation with DAMPs and in expansion of MerTK. Excessive bacterial translocation may also over-stimulate peritoneal macrophages with PAMPs, leading accumulation of inflammatory cytokines, evidenced by higher ascitic concentrations of TNF-α and IL-1β, and ultimately to endotoxin tolerance. Coupled with this is an attenuated inflammatory response to further LPS challenge, manifested as impaired cytokine production and oxidative burst, but preserved bacterial phagocytosis, leading to an immunotolerant peritoneal compartment as risk of infection.

In summary, key findings in this chapter include:

- Monocyte MerTK MFI expression was significantly enhanced by exposure to ACLF ascites compared to healthy plasma *in vitro*, higher in non-survivors at 90-days and correlated with ascitic cell death marker M65 and pro-inflammatory cytokines (including TNF-α, IL-1β and IL-12p70).
- Immunosuppressive MerTK+ HLA-DR- monocyte subsets and M-MDSCs were non-significantly elevated in ACLF ascites, adding to the hypothesis of an immunotolerant microenvironment.
- *Ex-vivo* phenotyping of peritoneal macrophages from patients with cirrhosis revealed a large peritoneal macrophage population described as CD14++ CD16++ (39%) and no CD14^{low} CD16+ subset, in line with previously published work.

- Most peritoneal macrophages (80%) expressed MerTK, Axl expression was low (2.4%) and Tyro3 variable.
- MerTK positive macrophages had high expression of activation markers (HLA-DR, CD11b and CD86), immunotolerant markers (CD206, CD163 and PD-1) and homing markers (CCR5 and CCR7).
- Cirrhotic peritoneal macrophages demonstrated higher MerTK and lower HLA-DR than ovarian cancer ascites and *in vitro* monocyte-derived macrophages.
- No difference in the percentage of MerTK+ peritoneal macrophages was observed between stable cirrhosis, acute decompensation and ACLF, nor in those who had subsequent SBP and those that did not.
- Peritoneal macrophage MerTK% correlated with circulating mean platelet volume, a marker of liver fibrosis.
- The freeze/thaw process in peritoneal macrophage phenotyping reduced expression of MerTK and CD16.
- Apoptotic cell marker M30 and necrotic cell marker M65 were both elevated overall in ascites compared to plasma, and more in ACLF ascites compared with stable cirrhosis.
- In ACLF, plasma M30 concentration exceeded ascites M30, opposite to that seen in cirrhosis without organ failure, perhaps due to apoptosis of cells in other organs and accumulation in the circulation.
- Apoptotic neutrophil efferocytosis increased MerTK expression; increased cell death in the peritoneal compartment in ACLF (as indicated by higher M65), may promote efferocytosis and explain the observed increase in MerTK expression.
- Peritoneal macrophages had impaired LPS-stimulated TNF-α and IL-6 production compared to healthy monocytes with lowest production by the MerTK+ HLA-DR- subpopulation.
- No difference was seen in LPS-stimulated proinflammatory cytokine production between MerTK+ and MerTK- subpopulations though previously described artefactual reduction in MerTK by fixation buffer and the freeze/thaw process prevented valid conclusions.

- Attenuated LPS-generated cytokines by peritoneal macrophages represents a translational aspect of the data; given the known role of MerTK in dampening cytokine responses to TLR-stimuli and its high expression on peritoneal macrophages, modulation of MerTK signalling represents a potential immunotherapeutic target.
- Peritoneal macrophage bacteria-induced lysosomal oxidative burst was impaired compared to health monocytes, with lowest production in MerTK+ HLA-DR- subsets, representing another potential immunotherapeutic target.
- Ingestion of *E. coli* BioParticles^{TM} resulted in lower MerTK and higher Axl peritoneal macrophage expression.
- Both bacterial and apoptotic cell phagocytosis capacity of peritoneal macrophages were preserved compared to healthy monocytes
- The sample size for phenotypic and functional work on ACLF peritoneal macrophages was small (n=3) and requires expansion.
- Ascites in ACLF had a higher concentration of inflammatory cytokines (TNF-α and IL-1β) and substances related to anaerobic metabolism (alanine, acetone and lactate).
- Transcriptomic profiling of steady-state MerTK+ macrophages showed upregulation of genes associated with immunotolerance (*C1q*, *APOE*, *LIPA, NR1H3*) and downregulated inflammasome (*NOD2*, *NLRP3*, *CASP1*) and superoxide anion generation (*FRP1*, *FRP2*) genes.
- LPS-stimulation of MerTK+ peritoneal macrophages resulted in upregulation immunosuppressive genes (TREM-2 and SIGLEC-1) in contrast to healthy monocyte-derived macrophages which had a classical inflammatory response.
- Areas of future research should focus on:
    a) evaluating gene transcription and pathway interactions across aetiologies and severity of liver disease, including ACLF, and the impact of their modulation on peritoneal macrophage functional capacity and susceptibility to infections such as SBP.

b) The biological role of Axl and Tyro3, and how the TAM receptors may co-operate or diverge, in liver disease.

c) Other strategies to dynamically identify patients with cirrhosis and ascites at risk of SBP which may lead to immune-enhancing drug discovery and avoid the need for prophylactic or therapeutic antibiotics which promote antimicrobial resistance.

CHAPTER 4

4. HEPATIC MACROPHAGE PHENOTYPE AND FUNCTION IN ADVANCED LIVER CIRRHOSIS

4.1. Background and Aims

The liver is an immunometabolic organ, specialised to enable liver tissue cells direct access from the blood, with high vascularity, permeable fenestrated endothelia and slow blood flow. Extensive liver capillary systems, called sinusoids, are lined with a multitude of specialised cells including hepatic sinusoidal endothelial cells (HSEC), intravascular resident macrophages (Kupffer cells) and liver dendritic cells (DCs) (Shetty, Lalor & Adams, 2018). All are capable of antigen presentation, cytokine and chemokine generation. Under normal conditions in healthy individuals, there is constant exposure to nonself antigens, including nutrients and resident microbial products (e.g. LPS) from the gut, such that there are mechanisms in place to ensure tolerance and maintenance of liver homeostasis, but also immune activation when a pathogenic or harmful antigen is encountered (Weston, Zimmermann & Adams, 2019). The liver comprises approximately 80% of the body's macrophage population in addition to being patrolled by myeloid cells including blood monocytes which monitor the liver vasculature and can infiltrate into the liver (Tacke & Zimmermann, 2014). These can become monocyte-derived macrophages (MoMFs) or liver DCs but are independent from the local resident Kupffer cells which are self-renewing and derived from either the foetal yolk sac or haemopoietic stem cells (Weston, Zimmermann & Adams, 2019). The liver is located in the peritoneal cavity and in contact with peritoneal fluid; peritoneal macrophages, noted to be *GATA-6* expressing in murine models, may also enter liver subcapsular regions during liver injury, though in humans this process is not well defined (Wang & Kubes, 2016). In the human, there are no reliable markers to distinguish tissue-resident Kupffer cells, infiltrating monocyte-derived macrophages or peritoneal macrophages (Heymann & Tacke, 2016). The three monocyte/macrophage subsets have been identified in liver tissue: classical CD14++ CD16-, intermediate CD14++ CD16+ and nonclassical CD14+ CD16++. In chronic liver injury, monocytes (especially intermediate CD14++ CD16+) accumulate in the liver from increased monocyte recruitment mediated by CX_3CL1 and local differentiation from CD14++ CD16- cells in

response to TGF-β and IL-10, (Liaskou *et al.*, 2012). These CD14++ CD16+ hepatic macrophages are pro-inflammatory, phagocytic and profibrogenic, the latter due to activation of hepatic stellate cells. (Liaskou *et al.*, 2012).

Our group has previously demonstrated an expansion of a pro-restorative MerTK+ HLA-DR^{high} macrophage phenotype during the resolution phase after acute liver failure, characterised by enhanced efferocytosis and dampened innate immune responses (Triantafyllou *et al.*, 2018a). There has been no prior evaluation of MerTK and Axl in cirrhotic liver disease. To further understand the phenotype and function of hepatic macrophages in cirrhosis, particularly in regards to TAM receptors, further exploration is required.

Hypothesis and aims:

In advanced cirrhosis, it is hypothesised that hepatic macrophages have higher expression of TAM receptors in comparison to non-cirrhotic control.

Hence in this chapter, the aim was to:

- Establish the phenotype of hepatic macrophages, in particular with regards to TAM receptors
- Assess the functional profile of hepatic macrophages

4.2. Materials and Methods

4.2.1. Patient Recruitment

Liver mononuclear cells were isolated from liver tissue from explanted whole livers in adult patients undergoing orthoptic liver transplantation at the Queen Elizabeth Hospital (Birmingham, UK). Diseased (06/Q2708/11) and non-transplanted donor (06/Q2702/61) liver tissue was collected with local research ethics committee approval and patient consent. Clinical, haematological and biochemical parameters were recorded, with blood tests performed routinely prior to transplant in patients using a haematology analyser (Siemens Advia 2120, Berks, UK).

4.2.2. Isolation of Hepatic Mononuclear Cells

Sections of liver were provided by the histopathology department at Queen Elizabeth Hospital's Liver Unit and left at 4°C in RPMI-1640 medium. Liver tissue was weighed and hepatic mononuclear cells (HMCs) isolated based on a previously described protocol (Liaskou *et al.*, 2012). In short, tissue was rinsed in cold PBS, diced into small 5mm cubes using two scalpels on a petri dish and suspended in a glass beaker containing RPMI-1640. Where the weight was greater than 150g, liver tissue in RPMI was transferred to Stomacher® 400 classic bags (Seward, UK), heat sealed and mechanically digested using a Stomacher® 400 Circulator (Cole-Palmer Instrument, UK) for 5 mins at speed 260rpm. If the weight was less than 150g, liver tissue was mechanically digested was with C-tubes (Miltenyi, UK) and a gentleMACS™ Dissociator (Miltenyi, UK). The digested tissue homogenate was poured through a fine mesh beaker and washed through with 600mls cold PBS. The perfusate was divided between twelve 50ml Falcon tubes and centrifuged at 800*g* for 5 minutes. The pellets were resuspended in PBS, combined and washed in sequentially fewer Falcon tubes until 3 tubes were left. The cell solution was layered on Ficoll Paque™ (GE Healthcare, UK), centrifuged and HMC layer aspirated with a Pasteur pipette. The HMCs were washed with PBS and red cells removed by lysis with ACK buffer (Life Technologies, UK) as per 3.2.8. Cells were counted manually using a Neubauer haemocytometer

(Marienfeld, Germany) and 0.4% Trypan blue solution. Cells were either used immediately for fresh experiments or frozen using 5-10 million cells per cryovial in 1ml of CryoStor® CS5 cell cryopreservation media and graduated cooling in a polycarbonate freezing container (Thermo Scientific, UK) at -80°C.

4.2.3. Flow cytometry of hepatic mononuclear cells for immunophenotyping

To identify hepatic macrophages, HMCs were incubated with a monoclonal antibody mixture; the common backbone of antibodies used for all samples included mouse anti-human CD14 PE-Cy7, CD16 APC-H7 (BD Biosciences, UK), HLA-DR PerCP Cy5.5 (eBioscience, UK) and MerTK APC (R&D Systems, UK). Other compatible antibody combinations were used with a full list of all monoclonal antibodies used provided in Appendix O. For six of the resection specimens, Axl and CD163 antibodies were not available for inclusion in the monoclonal antibody panel and so not included in the analysis of the expression of the markers; instead, the donor livers (n=4) and resection specimen (n=1) were grouped together as 'normal liver'. A fixed viability dye (Zombie Aqua™, BioLegend, UK) was used on a portion of liver specimens (n=4: donor, n=2 and cirrhotic, n=2) to verify the percentage of dead cells with the HMC isolation method. The method used for staining is described in 3.2.10. Fluorescence minus one (FMO) controls were routinely used for CD16 and MerTK. The former was used to identify hepatic macrophage subsets as $CD14_{low}$ CD16++, CD14++ CD16+ and CD14++ CD16-, as has been previously described in published literature (Liaskou *et al.*, 2012). Isotype controls were used for all other receptors including HLA-DR and Axl. The compensation for the fixable viability dye involved heating live cells in a heat block at 65°C for one minute to render them necrotic, mixing with untreated live cells and staining with Zombie Aqua™ dye. The CyAn™ ADP Flow Cytometer (Beckman Coulter, USA) was used for analysis at the University of Birmingham, calibrated weekly. Samples containing HMCs suspended in flow cytometry staining buffer were prepared for acquisition using CellTrics® 50μm filters (Sysmex, Germany) to minimize blockage of the flow cytometer fluidics system with particulate matter. UltraComp compensation beads (ThermoFisher Scientific, UK) were used to compensate for spectral overlap, though the compensation was conducted post-acquisition at software

level using FlowJo v10.4.2 (FlowJo LLC, USA). If there were time constraints on sample acquisition, samples for phenotyping were fixed by resuspending cells in fixation buffer (1% formaldehyde/PBS), left at 4°C overnight and acquired the following day.

4.2.4. Measurement of LPS-Stimulated Liver Macrophage TNF-α Production

Thawed liver mononuclear cells were stimulated with LPS 100 ng/ml in a 24-well plate, with cell concentration of 500,000 cells per well in complete media. After five hours, well contents were aspirated, centrifuged at 1940*g* in Eppendorfs to sediment cells, and the supernatant stored immediately at -80°C. The concentration of TNF-α was determined in thawed supernatants using the EASIA, as previously described (3.2.16).

4.2.5. pHrodo™ Phagocytosis Assay for Liver Macrophages

The phagocytosis of liver macrophages of *E. coli* BioParticles™ was determined using the pHrodo™ assay, using the method as previously described (3.2.21). These assays were performed *ex-vivo*, immediately after acquisition of liver mononuclear cells, with 500,000 cells in a 250µl volume of RPMI and 10% AB serum (for opsonins), and 20µl of BioParticles added for 60 minutes. In addition to cirrhosis liver specimens (n=3, ALD), normal liver (n=2, donor liver) was used as a comparator group.

4.2.6. Flow Cytometric Analysis

As per peritoneal macrophages, described in 3.2.11, hepatic macrophages were gated using an HLA-DR versus CD16 gating strategy (Abeles *et al.*, 2012). To ensure consistency, gates were set according to the negative cloud (using FMO or isotype controls), ensuring to keep <3% positive events at the gate position. Autofluorescence of hepatic macrophages was identified and attempts to minimise the effect were made by using red cell lysis, cell strainers (aforementioned) and compensating for the autofluorescent peak using unstained samples in compensation matrices.

4.3. Results

4.3.1. Characteristics of explanted liver

A total of 33 liver samples were obtained from explants between October 2015 and October 2016 at the Centre of Liver Research at the University of Birmingham. Of the livers deemed 'normal', there was 6 donor livers, unsuitable for transplantation, and 6 resection margin liver tissue from a colorectal cancer metastasis. Of the 6 donor livers, 2 were discarded due to excessive fat in the cellular monolayer after density gradient separation, since obtaining a clear cellular suspension suitable for subsequent analysis was not possible. The pathological liver tissue aetiology was primarily alcoholic liver disease (ALD, n=8), autoimmune cholestatic liver disease (PSC or PBC, n=6), non-alcoholic fatty liver disease (NAFLD, n=2), cryptogenic (n=1) or metabolic (alpha-1 antitrypsin deficiency, n=1; hereditary haemochromatosis, n=1) (**Figure 4.1**).

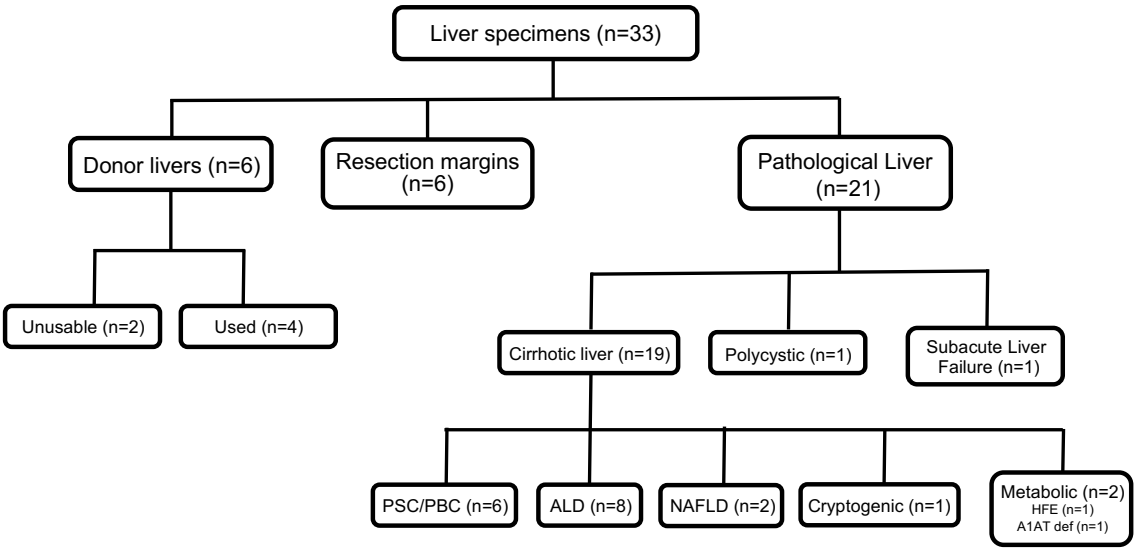


Figure 4.1 Liver explant aetiology

Total of 33 liver specimens obtained, of which 12 were 'normal' liver (donor liver or colorectal metastatic resection margin) and 21 were pathological liver tissue. Abbreviations: PSC = primary sclerosing cholangitis; PBC = primary biliary cholangitis; ALD = alcoholic liver disease; NAFLD = non-alcoholic fatty liver disease; HFE = hereditary haemochromatosis (homozygous C282Y), A1AT = alpha-1 antitrypsin.

Of the 31 viable liver tissue, 8 were stored only without immunophenotypic assays being performed due to time constraints. The polycystic liver and subacute liver failure specimens were not included in the final analysis due to low sample number for each (n=1). The data for one PSC/autoimmune liver was retrospectively discarded after phenotyping on discovering the patient was on azathioprine and prednisolone which could have affected the expression of surface markers on immune cells. This left a cohort of 10 normal livers (4 donor, 6 resection margins) and 11 cirrhotic livers (PSC/PBC, n=3; ALD n=6; haemochromatosis, n=1; A1AT deficiency, n=1) for same day phenotyping.

4.3.2. Clinical and Biochemical Correlations with Immunophenotype

As previously described, explanted liver (n=11) was compared with normal liver (resection margins, n=6; unusued donor liver, n=4). No patient clinical data was available for normal livers. Clinical data for explanted liver was obtained retrospectively (**Table 4.1**). No significant correlations between hepatic macrophage MerTK%, Axl%, HLA-DR% expression and clinical parameters were identified. Significant correlations (n=11), using Spearman's test, included CD163% and INR ($r= -0.648$, $p<0.05$), MerTK MFI and neutrophils ($r= 0.661$, $p<0.05$) and CX_3CR1% and serum creatinine ($r=0.609$, $p<0.05$). In patients on rifaximin prior to transplant (n=3), there was a trend towards lower MerTK+ HLA-DR- % and MerTK+ Axl- % frequency ($p=0.066$ for both) compared to those not on rifaximin (n=8).

Table 4.1 Summary of clinical and biochemical characteristics of patients recruited for phenotyping of liver explant specimens, just prior to liver transplant.

Variable	Frequencies / Median (range)
Age	58 (30-61)
Gender, male:female	9:2
Aetiology	
Alcohol	6
Autoimmune (PSC/PBC/AIH)	3
Metabolic (HFE / A1AT def.)	2
Haemoglobin, g/L	115 (103-159)
White cell count, x10^9/L	5.7 (2.1-8.6)
Neutrophil count, x10^9/L	3.45 (1.1-7.1)
Monocyte count, x10^9/L	0.65 (0.2-1.0)
Platelets, x10^9/L	101 (26-177)
Albumin, g/L	33.5 (21-45)
Total bilirubin, μmol/L	42.5 (14-103)
Serum sodium (Na), mmol/L	138.5 (126-143)
Serum creatinine, μmol/L	75.5 (48-166)
Alanine transaminase (ALT), U/L	33.5 (16-184)
Alkaline phosphatase (ALP), U/L	142 (54-531)
International normalised ratio	1.45 (1.2-3.9)
MELD score	15.5 (8-25)
UKELD score	53.5 (46-53)
Rifaximin pre-transplant, yes:no	3:8

4.3.3. Flow Cytometry Gating and Minimisation of Autofluorescence

The HLA-DR gating strategy was used during analysis of flow cytometry data (**Figure 4.2A**) (Triantafyllou *et al.*, 2018a). A fixable viability dye used for a portion of the liver specimens (n=4) identified high cell viability (mean = 92.5%) (**Figure 4.2B**). Autofluorescence is the natural background fluorescence of cells, unrelated to the specific fluorescent signals generated with immunophenotyping by flow cytometry, which is due to components native to the cells, e.g. mitochondria, lysosomes etc (Li *et al.*, 2012). The effect is the greatest with green- and red-channel fluorophores. This was identified on analysis of the liver mononuclear cell flow cytometric data; a post-acquisition compensation method, using the unstained cells for each sample and an unused channel on the flow cytometer, was applied to each analysis to minimise the effect of autofluorescence on the data (**Figure 4.2C**).

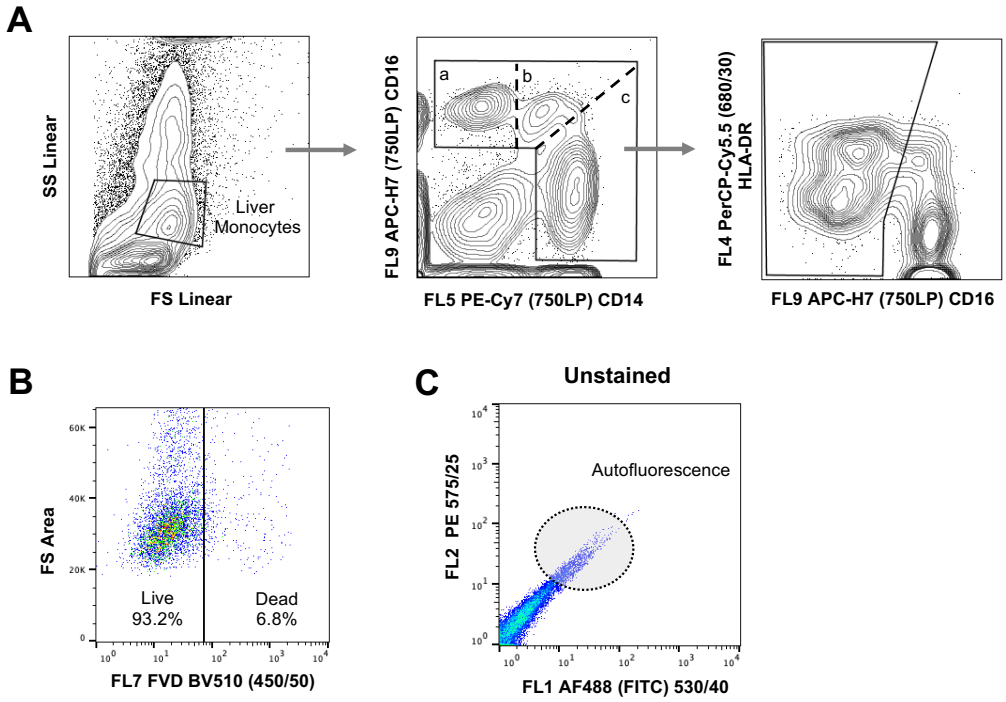


Figure 4.2 Liver mononuclear cell flow cytometry gating

(A) Contour plots HLA-DR gating strategy used to reliably identify macrophages with exclusion of neutrophils, NK cells and T-cells. Three CD16 subsets are highlighted (middle diagram): a) $CD14_{low}$ CD16++ b) CD14++ CD16+ c) CD14++ CD16- (B) Representative fixed viability dye plot demonstrating high cell viability in the liver cell isolation (C) Representative plot highlighting autofluorescent tail seen with tissue macrophages, most evidence on PE and FITC channels which can limit accuracy of data interpretation.

4.3.4. Immunophenotype of Hepatic Macrophages in Advanced Cirrhosis

Hepatic macrophage MerTK percentage expression was not significantly different between colorectal resection margin, donor liver and cirrhotic liver tissue (**Figure 4.3A**). Of note, the median MerTK % expression in the cirrhotic group was 25.7%. Axl percentage expression similarly was no different between normal and cirrhotic liver, with a median expression of 6.07% in the latter (**Figure 4.3B**). Tyro3 was not tested. No significant differences were identified in CD16 monocyte subsets between groups, though the dominant subset was CD14++ CD16- (**Figure 4.3C**).

Further interrogation of MerTK expression revealed that liver macrophage MerTK+ cells were $CD16^{high}$ $CD163^{high}$ $CD206^{high}$ HLA-DR^{high} $CCR5^{high}$, as observed with peritoneal macrophages in ascites of patients with cirrhosis (**Figure 4.3D**). The CD86 and CCR7 expression was not significant

(both p=0.09). In comparison to Axl-, liver macrophages that were Axl+ were also CD163^{high} CD206^{high} HLA-DR^{high} CD86^{high} (**Figure 4.3E**). However, when evaluating the frequency of hepatic macrophages expressing these TAM receptors as a percentage of the whole macrophage population, the majority (median 73.5%) were MerTK- Axl- and only a small number (median 4.19%) were double positive MerTK+ Axl+ (**Figure 4.3F**). No significant differences in the frequency of cells depending on MerTK+/- Axl+/- were identified between normal and cirrhotic liver. Pro-restorative MerTK+ HLA-DR^{high} hepatic macrophages have previously been described to accumulate in acute liver failure (Triantafyllou *et al.*, 2018a). Here, a significant increase in the proportion of MerTK+ HLA-DR$^{+/high}$ hepatic macrophages ($p<0.05$) and a trend towards increased frequency of MerTK+ HLA-DR+ macrophages (18.3 vs. 8.1%, p=0.07) as a percentage of total macrophages in cirrhotic liver compared with normal was observed (**Figure 4.3G**). When MerTK percentage expression in cirrhotic liver macrophages was compared by aetiology, no significant differences were identified though cohort sizes were small (**Figure 4.3H**). Axl expression did not significantly differ between aetiology (data not shown).

Thawed liver mononuclear cells were phenotyped to establish the CD68 expression of the macrophages obtained with this method (4.2.2), a marker often associated with hepatic macrophages (Antoniades *et al.*, 2012). The mean CD68 expression on normal liver tissue macrophages was 4.57% (n=3) and on cirrhotic liver 0.99% (n=1), suggesting that the isolation method and flow cytometry gating captured CD68^{low} CD14^{high} monocyte-derived macrophages rather than Kupffer cells, with the caveat of CD68 expression potentially being affected by the freeze-thaw process and its poor reliability as a distinguishing marker for liver-resident macrophages (Heymann & Tacke, 2016).

In the immunophenotyping of hepatic macrophages, some samples were acquired on the flow cytometer immediately, and some fixed with fixation buffer (4.2.3) for acquisition the following day. This fixation buffer was different to that used in ICCS experiments described in previous chapters. No significant difference in percentage of hepatic macrophages in cirrhotic livers expressing MerTK (p=0.42) and Axl (p=0.25) was noted between fresh and fixed samples (Appendix P).

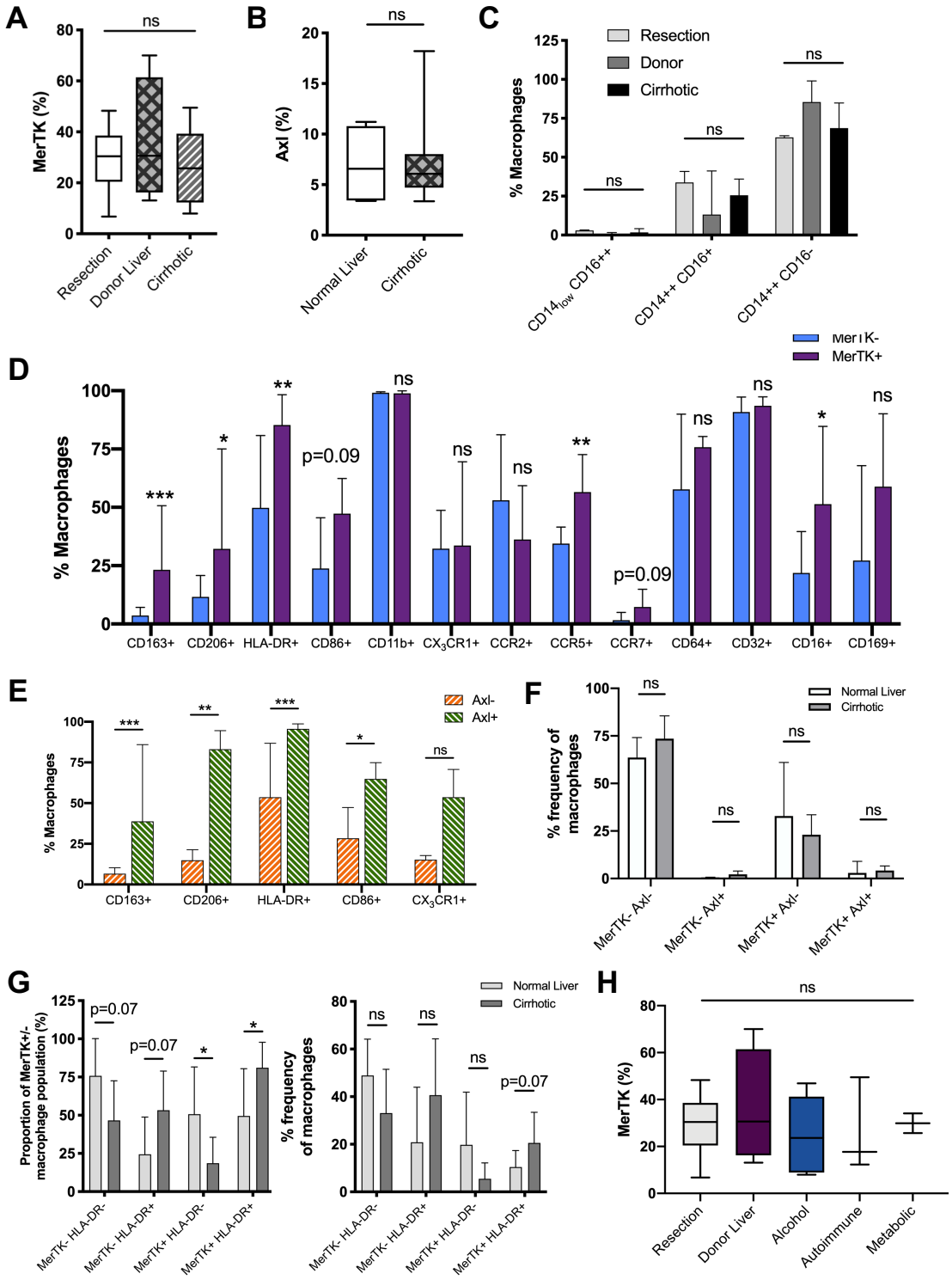


Figure 4.3 Immunophenotype of liver macrophages

(A) MerTK expression (%) on liver macrophages from specimens from colorectal metastases resection margins (n=7), unusued donor livers (n=4) and explant cirrhotic livers (n=11). (B) Axl expression (%) comparing normal (resection margin, n=1; donor liver, n=4) and cirrhotic liver (n=11). (C) Hepatic monocyte/macrophage subsets between resection margins (n=6), donor liver (n=4) and cirrhotic liver (n=11). (D) Comparison of expression (%) of surface markers between MerTK+ and MerTK- liver macrophages in cirrhotic livers for: M2 markers CD163 (n=10), CD206 (n=6); activation markers HLA-DR (n=11), CD86 (n=5), CD11b (n=4); migration markers

CX3CR1 (n=11), CCR2 (n=7), CCR5 (n=6), CCR7 (n=5); macrophage markers CD64 (n=4), CD32 (n=4), CD169 (n=4). (E) Expression (%) of surface markers in Axl- and Axl+ hepatic macrophages (CD163, n=10; CD206, n=6; HLA-DR, n=11; CD86, n=5; CX3CR1, n=3). (F) Percentage frequency of whole hepatic macrophage population of cells with combined MerTK+/- Axl+/- expression. (G) Proportion and frequency of macrophages according to MerTK+/- and HLA-DR+/- status in normal (n=5) and cirrhotic liver (n=11). (H) MerTK (%) expression according to aetiology (resection, n=6; donor liver, n=4; alcohol, n=6; autoimmune, n=3; metabolic, n=2). Data is presented as median with interquartile range. Statistical differences were detected by Mann-Whitney U for two groups or Kruskal Wallis with multiple comparison for greater than two groups. *p<0.05, **p<0.01, ***p<0.001

Sub-analysis of the monocyte/macrophage subsets by CD14/CD16 expression revealed no significant differences in MerTK, Axl nor CD163% expression between disease groups (**Figure 4.4A-C**). Significant reduction in the HLA-DR % expression CD14++ CD16- subset in donor liver ($p<0.05$) and cirrhosis ($p<0.01$) compared to resection margin liver specimen was observed, and likewise CX_3CR1% expression was significantly downregulated in cirrhotic hepatic macrophages in all subsets compared to resection margins (**Figure 4.4C**).

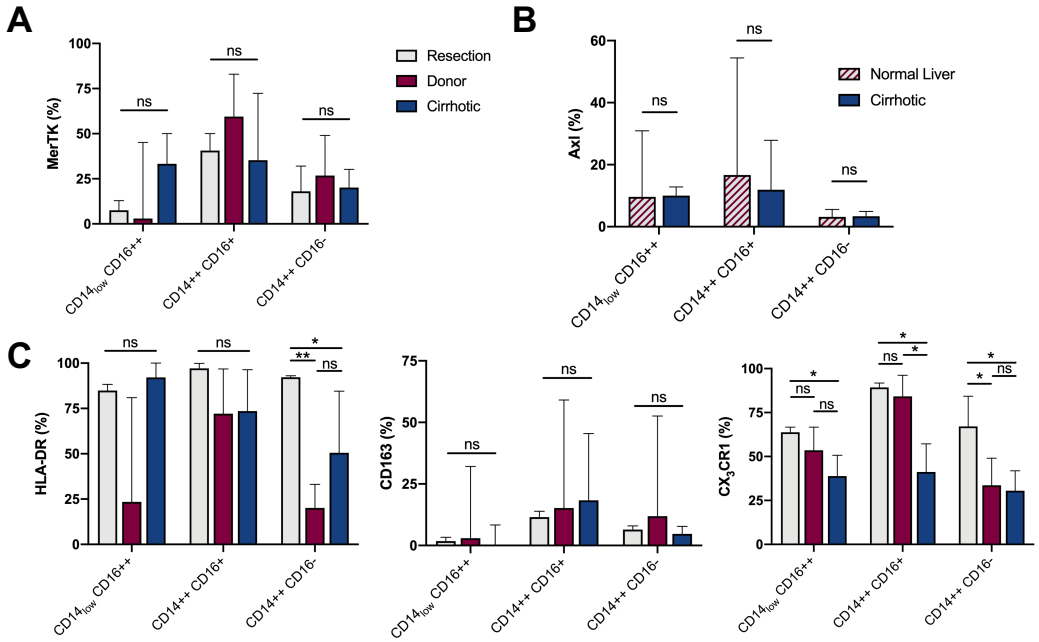


Figure 4.4 Hepatic macrophage surface marker expression according to CD16 subset

The cirrhotic liver macrophage population was analysed according to CD16 subsets: $CD14_{low}$ CD16++, CD14++ CD16+ and CD14++CD16-. (A) MerTK % expression between disease groups - colorectal liver metastasis resection margin (n=7), unused donor liver (n=4) and cirrhotic (n=11). (B) Axl % expression in CD16 subsets between normal liver (n=5) and cirrhotic (n=11). (C) HLA-DR, CD163 and CX3CR1 % expression in disease groups: colorectal liver metastasis resection margin (n=7), unused donor liver (n=4) and cirrhotic (n=11). Data is

presented as median with interquartile range. Statistical differences were detected by Mann-Whitney U for two groups or Kruskal Wallis with multiple comparison for greater than two groups. *p<0.05, **p<0.01, ***p<0.001.

4.3.5. Comparison of MerTK Expression Between Tissue Compartments

Comparison of the *ex-vivo* percentage of total monocytes/macrophages expressing MerTK in patients with cirrhosis demonstrated the lowest in circulating monocytes (median 3.2%), intermediate in hepatic macrophages (median 25.7%) and highest in peritoneal macrophages (median 80.2%), with significant differences between peritoneal macrophages and circulating monocytes (p<0.0001) and hepatic macrophages (p<0.001, Kruskal Wallis with Dunn's multiple comparison) (**Figure 4.5**).

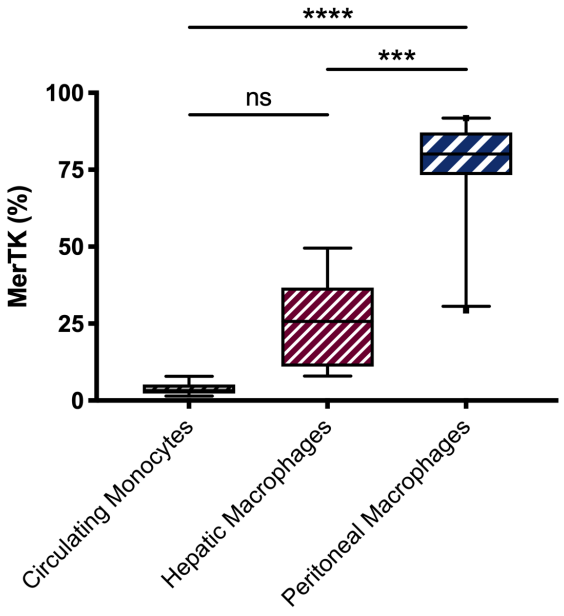


Figure 4.5 MerTK-expressing Monocyte/Macrophage Subsets in Tissue Compartments in Cirrhosis

Comparison of the percentage of total monocyte/macrophages expressing MerTK (%) measured *ex-vivo* by flow cytometry in circulating monocytes (whole blood phenotyping, n=9), hepatic macrophages (n=13) and peritoneal macrophages in ascites (n=29). Unpaired samples. Significance by Kruskal Wallis for non-parametric statistical analysis: p<0.0001. ***p<0.001, ****p<0.0001.

4.3.6. Antimicrobial Responses of Hepatic Macrophages

The pHrodo™ phagocytosis assay was performed on a small cohort of explant liver (n=3) vs. unused donor liver (n=2). No significant difference in percentage of macrophages containing BioParticles™

(47.9 vs. 64.3%, p=0.8) nor BioParticle™ MFI of macrophage population (3100 vs. 148, p=0.8, Mann Whitney) was identified. The range of results for both percentage (17.0-83.3%) and MFI (3.5-6200) was substantial and the sample size needs to be increased to make valid conclusions. LPS-stimulated TNF-α production, as measured using the TNF-α EASIA on cell culture supernatants, demonstrated impairment in cirrhosis (148.9 pg/ml, n=1) compared to normal liver (4116 pg/ml, n=3). Similarly, the cohort sizes are not sufficiently powered to make firm conclusions.

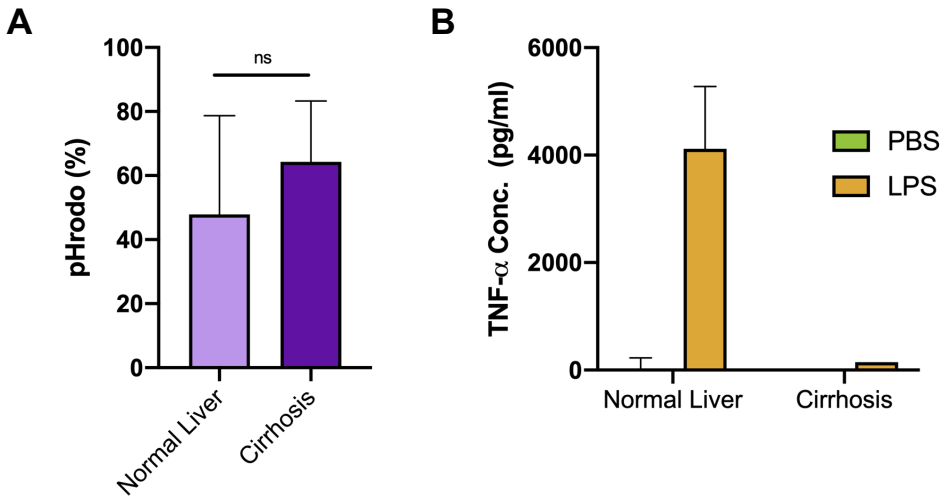


Figure 4.6 Phagocytosis and LPS-Stimulated TNF-α Production of Liver Macrophages

(A) *Ex-vivo* phagocytosis capacity of liver macrophages as measured by percentage engulfment of pHrodo™ BioParticles®, normal liver (n=2) vs. cirrhotic liver (n=3) (B) TNF-α cytokine concentration in LPS-stimulated liver macrophage supernatants, normal liver (n=3) vs. cirrhotic liver (n=1).

4.4. Discussion

In this chapter, the immunophenotype of hepatic macrophages was investigated using flow cytometry in explanted cirrhotic livers in comparison with normal liver tissue (colorectal cancer resection margins or unused donor liver). TAM receptors MerTK and Axl expression was studied in particular, with no major differences in the expression of these macrophage surface markers identified between these groups. In cirrhosis, the median MerTK% expression in hepatic macrophages was markedly less than the peritoneal compartment. The reason for the difference in expression between the compartments remains unclear. Perhaps it is due to a higher proportion of infiltrating monocytes in the liver detected by this method, which express MerTK at much lower levels, compared with resident macrophages, reflecting the much greater mix of cell types in the liver. Or perhaps it reflects the tissue microenvironment within the liver parenchyma and/or differentiation status, where there needs to be balance between immune tolerance and pro-inflammatory innate immune responses due to the liver's immune surveillance function. Human Kupffer cells, conventionally characterised by a CD68+ CD14+ TLR4+ CX_3CR1- phenotype, reside within the sinusoids and in some studies, are associated with higher MerTK expression (Triantafyllou *et al.*, 2018a; Weston, Zimmermann & Adams, 2019). CD68 expression was low in thawed liver parenchymal cells so it remains unclear whether Kupffer cells were part of the hepatic macrophage cell population identified in this chapter.

Hepatic MerTK+ cells were identified as exhibiting Fcγ-receptor $CD16^{high}$, HLA-DR^{high}, classical M2 markers ($CD163^{high}$ $CD206^{high}$) and tissue homing markers (e.g. $CCR5^{high}$). These markers were also observed in MerTK+ peritoneal macrophages (chapter 3), suggesting a clustering of surface markers, perhaps reflective of function. That said, interestingly CD14+HLA-DR+CD206+ intrahepatic macrophages in advanced viral liver disease were found to be pro-inflammatory and had no endotoxin tolerance (Tan-Garcia *et al.*, 2017). Although a viral aetiology was not included in this dataset, given MerTK+ hepatic macrophages are CD14+ HLA-DR+ CD206+, it highlights the need for further investigation of the cytokine signalling of macrophage subsets, exploration of antimicrobial responses in other aetiologies and in acute liver disease (e.g. ACLF and ALF). The latter would also be informative as a positive control for MerTK expression.

Axl+ hepatic macrophages were few in number, with only 6% expression, similar to peritoneal macrophage Axl expression. Axl+ macrophages have a similar CD163^{high} CD206^{high} HLA-DR^{high} CD86^{high} phenotype compared to MerTK+. Indeed, the data suggests that most Axl+ macrophages are MerTK+ (i.e. they are co-expressed), but most MerTK+ macrophages are Axl- (**Figure 4.3F**). Further work is needed to establish whether co-expression of TAM receptors, including Tyro3, impacts on function. However, there was no difference in MerTK/Axl combinations between normal and cirrhotic liver, and no difference in MerTK% between liver disease aetiologies.

MerTK+ HLA-DR+ macrophages have been previously identified by our group as a pro-restorative subset that was expanded in ALF (Triantafyllou *et al.*, 2018a). In this chapter, the proportion of MerTK+ hepatic macrophages expressing HLA-DR was expanded in cirrhotic livers compared to normal livers. However, the frequency of MerTK+ HLA-DR+ macrophages, as a percentage of the hepatic macrophage population, was not significantly raised, with only 18% observed in cirrhotic livers, compared to the 30-40% circulating in acute liver failure (Triantafyllou *et al.*, 2018a). The intense systemic inflammation seen in ALF, with high levels of DAMPs in sterile injury, may drive MerTK expression, and indeed MerTK+ HLA-DR+ macrophages are seen to surround areas of necrosis in the liver seen on confocal microscopy. The chronic inflammatory nature of cirrhosis with fibrosis as the overriding pathology rather than necrosis may explain why the MerTK+ HLA-DR+ subset was not significantly expanded. Although the cohort size was small, the trend towards lower MerTK% with rifaximin, a non-absorbable immunomodulatory antibiotic, perhaps hints towards a potential role of the gut microbiome in shaping the intrahepatic microenvironment (Patel *et al.*, 2018).

CD16 subtype analysis did not reveal an expanded CD14++ CD16+ (intermediate) population in cirrhotic livers compared with normal, at odds with previous descriptions (Liaskou *et al.*, 2012). Other authors have described the accumulation of CD14++ CD16+ monocytes in the circulation and liver of patients with cirrhosis, a population associated with proinflammatory cytokine signalling and pro-fibrogenic activation of hepatic stellate cells (Tacke, 2012; Liaskou *et al.*, 2012). The gating of the intermediate population can prove challenging since it is not always clearly delineated, particularly since CD14++ can begin to acquire CD16 in the liver and therefore there may be a spectrum of expression. Moreover, liver injury may promote the conversion of CD14++ CD16- cells to CD14++

CD16+ via cytokines IL-10 and TGF-β (Heymann & Tacke, 2016). The CX_3CR1-CX_3CL1 axis also has an anti-inflammatory and anti-fibrogenic effect. Downregulation of intrahepatic CX_3CR1 was observed in our data (**Figure 4.4C**), and supported by others, resulting in a pro-inflammatory state (Karlmark *et al.*, 2010; Tacke, 2012).

The functional data obtained - phagocytosis and TNF-α production after LPS stimulation - provides some substrate for speculation that macrophage bacterial phagocytosis was preserved in cirrhotic livers, whilst the TNF-α cytokine production/secretion appeared to be impaired. The cohort size was very small and firm conclusions cannot be made. More work is required to delineate the functional capabilities of hepatic macrophages.

Limitations to the study of the liver cell phenotype and function included the unavailability of explant tissue in patients transplanted for acute-on-chronic liver failure. These patients were only very rarely transplanted in this setting, and whilst attitudes to ACLF as a barrier to transplant are changing, only a small number of transplants are performed per annum in this cohort globally (Fernández & Saliba, 2018; O'Leary *et al.*, 2019). Accordingly, the expression of TAM receptors in intrahepatic macrophages in ACLF could not be investigated. Animal models of ACLF are not widely available or accepted with only one proposed rodent model published but not validated (Li *et al.*, 2017).

The data quality was undoubtedly affected by a number of methodological limitations. Firstly, the groups considered 'normal' liver for comparison were colorectal cancer resection margin liver tissue, and donor livers deemed unsuitable for transplantation. With the former, the presence of micrometastases and a more global change in liver immune cell phenotypes in the presence of cancer metastases cannot be excluded. In the latter case, donor livers are obtained from deceased individuals, sometimes in the absence of a cardiac output (donation after cardiac death – DCD – livers), transported across the United Kingdom in cold preservation fluid for varying lengths of time. They are usually unused for onward transplant because they are too fatty for transplantation or have prolonged cold ischaemic times. Both may make the donor liver more prone to injury and may influence the liver cell phenotype and function. In contrast, native livers explanted from transplant recipients may be stored for much less time. That said, each liver explant specimen had variations in the duration of time between

removal from the patient, storage in media, processing and immunostaining, which may have impacted on the results. Additionally, patients may be transplanted at different stages of liver disease and those on the transplant waiting list are not a homogenous population. For example, some patients with PSC may be transplanted without advanced cirrhosis in light of significant cholestasis or recurrent cholangitis, whereas most patients with ALD will have advanced cirrhosis. The actual method of mechanical digestion is a crude one, which blends together fibrous tissue, blood vessels and liver parenchyma although washing the tissue prior to mechanical digestion removes any PBMCs. Given the recognition that immune cells may have zonal differences, and there is a multitude of myeloid cell types including infiltrating monocytes, resident Kupffer cells, MDSCs, dendritic cells and endothelial cells, more discriminative immunophenotyping is required (Aizarani *et al.*, 2019). The intrahepatic microenvironment also impacts on macrophage phenotype, function and plasticity, and this requires further work for its characterisation. (Gordon, Plueddemann & Estrada, 2014; Tacke & Zimmermann, 2014)

The process of data anonymisation and subsequent collection of clinical data retrospectively (obtained by application to research administrative support staff) led to the discovery that the aetiology of some explants was incorrectly communicated to the laboratory, such that in some cases, the aetiology had to be recategorized dependent on the clinical history and/or native liver histology. Furthermore, no clinical data was available at the time of processing the liver tissue on the medication taken by patients; the phenotypic results of one patient was discounted due to pre-transplant immunosuppressant medication. No clinical data on previous episodes of sepsis was available; given TAM receptor activation can lead to increased susceptibility to infection, this data would have been highly informative.

In terms of analysis, despite attempts to minimise it, autofluorescence will have influenced the data quality. Additionally, data quality would have also been negatively impacted by the fact that fixable viability dye was not used routinely to exclude dead cells, some samples were run fresh and some fixed with fixation buffer, and isotype controls were used for most surface markers, which many would regard as suboptimal compared to the fluorescence minus one (FMO) control.

4.5. Conclusion

MerTK expression in the hepatic compartment was not proven to be elevated compared with 'normal' liver. However, in comparison to the peritoneal compartment, MerTK expression was substantially lower. Axl macrophage expression was low, similar to that observed for the peritoneal compartment. The previously described pro-restorative MerTK+ HLA-DR+ macrophage subset was not increased in absolute frequency in cirrhotic livers, perhaps indicative of absence of liver necrosis and predominance of fibrosis. Further work is needed to elucidate the expression of Tyro3, the functional attributes of hepatic macrophages and the corresponding role of TAM receptors, zonal differences within the liver, the impact of different aetiologies on TAM receptor expression, the expression in ACLF liver explants and how agonism or antagonism of TAM receptors at different time points could shape the phenotypic and functional characteristics, changing susceptibility to infection.

Key findings in this chapter are summarized as follows:

- No significant differences in percentage of MerTK-expressing hepatic macrophages were observed between 'normal' and cirrhotic liver, and between aetiologies of cirrhosis.
- The median MerTK% was 25%, higher than seen in circulating monocytes but lower than peritoneal macrophages in patients with cirrhosis and ascites.
- MerTK+ hepatic macrophages had a similar phenotype to peritoneal macrophages with CD16+ HLA-DR+ CD163+ CD206+ CCR5+ expression.
- Downregulation of CX_3CR1% hepatic macrophage expression was seen in cirrhosis compared to resection margins; the CX_3CR1-CX_3CL1 axis is anti-inflammatory and in combination with lower MerTK% expression could suggest the liver compartment is less immunotolerant than peritoneum; drug manipulation of MerTK and CX_3CR1 pathways represents a potentially translational aspect of the data.
- Further work from this chapter would include:
    a) More work on hepatic macrophage function (phagocytosis, efferocytosis, TLR-stimulated cytokine production)

b) Analysis of liver tissue and cells from patients with ACLF

c) Investigation of Axl and Tyro3 expression and function in the liver

d) The effect of TAM receptor agonism or antagonism, and CX_3CR1-CX_3CL1 axis targeting, on hepatic macrophage characteristics.

CHAPTER 5

5. MONOCYTE TRANSENDOTHELIAL MIGRATION

5.1. Background and Aims

Sterile liver injury results in the production of danger signals, so-called damage associated molecular patterns (DAMPs), and local inflammatory responses in which liver macrophages are crucial. The local pool of macrophages are augmented by recruitment of circulating and bone-marrow derived monocytes, which differentiate *in situ* to macrophages, contributing to the initiation, propagation and resolution of the hepatic inflammatory response (Triantafyllou *et al.*, 2018b). In ALF, this is accompanied by circulatory immune cell dysregulation (Antoniades *et al.*, 2006, 2012). In acute-on-chronic liver failure (ACLF), there is a primary liver injury and inflammation, associated with a systemic inflammatory response, multiorgan failure and subsequent immunosuppression with increased incidence of infection (Clària *et al.*, 2016a; Fernandez *et al.*, 2018). The trafficking of monocytes to and from the liver is fundamental in the pathophysiology of ACLF. In order to infiltrate the liver, monocytes must undergo transendothelial migration (TEM), a multi-step process involving adhesion to the hepatic sinusoidal endothelial cells (HSECs), and entry into the subendothelial space through diapedesis (Gerhardt & Ley, 2015; Muller, 2015). The process of reverse transmigration (RT), in which monocytes re-enter the circulation after entry into the tissues, may impact on the composition of circulating immune cells and interaction with the adaptive immune system (Randolph, 1998; Muller & Randolph, 1999). Indeed, RT has been proposed as a means for dendritic cells emigrating from liver to lymph nodes where they may present antigens to T-cells (Matsuno, 1996).

Zimmerman *et al.* previously studied monocyte migration across HSECs and identified that monocytes that stay in the subendothelial space adopt an anti-inflammatory macrophage-like phenotype that is highly phagocytic, refractory to LPS and promotes T-cell anergy (Zimmermann, Bruns & Weston, 2016). In contrast, reverse migrated monocytes, which preferentially express CD16, resemble DCs, with pro-inflammatory and T-cell activating properties.

Hypothesis and aims:

MerTK characterises an M2c-like anti-inflammatory macrophage phenotype (as seen in Chapters 3 & 4), with roles in macrophage migration and negative regulation of T-cell activation (Tang *et al.*, 2015; Cabezon *et al.*, 2015). Given this, the data from Chapter 2 and prior observations from Bernsmeier *et al*. (2015) showing that higher numbers of circulating and hepatic MerTK^{high} monocytes/macrophages are seen in ACLF with associated attenuated pro-inflammatory responses to LPS, it was hypothesised that monocyte TEM promotes acquisition of MerTK, which is more pronounced in ACLF, and is linked to dampened antimicrobial responses.

In this chapter, the aim was therefore to:

- Evaluate the phenotypic properties of monocytes in ACLF vs. healthy control and cirrhosis without organ failure (OF) as they migrate across HSEC in an *in vitro* TEM model
- Establish the functional characteristics of these migrating monocytes in ACLF
- Identify differences in the adhesion and numbers of migrating monocytes in ACLF compared to healthy by *in vitro* assay and using a flow-based adhesion assay.

5.2. Material and Methods

5.2.1. Hepatic Sinusoidal Endothelial Cell Culture

Human HSECs were isolated from explanted or resected liver, courtesy of research assistant Gill Muirhead at the Centre for Liver Research in Birmingham, using a method previously described (Zimmermann, Bruns & Weston, 2016). If the HSEC provided were at earlier passage stages (e.g. P2-4), their culture was continued and were sub-cultured as appropriate to prolong their use, with a maximum passage of P6. Briefly, sub-culture involved enzymatic dissociation of HSEC that were 80-90% confluent on light microscopy using TrypLE^{TM} Express (ThermoFisher Scientific, UK) for 4-5 minutes followed by deactivation by dilution with PBS. Cells were collected, washed, counted and resuspended in HSEC media containing 10% (v/v) heat-inactivated AB human serum (HD Supplies, Glasgow, UK), serum-free media (ThermoFisher Scientific, UK), 10ng/ml human recombinant vascular endothelial growth factor (PeproTech, Peterborough, UK), 10ng/ml hepatocyte growth factor (PeproTech, Peterborough, UK) and 1% penicillin-streptomycin-glutamine (ThermoFisher Scientific, UK). They were then seeded on the base of a T75 flask (Corning, UK) pre-treated with diluted rat-tail collagen type 1 (Sigma Aldrich, UK) at an optimal density of 5000 cells/cm^2, supplemented with HSEC media. Cells were kept in an incubator at 37°C (5% CO_2) and checked for confluence on alternate days with replacement of media (**Figure 5.1B**). When required, cells were split with enzymatic dissociation as described.

5.2.2. PBMC Isolation and CD14 Magnetic Bead Selection

PBMCs were isolated (2.2.3) from venesected whole blood in EDTA from volunteers with hereditary haemochromatosis (in the absence of liver disease), according to local research ethics committee approval and patient consent. PBMCs were subsequently frozen at -80°C. When required, PBMCs were thawed and CD14+ cells were positively selected using a pre-separation 30μm filter, CD14 magnetic beads, LS columns and a midiMACS^{TM} magnetic separator (Miltenyi Biotec, UK) (2.2.4). Two LS

columns were sequentially used to improve the CD14+ purity which was >95% as verified with flow cytometry.

5.2.3. Bidirectional *In Vitro* Transendothelial Monocyte Migration Assay

Each assay was performed over a four-day period, based on the method described (Zimmermann, Bruns & Weston, 2016). On day one, the collagen matrix was prepared on ice by combining 3mg/ml bovine collagen I (Life Technologies, UK), 10x minimal essential medium (Life Technologies, UK), 1M sodium hydroxide, 1mM HEPES buffer (Sigma Aldrich, UK) and triple distilled water. The collagen mixture was aliquoted to 24-well cell culture standing inserts (pore size 0.4μm), that had been equilibrated with HSEC medium for 3 days prior, (Merck Millipore, Watford, UK), supplemented with serum-free media (SFM) containing 0.1% bovine albumin fraction V solution (BSA) (Life Technologies, UK) and 0.1% 100x penicillin-streptomycin-glutamine (ThermoFisher Scientific, UK) and kept at 37°C. Subsequently, the collagen gels were overlayered with 50μl of 50μg/ml fibronectin (Life Technologies, UK) for 20 minutes at 37°C. After four hours, each cell insert was seeded with $5.5x10^4$ HSEC and left overnight at 37°C 5% CO_2. On day two, HSEC media was replaced with fresh HSEC media, supplemented with 10ng/ml TNF-α (PeproTech, UK) and 10ng/ml IFN-γ (PeproTech, UK). PBMCs were thawed and CD14 cells isolated as per 5.2.2. CD14+ cells were mixed with 25% plasma from patients with ACLF, cirrhosis without OF or healthy subjects, and complete media (RPMI with 10% fetal bovine serum and 1% penicillin-flucloxacillin-streptomycin) and added to each well of a separate 24-well plate at 2 million cells/ml/well. After 24 hours, on day three, 2 x 10^6 CD14+ monocytes were added in SFM/0.1% BSA to each cell insert. After 1.5 hours, nonadherent cells were washed off, collected and medium replaced with SFM/2.5% FBS. The plate was returned to the incubator, and non-migrated monocytes subjected to immunophenotyping, or functional assays. After a further 24 hours, on day 4, SFM/2.5% FBS was added to each cell insert and after 4 hours, aspirated and thoroughly washed with ice-cold PBS/1mM ethylene glycol tetraacetic acid (EGTA) to collect the reverse migrated monocytes. To harvest the subendothelial monocytes, collagen plugs were resected using an 18G needle, and chemically digested by exposure to a collagenase solution containing 20%

collagenase from *Clostridium histolyticum* (Sigma Aldrich, UK), 20% heat inactivated human serum and 60% PBS, for 30 minutes at 37°C. Collagenase was inactivated with PBS/1mM EDTA. Cells were washed and aliquoted to polystyrene tubes for further assays (**Figure 5.1A**).

5.2.4. Immunophenotyping of Monocytes

Monocytes from the non-migrated, subendothelial and reverse migrated phases were immunophenotyped according to methods already previously described (2.2.6). CountBright™ Absolute counting beads (ThermoFisher Scientific, UK) were used count cells by flow cytometry. The panel used for phenotyping is listed in Appendix Q.

5.2.5. Intracellular Cytokine Staining and pHrodo™ Phagocytosis Assays

Intracellular cytokine staining (ICCS) assays were performed on non-migrated, subendothelial and reverse migrated monocytes as per 2.2.7. LPS at 100ng/ml was used to provide stimulus for generation of TNF-α and IL-6. Fixation buffer consisted of 1% formaldehyde/PBS. The pHrodo™ assay using Green *E. coli* BioParticles™ was used to assess phagocytosis (Life Technologies, UK) with the method previously described (3.2.21). The volume of particles used was 20µl in a 100µl volume (10% AB serum and 70% RPMI).

5.2.6. Flow Cytometric and Statistical Analysis

The flow cytometer used was the CyAn™ ADP (Beckman Coulter, USA). UltraComp eBeads (Life Technologies, UK) were used to compensate for spectral overlap but this required post-acquisition generation of compensation matrices using FlowJo v10.4.2 software (FlowJo LLC, USA). Unstained samples were used to optimally position histograms during acquisition. Relevant isotype and FMO controls were used (see Appendix R). Statistical analysis was undertaken using GraphPad Prism v7 and statistical difference between groups employed Mann Whitney U for two groups or Kruskal Wallis with Dunn's multiple comparison for more than two groups.

5.2.7. Migration Flow Assay

To determine whether monocytes exposed to ACLF plasma compared to healthy had different adhesion or migratory properties, an assay was employed to directly visualise these aspects under flow conditions, with the aim of imaging using high resolution phase contrast and fluorescence microscopy. The experiment used a unique porous glass membrane (μ-Slide Membrane ibiPore Flow, ibidi GmbH, Germany) which allows culture of HSEC and co-culture with monocytes under perfusion, in combination with existing perfusion apparatus already setup at the Centre for Liver Research in Birmingham. In short, the collagen mixture (as per 5.2.3) was smoothly pipetted through one port of the upper channel, taking care to avoid bubble formation. 1X minimal essential media (Life Technologies, UK) was passed through a 0.22μm Millex® syringe filter (Merck Millipore, UK) and into the lower channels to minimize air in the system. Caps were placed on all channel ports and the slide left in an incubator at 37°C for 1 hour. After this time, HSEC were seeded through the lower channels at a density of 1 x 10^6/ml and the slide left inverted on a petri dish in the incubator for 2 hours. Subsequently, HSECs were supplemented with 50μg/ml fibronectin in PBS through the lower channel and after 30 minutes, replaced with HSEC media. The following day, HSEC media was supplemented with 10ng/ml TNF-α (PeproTech, UK) and 10ng/ml IFN-γ (PeproTech, UK). Once the HSEC monolayer appeared confluent on light microscopy, the flow assay system was setup as previously described (Shetty *et al.*, 2014). In short, in a thermostatically-controlled transparent chamber at 37°C contained an inverted microscope, a 50ml glass syringe was setup in a syringe pump (Harvard Apparatus, USA) with thick and thin silicone tubing (ThermoFisher Scientific, UK) attached to flow chamber. Two syringes were attached via an electronic solenoid valve, at the influx, one containing THP-1 cells (ATCC, UK) (cultured as per 3.2.19) and the other media alone. Perfusion was set a rate of 0.28ml/min; leucocyte boluses lasted 5 minutes with 5 minutes of subsequent acellular media flow, the final 2 minutes of which monocytes were recorded in 10 random fields along the length of the microslide. Rolling and adherent cells could be estimated as per Shetty *et al*. (2014).

5.3. Results

5.3.1. Transendothelial Monocyte Migration

Isolated CD14+ monocytes were gated on flow cytometry software as described (**Figure 5.1C**). Comparison of monocyte MerTK% expression demonstrated highest expression in the reverse transmigrated monocytes, followed by subendothelial and then lowest in non-migrated monocytes. The only significant difference seen was in healthy controls between reverse transmigrated and non-migrated monocyte MerTK% (median: 56 vs. 25.3%, $p<0.01$), though in ACLF this difference was not significant (84.5 vs. 65.0%, $p=0.06$). Monocytes conditioned in ACLF plasma had significantly increased MerTK% expression compared with healthy (Kruskal Wallis with multiple comparison, $p<0.05$) in each phase of the migration assay, though the increase was not significant in monocytes conditioned in plasma from patients with cirrhosis without OF (**Figure 5.1D**). The overall MerTK% monocyte expression irrespective of the stage of migration or disease group was not different between CD14+ CD16- and CD14+ CD16+ (**Figure 5.1E**). ICCS experiments revealed the highest producers of TNF-α after LPS stimulation were subendothelial monocytes in healthy and cirrhosis groups, significantly greater than non-migrated in healthy (39.9 vs. 12.5%, $p<0.01$), but not significant in cirrhosis (30.8 vs. 8.0%, $p=0.06$). In ACLF, reverse migrated monocytes produced most TNF-α, significantly greater than non-migrated monocytes ($p<0.05$). However, there was no significant difference in TNF-α production between subendothelial and reverse transmigrated monocytes in any disease group **(Figure 5.1F**). In comparison with healthy controls, the TNF-α production in ACLF was significantly attenuated in subendothelial (18.1 vs. 39.9%, $p<0.05$) and reverse transmigrated monocytes (20.3 vs. 37.1%, $p=0.05$) but not significantly so in non-migrated (**Figure 5.1F**). There was a significant inverse correlation of MerTK% monocyte expression (as determined on immunophenotyping) and TNF-α% production ($p<0.05$), in all phases of migration when disease groups were combined (**Figure 5.1H**). LPS-stimulated monocyte IL-6% production was not significantly different between phases of migration in any disease group but was significantly different in ACLF reverse migrated monocytes when compared with healthy (20.3 vs. 37.1%, $p=0.05$). The preliminary data from these experiments is published in the Bernsmeier *et al*. paper including cell count

demonstrating higher cell counts in MerTK+ subendothelial and reverse migrated (Bernsmeier *et al.*, 2015).

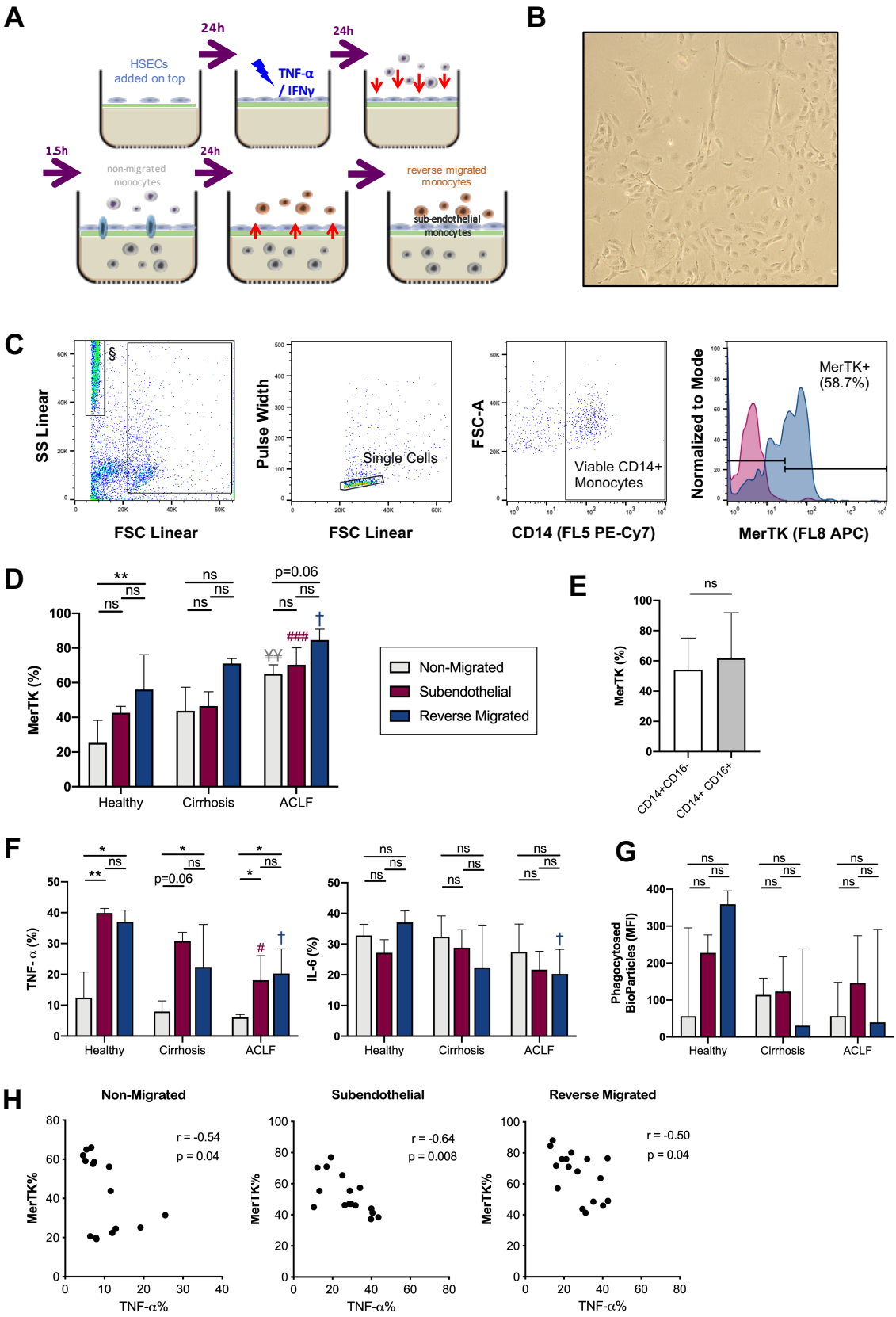


Figure 5.1 Transendothelial Migration Assay to Recapitulate Monocyte Entry into Tissue and Associated Phenotypic and Functional Attributes

(A) Schematic diagram of transendothelial migration model in which HSEC are layered on a collagen plug, activated with TNF-α and IFN-γ followed by the addition of plasma conditioned monocytes; non-migrated monocytes are collected after 90 minutes, and subendothelial and reverse transmigrated the following day. (B) Representative image from light microscope of HSEC growing on collage-coated flask – HSEC were sub-cultured when cells were 80-90% confluent. (C) Representative flow cytometry plots to highlight the gating strategy; isotype control = red histogram; stained tube for MerTK = blue histogram. Gated area denoted by § = counting beads (D) Phenotypic MerTK surface expression (%) on CD14+ selected monocytes in the different phases of migration: healthy (n=6), cirrhosis without OF (n=5) and ACLF (n=6) (E) MerTK% expression according to CD16+ or CD16- of monocytes in all phases of migration and all disease groups (F) LPS-stimulated TNF-α and IL-6 production of monocytes according to disease group and migration stage. (G) Median fluorescence intensity (MFI) of CD14+ monocytes exposed to *E. coli* Green pHrodoTM BioParticles™ as a measure of phagocytosis capacity by disease group and migration stage (n, as per (D)). (H) Correlation (Spearman's rank) of MerTK% and TNF-α% if different migration phases. Statistical analysis was by non-parametric testing: Mann Whitney U for two groups, Kruskal Wallis with Dunn's multiple comparison between means for migration phases within disease categories, but using healthy as control when comparing between disease groups. */#/¥/ †, $p<0.05$, **$p<0.01$, ***$p<0.001$.

The phagocytosis of *E. coli* BioParticles™ did not reveal any significant differences in percentage particle uptake (data not shown). MFI showed greater discriminant properties, but nevertheless was highly variable and did not demonstrate significant differences between migration phases or between disease groups (**Figure 5.1G**).

5.3.2. Flow Based Adhesion Assay

The flow-based adhesion assay to investigate the adhesion, rolling and migration of THP-1 monocytes conditioned in plasma from patients with ACLF and cirrhosis without OF, compared with healthy control plasma, could not be reliably interpreted due to small non-confluent areas of HSEC identified on the porous membrane of the flow slide, which occurred consistently with repeat attempts (**Figure 5.2A&B**). Although monocytes were visualised on phase contrast microscopy to adhere and roll, a confluent monolayer is required to properly enumerate the number of cells interacting with the endothelium. Using current experimental setup, the size and number of non-confluent areas varied between experiments, despite alterations to the protocol such as modifying the seeding density of HSEC, such that the variability between experiments prevented detailed analysis (**Figure 5.2C**).

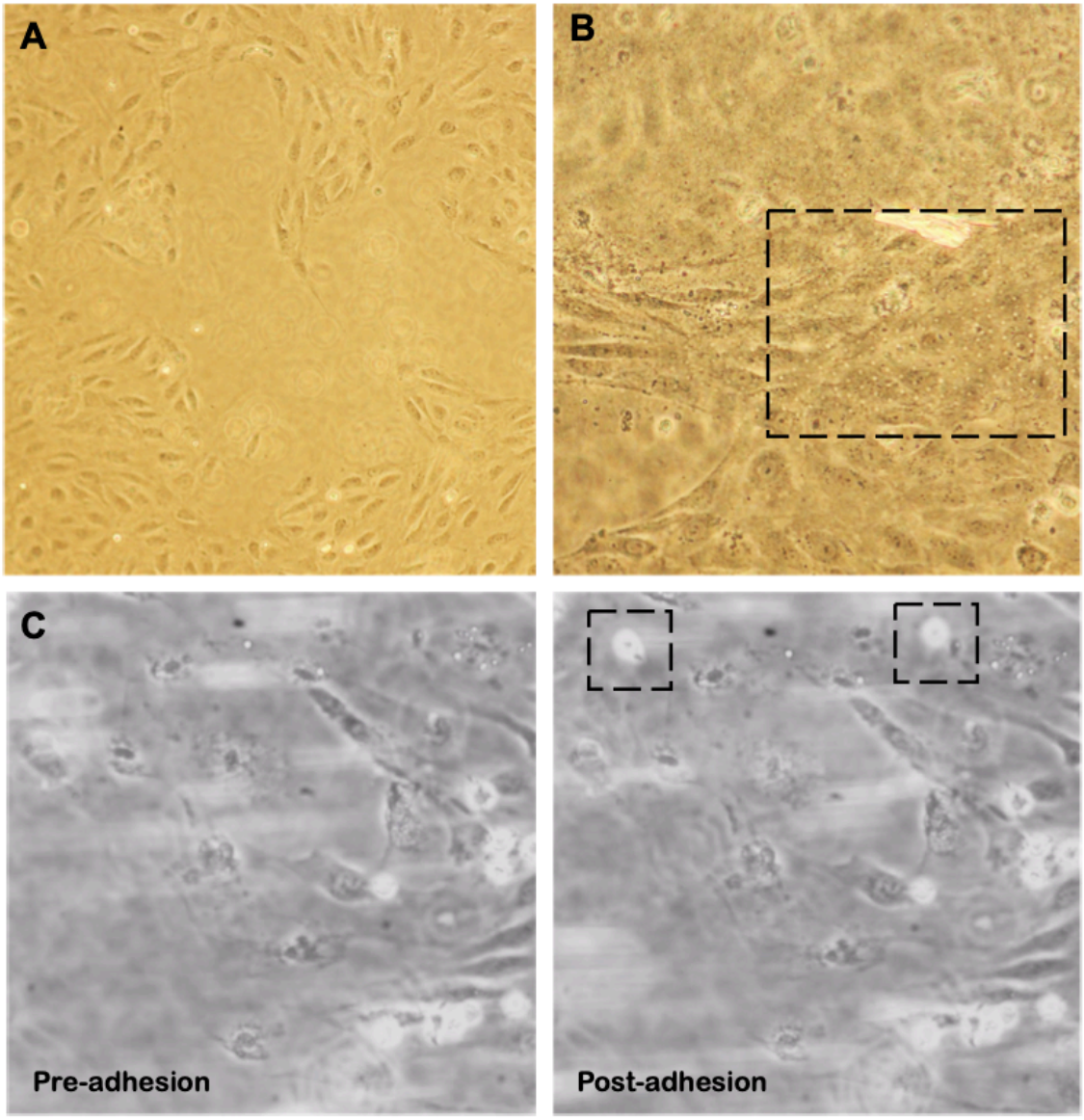


Figure 5.2 Images from Flow-Based Monocyte Adhesion Assay

(A) Light microscopy image taken at 10x magnification of HSEC growing on µSlide pore membrane demonstrating non-confluent areas (B) Areas with no growth and pore membrane visible (white dots within black box) (C) Sequential still images from video of flow chamber microscope (10x magnification) during flow of THP-1 monocytes highlight monocyte adhesion (black box).

5.4. Discussion

Zimmerman and co-authors previously identified that classical CD14+ CD16- monocytes acquire CD16 during the RT process, and these monocytes are HLA-DR^{high} CD163^{high} CD206^{high} CD86^{low}. They surmised that in the subendothelial space, monocytes either differentiate into macrophage-like cells, with high phagocytic activity, LPS-tolerance and anergic effects on T-cells, or dendritic-like cells which reverse migrate back into the vessel lumen, potentially homing towards draining lymph nodes. These DC-like cells have poorer phagocytic capabilities but have pro-inflammatory cytokine responses to LPS, and activate T-cells (Zimmermann, Bruns & Weston, 2016). The data in this chapter verified that monocytes also acquire MerTK during the transmigration process, with sequentially higher MerTK% expression from non-migrated, subendothelial and reverse migrated phases. In monocytes conditioned in ACLF plasma, which already had higher MerTK expression compared with healthy, TEM enhances MerTK expression even further. There was no difference in MerTK% expression between CD14+ CD16- and CD14+ CD16+ subsets, corroborating the observation in the liver (4.3.4) and highlighting the plasticity of the cells. As expected, the ACLF-conditioned monocytes had attenuated TNF-α responses to LPS stimulation, corroborating with data from the circulation in Chapter 2. Generally, as monocytes migrate through the endothelium, they became more responsive to LPS, though there were no significant differences between subendothelial and reverse migrated monocytes, contrary to the Zimmerman *et al*. findings. Concordant with its known function as an immunoregulatory receptor, monocyte MerTK% expression inversely correlated with TNF-α% in the assay. However, if this was a straightforward linear biological relationship, one would expect reverse migrated monocytes, with the highest MerTK% expression, to have the lowest TNF-α production on LPS stimulation, which we found to be opposite. This points to a more complicated multi-factorial picture, perhaps due to more complex interaction between components of the serum and the extracellular matrix used in the experiment or even metabolism related. The phagocytosis experiments yielded highly variable data, discordant from Zimmerman's findings of highly phagocytic subendothelial monocytes. Taken together, one can infer that monocytes in ACLF, with already high MerTK expression, transmigrate into liver tissue, where they may encounter apoptotic cells or debris in liver injury, may efferocytose these, increasing their

MerTK expression, and some may reverse migrate with even higher expression, thus compounding the problem. This dampens the pro-inflammatory responses to subsequent microbial challenge. Reverse migrated monocytes exit tissue, recirculate and either home to lymph nodes where they negatively regulate adaptive immune responses or to other tissues. Supporting this recirculation theory is the observation that there is higher *ex-vivo* expression of lymph node homing marker CCR7 on MerTK+ peritoneal macrophages (**Figure 3.4C**), higher CCR7 in MerTK+ monocytes in ACLF and increased frequency of MerTK+ CD68+ lymph node macrophages identified in non-follicular regions in decompensated cirrhosis compared with pathological controls (cf. Bernsmeier *et al.*, 2015).

There were a number of limitations to the *in vitro* transmigration experimental work and inferences that require consideration. Firstly, the transmigration assay was labour-intensive, involved multiple steps and reagents and highly sensitive to error. Imperfect assays were sometimes only identified when acquiring cells on the flow cytometer on the fourth day and the factors for which sometimes not easily identifiable. Recognisable faults included failure of the collagen to set, non-confluent HSEC monolayers (which also affected the flow-based adhesion assay) and retraction of the monolayer from the edges of the cell insert. Gaps in the endothelial cell monolayer or at the edges lead to unregulated monocyte migration through the spaces, into and out of the gel plug, and therefore not representative of what happens *in vivo*. Accordingly, the experiments proved difficult to consistently and successfully replicate. Great lengths were taken to optimise the conditions from the prior protocol including optimisation of pH, changing batches of bovine collagen and finding the ideal fibronectin concentration, which had some success. Alternative methods may have been useful to complement the experiment, e.g. immunohistocytochemistry of liver tissue or perfusion of cells through explanted human liver wedges and subsequent cell extraction and flow cytometry. Technology has also advanced now such that there is a spectrum of microfluidic-based 2D/3D cell culture chips, allowing the detailed study of cell-to-cell interactions in a representative microenvironment (Rothbauer, Zirath & Ertl, 2018).

Other ways in which the assay could have been improved include using a fixable viability dye to highlight dead cells on flow cytometric analysis and keeping the aetiology and passage of the HSEC

consistent, given that HSEC are not immunologically inert, though this would prove difficult due to the availability of HSEC (Shetty, Lalor & Adams, 2018). It is also likely that the volume of pHrodo™ BioParticles™ (20µl) was too high, since subsequent optimisation experiments would suggest that 5µl was enough and may have provided better discrimination and more reliable results (Appendix T).

Other theoretical aspects require consideration. Non-migrated monocytes may not migrate due to pre-programming, competition for adhesion binding sites or because they underwent apoptosis or necrosis, all of which could affect their phenotype and function. Indeed, MerTK is a marker of cell survival and chemotherapy-resistance when ectopically expressed on cancer cells (Tworkoski *et al.*, 2013). But, it also has a role in cell motility (Tang *et al.*, 2015). Could monocytes that already express higher MerTK be selected, or have greater ability, for transmigration? Furthermore, the plasticity of cells in their microenvironment is not considered in this model; aside from the conditioning of monocytes in plasma, there are no other microenvironmental cues once they are introduced into the cell inserts lined with HSEC. Finally, reverse migration of myeloid cells has been proposed as a means of sampling a tissue environment and communicating with the adaptive immune system (Muller & Randolph, 1999). Whilst it has been studied extensively in the zebrafish and in some murine models *in vivo*, human data is *in vitro* and therefore some may argue its relevance in physiology and pathophysiology is of doubt (Nourshargh, Renshaw & Imhof, 2016). In human neutrophils, only a tiny proportion (~0.25%) reverse migrated in one study (Buckley *et al.*, 2006).

Further work should include providing microenvironmental cues to assess monocyte behaviour, e.g. using apoptotic hepatocytes in the collagen matrix to better recapitulate liver injury, assessing the expression of other TAM receptors during the migration process and exploring the response to other TLR agonists, e.g. bacterial DNA (CpG) and bacterial lipopeptide (Pam_3CSK_4). Blocking monocyte recruitment by HSEC using VCAM-1 inhibition or pertussis toxin and observation as to whether there is modulation of monocyte phenotype in this setting would elucidate the role of adhesion

molecule-monocyte interaction. Using an inhibitor of MerTK in this model would also provide valuable insight into its function.

5.5. Conclusion

In this chapter, a novel transwell migration assay was employed to investigate the phenotypic and functional characteristics of isolated healthy monocytes, conditioned in plasma from patients with ACLF (and healthy controls), as they migrate across hepatic sinusoidal endothelium, cultured from explanted liver tissue. The assay enabled assessment of monocytes in the non-migrated, subendothelial and reverse migrated phases as a biological model for monocyte entry into, and exit out of, tissue compartments. Here, it was demonstrated that monocytes conditioned in ACLF plasma had increased MerTK expression compared to healthy control, which was further increased by entry into the subendothelial space, and even further enhanced by reverse migration out. Inversely correlated with MerTK percentage expression was LPS-stimulated TNF-α production. The findings are hypothesised to recapitulate monocyte trafficking to the injured liver, where they acquire MerTK and become LPS-tolerant; if they encounter apoptotic cells from liver injury, MerTK may be further enhanced, increasing the susceptibility to infection. In ACLF, where liver injury is greater compared to cirrhosis without organ failure, this may be one mechanism by which MerTK expression is propagated, increasing the risk of infection even more.

Key findings from this chapter include:

- The highest percentage of monocytes expressing MerTK was seen in the reverse migrated phase, suggesting monocytes acquire MerTK as they enter and exit tissue.
- The highest LPS-stimulated TNF-α production was observed in subendothelial monocytes in healthy controls and cirrhosis without organ failure.
- In ACLF plasma-conditioned monocytes, LPS-triggered TNF-α production was less compared to healthy control, and more in the reverse migrated monocytes compared to the subendothelial, perhaps suggesting ACLF monocytes are programmed to be tolerant when they enter tissue.

- When all migration phases were considered together, there was an inverse correlation between MerTK% and LPS-triggered TNF-α production *in vitro*.
- The migration experimental data adds to a recirculation theory whereby monocytes enter injured liver, upregulate MerTK becoming tolerant to LPS, and reverse migrate to re-enter the circulation, or homing to lymph nodes or other tissues, explaining the compartmental enhancement of MerTK in ACLF, predisposing to infection (see 7.2.6).
- No significant differences were observed with bacterial phagocytosis though the variability of results in the ACLF group was high.
- The week-long transmigration assay was sensitive to error with wells sometimes demonstrating non-confluent HSEC growth which therefore needed to be discarded.
- The flow-based adhesion assay performed to investigate differences in monocyte adhesion and rolling of THP-1 monocytes conditioned in ACLF plasma vs. healthy was limited by non-confluent growth of HSEC on the ibiPore Flow μ-slide membrane allowing monocytes to bypass HSEC.
- Further work should include:
    a) Modifying the transwell assay to include apoptotic hepatocytes or ascites from ACLF (vs. cirrhosis without OF) in the collagen matrix.
    b) Expanding the functional readouts to include oxidative burst and efferocytosis
    c) Use of microfluidic 3D liver chips which provide a more advanced model to study monocyte migration.

CHAPTER 6

6. INHIBITION OF MER TYROSINE KINASE SIGNALLING

6.1. Background and Aims

The innate immune system must be carefully regulated, such that mechanisms to switch on an inflammatory response to an insult (injurious or infectious) must be tied to mechanisms to switch it off. Whilst toll-like receptor (TLR) signalling and pro-inflammatory cytokine production is necessary to overcome bacterial, viral and fungal infection, over-exuberant or prolonged signalling can result in chronic inflammation and immunopathology (Lemke & Rothlin, 2008). TAM receptors are key mediators in immune homeostasis, functioning to clear apoptotic cells and debris, and acting as inhibitors of the inflammatory response to prevent its dysregulation (Rothlin *et al.*, 2007, 2015). Activation of TAM receptors leads to an IFNAR-STAT1-dependent modulation of SOCS1 and SOCS3 gene expression, which are negative regulators of TLR signalling at multiple levels (Rothlin *et al.*, 2007). In diseases in which MerTK is over-expressed, inhibition of its signalling pathway may represent a promising strategy to enhance innate immune responses. Inhibition has been mostly studied in oncology, where MerTK has been observed to be ectopically expressed in B- and T-cell acute lymphoblastic leukaemia (ALL), acute myeloid leukaemia (AML), non-small cell lung cancer (NSCLC), glioblastoma multiforme (GBM) and metastatic melanoma (Graham, 2006; Wang *et al.*, 2013, 2013; Lee-Sherick *et al.*, 2013; Xie *et al.*, 2015). Here, MerTK inhibition via short hairpin RNA (shRNA) or monoclonal antibody was observed to increase tumour cell apoptosis, reduction in colony formation and inhibited invasion of cancer cells (Cummings *et al.*, 2013; Schlegel *et al.*, 2013; Knubel *et al.*, 2014). However, theoretically there is a risk of host antibody formation against MerTK antagonist antibodies, potentially leading to infusion reactions and delayed hypersensitivity. Small molecule inhibitors however are less immunogenic and have shown promise in preclinical models. UNC569 potently inhibits MerTK phosphorylation and downstream signalling, suppressing tumour cell survival and proliferation in ALL cell lines (Christoph *et al.*, 2013).

Our group demonstrated the expansion of MerTK+ monocytes in ACLF patients and provided proof-of-principle data that inhibition of MerTK signalling, using the selective small molecule inhibitor UNC569 on healthy monocytes conditioned for 24 hours in ACLF plasma, was able to enhance TNF-α and IL-6 production after LPS stimulation (Bernsmeier *et al.*, 2015). However, UNC569 has off-target effects, namely inhibition of the human *ether-a-go-go*-related gene potassium channel (hERG), which can lead to the pro-arrhythmogenic cardiac long QT syndrome and sudden death, a reason for the withdrawal of several Food and Drug Administration (FDA)-approved drugs in the United States (Liu *et al.*, 2013). Other iterations of the agent have been developed including UNC1062 and UNC1666 which have enhanced MerTK potency and reduced activity against hERG but have had poor pharmacokinetic profiles, preventing their progression to preclinical oncology studies (Huey *et al.*, 2016). The latest iteration, UNC2025, is highly selective for MerTK, with > 45x selectivity than for Tyro3 and Axl, a half maximal inhibitory concentration (IC_{50}) of 2.7nM in cellular assays, and a good side effect profile in animal cancer models (Huey *et al.*, 2016; Deryckere *et al.*, 2017).

Other methods of blocking the MerTK signalling pathway, for example through Gas6 inhibition or LXR-α pathway antagonism, may also represent alternative strategies (Kariolis *et al.*, 2016; Kimani *et al.*, 2017). Sequestration of Gas6, a ligand for the MerTK receptor, may limit its signalling pathway. Similarly, given LXR-α signalling increases MerTK transcription, modulation of LXR-α may also interrupt MerTK pathways (Kim *et al.*, 2016). By blocking the MerTK signalling pathway, the immunotherapeutic potential of these inhibitors can be explored in addition to off-target effects.

Hypothesis and aims:

In light of the expansion of MerTK+ monocytes in ACLF and proof-of-principle data that UNC569 could restore LPS-stimulated pro-inflammatory cytokine secretion, it was hypothesis that blockade of the MerTK pathway could modify monocyte/macrophage phenotype and function. Hence, in this chapter, the aims were:

- Titration of the MerTK inhibitor UNC2025 inhibitor according to its effects on cytokine production and cell survival.
- Impact of other MerTK inhibition strategies on cytokine signalling, including inhibitors of Gas6, IL-10, IL-17 and LXR-α.

6.2. Materials and Methods

6.2.1. Reconstitution of UNC2025

Lyophilized UNC2025 (trans-4-[2-(butylamino)-5-[4-[(4-methyl-1-piperazinyl) methyl] phenyl]-7H-pyrrolol[2,3-d]pyrimidin7-yl]-cyclohexanol), conjugated with hydrochlorate, was provided courtesy of Professor Shelly Earp (University of North Carolina, USA). Molecular weight was 586.04 g/L. The powder was weighed, resuspended in dimethyl sulfoxide (DMSO) and vortexed; of note, solubility of UNC2025 in DMSO was up to 25mg/ml. Inert gas purging with nitrogen was recommended but not performed due to unavailability of a suitable nitrogen source. The soluble UNC2025 was aliquoted with stock concentration made up to 10mM. Vials were frozen at -20°C and were for single-use only in subsequent experiments. DMSO was used at same concentration as vehicle to establish the effect of DMSO.

6.2.2. UNC2025 Titration Experiments

Previously UNC569 was used at an optimum concentration of 2μM on healthy CD14+ selected human monocytes, conditioned in 25% healthy donor or ACLF plasma for 16 hours (Bernsmeier *et al.*, 2015). The only published UNC2025 titration experiments evaluated its impact on survival of MerTK+ primary cells or cell lines (measured by relative colony number), with no effect of 500nM UNC2025 on healthy human bone marrow mononuclear cells (absent MerTK expression), a reduction in colony number at 500nM in umbilical cord blood mononuclear cells (low MerTK expression) and an IC_{50} of 70nM in AML cell lines (>80% MerTK expression) (Deryckere *et al.*, 2017). No evidence exists for its effect on cytokine production or survival of human peritoneal macrophages or circulating monocytes.

Here, UNC2025 titration experiments evaluated the dose range of 100nM to 5μM in order to identify an optimum concentration.

To evaluate the effect of differing UNC2025 concentrations on cytokine production, thawed ascitic cells, at a concentration of one million per ml of complete media in a 24-well plate, were pre-treated with UNC2025 or DMSO vehicle at different concentrations for 2 hours, and were subsequently stimulated with 100ng/ml of LPS for 4 hours. Golgi Stop (0.25μl) was added to each well after one hour and the assay performed as per previously described protocol (2.2.7). In the first experiment, ascitic cells (n=1), were exposed to UNC2025 at a concentration range of 0, 500nM, 1μM and 2μM, with corresponding DMSO vehicle concentrations. In the second experiment, ascitic cells (n=1), healthy PBMCs (n=1) and ACLF PBMCs (n=1) were exposed to UNC2025 at 0, 100nM, 500nM and 5μM concentrations, again with DMSO vehicle for comparison. The flow cytometric monoclonal antibody panel included CD14 PE-Cy7, CD16 APC-H7 and TNF-α PE (BD Biosciences, UK), HLA-DR PerCP Cy5.5 (Life Technologies, UK) and IL-6 Brilliant Violet 421 (BioLegend, UK). Fixable viability dye eFluor 506 (Life Technologies, UK) was used. MerTK was excluded from the panel to avoid any interference the antibody binding may have on the action of UNC2025, though a separate well with untreated and unstimulated cells was used a control to identify the expression of MerTK of the cells at baseline.

To investigate the effect of different UNC2025 concentrations on cell survival, an apoptosis assay was performed using Annexin V FITC and 7-AAD PerCP (BioLegend, UK). In short, after pre-incubation of UNC2025 and subsequent stimulation with LPS for 4 hours, cells were retrieved, washed in PBS and stained with CD14 PE-Cy7 for 20 minutes at room temperature. They were subsequently stained with Annexin V and 7-AAD in Annexin V buffer, and after 15 minutes at room temperature, acquired on the flow cytometer (BD FACS Fortessa) within 1 hour as per manufacturer's recommendations.

6.2.3. Measurement of Pro-inflammatory Cytokines and Apoptosis Markers by ELISA

In similar conditions to the experiment above (6.2.2), but in separate wells, thawed ascitic mononuclear cells were pre-incubated for 2 hours with UNC2025 of varying concentrations (0, 500nM, 1μM, 2μM and 5μM). After this time, LPS (100ng/ml) was added and the cell culture supernatant was collected after 4 hours. No Golgi Stop^{TM} was added. Supernatants were analysed by using TNF-α EASIA (n=1), IL-6 ELISA (n=5) (3.2.16) and M30 ELISA (n=1) (3.2.17).

6.2.4. Effect of UNC2025 on Efferocytosis of Apoptotic Neutrophils

To determine whether inhibition of MerTK signalling could affect efferocytosis, the capacity of healthy PBMCs (n=2) and ACs (n=1) to engulf healthy apoptotic neutrophils, in the presence or absence of UNC2025 at 500nM, was evaluated *in vitro*. Neutrophils were rendered apoptotic by culture for 20hrs and pre-stained with Cell Tracker Violet (BMQC+) as per previous protocol (3.2.20). They were then co-cultured with PBMCs and ACs in the presence or absence of UNC2025 at 500nM. PBMCs were evaluated in one experiment with PBMC-to-neutrophil ratio of 1:4 and ACs in another experiment with AC-to-neutrophil ratio of 1:2. Ideally, the ratio for the latter should have been 1:4 but the neutrophil isolation for that particular experiment generated insufficient neutrophils. Hence, the efferocytic capacity between PBMCs and ACs cannot be compared. Cells that had efferocytosed apoptotic neutrophils were deemed to be CD14+ BMQC+ on flow cytometric analysis. Gates were set using FMO for BMQC.

6.2.5. Proinflammatory Cytokine Production of PBMCs Conditioned in Ascites +/- Antagonists

Ex-vivo PBMCs were isolated as per protocol (2.2.3) with ACK lysis buffer used to remove erythrocytes. After cell counting, 500,000 cells were allocated per well of a 48-well plate, in combination with 50% ascites from ACLF patients (n=5), 50% plasma from healthy volunteers (n=6) or glutamate-containing complete media alone. Antagonists were added to select wells: 5μM GSK2033 (LXR- α antagonist, Tocris, UK), 5μg/ml Gas6 polyclonal goat IgG antibody (R&D, UK), 5μg/ml

IL-10 Ultra-LEAF^{TM} purified anti-human antibody (BioLegend, UK), 2.5μg/ml IL-17 antibody (R&D, UK) and 500nM UNC2025 (6.2.1). Cells were incubated for 24 hours at 37°C 5% CO_2 after which time LPS 100ng/ml was added to the wells for 4 hours. The intracellular cytokines staining protocol (2.2.7) was followed. Isotype controls were used for TNF-α and IL-6 and FMOs for MerTK, Axl and HLA-DR. Isotype controls were also used for Gas6 antibody (goat polyclonal IgG1, R&D, UK), IL-10 LEAF rat IgG2α and DMSO vehicle for UNC2025, all used at the same concentrations as their counterparts. The flow cytometry panel used is listed in Appendix S.

6.2.6. Reconstitution and Concentrations of MerTK Signalling Antagonists

Reconstitution of lyophilized antagonists were performed as per manufacturer's recommendations. In short, GSK2033 was reconstituted in DMSO to a stock concentration of 10mM and experimental target concentration of 5μM as previously used with Th17 CD4+ T-cells (Solt, Kamenecka & Burris, 2012). Gas6 polyclonal goat IgG was reconstituted in sterile PBS to a stock concentration of 1mg/ml and a target of 5μg/ml, a concentration previously used with CD14+ macrophages to block Gas6 (Zizzo *et al.*, 2012). The IL-10 Ultra-LEAF^{TM} anti-human neutralizing antibody did not require reconstitution; stock concentration was 1mg/ml and was diluted in media to a target of 5μg/ml (Jin *et al.*, 2014; Cates *et al.*, 2015). IL-17 neutralizing polyclonal goat IgG antibody was reconstituted in PBS to a stock concentration of 0.2mg/ml and a target of 2.5μg/ml. Published studies involving the neutralizing IL-17 antibody have used a concentration range of 1-10μg/ml on human cells (Witowski *et al.*, 2007; Shahrara *et al.*, 2009; Xing *et al.*, 2013).

6.3. Results

6.3.1. UNC2025 Concentrations Above 500nM Reduce Ascitic Cell Survival and Impair LPS-stimulated Pro-Inflammatory Cytokine Production

In the first flow cytometry experiment to investigate the effect of UNC2025 on ascitic macrophage LPS-stimulated cytokine production, the highest TNF-α production was seen when no UNC2025 or vehicle was added (MFI 477; TNF-α 36.3%). Preincubation with 500nM UNC2025 resulted in marked reduction in TNF-α production (MFI 111; 8.11%) with comparably more produced with DMSO vehicle, suggesting that this concentration of UNC2025 impaired LPS-stimulated TNF-α generation (**Figure 6.1B**). Similar results were obtained when higher concentrations were used. Likewise, IL-6 (%) was impaired with 500nM UNC2025 though there was not a marked difference when compared with DMSO vehicle. Little difference was seen in IL-6 expression by MFI even at 1μM concentrations of UNC2025. Similarly, HLA-DR MFI expression showed only a slight reduction with 1μM UNC2025 and was associated with little difference in percentage expression of HLA-DR. The post-LPS stimulated MerTK expression of the AC sample used in experiment 1 was 63.2%. A second experiment aimed to evaluate a wider UNC2025 dose range (100nM to 5μM) across ACs and PBMCs but unfortunately, the LPS used did not stimulate the cells at all (a different batch was used). However, while the first titration experiment only used thawed ACs from one patient, the data was corroborated by the ELISA results showing that the TNF-α concentration (pg/ml) in supernatants obtained from LPS-stimulated ACs (n=1) progressively declined as the concentration of pre-incubated UNC2025 increased from 500nM to 10μM. Similarly, the IL-6 concentration (pg/ml) in supernatants (n=5) declined as the UNC2025 concentration increased (**Figure 6.1C**). The IL-6 concentration in two supernatants across different UNC2025 concentrations was negligible and therefore likely that either the cells were non-viable or the LPS used did not adequately stimulate the cells. The reason for diminishing cytokine production with higher UNC2025 concentration may be increased cell death with potent MerTK signalling inhibition.

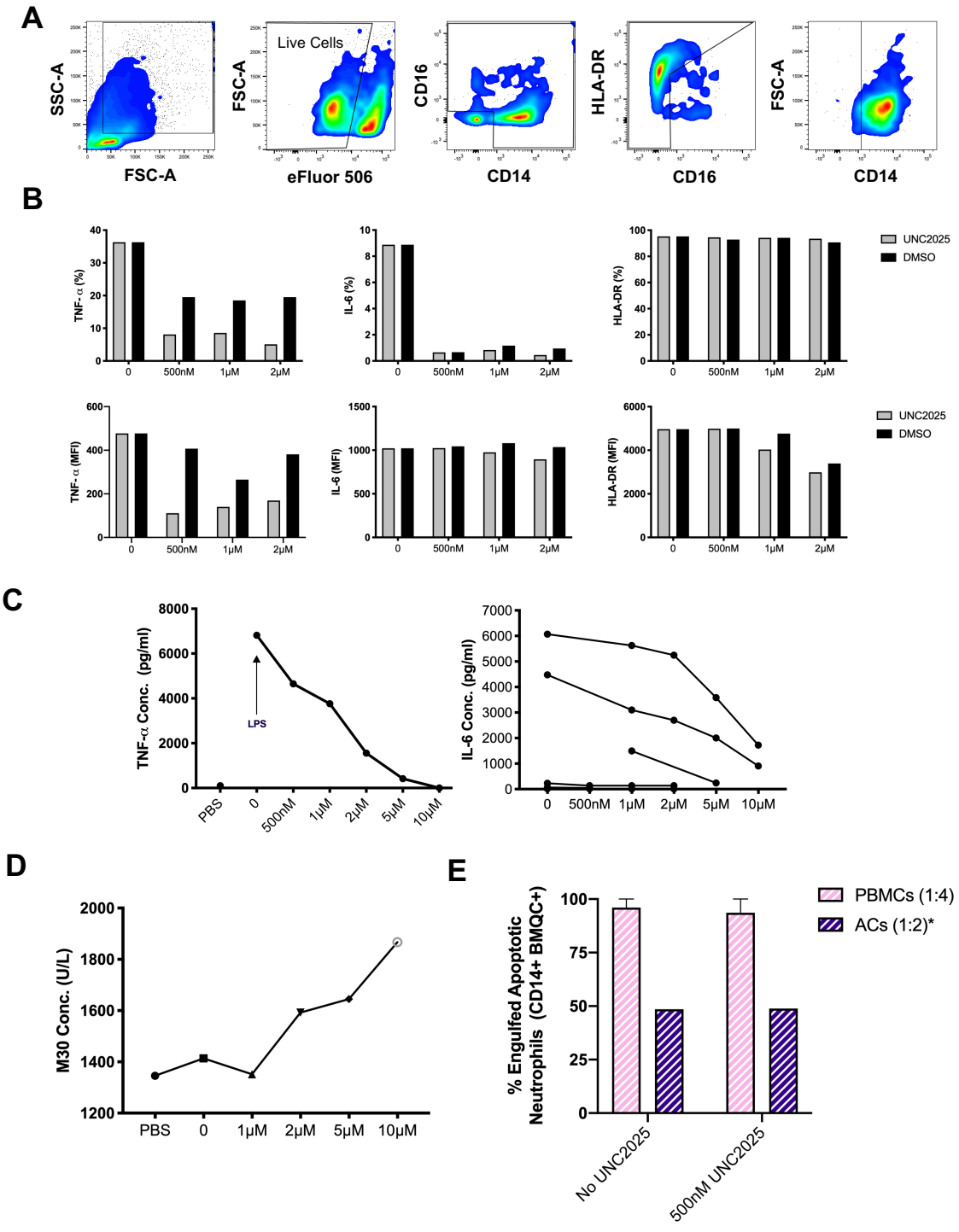


Figure 6.1 Effect of MerTK Signalling Inhibitor UNC2025 Concentration on LPS-Stimulated Cytokine Production, Cell Survival and Efferocytosis

(A) Validated DR-gating strategy used for flow cytometry analysis of ascitic cell cytokine production (B) Effect of 2hr precubated-UNC2025 concentration on LPS (100ng/ml)-stimulated peritoneal macrophage (n=1) HLA-DR expression, and TNF-α and IL-6 production (% - top row; median fluorescence intensity – bottom row) (C) UNC2025 concentration (x-axis) and effect on LPS-stimulated AC supernatant cytokine concentrations with TNF-α EASIA (n=1) and IL-6 ELISA (n=5) (D) Effect of pre-incubated UNC2025 concentration (x-axis) on

LPS-stimulated AC M30 (apoptosis marker) concentration (U/L) (n=1) (E) Effect of 500nM UNC2025 on efferocytosis of PBMCs (n=2) and ACs (n=1) of apoptotic BMQC (cell tracker violet)-stained neutrophils. *Ascitic cell to apoptotic neutrophil ratio was 1:2 in comparison to PBMC to apoptotic neutrophil ratio of 1:4. Where relevant, data expressed as mean with standard error of margin.

An experiment to measure this with flow cytometry was unsuccessful due to poor initial cell viability of the sample used. However, M30 concentration (U/L) in supernatants of ACs (n=1) stimulated with LPS and pre-incubated with varying UNC2025 concentrations demonstrated increased early apoptosis with higher UNC2025 concentrations beyond 1μM (**Figure 6.1D**). The addition of 500nM UNC2025 appeared not to have an impact on efferocytosis for PBMCs and ACs (**Figure 6.1E**).

Taken together, the experiments demonstrated that UNC2025 concentrations of ≥ 500nM impaired LPS-stimulated TNF-α and IL-6 production, possibly attributed to poorer cell survival. The sample sizes for these experiments were very small so firm conclusions cannot be made. Experiments were hindered by poor initial cell viability after thawing, and a problematic batch of LPS. Further work is required to expand the datasets and moreover, evaluate the dose range from 0 to 500nM by ICCS and flow cytometry, and transcriptomic profiling.

6.3.2. LXR-α Antagonist GSK2033 Enhances LPS-Stimulated TNF-α Production in PBMCs Conditioned in 50% Ascites from Patients with ACLF

Healthy PBMCs from the same donor cultured in ascites from ACLF patients demonstrated a large reduction in LPS-stimulated TNF-α MFI compared to PBMCs cultured in healthy control plasma (TNF-α MFI: 996 vs. 2458, p=0.08), though there was some overlap with healthy control. This highlighted that the ascitic microenvironment in ACLF may promote immunotolerance (**Figure 6.2A**). There was no significant difference between PBS and LPS-stimulated TNF-α in PBMCs in ACLF ascites, pointing to endotoxin tolerance. To evaluate the immunotherapeutic potential of MerTK pathway antagonists, PBMCs cultured in ACLF ascites were simultaneously exposed to one of

UNC2025 (500nM), Gas6 antibody, IL-17 antibody, IL-10 antibody or LXR-α antagonist GSK2033 for 24 hours, followed by LPS stimulation, and TNF-α production was analysed by ICCS.

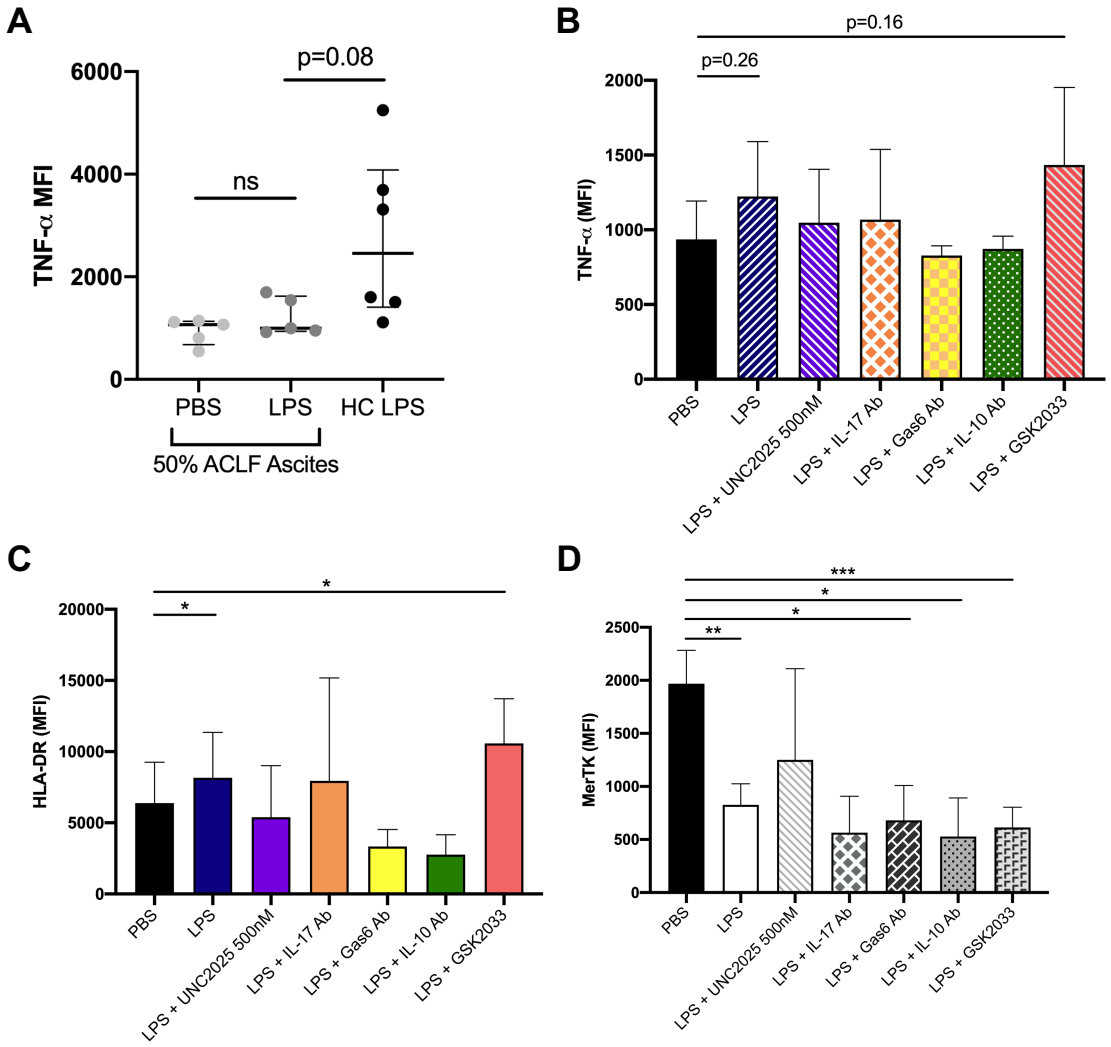


Figure 6.2 Effect of MerTK antagonists on LPS-Stimulated TNF-α Production, and HLA-DR and MerTK Expression in PBMCs Exposed to 50% Ascites from Patients with ACLF

(A) Monocyte TNF-α production (MFI) determined by flow cytometric intracellular cytokine staining (ICCS) from PBMCs cultured for 24 hours in 50% ascites from patients with ACLF stimulated with PBS (n=5) or LPS (n=5) for 4 hours compared with LPS-stimulated PBMCs in 50% healthy control plasma (B) Monocyte TNF-α production (MFI) of PBMCs in 50% ACLF ascites exposed to MerTK antagonists for 24 hours: UNC2025 500nM (n=4), IL-17 neutralizing antibody (n=4), Gas6 neutralizing antibody (n=3), IL-10 neutralizing antibody (n=3) and LXR-α antagonist GSK2033 (n=5). (C) HLA-DR monocyte expression (MFI) with aforementioned exposure to antagonists (D) MerTK monocyte expression (MFI) with aforementioned exposure to antagonists. All data is expressed as median with interquartile range. In (A), difference between PBS and LPS in PBMCs in ACLF ascites was paired so Wilcoxon paired-rank test was used; difference between LPS-stimulated PBMCs in 50% ACLF and healthy control plasma (n=6) was not paired and Mann Whitney U test was used. In (B), (C) and (D), a mixed effects analysis was used (assuming normality – verified with Shapiro-Wilkes analysis) since some paired values were missing, with Dunnett's multiple comparison's test using PBS as the control group and assuming an alpha

of 0.05 and adjustment of p-values for multiple comparisons. Where not indicated, differences between PBS and a group is assumed non-significant. Where stated, *p<0.05 **p<0.01, ***p<0.001

Using a mixed-effects model and PBS as control, there was no significant change in LPS-evoked TNF-α production observed with any agent, though the greatest increase being GSK2033 (p=0.16 by mixed effects model). The only agent which increased monocyte TNF-α production compared with LPS alone was GSK2033 (median 996 vs. 1095, p=0.06 by Wilcoxon signed rank) (**Figure 6.2B**). There were no significant differences between the viability of cells exposed to the different agents, as assessed by comparison of viability dye MFI of the whole cell population and the aforementioned mixed-effects model (data not shown). Likewise, GSK2033 increased monocyte HLA-DR expression (median 7049 vs. 10202, p<0.05 by mixed effects model) when compared with PBS (**Figure 6.2C**). Other agents did not have any significant effect on HLA-DR expression, though the sample size was small. In terms of effect on monocyte MerTK surface expression, as previously described, LPS exposure results in a significant downregulation (p<0.01); the only agent to further downregulate MerTK was GSK2033 (p<0.001 when compared with PBS in mixed-effects model or p=0.06 when compared with LPS alone by Wilcoxon signed rank) (**Figure 6.2D**). The binding of UNC2025 or polyclonal Gas6 IgG antibody may have affected the binding of the MerTK APC IgG1 antibody used for staining and vice versa, so these results should be interpreted with caution.

6.4. Discussion

In the immunological response to sepsis and ACLF (both SIRS-mediated diseases), both pro- and anti-inflammatory responses are activated at incipience but the pro-inflammatory response predominates. As they progress, the anti-inflammatory response becomes predominant. (Hotchkiss *et al.*, 2009; Berry *et al.*, 2010a). With good supportive measures in intensive care, most patients survive the early cytokine storm and enter the later phase of immuneparesis, where the immune system is unable to effectively combat microbial challenge, leading to either incomplete clearance of the primary infection, or development of new secondary infections. In severe sepsis and ACLF, this is usually the cause of death despite the use of potent antimicrobial drugs (Fernandez *et al.*, 2018). The TAM receptor signalling pathway is a negative regulator of monocyte and macrophage inflammatory responses, after initiation of the inflammatory process (Rothlin *et al.*, 2007). Upregulation of MerTK monocyte expression has been observed in severe sepsis and ACLF, and is likely to be a key mediator in the later phase of immunosuppression (Guignant *et al.*, 2013; Bernsmeier *et al.*, 2015). The cellular mechanisms for upregulation of MerTK are multimodal; as demonstrated in chapter 3 and supported by literature, efferocytosis itself promotes a M2c-like restorative phenotype, and the effect of mediators in ACLF ascites, rich in cytokines and apoptotic/necrotic material, enhanced MerTK expression (Fadok *et al.*, 1998; Zizzo *et al.*, 2012). Modulating MerTK signalling therefore represents a promising immunotherapeutic strategy, and work by our group demonstrated 2μM UNC569, a selective MerTK inhibitor, was able to augment LPS-stimulated pro-inflammatory cytokine responses in ACLF plasma-conditioned CD14+ isolated monocytes (Bernsmeier *et al.*, 2015).

In this chapter, a more potent and selective MerTK inhibitor, UNC2025, was evaluated on an ascitic mononuclear population, to test the hypothesis that it could equally augment LPS-stimulated pro-inflammatory cytokine responses. The range of 500nM to 10μM was used to ensure complete inhibition of MerTK phosphorylation and disruption of the signalling pathway. However, at a concentration of 500nM UNC2025, cytokine production (TNF-α and IL-6) was lower compared to no pre-incubation with UNC2025, both on flow cytometry and ELISA readouts. There was a progressive

decline in cytokine production with increasing UNC2025 concentration, in parallel with an increasing M30 concentration, suggesting increased cell apoptosis may be responsible for declining cytokine production. Indeed, MerTK has a role in survival of macrophages exposed to oxidative stress, and inhibition of ectopically-expressed MerTK on tumour cells results in their death (Anwar *et al.*, 2009; Knubel *et al.*, 2014). A concentration of 500nM did not appear to impact on efferocytosis. Further UNC2025 titration work is needed in the 0-500nM concentration range to identify the optimum concentration to enhance inflammatory cytokine responses to microbial challenge whilst minimising apoptosis and maintaining efferocytosis. Furthermore, a mononuclear cell population was chosen, rather than an isolated CD14+ population or a cell sorted macrophage population, on which to use UNC2025; this reflected a more *in vivo* scenario if the MerTK inhibitor were to be used as an immunotherapeutic drug but the effect on a pure macrophage population is not known, which subsequent work would need to address. UNC2025 may also have off-target effects; over-exuberant pro-inflammatory responses, autoimmunity due to inadequate clearance of apoptotic or necrotic material and inadequate resolution responses are risks of MerTK inhibition. One could argue that resolution responses do however have a number of parallel mechanisms and there is therefore redundancy in the system (Ortega-Gómez, Perretti & Soehnlein, 2013). UNC2025 is also known to decrease platelet activation, which might increase risk of haemorrhage (Branchford *et al.*, 2018). Some authors report ACLF may be a state associated with higher bleeding risk compared with AD, so use of UNC2025 in ACLF would need to evaluate this (Fisher *et al.*, 2018). Clearly for such an inhibitory strategy to work, identification of the phase of the immune response that a patient with ACLF is in, the degree of MerTK expression / signalling and the optimal dose and timing would need to be established. Whilst mouse models of ACLF are lacking, murine experiments with acute and chronic liver injury and use of UNC2025 would help to define these.

Other strategies to impede MerTK signalling may also be promising, including neutralisation of TAM ligands (e.g. Gas6), cytokines that enhance MerTK expression (e.g. IL-10 and IL-17; cf. Chapter 3) and inhibition of LXR-α. Two outputs as a measure for improved response to microbial challenge includes

pro-inflammatory cytokine signalling (e.g. TNF-α) and increased antigen presentation capabilities (HLA-DR expression). The sample size was small and so differences between groups were not significant. Exposure of the cells in ACLF ascites to IL-10, IL-17 and Gas6 neutralising antibodies resulted in reduced MerTK expression, though impaired LPS-stimulated TNF-α production and lower HLA-DR expression compared to LPS alone (**Figure 6.2B&C**). UNC2025 500nM demonstrated similar outcomes though it's effect on MerTK expression was less striking.

The only agent to improve TNF-α production and HLA-DR expression was LXR-α antagonist GSK2033. It is known that the gene encoding MerTK (*Mertk*) is an LXR-responsive gene (A-Gonzalez *et al.*, 2009a). LXRs have a pivotal role in regulating reverse cholesterol transport and sterol homeostasis in macrophages (Hong & Tontonoz, 2014). When phagocytes ingest apoptotic cells, degradation of their lipid membranes and organelles leads to oxysterol accumulation; failure to clear this leads to toxic effects such as lysosomal dysfunction, endoplasmic reticular stress and mitochondrial dysfunction (Gibson, Domingues & Vieira, 2018). Activation of LXR by apoptotic cells works to clear these intracellular lipids using ABC family membrane transporters (e.g. ABCA1) and inducing the expression of cholesterol acceptors such as APOE (Hong & Tontonoz, 2014). Enhanced LXR-driven transcription of MerTK, and subsequent Gas6-MerTK signalling-driven LXR transcription, further promotes apoptotic cell clearance and cholesterol homeostasis in a positive feedback loop (Choi *et al.*, 2015). Upregulated transcription of *NR1H3* (LXR gene) and *APOE* was observed in MerTK+ peritoneal macrophage in Chapter 3. But linked to both LXR and MerTK is associated innate immune suppression, part of the resolution response to inflammation and tissue injury, to avoid unwanted immune responses against intracellular antigens. In murine experiments, apoptotic thymocytes promoted the expression of immunosuppressive mediators TGF-β and IL-10 in wild type macrophages though induction of these genes was impaired in $LXR^{-/-}$ macrophages (A-Gonzalez *et al.*, 2009a). LXR antagonist GSK2033 likely changes this balance and therefore represents a potential immunotherapeutic agent to augment inflammatory responses in ACLF. However, as with direct MerTK inhibition, this could impact on resolution responses and cholesterol efflux mechanisms, leading to off-target effects. These may

include promotion of atherosclerosis and progression of coronary heart disease which could have important implications in patients with NAFLD, a leading cause for liver disease in the Western world (Haas, Francque & Staels, 2016). With all the antagonists tested, concentrations used were based on published papers but further work is required to titrate according to effect to ascertain optimum concentrations.

6.5. Conclusion

Data presented in previous chapters has identified increased expression of MerTK in ACLF on circulating monocytes and peritoneal macrophages and linked this to attenuated responses to microbial challenge. Accordingly, modulation of the MerTK signalling pathway represents a promising strategy to reversing these innate immune defects. Likewise, given the observations of the MerTK-upregulating effect of IL-10 and IL-17, and association of the LXR-α pathway, their antagonism also provided other potential means of immune augmentation in ACLF. Here, a novel potent MerTK inhibitor UNC2025 was trialled for the first time on human peritoneal macrophages from patients with cirrhosis. It was demonstrated that UNC2025 at concentrations beyond 500nM did not augment pro-inflammatory cytokine responses of ascitic peritoneal macrophages to LPS stimulation, most likely due to excessive cell death. Further work is required to test a lower concentration range and expand the small dataset. LXR-α antagonism showed promise with improved TNF-α production and upregulated HLA-DR, albeit non-significant, in PBMCs cultured in ACLF ascites and subsequently LPS-stimulated. Again, further work is required to evaluate all the antagonists tested more robustly, with dose titration experiments and impacts on other functional cellular processes such as efferocytosis, pathogen phagocytosis and oxidative burst. The best strategy to improve innate immune responses in the immunosuppressive phase of ACLF is likely to involve multi-pathway modulation but requires a robust, dynamic and point-of-care method of determining the degree of immunosuppression and liver regeneration in patients with ACLF in order to tailor modulation to the individual.

Key findings of this chapter include:

- PBMCs cultured in ascites from ACLF patients demonstrated impaired LPS-stimulated TNF-α production compared to those cultured in healthy control plasma, supporting the immunotolerant microenvironment hypothesis of cirrhosis and ACLF.
- Concentrations of MerTK inhibitor UNC2025 greater than 1μM induced greater cell death in peritoneal macrophages.
- No improvement in LPS-stimulated TNF-α production in ascites-cultured PBMCs was observed with the tested UNC2025 concentrations equal to or greater than 500nM.
- Antagonism of Gas6, IL-10 and IL-17 did not demonstrate any augmentation of LPS-stimulated TNF-α production.
- Only LXR-α antagonist GSK2033 generated a non-significant improvement in TNF-α and a significant increase in HLA-DR, suggesting improved antigen-presenting capabilities.
- The effect of LXR-α antagonist GSK2033 on these readouts is a potentially translational finding; currently no clinical drug equivalent exists. Further experimental data is required.
- Dose titration and experimental condition optimisation is required for all antagonists used.
- Theoretical off-target effects of UNC2025 could include risks of the patient developing autoimmunity, impairment in resolution responses and reduced platelet activation (the latter perhaps increasing the risk of bleeding in ACLF). These require further experimental evaluation.
- The effect of antagonists on the observed defective peritoneal macrophage oxidative burst warrants exploration.

CHAPTER 7

7. GENERAL DISCUSSION

7.1. Introduction

Mortality from liver cirrhosis in the UK in increasing (Williams & Horton, 2013). Compared to the healthy population, these patients are at increased risk of bacterial infection which is linked to the development of organ failure (ACLF) and death (Jalan *et al.*, 2014a). Even in patients with ACLF in which organ failure has not been precipitated by infection, there is a higher risk of sepsis and subsequent poorer outcomes (Fernandez *et al.*, 2018). One of the commonest and most serious infections in decompensated cirrhosis is SBP. The pathogenesis of SBP is described by the pathological bacterial translocation hypothesis in which there is gut dysbiosis, increased intestinal permeability to gut bacteria and bacterial products, and hepatocyte injury (Wiest, Lawson & Geuking, 2014). Kupffer cells in the liver are activated by PAMPs and DAMPs, initiating a pro-inflammatory response, with recruitment of bone-marrow derived monocytes to the liver, differentiation into inflammatory macrophages to expand the macrophage pool and further tissue injury. This innate immune activation is self-perpetuating and eventually may result in pro-inflammatory cytokine release into the systemic circulation resulting in SIRS, and in some cases vascular endothelial dysfunction and microcirculatory disturbances causing organ failure (OF) (Clària *et al.*, 2016a). Paradoxically, in parallel to SIRS, a compensatory anti-inflammatory response syndrome (CARS) develops due to liver-generated anti-inflammatory mediators. In combination with efferocytosis of apoptotic cells, they functionally re-programme liver macrophages to a pro-restorative type, promoting resolution of inflammation and tissue homeostasis (Triantafyllou *et al.*, 2018b). Spillover of these anti-inflammatory mediators into the systemic circulation can propagate CARS, resulting in a multi-modal immuneparesis, in which monocyte dysfunction is a key part, increasing the susceptibility to infection. TAM (Tyro3, Axl and MerTK) receptors are expressed on the surface of macrophages and dendritic cells whose signalling serves to promote clearance of apoptotic cells with exposed “eat me” signal phosphatidylserine, coupled with dampening of pro-inflammatory cytokine responses (Lemke & Rothlin, 2008). Bernsmeier *et al.* identified an expansion of MerTK+ circulating monocytes in ACLF associated with liver disease

severity, risk of subsequent infection and mortality (Bernsmeier *et al.*, 2015). In this thesis, it was sought to investigate the expression and function of TAM receptors (Tyro3, Axl and MerTK) on monocytes and macrophages in tissue compartments (circulation, peritoneum and liver) in patients with cirrhosis and ACLF to identify their role in immuneparesis and potentially yield an immunotherapeutic target to improve antimicrobial responses in these patients, reduce susceptibility to infection (including SBP) and improve survival. The importance of strategies to resolve immuneparesis is increasingly being recognised given the emergence of MDR organisms globally (Piano *et al.*, 2018).

7.2. Synthesis of Findings

7.2.1. Circulation

In the circulation, the data presented in this thesis internally validated the expansion of MerTK+ circulating monocytes in patients with ACLF compared to healthy controls and patients with decompensated cirrhosis without OF, correlating with disease severity scores and relating to short-term mortality (Bernsmeier *et al.*, 2015). The percentage of circulating Axl+ monocytes was low (highest in cirrhosis without OF with a median of 1.2%). Tyro3+ monocytes were variable with no significant differences between groups. This identifies the proportion of MerTK+ monocytes as the most important discriminator in ACLF and negates the hypothesis that other TAM receptors (Tyro3 and Axl) are expanded circulation, with capacity to predict outcome. However, when considering the expression of the TAM receptors in the CD14+ population by median fluorescence intensity (MFI), all are increased in ACLF and similarly, the percentage frequency of CD14+ monocytes expressing all three receptors was increased. This would suggest the factors upregulating one may well apply to the others, but previous authors have proposed a differential function of the receptors. For example, Axl mRNA has been shown to be upregulated with inflammatory signals such as LPS and poly I:C, whilst MerTK upregulation is driven by tolerogenic stimuli such as IL-10 (Zagórska *et al.*, 2014). These opposing roles of MerTK and Axl have been supported by other experimental studies (Zhen, Priest & Shao, 2016). Indeed, in chapter 2, ICCS experiments performed on PBMCs demonstrated Axl+ monocytes had a higher relative LPS-stimulated TNF-α production compared to MerTK+. In chapter 3, this was

also observed in Axl+ peritoneal macrophages in addition to an association with increased phagocytic capacity. But given the low level of Axl+ monocytes (and macrophages), overall this made little difference to the considerably blunted TNF-α (and IL-6) responses in ACLF. It is unclear whether Axl is simply associated with cells that are responsive to LPS or microbial challenge (as per Zagorska's findings of its enhancement in inflammatory environments) rather than being less inhibitory than MerTK. Using an Axl inhibitor in the assays would be very useful to establish the mechanism. Nevertheless, enhancing Axl expression may represent a potential novel immunotherapeutic angle to improve attenuated pro-inflammatory cytokine responses in ACLF, perhaps by priming with poly I:C (TLR3 agonist) which has been used to improve host defence against gram-negative bacteria in the intestine (Ruiz *et al.*, 2016). Transcriptomic profiling of MerTK+ monocytes in patients with alcohol-related decompensated cirrhosis revealed these cells are primed for efferocytosis with upregulation of genes for phagocytic receptors, antigen presentation, *C1q*, and *LIPA*. Complement component C1q is known to act in steady-state as an autocrine and paracrine signal, enhancing MerTK expression, promoting efferocytosis and limiting TNF-α production in murine and human macrophages (Galvan *et al.*, 2012; Hulsebus *et al.*, 2016; Ghebrehiwet, Hosszu & Peerschke, 2017). Ingestion of apoptotic bodies in efferocytosis involves their lysosomal degradation, generating intracellular lipids which in turn results in inflammasome activation. Lysosomal acid lipase (LIPA) is an endocytic enzyme that hydrolyses cholesterol esters into free cholesterol, the efflux of which is mediated by LXR, controls inflammasome activation and maintains metabolic homeostasis (Viaud *et al.*, 2018). LXR promotes MerTK transcription, priming the cell for further efferocytosis and suppressing the production of inflammatory mediators (A-Gonzalez *et al.*, 2009a). The upregulation of phagocytic and antigen-presentation genes suggests these MerTK+ cells could be macrophage-dendritic cell-like hybrids, that function to clear apoptotic cell debris, especially in organ injury, and dampen innate immune responses to pathogens. MerTK is also know to negatively regulate T-cell activation suggesting a potential interaction with the adaptive immune system in susceptibility to infection (Cabezon *et al.*, 2015). Impaired phagocytosis was also identified on live cell imaging of ACLF plasma-conditioned monocytes challenged with fluorescent *E. coli* BioParticles™, contradicting the hypothesis that

phagocytosis was enhanced in ACLF and adding to the corroborating work by Bernsmeier *et al.* but the role of TAM receptors in this has not been elucidated (Bernsmeier *et al.*, 2018).

7.2.2. Peritoneum

In the peritoneum, the percentage of *ex-vivo* macrophages expressing MerTK was high (median 80%), Axl low (2.35%) and Tyro3 mixed (47%), confirming the original hypothesis of MerTK expansion in this compartment. Compared to *in vitro* healthy MDMs, expression of MerTK and CD163 was higher, and Axl lower. The large granular CD14++ CD16++ subset, one-third of the CD14+ cells, had higher MerTK and Axl expression compared to other subsets and the CD14++ CD16++ MerTK+ percentage of macrophages was higher in the AD-ACLF groups compared to stable cirrhosis. However, none of the TAM receptors' expression was able to predict the development of subsequent SBP. In the peritoneal compartment, macrophage TAM receptor expression and the factors leading to SBP may be dynamic and a single snapshot may not be enough to predict its development. Interestingly, peritoneal macrophages from the ascites of patients with advanced ovarian cancer showed no significant differences in TAM receptor expression compared to cirrhotic peritoneal macrophages, apart from only a trend ($p=0.15$) towards higher MerTK% expression in cirrhosis. Here, ovarian cancer ascites acted as a pathological control; it is known that defects in innate and adaptive immunity predispose to cancer progression and reduced survival, hence the role for immunotherapy (McCloskey *et al.*, 2018). But the incidence of SBP in ovarian cancer ascites is very low, suggesting that pathological bacterial translocation, including impairment in hepatic reticuloendothelial function and portosystemic shunting, is pivotal (Bac, de Marie & van Blankenstein, 1996). Further work comparing TAM receptor expression of peritoneal macrophages in ascites from different sources, e.g. abdominal washout during diagnostic laparoscopy, continuous ambulatory peritonitis, cardiac or pancreatic ascites, would be useful to see if there are phenotyping differences that influence the risk of SBP seen in cirrhosis.

Peritoneal macrophages from cirrhosis exhibited preserved bacterial phagocytosis, enhanced efferocytic capabilities but impaired LPS-stimulated TNF-α and IL-6 cytokine signalling and *E.*

coli-stimulated oxidative burst. Peritoneal macrophages had higher resting burst, and MerTK+ cells were associated with lower oxidative burst. Gene expression profiling corroborated with downregulation of superoxide anion generated genes in MerTK+ peritoneal macrophages compared to MerTK-. Like circulating MerTK+ monocytes, upregulated genes at steady-state were those needed for efficient efferocytosis and intracellular lipid metabolism, including *LIPA*, *APOE* and *C1q*. With exposure to LPS, MerTK+ MDM reacted in a classical way with upregulation of TLR4 and NOD1/2 signalling. However, MerTK+ peritoneal macrophages from patients with advanced alcohol-related cirrhosis did not respond in a similar way but instead upregulated anti-apoptotic and anti-inflammatory genes. This demonstrates the anergic state of MerTK+ peritoneal macrophages but also since MerTK+ MDM can generate a normal TLR4 response, that MerTK does not define the cell and that they are truly plastic in nature, subject to multiple mediating factors (Sica, Invernizzi & Mantovani, 2013).

Of course, the ascitic microenvironment exerts an effect on the cells. Healthy PBMCs exposed to ascites were >94% MerTK+ after 48 hours. Indeed, MerTK is a macrophage marker, and in this setting expression of the receptor by MFI was a better indicator (Xue *et al.*, 2014). Notably, ACLF ascites increased MerTK MFI expression in healthy PBMCs (confirming the original hypothesis of its expression in ACLF), reduced HLA-DR MFI and increased the MerTK+ HLA-DR- (%) subset, previously described as immunosuppressive (Triantafyllou *et al.*, 2018a). The latter correlates with a non-significant increase in M-MDSCs, an immunosuppressive subpopulation of myeloid cells, and there may be overlap between the two. These markers predicted poor short-term survival in ACLF but not cirrhosis without OF; due to incomplete recording of clinical data, it is not known whether deaths were due to *de novo* or unresolved sepsis in these patients. In keeping with the divergent roles, ACLF ascites diminished Axl expression. It also promoted an M-MDSC-like phenotype (which correlated with MerTK+ HLA-DR- and thus could represent the same cells) (Bronte *et al.*, 2016). These cells are biologically immunosuppressive but did not exhibit differences in MerTK expression. However, a recent study in melanoma-bearing mice identified that M-MDSCs in TAM receptor knockouts did not exhibit the same immunosuppressive activity implicating a potential role (Holtzhausen *et al.*, 2019).

Further work to test T-cell suppressive capabilities of these *in vitro* M-MDSCs with and without TAM receptor pharmacological blockade in ACLF ascites would be informative.

Whilst recombinant IL-10 or the IL-10/IL-17 combination synergistically promoted MerTK and Axl MFI expression, the prevailing cytokines in ACLF ascites were TNF-α and IL-1β. The paradoxical mix of pro-inflammatory cytokines yet immunotolerant cellular responses to microbial ligands has been reported in the circulation and this dichotomy is recognised by the cirrhosis-associated immune dysfunction model (Albillos, Lario & Alvarez-Mon, 2014; Bernsmeier *et al.*, 2015; Clària *et al.*, 2016a). There are many unmeasured cytokines of relevance, e.g. TGF-β, IL-8, and given their effect may be context and tissue-dependent, the complex interplay of cytokines in the inflammatory milieu requires more investigation. Since SBP is defined by neutrophil infiltration, the dynamic response and interaction of IL-8 with bacterial DNA would be useful to study. Also, of particular interest is the higher concentration of cell death marker M65 in the ascites vs. plasma and in ACLF vs. stable cirrhosis or AD. Given the much lower cell numbers of the peritoneal compartment, the higher levels are surprising. Perhaps there is increased cell death in the peritoneal compartment in ACLF due to fragility of the mesothelial cells, made worse by a metabolically stressed ascitic microenvironment with preferential anaerobic and lipid metabolism. Necrotic cells or M65 may accumulate in ascites from the injured liver which lies within the peritoneal cavity in direct contact with ascites, or from the circulation. Higher circulating M30 and M65 has already been observed in ACLF (Cao *et al.*, 2015; Macdonald *et al.*, 2018). Efferocytosis data from Chapter 3 suggests peritoneal macrophages from cirrhotic patients maintain a good efferocytic index (though not tested against MDMs) and MerTK and Axl% increases after efferocytosis. Indeed efferocytosis itself promotes an immunosuppressive microenvironment, with increased local IL-10 production amongst others (Fadok *et al.*, 1998; Liu *et al.*, 2006). Axl% increase after efferocytosis was much greater in healthy monocytes compared with cirrhotic peritoneal macrophages suggesting circulatory monocytes retain potential to become DC-like whilst peritoneal macrophages are committed to their lineage, perhaps indicating that these were tissue-resident cells (Seitz *et al.*, 2007). TAM receptor ligands Gas6 and Galectin-3 were not significantly raised in ascites but their concentration may be dynamic, and may not be representative of TAM signalling. Further

work is needed to decipher if TAM signalling is heightened in peritoneal macrophages by, for example, using phosphoflow or Western Blot techniques. Ascites bacterial DNA quantification did not reveal any significant associations; further work is needed to validate the assay and expand the cohort. The effect of TLR9 agonist CpG, an analogue of bacterial DNA, on peritoneal immune cells in cirrhotic ascites should be investigated. Recent murine studies on Gata-6+ peritoneal macrophages which can migrate to the subcapsular space to sites of liver injury, and also inadvertently harbour Staphylococcus aureus during infection, are very intriguing (Wang & Kubes, 2016; Jorch *et al.*, 2019). Whilst *GATA-6* was not upregulated in our transcriptomic data, the relationship between Gata-6, CRIg and TAM receptors would be interesting to study.

7.2.3. Liver

In both tissue compartments (peritoneum and liver), and in corroboration with previous work, MerTK+ and Axl+ macrophages both had a $CD16^{high}$ $HLA\text{-}DR^{high}$ $CD206^{high}$ $CD163^{high}$ phenotype. Whilst polarisation does not reflect the plasticity of macrophages, these cell markers do place them in the anti-inflammatory M2c category. There was no significant difference in MerTK expression between normal and cirrhotic liver, refuting the hypothesis, and MerTK+ Axl+ macrophages were of low frequency. Comparing the compartments in patients with decompensated cirrhosis by *ex-vivo* MerTK% expression, lowest was the circulation, intermediate was liver and highest was peritoneum, perhaps reflecting their degree of immunotolerance or tissue homeostasis in these compartments, or even the diversity of cell populations. Macrophages in the liver are abundant, heterogenous and have substantially diverse functions whereas peritoneal macrophages are scant and their primary function is likely tissue homeostasis (Kubicka *et al.*, 1996; Heymann & Tacke, 2016). The scant data on potentially attenuated cytokine signalling in hepatic macrophages needs extended study.

7.2.4. Transendothelial Migration

The transendothelial migration model suggested monocytes acquire MerTK as they enter tissue, and in those that reverse migrate, the highest MerTK expression is observed. This may due to enhanced tissue

differentiation as monocytes migrate or possibly because MerTK+ monocytes are more motile and better suited to migration (Tang *et al.*, 2015). In the tissues, subendothelial monocytes may sample the microenvironment; in ACLF, the microenvironment may be rich in apoptotic bodies and their endocytosis and efferocytosis may promote MerTK further. Some DC-like cells reverse transmigrate, homing to lymph nodes via circulation or lymphatics to present auto-antigen to T-cells and tolerising them (Bernsmeier *et al.*, 2015). These reverse migrated MerTK+ cells (with expanded HLA-DR- subset in liver injury) may also recirculate into tissue such that their tolerogenic effect becomes widespread (recirculation hypothesis) (**Figure 7.1**). This is supported by enhanced CCR5 and CCR7 (tissue and lymph node homing markers) identified on MerTK+ cells. Expanded MerTK+ monocyte subsets result in impaired pro-inflammatory cytokine (e.g. TNF-α) production in response to microbial ligands, confirming the proposed hypothesis. The MerTK+ HLA-DR- subset is the most immunotolerant. MerTK is also a negative regulator of T-cell activation, hindering the adaptive arm of the immune response to pathogens, though this requires further exploration in liver disease (Cabezon *et al.*, 2015).

7.2.5. Inhibition of MerTK Signalling Pathways

Whilst no MerTK signalling pathway antagonist had a significant impact, the LXR-α antagonist GSK2033 showed greatest promise in reversing the blunted LPS-evoked TNF-α secretion, highlighting the link between MerTK and LXR-α signalling. UNC2025 was not adequately titrated and further work is needed to identify the optimal concentration, duration of exposure and effect on different cell types. Bernsmeier *et al.* (2015) showed proof of principle data for UNC569 to reverse the immuneparesis in monocytes conditioned in ACLF plasma, but this was a CD14+ monocyte pure population and less reflective of the *in vivo* effect (Bernsmeier *et al.*, 2015). The argument against inhibiting MerTK or other TAM receptor pathways will be that resolution and homeostatic responses might be impaired, meaning failure to clear dead cells, stifling liver regeneration in AD or ACLF and potentially increasing the risk of autoimmune phenomena if auto-antigens are not appropriately cleared. The counter-argument is that there is redundancy in the efferocytic responses; multiple efferocytosis receptors exist (e.g. Tim-4, stabilin-1 and -2, BAI-1, RAGE, CD36, $\alpha_v\beta_3$ integrin, complement

receptors and CD91) and blockade of a single receptor has never been shown to abolish efferocytosis (Greenlee-Wacker, 2016). The importance and co-operation of each receptor in liver disease remains to be fully investigated.

Other immunotherapeutic strategies and their impact on TAM signalling should be investigated further. Data in this thesis, supported by work by other authors, confirm higher circulating and ascitic concentrations of cell death markers M30 and M65 (Macdonald *et al.*, 2018). However, a study of a pan-caspase inhibitor to limit caspase-mediated hepatocyte death did not generate favourable results in ACLF (Mehta *et al.*, 2018). Other such agents targeting cell death may justify further work. Albumin has recently been shown to counteract the immunosuppressive action of lipid mediators (generated by cell death and efferocytosis); how this impacts on TAM receptor expression and function should also be explored (China *et al.*, 2018).

7.2.6. Re-circulation Hypothesis: MerTK+ Monocytes/Macrophages Promote Immuneparesis in Compartments in ACLF

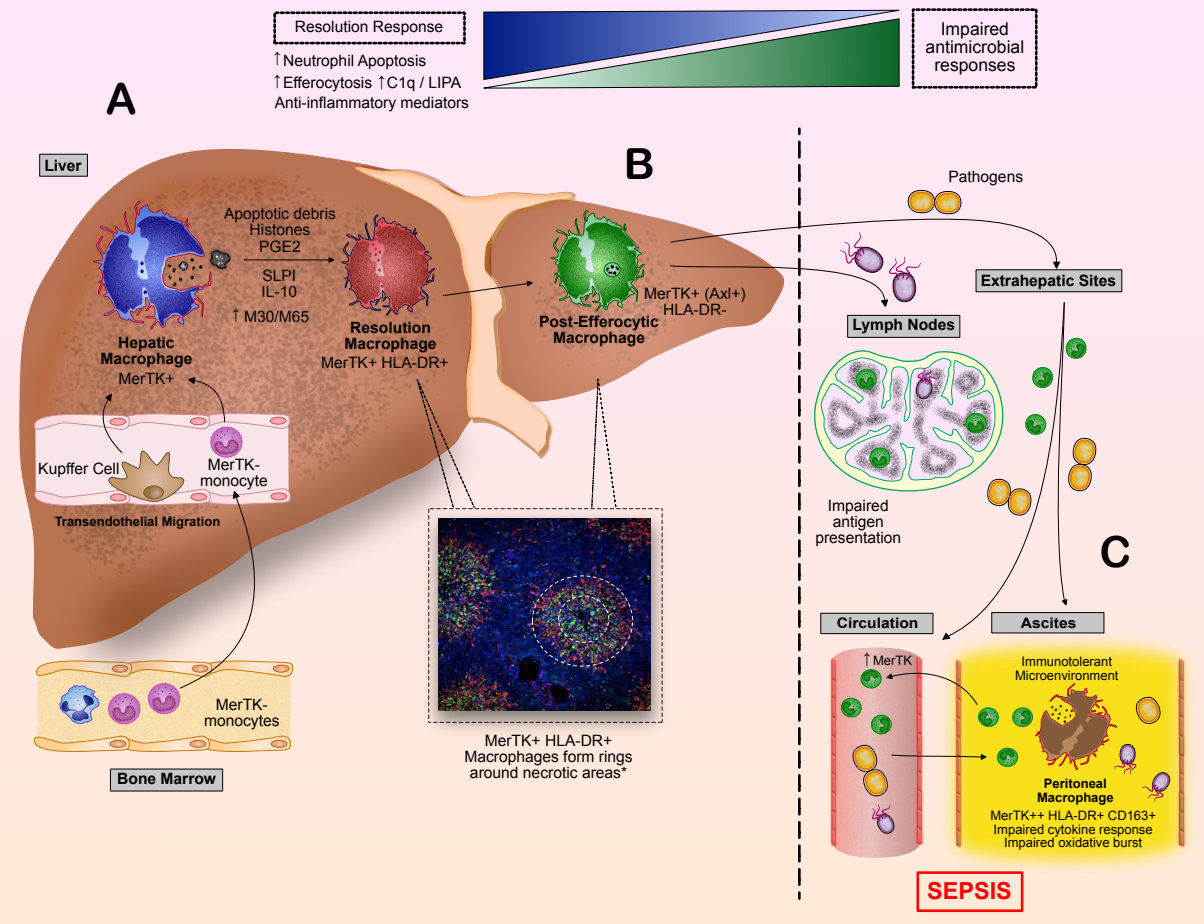


Figure 7.1 Schematic Diagram Proposing the Evolution of MerTK+ Monocytes / Macrophages in Compartments in Liver Injury

(A) A primary liver injury results in apoptosis and necrosis of hepatocytes, resident and infiltrating immune cells (e.g. neutrophils). DAMP-release triggers a local hepatic inflammatory response, myeloid cell recruitment and further hepatic pro-inflammatory cytokine production, spilling over into the circulation. A systemic inflammatory response (SIRS) ensues, seen commonly in ACLF, with bystander damage to other organs causing multi-organ injury. **(B)** Concurrently, a compensatory anti-inflammatory response commences, where apoptotic bodies, histones and nuclear material from necrosis promotes a resolution response, where efferocytosis by resident and monocyte-derived macrophages promotes MerTK+ HLA-DR+ subset expansion in the liver, and generates lipid mediators (resolvins), IL-10, PGE_2 and SLPI, amongst others, further enhancing MerTK expression with associated attenuated pro-inflammatory responses. Some post-efferocytic MerTK+ HLA-DR- macrophages may reverse migrate back into the circulation (recirculation) or lymph nodes resulting in impaired antimicrobial responses in these compartments. **(C)** The peritoneum is already an immunotolerant compartment due to chronic immune stimulation and endotoxin tolerance from low-grade chronic liver injury in cirrhosis and pathological bacterial translocation. Located adjacent to the injured liver, ascites accumulates apoptotic debris, lipids and PGE_2, and M-MDSCs and MerTK+ HLA-DR- macrophages accumulate either from the circulation or through direct paracellular routes (? GATA6-expressing). Further efferocytosis promotes even greater MerTK expression, increasing the susceptibility to SBP. Peritoneal macrophages in advanced cirrhosis exhibit poor cytokine

responses and impaired oxidative burst, relying on neutrophil infiltration to overcome the infection. In patients where exhaustion of the immune system is too great or the bacterial load or virulence overcomes the immune response, endothelial dysfunction and circulatory disturbance propagates organ failure and ultimately leads to death. *confocal microscopy image from Triantafyllou *et al.* (2018), with permission from BMJ Publishing Group (Appendix U).

7.3. Limitations

Aside from those specified in the discussion of each chapter, the major limitation to the study which has focused on patients with ACLF, has been the relative paucity of patients with ACLF and access to tissue from compartments. Liver transplant is very rarely performed on patients with cirrhosis and multiple organ failure and so no liver explants were available in ACLF for analysis. Equally, therapeutic abdominal paracentesis, to relieve the abdominal distension from large volume ascites, is rarely and cautiously performed on patients with organ failure due to the risk of paracentesis-induced circulatory dysfunction (PICD), a condition occurring after removal of a large volume of ascites in patients with advanced cirrhosis leading to haemodynamic instability from fluid shifts, and exacerbation of renal dysfunction (Hussain *et al.*, 1969). As a consequence, large volumes are rarely drained from patients with ACLF, and given the low cell numbers in the peritoneum compared to blood, there is little sample available for experimental assays. Furthermore, the paracentesis procedure itself may not be as innocuous as once thought: some authors report that PICD may enhance bacterial translocation provoking monocyte activation, which would naturally influence the results presented in this thesis (Carl *et al.*, 2014; Moreau, 2014). Albumin is given routinely during paracentesis to reduce the risk of PICD, and recently albumin has been shown to have immunomodulatory effects (China *et al.*, 2018).

There are inherent challenges with the ACLF cohort. Firstly, patients with ACLF are a heterogenous group, with varying aetiologies, co-morbidities, alcohol consumption and diet, none of which are accounted for in the analysis. Accounting for confounders require a very large dataset which was not possible in the study period with a single recruiter and only two sites. Most of the ACLF patients were recruited from King's College Hospital (KCH), a tertiary referral centre, to where many of the ACLF patients were transferred from smaller hospitals. Hence, baseline samples were taken on admission to

KCH liver ITU but each patient may have had a variable duration in hospital. Longitudinal data collection, particularly with regard to subsequent sepsis, was challenging due to incomplete clinical records, difficulties in identifying sepsis, subsequent liver transplantation or transfer of the patients back to their referring centres. Sequential sampling of ascites was not possible since paracentesis is only performed on clinical indications rather than specified intervals due to the higher risk of complications (e.g. 0.1% risk of bowel perforation) (Runyon, 2012). Both AD and ACLF are dynamic processes and sequentially sampling would have been useful. Since there is no healthy control version of ascites, an adequate comparator group for peritoneal macrophages in ascites of patients with cirrhosis was lacking. Healthy monocyte-derived macrophages were perhaps the best comparator, but other *ex-vivo* groups, e.g. abdominal washout in laparoscopic surgery or peritoneal dialysis effluent, would have added to the dataset. More cases of SBP would have also been useful for comparison, but there is already a body of published work on immune cells during SBP and what is observed does not equate to compartmental susceptibility to SBP.

In the experimental work, identification of how much the freeze-thaw process and fixation affect surface expression of TAM receptors would help to homogenize the dataset. In some cases, fixable viability dyes (FVD) were not used especially on *ex-vivo* samples due to presumption of high cell viability. Whilst this was demonstrated in examples, the degree of cell death cannot be accurately predicted in each case, and so use of FVD should be routine even on *ex-vivo* samples. Finally, TAM receptors all have soluble counterparts, the cleaved form of their receptors, such that just measuring surface receptors may be only half the story. These soluble forms have been measured in a variety of other diseases including SLE, pre-eclampsia, rheumatoid arthritis and diabetic nephropathy, and they are not immunologically inert, often acting as decoy receptors by sequestering ligands (Ballantine *et al.*, 2015; Ochodnicky *et al.*, 2017; Xu *et al.*, 2018; Peng *et al.*, 2018). Little is known about their concentration, kinetics and interactions with ligands and immune cells in liver disease.

7.4. Future Directions

The TAM receptors are efferocytic receptors and signalling pathways with the dual function of attenuating pro-inflammatory cytokine responses to DAMP and PAMP stimuli during the resolution or tissue repair phase of inflammation or injury. A prolonged or excessive compensatory anti-inflammatory response increases the susceptibility to infection. The overall and compartmental balance of pro-inflammatory and anti-inflammatory factors, cellular and microenvironmental, may be the crucial determinant.

The challenge in the evolution of disease from stable cirrhosis to decompensated to ACLF, is the identification of the mechanisms that trigger progression of disease including the development of organ injury and to accurately identify where the balance of immune homeostasis lies. Measuring TAM receptors, either surface or soluble, at a single time point or sequentially, may be able to predict the development of sepsis due to immuneparesis and warrants further study. Their dynamic and differential expression in tissue compartments should be explored. Axl, for example, is highly expressed in murine alveolar macrophages and inhibition can improve pro-inflammatory responses to pulmonary aspergillosis (Shibata *et al.*, 2014; Shibata & Ato, 2017).

TAM immunotherapeutics remains a potential strategy to augment a weakened immune system. This may be MerTK inhibition with small molecule inhibitors, potentiating Axl or influencing receptor cleavage. This may translate to drugs delivered into the systemic circulation or directly into tissue compartments.

CHAPTER 8

8. REFERENCES

Abdel-Misih, S.R.Z. & Bloomston, M. (2010) Liver Anatomy. *Surgical Clinics of North America*. [Online] 90 (4), 643–653. Available from: doi:10.1016/j.suc.2010.04.017.

Abeles, R.D., McPhail, M.J., Sowter, D., Antoniades, C.G., et al. (2012) CD14, CD16 and HLA-DR reliably identifies human monocytes and their subsets in the context of pathologically reduced HLA-DR expression by CD14hi/CD16neg monocytes: Expansion of CD14hi/CD16pos and contraction of CD14lo/CD16pos monocytes in acute liver fail. *Cytometry Part A*. [Online] 81A (10), 823–834. Available from: doi:10.1373/clinchem.2005.052639.

Acharya, C. & Bajaj, J.S. (2019) Altered Microbiome in Patients With Cirrhosis and Complications. *Clinical Gastroenterology and Hepatology*. [Online] 17 (2), 307–321. Available from: doi:10.1016/j.cgh.2018.08.008.

Adam, R., Karam, V., Delvart, V., O'Grady, J., et al. (2012) Evolution of indications and results of liver transplantation in Europe. A report from the European Liver Transplant Registry (ELTR). *Journal of Hepatology*. [Online] 57 (3), 675–688. Available from: doi:10.1016/j.jhep.2012.04.015.

A-Gonzalez, N., Bensinger, S.J., Hong, C., Beceiro, S., et al. (2009a) Apoptotic Cells Promote Their Own Clearance and Immune Tolerance through Activation of the Nuclear Receptor LXR. *Immunity*. [Online] 31 (2), 245–258. Available from: doi:10.1016/j.immuni.2009.06.018.

A-Gonzalez, N., Bensinger, S.J., Hong, C., Beceiro, S., et al. (2009b) Apoptotic cells promote their own clearance and immune tolerance through activation of the nuclear receptor LXR. *Immunity*. [Online] 31 (2), 245–258. Available from: doi:10.1016/j.immuni.2009.06.018.

Ahmed, A.M.M., Bomford, A., Nouri-Aria, K.T., Davies, T., et al. (2011) Peritoneal macrophages from patients with cirrhotic ascites show impaired phagocytosis and vigorous respiratory burst. *Results in immunology*. [Online] 1 (1), 53–59. Available from: doi:10.1016/j.rinim.2011.08.004.

Aizarani, N., Saviano, A., Sagar, Mailly, L., et al. (2019) A human liver cell atlas reveals heterogeneity and epithelial progenitors. *Nature*. [Online] 572 (7768), 199–204. Available from: doi:10.1038/s41586-019-1373-2.

Akalu, Y.T., Rothlin, C.V. & Ghosh, S. (2017) TAM receptor tyrosine kinases as emerging targets of innate immune checkpoint blockade for cancer therapy. *Immunological Reviews*. [Online] 276 (1), 165–177. Available from: doi:10.1111/imr.12522.

Albillos, A., Lario, M. & Alvarez-Mon, M. (2014) Cirrhosis-associated immune dysfunction: Distinctive features and clinical relevance. *Journal of Hepatology*. [Online] Available from: doi:10.1016/j.jhep.2014.08.010.

Alciato, F., Sainaghi, P.P., Sola, D., Castello, L., et al. (2010) TNF-α, IL-6, and IL-1 expression is inhibited by GAS6 in monocytes/macrophages. *Journal of Leukocyte Biology*. [Online] 87 (5), 869–875. Available from: doi:10.1189/jlb.0909610.

Allen, A.M., Kim, W.R., Moriarty, J.P., Shah, N.D., et al. (2016) Time trends in the health care burden and mortality of acute on chronic liver failure in the United States. *Hepatology*. [Online] 64 (6), 2165–2172. Available from: doi:10.1002/hep.28812.

Alvarez-Silva, C., Schierwagen, R., Pohlmann, A., Magdaleno, F., et al. (2019) Compartmentalization of Immune Response and Microbial Translocation in Decompensated Cirrhosis. *Frontiers in Immunology*. [Online] 10, 69. Available from: doi:10.3389/fimmu.2019.00069.

Amathieu, R., Triba, M.N., Nahon, P., Bouchemal, N., et al. (2014) Serum 1H-NMR Metabolomic Fingerprints of Acute-On-Chronic Liver Failure in Intensive Care Unit Patients with Alcoholic Cirrhosis Petras Dzeja (ed.). *PLoS ONE*. [Online] 9 (2), e89230. Available from: doi:10.1371/journal.pone.0089230.

Andreu, M., Sola, R., Sitges-Serra, A., Alia, C., et al. (1993) Risk factors for spontaneous bacterial peritonitis in cirrhotic patients with ascites. *YGAST*. 104 (4), 1133–1138.

Angeli, P., Bernardi, M., Villanueva, C., Francoz, C., et al. (2018) EASL Clinical Practice Guidelines for the management of patients with decompensated cirrhosis. *Journal of Hepatology*. [Online] 69 (2), 406–460. Available from: doi:10.1016/j.jhep.2018.03.024.

Antoniades, C.G., Berry, P.A., Davies, E.T., Hussain, M., et al. (2006) Reduced monocyte HLA-DR expression: a novel biomarker of disease severity and outcome in acetaminophen-induced acute liver failure. *Hepatology*. [Online] 44 (1), 34–43. Available from: doi:10.1002/hep.21240.

Antoniades, C.G., Quaglia, A., Taams, L.S., Mitry, R.R., et al. (2012) Source and characterization of hepatic macrophages in acetaminophen-induced acute liver failure in humans. *Hepatology*. [Online] 56 (2), 735–746. Available from: doi:10.4049/jimmunol.171.3.1507.

Anty, R., Anty, R., Tonohouan, M., Tonohouan, M., et al. (2014) Low Levels of 25-Hydroxy Vitamin D are Independently Associated with the Risk of Bacterial Infection in Cirrhotic Patients. *Clinical and Translational Gastroenterology*. [Online] 5, e56–e56. Available from: doi:10.1038/ctg.2014.6.

Anwar, A., Keating, A.K., Joung, D., Sather, S., et al. (2009) Mer tyrosine kinase (MerTK) promotes macrophage survival following exposure to oxidative stress. *Journal of leukocyte biology*. [Online] 86 (1), 73–79. Available from: doi:10.1189/jlb.0608334.

Aronoff, D.M., Canetti, C. & Peters-Golden, M. (2004) Prostaglandin E2 Inhibits Alveolar Macrophage Phagocytosis through an E-Prostanoid 2 Receptor-Mediated Increase in Intracellular Cyclic AMP. *The Journal of Immunology*. [Online] 173 (1), 559–565. Available from: doi:10.4049/jimmunol.173.1.559.

Artru, F., Louvet, A., Ruiz, I., Levesque, E., et al. (2017) Liver transplantation in the most severely ill cirrhotic patients: A multicenter study in acute-on-chronic liver failure grade 3. *Journal of Hepatology*. [Online] 67 (4), 708–715. Available from: doi:10.1016/j.jhep.2017.06.009.

Arvaniti, V., Arvaniti, V., D'Amico, G., D'Amico, G., et al. (2010) Infections in patients with cirrhosis increase mortality four-fold and should be used in determining prognosis. *Gastroenterology*. [Online] 139 (4), 1246-56-1256.e1-5. Available from: doi:10.1053/j.gastro.2010.06.019.

Asrani, S.K., Devarbhavi, H., Eaton, J. & Kamath, P.S. (2019) Burden of liver diseases in the world. *Journal of Hepatology*. [Online] 70 (1), 151–171. Available from: doi:10.1016/j.jhep.2018.09.014.

Asrani, S.K., Simonetto, D.A. & Kamath, P.S. (2015) Acute-on-Chronic Liver Failure. *Clinical Gastroenterology and Hepatology*. [Online] 13 (12), 2128–2139. Available from: doi:10.1016/j.cgh.2015.07.008.

Assimakopoulos, S.F., Tsamandas, A.C., Tsiaoussis, G.I., Karatza, E., et al. (2012) Altered intestinal tight junctions' expression in patients with liver cirrhosis: a pathogenetic mechanism of intestinal hyperpermeability: INTESTINAL TIGHT JUNCTIONS IN CIRRHOSIS. *European Journal of Clinical Investigation*. [Online] 42 (4), 439–446. Available from: doi:10.1111/j.1365-2362.2011.02609.x.

van Baal, J.O.A.M., Van de Vijver, K.K., Nieuwland, R., van Noorden, C.J.F., et al. (2017) The histophysiology and pathophysiology of the peritoneum. *Tissue and Cell*. [Online] 49 (1), 95–105. Available from: doi:10.1016/j.tice.2016.11.004.

Bac, D.J., de Marie, S. & van Blankenstein, M. (1996) Spontaneous bacterial peritonitis complicating malignancy-related ascites. *Digestive Diseases and Sciences*. [Online] 41 (1), 131–132. Available from: doi:10.1007/BF02208594.

Bachmann, M.F. & Oxenius, A. (2007) Interleukin 2: From immunostimulation to immunoregulation and back again. *EMBO Reports*. [Online] 8 (12), 1142–1148. Available from: doi:10.1038/sj.embor.7401099.

von Baehr, V., Döcke, W.D., Plauth, M., Liebenthal, C., et al. (2000) Mechanisms of endotoxin tolerance in patients with alcoholic liver cirrhosis: role of interleukin 10, interleukin 1 receptor antagonist, and soluble tumour necrosis factor receptors as well as effector cell desensitisation. *Gut*. [Online] 47 (2), 281–287. Available from: doi:10.1136/gut.47.2.281.

Bain, C.C. & Jenkins, S.J. (2018) The biology of serous cavity macrophages. *Cellular Immunology*. [Online] 330, 126–135. Available from: doi:10.1016/j.cellimm.2018.01.003.

Bajaj, J.S., O'Leary, J.G., Reddy, K.R., Wong, F., et al. (2012) Second infections independently increase mortality in hospitalized patients with cirrhosis: the North American consortium for the study of end-stage liver disease (NACSELD) experience. *Hepatology*. [Online] 56 (6), 2328–2335. Available from: doi:10.1002/hep.25947.

Bajaj, J.S., O'Leary, J.G., Reddy, K.R., Wong, F., et al. (2014) Survival in infection-related acute-on-chronic liver failure is defined by extrahepatic organ failures. *Hepatology*. [Online] 60 (1), 250–256. Available from: doi:10.1002/hep.27077.

Bal, C.K., Daman, R. & Bhatia, V. (2016) Predictors of fifty days in-hospital mortality in decompensated cirrhosis patients with spontaneous bacterial peritonitis. *World Journal of Hepatology*. [Online] 8 (12), 566. Available from: doi:10.4254/wjh.v8.i12.566.

Ballantine, L., Midgley, A., Harris, D., Richards, E., et al. (2015) Increased soluble phagocytic receptors sMer, sTyro3 and sAxl and reduced phagocytosis in Juvenile-onset Systemic Lupus Erythematosus. *Pediatric Rheumatology*. [Online] 13 (1), 10. Available from: doi:10.1186/s12969-015-0007-y.

Bárcena, C., Stefanovic, M., Tutusaus, A., Joannas, L., et al. (2015) Gas6/Axl pathway is activated in chronic liver disease and its targeting reduces fibrosis via hepatic stellate cell inactivation. *Journal of Hepatology*. [Online] 63 (3), 670–678. Available from: doi:10.1016/j.jhep.2015.04.013.

Barth, N.D., Marwick, J.A., Heeb, M.J., Gale, A.J., et al. (2018) Augmentation of Human Monocyte Responses to Lipopolysaccharide by the Protein S and Mer/Tyro3 Receptor Tyrosine Kinase Axis. *The Journal of Immunology*. [Online] 201 (9), 2602–2611. Available from: doi:10.4049/jimmunol.1800249.

Bayik, D., Tross, D., Haile, L.A., Verthelyi, D., et al. (2017) Regulation of the maturation of human monocytes into immunosuppressive macrophages. *Blood Advances*. [Online] 1 (26), 2510–2519. Available from: doi:10.1182/bloodadvances.2017011221.

Bellan, M., Castello, L.M. & Pirisi, M. (2018) Candidate Biomarkers of Liver Fibrosis: A Concise, Pathophysiology-oriented Review. *Journal of Clinical and Translational Hepatology*. [Online] 6 (3), 1–9. Available from: doi:10.14218/JCTH.2018.00006.

Bernal, W., Jalan, R., Quaglia, A., Simpson, K., et al. (2015) Acute-on-chronic liver failure. *Lancet*. [Online] Available from: doi:10.1016/S0140-6736(15)00309-8.

Bernardi, M., Moreau, R., Angeli, P., Schnabl, B., et al. (2015) Mechanisms of decompensation and organ failure in cirrhosis: From peripheral arterial vasodilation to systemic inflammation hypothesis. *Journal of Hepatology*. [Online] 63 (5), 1272–1284. Available from: doi:10.1016/j.jhep.2015.07.004.

Bernsmeier, C., Pop, O.T., Singanayagam, A., Triantafyllou, E., et al. (2015) Patients with acute-on-chronic liver failure have increased numbers of regulatory immune cells expressing the receptor tyrosine kinase MERTK. *Gastroenterology*. [Online] 148 (3), 603-615.e14. Available from: doi:10.1053/j.gastro.2014.11.045.

Bernsmeier, C., Triantafyllou, E., Brenig, R., Lebosse, F.J., et al. (2018) CD14+ CD15- HLA-DR- myeloid-derived suppressor cells impair antimicrobial responses in patients with acute-on-chronic liver failure. *Gut*. [Online] 67 (6), 1155–1167. Available from: doi:10.1136/gutjnl-2017-314184.

Berry, P.A., Antoniades, C.G., Carey, I., McPhail, M.J.W., et al. (2010a) Severity of the compensatory anti-inflammatory response determined by monocyte HLA-DR expression may assist outcome prediction in cirrhosis. *Intensive care medicine*. [Online] 37 (3), 453–460. Available from: doi:10.1001/archsurg.1997.01430280099016.

Berry, P.A., Antoniades, C.G., Hussain, M.J., McPhail, M.J.W., et al. (2010b) Admission levels and early changes in serum interleukin-10 are predictive of poor outcome in acute liver failure and decompensated cirrhosis. *Liver International*. [Online] 30 (5), 733–740. Available from: doi:10.1111/j.1478-3231.2010.02219.x.

Berzigotti, A., Seijo, S., Reverter, E. & Bosch, J. (2013) Assessing portal hypertension in liver diseases. *Expert Review of Gastroenterology & Hepatology*. [Online] 7 (2), 141–155. Available from: doi:10.1586/egh.12.83.

Bird, G., Senaldi, G., Pano, M., Rolando, N., et al. (1992) Activation of the Classical Complement Pathway in Spontaneous Bacterial Peritonitis. *Gut*. 33 (3), 307–311.

Blasco-Algora, S., Masegosa-Ataz, J., Gutiérrez-García, M.L., Alonso-López, S., et al. (2015) Acute-on-chronic liver failure: Pathogenesis, prognostic factors and management. *World journal of gastroenterology: WJG*. [Online] 21 (42), 12125–12140. Available from: doi:10.3748/wjg.v21.i42.12125.

Blasi, A., Calvo, A., Prado, V., Reverter, E., et al. (2018) Coagulation Failure in Patients With Acute-on-Chronic Liver Failure and Decompensated Cirrhosis: Beyond the International Normalized Ratio. *Hepatology (Baltimore, Md.)*. [Online] 68 (6), 2325–2337. Available from: doi:10.1002/hep.30103.

Bonnel, A.R., Bunchorntavakul, C. & Reddy, K.R. (2011) Immune dysfunction and infections in patients with cirrhosis. *Clinical gastroenterology and hepatology : the official clinical practice*

journal of the American Gastroenterological Association. [Online] 9 (9), 727–738. Available from: doi:10.1016/j.cgh.2011.02.031.

Borzio, M., Salerno, F., Piantoni, L., Cazzaniga, M., et al. (2001) Bacterial infection in patients with advanced cirrhosis: a multicentre prospective study. *Digestive and Liver Disease*. [Online] 33 (1), 41–48. Available from: doi:10.1016/S1590-8658(01)80134-1.

Branchford, B.R., Stalker, T.J., Law, L., Acevedo, G., et al. (2018) The small-molecule MERTK inhibitor UNC2025 decreases platelet activation and prevents thrombosis. *Journal of Thrombosis and Haemostasis*. [Online] 16 (2), 352–363. Available from: doi:10.1111/jth.13875.

Bronte, V., Brandau, S., Chen, S.-H., Colombo, M.P., et al. (2016) Recommendations for myeloid-derived suppressor cell nomenclature and characterization standards. *Nature communications*. [Online] 7, 12150. Available from: doi:10.1038/ncomms12150.

Bruns, T., Lutz, P., Stallmach, A. & Nischalke, H.D. (2015) Low ascitic fluid protein does not indicate an increased risk for spontaneous bacterial peritonitis in current cohorts. *Journal of Hepatology*. [Online] 63 (2), 527–528. Available from: doi:10.1016/j.jhep.2015.03.040.

Bruns, T., Peter, J., Hagel, S., Herrmann, A., et al. (2011) The augmented neutrophil respiratory burst in response to Escherichia coli is reduced in liver cirrhosis during infection. *Clinical and experimental immunology*. [Online] 164 (3), 346–356. Available from: doi:10.1111/j.1365-2249.2011.04373.x.

Bruns, T., Reuken, P.A., Fischer, J., Berg, T., et al. (2012) Further evidence for the relevance of TLR2 gene variants in spontaneous bacterial peritonitis. *Journal of Hepatology*. [Online] 56 (5), 1207–1208. Available from: doi:10.1016/j.jhep.2011.09.010.

Buckley, C.D., Ross, E.A., McGettrick, H.M., Osborne, Chloe.E., et al. (2006) Identification of a phenotypically and functionally distinct population of long-lived neutrophils in a model of reverse endothelial migration. *Journal of Leukocyte Biology*. [Online] 79 (2), 303–311. Available from: doi:10.1189/jlb.0905496.

Cabezon, R., Carrera-Silva, E.A., Florez-Grau, G., Errasti, A.E., et al. (2015) MERTK as negative regulator of human T cell activation. *Journal of leukocyte biology*. [Online] 97 (4), 751–760. Available from: doi:10.1189/jlb.3A0714-334R.

Cai, B., Cai, J., Luo, Y., Chen, C., et al. (2015) The Specific Roles of JAK/STAT Signaling Pathway in Sepsis. *Inflammation*. [Online] 38 (4), 1599–1608. Available from: doi:10.1007/s10753-015-0135-z.

Caly, W.R. & Strauss, E. (1993) A prospective study of bacterial infections in patients with cirrhosis. *Journal of Hepatology*. [Online] 18 (3), 353–358. Available from: doi:10.1016/S0168-8278(05)80280-6.

Camenisch, T.D., Camenisch, T.D., Koller, B.H., Koller, B.H., et al. (1999) A novel receptor tyrosine kinase, Mer, inhibits TNF-alpha production and lipopolysaccharide-induced endotoxic shock. *Journal of immunology (Baltimore, Md. : 1950)*. 162 (6), 3498–3503.

Canton, J. (2014) Phagosome maturation in polarized macrophages. *Journal of leukocyte biology*. [Online] 96 (5), 729–738. Available from: doi:10.1189/jlb.1MR0114-021R.

Cao, Z., Li, F., Xiang, X., Liu, K., et al. (2015) Circulating cell death biomarker: good candidates of prognostic indicator for patients with hepatitis B virus related acute-on-chronic liver failure. *Scientific Reports*. [Online] 5 (1), 14240. Available from: doi:10.1038/srep14240.

Capobianco, A., Cottone, L., Monno, A., Manfredi, A.A., et al. (2017) The peritoneum: healing, immunity, and diseases. *The Journal of pathology*. [Online] 243 (2), 137–147. Available from: doi:10.1002/path.4942.

Carl, D.E., Ghosh, S., Cheng, J., Gehr, T.W.B., et al. (2014) Post-paracentesis circulatory derangements are related to monocyte activation. *Liver International*. [Online] 34 (7), 1001–1007. Available from: doi:10.1111/liv.12450.

Carrera Silva, E.A., Chan, P.Y., Joannas, L., Errasti, A.E., et al. (2013) T Cell-Derived Protein S Engages TAM Receptor Signaling in Dendritic Cells to Control the Magnitude of the Immune Response. *Immunity*. [Online] 39 (1), 160–170. Available from: doi:10.1016/j.immuni.2013.06.010.

Cates, A.M., Holden, V.I., Myers, E.M., Smith, C.K., et al. (2015) Interleukin 10 hampers endothelial cell differentiation and enhances the effects of interferon α on lupus endothelial cell progenitors. *Rheumatology*. [Online] 54 (6), 1114–1123. Available from: doi:10.1093/rheumatology/keu431.

Cavaillon, J.-M. (2001) Pro- versus anti-inflmmatory cytokines: myth or reality. *Cellular and Molecular Biology*. 47 (4), 695–702.

Cavaillon, J.-M. & Annane, D. (2016) Invited review: Compartmentalization of the inflammatory response in sepsis and SIRS. *Journal of Endotoxin Research*. [Online] 12 (3), 151–170. Available from: doi:10.1164/ajrccm.152.5.7582314.

Cazzaniga, M., Dionigi, E., Gobbo, G., Fioretti, A., et al. (2009) The systemic inflammatory response syndrome in cirrhotic patients: Relationship with their in-hospital outcome. *Journal of Hepatology*. [Online] 51 (3), 475–482. Available from: doi:10.1016/j.jhep.2009.04.017.

Ceylan, B., Mete, B., Fincanci, M., Aslan, T., et al. (2013) A new model using platelet indices to predict liver fibrosis in patients with chronic hepatitis B infection. *Wiener klinische Wochenschrift*. [Online] 125 (15–16), 453–460. Available from: doi:10.1007/s00508-013-0394-3.

Cheong, H.S., Lee, S.O., Choi, C.-B., Sung, Y.-K., et al. (2007) MERTK polymorphisms associated with risk of haematological disorders among Korean SLE patients. *Rheumatology*. [Online] 46 (2), 209–214. Available from: doi:10.1093/rheumatology/kel182.

China, L., Maini, A., Skene, S.S., Shabir, Z., et al. (2018) Albumin Counteracts Immune-Suppressive Effects of Lipid Mediators in Patients With Advanced Liver Disease. *Clinical Gastroenterology and Hepatology*. [Online] 16 (5), 738-747.e7. Available from: doi:10.1016/j.cgh.2017.08.027.

Choi, J.-Y., Park, H.-J., Lee, Y.-J., Byun, J., et al. (2013) Upregulation of Mer Receptor Tyrosine Kinase Signaling Attenuated Lipopolysaccharide-Induced Lung Inflammation. *Journal of Pharmacology and Experimental Therapeutics*. [Online] 344 (2), 447–458. Available from: doi:10.1124/jpet.112.199778.

Choi, J.-Y., Seo, J.Y., Yoon, Y.-S., Lee, Y.-J., et al. (2015) Mer signaling increases the abundance of the transcription factor LXR to promote the resolution of acute sterile inflammation. *Science signaling*. [Online] 8 (365), ra21–ra21. Available from: doi:10.1126/scisignal.2005864.

Christoph, S., DeRyckere, D., Schlegel, J., Frazer, J.K., et al. (2013) UNC569, a Novel Small-Molecule Mer Inhibitor with Efficacy against Acute Lymphoblastic Leukemia In Vitro and In Vivo. *Molecular Cancer Therapeutics*. [Online] 12 (11), 2367–2377. Available from: doi:10.1158/1535-7163.MCT-13-0040.

Clària, J., Clària, J., Stauber, R.E., Stauber, R.E., et al. (2016a) Systemic inflammation in decompensated cirrhosis: Characterization and role in acute-on-chronic liver failure. *Hepatology*. [Online] Available from: doi:10.1002/hep.28740.

Clària, J., Moreau, R., Fenaille, F., Amorós, A., et al. (2019) Orchestration of Tryptophan-Kynurenine Pathway, Acute Decompensation, and Acute-on-Chronic Liver Failure in Cirrhosis. *Hepatology*. [Online] 69 (4), 1686–1701. Available from: doi:10.1002/hep.30363.

Clària, J., Stauber, R.E., Coenraad, M.J., Moreau, R., et al. (2016b) Systemic inflammation in decompensated cirrhosis: Characterization and role in acute-on-chronic liver failure: Clària, Stauber et al. *Hepatology*. [Online] 64 (4), 1249–1264. Available from: doi:10.1002/hep.28740.

Condamine, T., Condamine, T., Gabrilovich, D.I. & Gabrilovich, D.I. (2011) Molecular mechanisms regulating myeloid-derived suppressor cell differentiation and function. *Trends in immunology*. [Online] 32 (1), 19–25. Available from: doi:10.1016/j.it.2010.10.002.

Cummings, C.T., Deryckere, D., Earp, H.S. & Graham, D.K. (2013) Molecular pathways: MERTK signaling in cancer. *Clinical Cancer Research*. [Online] 19 (19), 5275–5280. Available from: doi:10.1158/1078-0432.CCR-12-1451.

Curry, N., McCallum, R.W. & Guth, P.H. (1974) Spontaneous Peritonitis in Cirrhotic Ascites. *American Journal of Digestive Diseases*. 19 (8).

D'Amico, G., Garcia-Tsao, G. & Pagliaro, L. (2006) Natural history and prognostic indicators of survival in cirrhosis: A systematic review of 118 studies. *Journal of Hepatology*. [Online] 44 (1), 217–231. Available from: doi:10.1016/j.jhep.2005.10.013.

D'Amico, G., Morabito, A., D'Amico, M., Pasta, L., et al. (2018) Clinical states of cirrhosis and competing risks. *Journal of Hepatology*. [Online] 68 (3), 563–576. Available from: doi:10.1016/j.jhep.2017.10.020.

Davies, L.C., Jenkins, S.J., Allen, J.E. & Taylor, P.R. (2013) Tissue-resident macrophages. *Nature immunology*. [Online] 14 (10), 986–995. Available from: doi:10.1038/ni.2705.

Dengler, M., Staufer, K., Huber, H., Stauber, R., et al. (2017) Soluble Axl is an accurate biomarker of cirrhosis and hepatocellular carcinoma development: results from a large scale multicenter analysis. *Oncotarget*. [Online] 8 (28). Available from: doi:10.18632/oncotarget.17598 [Accessed: 19 September 2019].

Deryckere, D., Lee-Sherick, A.B., Huey, M.G., Hill, A.A., et al. (2017) UNC2025, a MERTK Small-Molecule Inhibitor, Is Therapeutically Effective Alone and in Combination with Methotrexate in Leukemia Models. *Clinical cancer research : an official journal of the American Association for Cancer Research*. [Online] 23 (6), 1481–1492. Available from: doi:10.1158/1078-0432.CCR-16-1330.

Dever, J.B. & Sheikh, M.Y. (2015) Review article: spontaneous bacterial peritonitis - bacteriology, diagnosis, treatment, risk factors and prevention. *Alimentary Pharmacology and Therapeutics*. [Online] 41 (11), 1116–1131. Available from: doi:10.1111/apt.13172.

Doherty, D.G. (2015) Immunity, tolerance and autoimmunity in the liver: A comprehensive review. *Journal of autoimmunity*. [Online] Available from: doi:10.1016/j.jaut.2015.08.020.

Doi, H., Tanoue, S. & Kaplan, D.E. (2014) Peripheral CD27−CD21− B-cells represent an exhausted lymphocyte population in hepatitis C cirrhosis. *Clinical Immunology*. [Online] 150 (2), 184–191. Available from: doi:10.1016/j.clim.2013.12.001.

Dona, A.C., Jiménez, B., Schäfer, H., Humpfer, E., et al. (2014) Precision High-Throughput Proton NMR Spectroscopy of Human Urine, Serum, and Plasma for Large-Scale Metabolic Phenotyping. *Analytical Chemistry*. [Online] 86 (19), 9887–9894. Available from: doi:10.1021/ac5025039.

Dorhoi, A. & Du Plessis, N. (2017) Monocytic Myeloid-Derived Suppressor Cells in Chronic Infections. *Frontiers in Immunology*. [Online] 8 (JAN), 1895. Available from: doi:10.3389/fimmu.2017.01895.

Dransfield, I., Zagórska, A., Lew, E.D., Michail, K., et al. (2015) Mer receptor tyrosine kinase mediates both tethering and phagocytosis of apoptotic cells. *Cell death & disease*. [Online] 6, e1646. Available from: doi:10.1038/cddis.2015.18.

Duseja, A. & Singh, S.P. (2017) Toward a Better Definition of Acute-on-Chronic Liver Failure. *Journal of Clinical and Experimental Hepatology*. [Online] 7 (3), 262–265. Available from: doi:10.1016/j.jceh.2017.05.002.

Elliott, M.R., Koster, K.M. & Murphy, P.S. (2017) Efferocytosis Signaling in the Regulation of Macrophage Inflammatory Responses. *The Journal of Immunology*. [Online] 198 (4), 1387–1394. Available from: doi:10.4049/jimmunol.1601520.

Engelmann, C., Becker, C., Boldt, A., Herta, T., et al. (2016a) Ascites' neutrophil function is significantly impaired in patients with decompensated cirrhosis but can be restored by autologous plasma incubation. *Scientific Reports*. [Online] 6 (1), 37926. Available from: doi:10.1038/srep37926.

Engelmann, C., Krohn, S., Prywerek, D., Hartmann, J., et al. (2016b) Detection of molecular bacterascites in decompensated cirrhosis defines a risk with decreased survival. *European journal of gastroenterology & hepatology*. [Online] 28 (11), 1285–1292. Available from: doi:10.1097/MEG.0000000000000712.

Facciorusso, A., Papagiouvanni, I., Cela, M., Buccino, V.R., et al. (2019) Comparative efficacy of long-term antibiotic treatments in the primary prophylaxis of spontaneous bacterial peritonitis. *Liver International*. [Online] liv.14109. Available from: doi:10.1111/liv.14109.

Fadok, V.A., Bratton, D.L., Konowal, A., Freed, P.W., et al. (1998) Macrophages that have ingested apoptotic cells in vitro inhibit proinflammatory cytokine production through autocrine/paracrine mechanisms involving TGF-beta, PGE2, and PAF. *Journal of Clinical Investigation*. [Online] 101 (4), 890–898. Available from: doi:10.1172/JCI1112.

Fagan, K.J., Rogers, G.B., Melino, M., Arthur, D.M., et al. (2015) Ascites Bacterial Burden and Immune Cell Profile Are Associated with Poor Clinical Outcomes in the Absence of Overt Infection Golo Ahlenstiel (ed.). *PLoS ONE*. [Online] 10 (3), e0120642-15. Available from: doi:10.1371/journal.pone.0120642.

Fernandez, J., Acevedo, J., Wiest, R., Gustot, T., et al. (2017) Bacterial and fungal infections in acute-on-chronic liver failure: prevalence, characteristics and impact on prognosis. *Gut*. [Online] gutjnl-2017-314240. Available from: doi:10.1136/gutjnl-2017-314240.

Fernandez, J., Acevedo, J., Wiest, R., Gustot, T., et al. (2018) Bacterial and fungal infections in acute-on-chronic liver failure: prevalence, characteristics and impact on prognosis. *Gut*. [Online] 67 (10), 1870–1880. Available from: doi:10.1136/gutjnl-2017-314240.

Fernandez, J., Navasa, M., Gómez, J., Colmenero, J., et al. (2002) Bacterial infections in cirrhosis: Epidemiological changes with invasive procedures and norfloxacin prophylaxis. *Hepatology*. [Online] 35 (1), 140–148. Available from: doi:10.1053/jhep.2002.30082.

Fernández, J. & Saliba, F. (2018) Liver transplantation in patients with ACLF and multiple organ failure: Time for priority after initial stabilization. *Journal of Hepatology*. [Online] 69 (5), 1004–1006. Available from: doi:10.1016/j.jhep.2018.09.002.

Fernandez, J., Tandon, P., Mensa, J. & Garcia-Tsao, G. (2015) Antibiotic prophylaxis in cirrhosis: Good and bad. *Hepatology*. [Online] Available from: doi:10.1002/hep.28330.

Fischer, J., Silva, T.E., Soares e Silva, P.E., Colombo, B.S., et al. (2017) From stable disease to acute-on-chronic liver failure: Circulating cytokines are related to prognosis in different stages of cirrhosis. *Cytokine*. [Online] 91, 162–169. Available from: doi:10.1016/j.cyto.2016.12.017.

Fisher, C., Patel, V.C., Stoy, S.H., Singanayagam, A., et al. (2018) Balanced haemostasis with both hypo- and hyper-coagulable features in critically ill patients with acute-on-chronic-liver failure. *Journal of critical care*. [Online] 43, 54–60. Available from: doi:10.1016/j.jcrc.2017.07.053.

Foreman, M.G., Mannino, D.M. & Moss, M. (2003) Cirrhosis as a risk factor for sepsis and death - Analysis of the National Hospital Discharge Survey. *Chest*. [Online] 124 (3), 1016–1020. Available from: doi:10.1378/chest.124.3.1016.

Gäbele, E., Mühlbauer, M., Paulo, H., Johann, M., et al. (2009) Analysis of monocyte chemotactic protein-1 gene polymorphism in patients with spontaneous bacterial peritonitis. *World Journal of Gastroenterology*. [Online] 15 (44), 5558–5562. Available from: doi:10.3748/wjg.15.5558.

Gabrilovich, D.I. (2017) Myeloid-Derived Suppressor Cells. *Cancer immunology research*. [Online] 5 (1), 3–8. Available from: doi:10.1158/2326-6066.CIR-16-0297.

Galvan, M.D., Foreman, D.B., Zeng, E., Tan, J.C., et al. (2012) Complement Component C1q Regulates Macrophage Expression of Mer Tyrosine Kinase To Promote Clearance of Apoptotic Cells. *The Journal of Immunology*. [Online] 188 (8), 3716–3723. Available from: doi:10.4049/jimmunol.1102920.

Gerhardt, T. & Ley, K. (2015) Monocyte trafficking across the vessel wall. *Cardiovascular Research*. [Online] 107 (3), 321–330. Available from: doi:10.1093/cvr/cvv147.

Ghebrehiwet, B., Hosszu, K.H. & Peerschke, E.I.B. (2017) C1q as an autocrine and paracrine regulator of cellular functions. *Molecular Immunology*. [Online] 84, 26–33. Available from: doi:10.1016/j.molimm.2016.11.003.

Ghosn, E.E.B., Cassado, A.A., Govoni, G.R., Fukuhara, T., et al. (2010) Two physically, functionally, and developmentally distinct peritoneal macrophage subsets. *Proceedings of the National Academy of Sciences*. [Online] 107 (6), 2568–2573. Available from: doi:10.1073/pnas.0915000107.

Gibson, M.S., Domingues, N. & Vieira, O.V. (2018) Lipid and Non-lipid Factors Affecting Macrophage Dysfunction and Inflammation in Atherosclerosis. *Frontiers in Physiology*. [Online] 9, 654. Available from: doi:10.3389/fphys.2018.00654.

Gines, P., Rimola, A., Rimola, A., PLANAS, R., et al. (1990) Norfloxacin Prevents Spontaneous Bacterial Peritonitis Recurrence in Cirrhosis - Results of a Double-Blind, Placebo-Controlled Trial. *Hepatology*. [Online] 12 (4), 716–724. Available from: doi:10.1002/hep.1840120416.

Ginhoux, F., Schultze, J.L., Murray, P.J., Ochando, J., et al. (2016) New insights into the multidimensional concept of macrophage ontogeny, activation and function. *Nature Immunology*. [Online] 17 (1), 34–40. Available from: doi:10.1038/ni.3324.

Giuntoli, R.L.I., Webb, T.J., Zoso, A., Rogers, O., et al. (2009) Ovarian Cancer-associated Ascites Demonstrates Altered Immune Environment: Implications for Antitumor Immunity. *Anticancer Research*. 29 (8), 2875–2884.

Gordon, S., Plueddemann, A. & Estrada, F.M. (2014) Macrophage heterogeneity in tissues: phenotypic diversity and functions. *Immunological reviews*. [Online] 262 (1), 36–55. Available from: doi:10.1111/imr.12223.

Gordon, S. & Taylor, P.R. (2005) Monocyte and macrophage heterogeneity. *Nature Reviews Immunology*. [Online] 5 (12), 953–964. Available from: doi:10.1038/nri1733.

Graham, D.K. (2006) Ectopic Expression of the Proto-oncogene Mer in Pediatric T-Cell Acute Lymphoblastic Leukemia. *Clinical Cancer Research*. [Online] 12 (9), 2662–2669. Available from: doi:10.1158/1078-0432.CCR-05-2208.

Graham, D.K., DeRyckere, D., Davies, K.D. & Earp, H.S. (2014) The TAM family: phosphatidylserine-sensing receptor tyrosine kinases gone awry in cancer. *Nature Reviews Cancer*. [Online] 14 (12), 769–785. Available from: doi:10.1038/nrc3847.

Greenlee-Wacker, M.C. (2016) Clearance of apoptotic neutrophils and resolution of inflammation. *Immunological Reviews*. [Online] 273 (1), 357–370. Available from: doi:10.1111/imr.12453.

Gregory, S.H. & Wing, E.J. (1998) Neutrophil–Kupffer-cell interaction in host defenses to systemic infections. *Immunology today*. 19 (11), 507–510.

Gudowska, M., Gruszewska, E., Cylwik, B., Panasiuk, A., et al. (2015) *Galectin-3 Concentration in Liver Diseases*. 45 (6), 5.

Guignant, C., Venet, F., Planel, S., Demaret, J., et al. (2013) Increased MerTK expression in circulating innate immune cells of patients with septic shock. *Intensive care medicine*. [Online] 39 (9), 1556–1564. Available from: doi:10.1097/CCM.0b013e3181ab858a.

Guillot, A. & Tacke, F. (2019) Liver Macrophages: Old Dogmas and New Insights. *Hepatology Communications*. [Online] 3 (6), 730–743. Available from: doi:10.1002/hep4.1356.

Gustot, T., Fernandez, J., Garcia, E., Morando, F., et al. (2015) Clinical Course of acute-on-chronic liver failure syndrome and effects on prognosis: HEPATOLOGY, Vol. XX, No. X, 2015. *Hepatology*. [Online] 62 (1), 243–252. Available from: doi:10.1002/hep.27849.

Haas, J.T., Francque, S. & Staels, B. (2016) Pathophysiology and Mechanisms of Nonalcoholic Fatty Liver Disease. *Annual review of physiology*. [Online] 78, 181–205. Available from: doi:10.1146/annurev-physiol-021115-105331.

Hackstein, C.-P., Assmus, L.M., Welz, M., Klein, S., et al. (2017) Gut microbial translocation corrupts myeloid cell function to control bacterial infection during liver cirrhosis. *Gut*. [Online] 66 (3), 507–518. Available from: doi:10.1136/gutjnl-2015-311224.

Hafizi, S. & Dahlbäck, B. (2006) Gas6 and protein S. Vitamin K-dependent ligands for the Axl receptor tyrosine kinase subfamily. *The FEBS journal*. [Online] 273 (23), 5231–5244. Available from: doi:10.1111/j.1742-4658.2006.05529.x.

Harputluoglu, M.M.M., Dertli, R., Otlu, B., Demirel, U., et al. (2016) Nucleotide-Binding Oligomerization Domain-Containing Protein 2 Variants in Patients with Spontaneous Bacterial Peritonitis. *Digestive Diseases and Sciences*. [Online] 61 (6), 1545–1552. Available from: doi:10.1007/s10620-015-4024-y.

Hernaez, R., Solà, E., Moreau, R. & Ginès, P. (2017) Acute-on-chronic liver failure: an update. *Gut*. [Online] 66 (3), 541–553. Available from: doi:10.1136/gutjnl-2016-312670.

Heymann, F. & Tacke, F. (2016) Immunology in the liver - from homeostasis to disease. *Nature Reviews Gastroenterology & Hepatology*. [Online] 13 (2), 88–110. Available from: doi:10.1038/nrgastro.2015.200.

Ho, H.-L. & Huang, H.-C. (2015) Molecular mechanisms of circulatory dysfunction in cirrhotic portal hypertension. *Journal of the Chinese Medical Association*. [Online] 78 (4), 195–203. Available from: doi:10.1016/j.jcma.2014.10.004.

Holland, S.J., Pan, A., Franci, C., Hu, Y., et al. (2010) R428, a Selective Small Molecule Inhibitor of Axl Kinase, Blocks Tumor Spread and Prolongs Survival in Models of Metastatic Breast Cancer. *Cancer Research*. [Online] 70 (4), 1544–1554. Available from: doi:10.1158/0008-5472.CAN-09-2997.

Holtzhausen, A., Harris, W., Ubil, E., Hunter, D.M., et al. (2019) TAM Family Receptor Kinase Inhibition Reverses MDSC-Mediated Suppression and Augments Anti–PD-1 Therapy in Melanoma. *Cancer Immunology Research*. [Online] Available from: doi:10.1158/2326-6066.CIR-19-0008.

Hong, C. & Tontonoz, P. (2014) Liver X receptors in lipid metabolism: opportunities for drug discovery. *Nature Reviews Drug Discovery*. [Online] 13 (6), 433–444. Available from: doi:10.1038/nrd4280.

Hotchkiss, R.S., Coopersmith, C.M., McDunn, J.E. & Ferguson, T.A. (2009) *Tilting toward immunosuppression*. 2.

Hotchkiss, R.S., Monneret, G. & Payen, D. (2013) Immunosuppression in sepsis: a novel understanding of the disorder and a new therapeutic approach. *The Lancet Infectious Diseases*. [Online] 13 (3), 260–268. Available from: doi:10.1016/S1473-3099(13)70001-X.

Huey, M., Minson, K., Earp, H., DeRyckere, D., et al. (2016) Targeting the TAM Receptors in Leukemia. *Cancers*. [Online] 8 (11), 101. Available from: doi:10.3390/cancers8110101.

Hulsebus, H.J., O'Conner, S.D., Smith, E.M., Jie, C., et al. (2016) Complement Component C1q Programs a Pro-Efferocytic Phenotype while Limiting TNFα Production in Primary Mouse and Human Macrophages. *Frontiers in Immunology*. [Online] 7. Available from: doi:10.3389/fimmu.2016.00230 [Accessed: 22 September 2019].

Hume, D.A. (2015) The Many Alternative Faces of Macrophage Activation. *Frontiers in Immunology*. [Online] 6 (JUL), 370. Available from: doi:10.3389/fimmu.2015.00370.

Hussain, W., Khalid, A.B., Usmani, T., Ghufran, A., et al. (1969) Low dose albumin for the prevention of renal impairment following large volume paracentesis in cirrhosis. *Pakistan Journal of*

Medical Sciences. [Online] 31 (3). Available from: doi:10.12669/pjms.313.7281 [Accessed: 23 September 2019].

Ikarashi, M., Nakashima, H., Kinoshita, M., Sato, A., et al. (2013) Distinct development and functions of resident and recruited liver Kupffer cells/macrophages. *Journal of Leukocyte Biology*. [Online] 94 (6), 1325–1336. Available from: doi:10.1189/jlb.0313144.

Ingersoll, M.A., Spanbroek, R., Lottaz, C., Gautier, E.L., et al. (2010) Comparison of gene expression profiles between human and mouse monocyte subsets. *Blood*. [Online] 115 (3), e10–e19. Available from: doi:10.1182/blood-2009-07-235028.

Irvine, K.M., Banh, X., Gadd, V.L., Wojcik, K.K., et al. (2016) CRIg-expressing peritoneal macrophages are associated with disease severity in patients with cirrhosis and ascites. *JCI insight*. [Online] 1 (8), e86914. Available from: doi:10.1172/jci.insight.86914.

Jalan, R., Fernandez, J., Wiest, R., Schnabl, B., et al. (2014a) Bacterial infections in cirrhosis: a position statement based on the EASL Special Conference 2013. *Journal of Hepatology*. [Online] 60 (6), 1310–1324. Available from: doi:10.1016/j.jhep.2014.01.024.

Jalan, R., Saliba, F., Pavesi, M., Amoros, A., et al. (2014b) Development and validation of a prognostic score to predict mortality in patients with acute-on-chronic liver failure. *Journal of Hepatology*. [Online] 61 (5), 1038–1047. Available from: doi:10.1016/j.jhep.2014.06.012.

Jalan, R., Stadlbauer, V., Sen, S., Cheshire, L., et al. (2012) Role of predisposition, injury, response and organ failure in the prognosis of patients with acute-on-chronic liver failure: a prospective cohort study. *Critical Care*. [Online] 16 (6), R227. Available from: doi:10.1186/cc11882.

Jang, J.C., Li, J., Gambini, L., Batugedara, H.M., et al. (2017) Human resistin protects against endotoxic shock by blocking LPS–TLR4 interaction. *Proceedings of the National Academy of Sciences*. [Online] 114 (48), E10399–E10408. Available from: doi:10.1073/pnas.1716015114.

Jenne, C.N. & Kubes, P. (2013) Immune surveillance by the liver. *Nature Immunology*. [Online] 14 (10), 996–1006. Available from: doi:10.1038/ni.2691.

Jin, J.-O., Zhang, W., Wong, K.-W., Kwak, M., et al. (2014) Inhibition of Breast Cancer Resistance Protein (ABCG2) in Human Myeloid Dendritic Cells Induces Potent Tolerogenic Functions during LPS Stimulation Yuntao Wu (ed.). *PLoS ONE*. [Online] 9 (8), e104753. Available from: doi:10.1371/journal.pone.0104753.

Johansson, U., Bloxham, D., Couzens, S., Jesson, J., et al. (2014) Guidelines on the use of multicolour flow cytometry in the diagnosis of haematological neoplasms. *British Journal of Haematology*. [Online] 165 (4), 455–488. Available from: doi:10.1111/bjh.12789.

Jorch, S.K., Surewaard, B.G.J., Hossain, M., Peiseler, M., et al. (2019) Peritoneal GATA6+ macrophages function as a portal for Staphylococcus aureus dissemination. *Journal of Clinical Investigation*. [Online] 10.1172/JCI127286. Available from: doi:10.1172/JCI127286.

Kapellos, T.S., Bonaguro, L., Gemünd, I., Reusch, N., et al. (2019) Human Monocyte Subsets and Phenotypes in Major Chronic Inflammatory Diseases. *Frontiers in Immunology*. [Online] 10, 2035. Available from: doi:10.3389/fimmu.2019.02035.

Kariolis, M.S., Miao, Y.R., Diep, A., Nash, S.E., et al. (2016) Inhibition of the GAS6/AXL pathway augments the efficacy of chemotherapies. *Journal of Clinical Investigation*. [Online] 127 (1), 183–198. Available from: doi:10.1172/JCI85610.

Karlmark, K.R., Zimmermann, H.W., Roderburg, C., Gassler, N., et al. (2010) The fractalkine receptor CX3CR1 protects against liver fibrosis by controlling differentiation and survival of infiltrating hepatic monocytes. *Hepatology*. [Online] 52 (5), 1769–1782. Available from: doi:10.1002/hep.23894.

Karvellas, C.J., Garcia-Lopez, E., Fernandez, J., Saliba, F., et al. (2018) Dynamic Prognostication in Critically Ill Cirrhotic Patients With Multiorgan Failure in ICUs in Europe and North America: A Multicenter Analysis*. *Critical Care Medicine*. [Online] 46 (11), 1783–1791. Available from: doi:10.1097/CCM.0000000000003369.

Khanam, A., Trehanpati, N., Riese, P., Rastogi, A., et al. (2017) Blockade of Neutrophil's Chemokine Receptors CXCR1/2 Abrogate Liver Damage in Acute-on-Chronic Liver Failure. *Frontiers in Immunology*. [Online] 8, 464. Available from: doi:10.3389/fimmu.2017.00464.

Kim, S.-Y., Lim, E.-J., Yoon, Y.-S., Ahn, Y.-H., et al. (2016) Liver X receptor and STAT1 cooperate downstream of Gas6/Mer to induce anti-inflammatory arginase 2 expression in macrophages. *Scientific reports*. [Online] 6 (1), 29673. Available from: doi:10.1038/srep29673.

Kimani, S.G., Kumar, S., Bansal, N., Singh, K., et al. (2017) Small molecule inhibitors block Gas6-inducible TAM activation and tumorigenicity. *Scientific Reports*. [Online] 7 (1), 43908. Available from: doi:10.1038/srep43908.

Knubel, K.H., Pernu, B.M., Sufit, A., Nelson, S., et al. (2014) MerTK inhibition is a novel therapeutic approach for glioblastoma multiforme. *Oncotarget*. [Online] 5 (5), 1338–1351. Available from: doi:10.18632/oncotarget.1793.

Korf, H., du Plessis, J., van Pelt, J., De Groote, S., et al. (2019) Inhibition of glutamine synthetase in monocytes from patients with acute-on-chronic liver failure resuscitates their antibacterial and inflammatory capacity. *Gut*. [Online] 68 (10), 1872–1883. Available from: doi:10.1136/gutjnl-2018-316888.

Krag, A., Wiest, R., Albillos, A. & Gluud, L.L. (2012) The window hypothesis: haemodynamic and non-haemodynamic effects of β-blockers improve survival of patients with cirrhosis during a window in the disease: Figure 1. *Gut*. [Online] 61 (7), 967–969. Available from: doi:10.1136/gutjnl-2011-301348.

Krag, A., Wiest, R. & Gluud, L.L. (2010) Fluoroquinolones in the Primary Prophylaxis of Spontaneous Bacterial Peritonitis: *American Journal of Gastroenterology*. [Online] 105 (6), 1444. Available from: doi:10.1038/ajg.2010.126.

Kubicka, U., Olszewski, W.L., Tarnowski, W., Bielecki, K., et al. (1996) Normal Human Immune Peritoneal Cells: Subpopulations and Functional Characteristics. *Scandinavian Journal of Immunology*. [Online] 44 (2), 157–163. Available from: doi:10.1046/j.1365-3083.1996.d01-297.x.

Laleman, W., Clària, J., Van der Merwe, S., Moreau, R., et al. (2018) Systemic Inflammation and Acute-on-Chronic Liver Failure: Too Much, Not Enough. *Canadian journal of gastroenterology & hepatology*. [Online] 2018 (4, article r108), 1–10. Available from: doi:10.1155/2018/1027152.

Lario, M., Muñoz, L., Ubeda, M., Borrero, M.-J., et al. (2013) Defective thymopoiesis and poor peripheral homeostatic replenishment of T-helper cells cause T-cell lymphopenia in cirrhosis. *Journal of Hepatology*. [Online] 59 (4), 723–730. Available from: doi:10.1016/j.jhep.2013.05.042.

Lechner, M.G., Liebertz, D.J. & Epstein, A.L. (2010) Characterization of cytokine-induced myeloid-derived suppressor cells from normal human peripheral blood mononuclear cells. *Journal of immunology (Baltimore, Md. : 1950)*. [Online] 185 (4), 2273–2284. Available from: doi:10.4049/jimmunol.1000901.

Lee, Y.-J., Han, J.-Y., Byun, J., Park, H.-J., et al. (2012a) Inhibiting Mer receptor tyrosine kinase suppresses STAT1, SOCS1/3, and NF-κB activation and enhances inflammatory responses in lipopolysaccharide-induced acute lung injury. *Journal of Leukocyte Biology*. [Online] 91 (6), 921–932. Available from: doi:10.1189/jlb.0611289.

Lee, Y.-J., Han, J.-Y., Byun, J., Park, H.-J., et al. (2012b) Inhibiting Mer receptor tyrosine kinase suppresses STAT1, SOCS1/3, and NF-κB activation and enhances inflammatory responses in lipopolysaccharide-induced acute lung injury. *Journal of Leukocyte Biology*. [Online] 91 (6), 921–932. Available from: doi:10.1189/jlb.0611289.

Lee-Sherick, A.B., Eisenman, K.M., Sather, S., McGranahan, A., et al. (2013) Aberrant Mer receptor tyrosine kinase expression contributes to leukemogenesis in acute myeloid leukemia. *Oncogene*. [Online] 32 (46), 5359–5368. Available from: doi:10.1038/onc.2013.40.

Lemke, G. & Rothlin, C.V. (2008) Immunobiology of the TAM receptors. *Nature Reviews Immunology*. [Online] 8 (5), 327–336. Available from: doi:10.1172/JCI22079.

Lemoine, M., Shimakawa, Y., Nayagam, S., Khalil, M., et al. (2016) The gamma-glutamyl transpeptidase to platelet ratio (GPR) predicts significant liver fibrosis and cirrhosis in patients with chronic HBV infection in West Africa. *Gut*. [Online] 65 (8), 1369–1376. Available from: doi:10.1136/gutjnl-2015-309260.

Levy, O., Calippe, B., Lavalette, S., Hu, S.J., et al. (2015) Apolipoprotein E promotes subretinal mononuclear phagocyte survival and chronic inflammation in age-related macular degeneration. *EMBO Molecular Medicine*. [Online] 7 (2), 211–226. Available from: doi:10.15252/emmm.201404524.

Li, F., Miao, L., Sun, H., Zhang, Y., et al. (2017) Establishment of a new acute-on-chronic liver failure model. *Acta Pharmaceutica Sinica B*. [Online] 7 (3), 326–333. Available from: doi:10.1016/j.apsb.2016.09.003.

Li, F., Yang, M., Wang, L., Williamson, I., et al. (2012) Autofluorescence contributes to false-positive intracellular Foxp3 staining in macrophages: A lesson learned from flow cytometry. *Journal of Immunological Methods*. [Online] 386 (1–2), 101–107. Available from: doi:10.1016/j.jim.2012.08.014.

Liao, C.-T., Andrews, R., Wallace, L.E., Khan, M.W.A., et al. (2017) Peritoneal macrophage heterogeneity is associated with different peritoneal dialysis outcomes. *Kidney international*. [Online] 91 (5), 1088–1103. Available from: doi:10.1016/j.kint.2016.10.030.

Liaskou, E., Zimmermann, H.W., Li, K.-K., Oo, Y.H., et al. (2012) Monocyte subsets in human liver disease show distinct phenotypic and functional characteristics. *Hepatology*. [Online] 57 (1), 385–398. Available from: doi:10.4049/jimmunol.172.7.4068.

Ling, L., Templeton, D. & Kung, H.-J. (1996) Identification of the Major Autophosphorylation Sites of Nyk/Mer, an NCAM-related Receptor Tyrosine Kinase. *Journal of Biological Chemistry*. [Online] 271 (31), 18355–18362. Available from: doi:10.1074/jbc.271.31.18355.

Liu, C.M., Aziz, M., Kachur, S., Hsueh, P.-R., et al. (2012) BactQuant: An enhanced broad-coverage bacterial quantitative real-time PCR assay. *BMC Microbiology*. [Online] 12 (1), 56. Available from: doi:10.1186/1471-2180-12-56.

Liu, G., Wu, C., Wu, Y. & Zhao, Y. (2006) Phagocytosis of apoptotic cells and immune regulation. *Scandinavian journal of immunology*. [Online] 64 (1), 1–9. Available from: doi:10.1111/j.1365-3083.2006.01771.x.

Liu, J., Zhang, W., Stashko, M.A., DeRyckere, D., et al. (2013) UNC1062, a new and potent Mer inhibitor. *European Journal of Medicinal Chemistry*. [Online] 65, 83–93. Available from: doi:10.1016/j.ejmech.2013.03.035.

Llacuna, L., Bárcena, C., Bellido-Martín, L., Fernández, L., et al. (2010) Growth arrest-specific protein 6 is hepatoprotective against murine ischemia/reperfusion injury. *Hepatology*. [Online] 52 (4), 1371–1379. Available from: doi:10.1002/hep.23833.

Lombardi, A., Zuccaro, V., Fagiuoli, S. & Bruno, R. (2019) Prophylaxis of spontaneous bacterial peritonitis: Is there still room for quinolones? *Journal of hepatology*. [Online] 70 (5), 1027–1028. Available from: doi:10.1016/j.jhep.2018.12.032.

Macdonald, S., Andreola, F., Bachtiger, P., Amorós, À., et al. (2018) Cell death markers in patients with cirrhosis and acute decompensation. *Hepatology (Baltimore, Md.)*. [Online] 67 (3), 989–1002. Available from: doi:10.1002/hep.29581.

Madenspacher, J.H., Azzam, K.M., Gong, W., Gowdy, K.M., et al. (2012) Apolipoproteins and Apolipoprotein Mimetic Peptides Modulate Phagocyte Trafficking through Chemotactic Activity. *Journal of Biological Chemistry*. [Online] 287 (52), 43730–43740. Available from: doi:10.1074/jbc.M112.377192.

Magiorakos, A.-P., Srinivasan, A., Carey, R.B., Carmeli, Y., et al. (2012) Multidrug-resistant, extensively drug-resistant and pandrug-resistant bacteria: an international expert proposal for interim standard definitions for acquired resistance. *Clinical Microbiology and Infection*. [Online] 18 (3), 268–281. Available from: doi:10.1111/j.1469-0691.2011.03570.x.

Mai, M., Stengel, S., Al-Herwi, E., Peter, J., et al. (2017) Genetic variants of TRAF6 modulate peritoneal immunity and the risk of spontaneous bacterial peritonitis in cirrhosis: A combined prospective-retrospective study. *Scientific reports*. [Online] 7 (1), 4914. Available from: doi:10.1038/s41598-017-04895-z.

Mandorfer, M., Mandorfer, M., Bota, S., Bota, S., et al. (2014) Nonselective β blockers increase risk for hepatorenal syndrome and death in patients with cirrhosis and spontaneous bacterial peritonitis. *YGAST*. [Online] 146 (7), 1680-16e1. Available from: doi:10.1053/j.gastro.2014.03.005.

Marciano, S., Díaz, J.M., Dirchwolf, M. & Gadano, A. (2019) Spontaneous bacterial peritonitis in patients with cirrhosis: incidence, outcomes, and treatment strategies. *Hepatic Medicine: Evidence and Research*. [Online] Volume 11, 13–22. Available from: doi:10.2147/HMER.S164250.

Markwick, L.J.L., Riva, A., Ryan, J.M., Cooksley, H., et al. (2015) Blockade of PD1 and TIM3 Restores Innate and Adaptive Immunity in Patients With Acute Alcoholic Hepatitis. *Gastroenterology*. [Online] 148 (3), 590-602.e10. Available from: doi:10.1053/j.gastro.2014.11.041.

Martin-Mateos, R., Alvarez-Mon, M. & Albillos, A. (2019) Dysfunctional Immune Response in Acute-on-Chronic Liver Failure: It Takes Two to Tango. *Frontiers in Immunology*. [Online] 10, 973. Available from: doi:10.3389/fimmu.2019.00973.

Matsuno, K. (1996) A life stage of particle-laden rat dendritic cells in vivo: their terminal division, active phagocytosis, and translocation from the liver to the draining lymph. *Journal of Experimental Medicine*. [Online] 183 (4), 1865–1878. Available from: doi:10.1084/jem.183.4.1865.

McCloskey, C., Rodriguez, G., Galpin, K. & Vanderhyden, B. (2018) Ovarian Cancer Immunotherapy: Preclinical Models and Emerging Therapeutics. *Cancers*. [Online] 10 (8), 244. Available from: doi:10.3390/cancers10080244.

McDonald, J.A.K., Mullish, B.H., Pechlivanis, A., Liu, Z., et al. (2018) Inhibiting Growth of Clostridioides difficile by Restoring Valerate, Produced by the Intestinal Microbiota. *Gastroenterology*. [Online] 155 (5), 1495-1507.e15. Available from: doi:10.1053/j.gastro.2018.07.014.

McPhail, M.J.W., Shawcross, D.L., Lewis, M.R., Coltart, I., et al. (2016) Multivariate metabotyping of plasma predicts survival in patients with decompensated cirrhosis. *Journal of Hepatology*. [Online] 64 (5), 1058–1067. Available from: doi:10.1016/j.jhep.2016.01.003.

Meertens, L., Carnec, X., Lecoin, M.P., Ramdasi, R., et al. (2012) The TIM and TAM Families of Phosphatidylserine Receptors Mediate Dengue Virus Entry. *Cell Host & Microbe*. [Online] 12 (4), 544–557. Available from: doi:10.1016/j.chom.2012.08.009.

Mehta, G., Mehta, G., Mookerjee, R.P., Sharma, V., et al. (2015) Systemic inflammation is associated with increased intrahepatic resistance and mortality in alcohol-related acute-on-chronic liver failure. *Liver International*. [Online] 35 (3), 724–734. Available from: doi:10.1111/liv.12559.

Mehta, G., Rousell, S., Burgess, G., Morris, M., et al. (2018) A Placebo-Controlled, Multicenter, Double-Blind, Phase 2 Randomized Trial of the Pan-Caspase Inhibitor Emricasan in Patients with Acutely Decompensated Cirrhosis. *Journal of Clinical and Experimental Hepatology*. [Online] 8 (3), 224–234. Available from: doi:10.1016/j.jceh.2017.11.006.

Merle, N.S., Noe, R., Halbwachs-Mecarelli, L., Fremeaux-Bacchi, V., et al. (2015) Complement System Part II: Role in Immunity. *Frontiers in Immunology*. [Online] 6. Available from: doi:10.3389/fimmu.2015.00257 [Accessed: 29 September 2019].

Michelena, J., Altamirano, J., Abraldes, J.G., Affò, S., et al. (2015) Systemic inflammatory response and serum lipopolysaccharide levels predict multiple organ failure and death in alcoholic hepatitis. *Hepatology*. [Online] Available from: doi:10.1002/hep.27779.

Mills, E.L., Ryan, D.G., Prag, H.A., Dikovskaya, D., et al. (2018) Itaconate is an anti-inflammatory metabolite that activates Nrf2 via alkylation of KEAP1. *Nature*. [Online] 556 (7699), 113–117. Available from: doi:10.1038/nature25986.

Min, Y.W., Min, Y.W., Lim, K.S., Lim, K.S., et al. (2014) Proton pump inhibitor use significantly increases the risk of spontaneous bacterial peritonitis in 1965 patients with cirrhosis and ascites: a propensity score matched cohort study. *Alimentary Pharmacology and Therapeutics*. [Online] 40 (6), 695–704. Available from: doi:10.1111/apt.12875.

Minasyan, H. (2016) Mechanisms and pathways for the clearance of bacteria from blood circulation in health and disease. *Pathophysiology : the official journal of the International Society for*

Pathophysiology / ISP. [Online] 23 (2), 61–66. Available from: doi:10.1016/j.pathophys.2016.03.001.

Moreau, R. (2014) Paracentesis-induced inflammation: a new syndrome? *Liver International*. [Online] n/a-n/a. Available from: doi:10.1111/liv.12545.

Moreau, R., Jalan, R. & Arroyo, V. (2015) Acute-on-Chronic Liver Failure: Recent Concepts. *Journal of Clinical and Experimental Hepatology*. [Online] 5 (1), 81–85. Available from: doi:10.1016/j.jceh.2014.09.003.

Moreau, R., Jalan, R., Ginès, P., Pavesi, M., et al. (2013) Acute-on-chronic liver failure is a distinct syndrome that develops in patients with acute decompensation of cirrhosis. *Gastroenterology*. [Online] 144 (7), 1426-37-1437.e1-9. Available from: doi:10.1053/j.gastro.2013.02.042.

Mücke, M.M., Rumyantseva, T., Mücke, V.T., Schwarzkopf, K., et al. (2017) Bacterial infection-triggered acute-on-chronic liver failure is associated with increased mortality. *Liver International*. [Online] Available from: doi:10.1111/liv.13568.

Mukherjee, S.K., Wilhelm, A. & Antoniades, C.G. (2016) TAM receptor tyrosine kinase function and the immunopathology of liver disease. *American Journal of Physiology-Gastrointestinal and Liver Physiology*. [Online] 310 (11), G899–G905. Available from: doi:10.1152/ajpgi.00382.2015.

Muller, W.A. (2015) Localized signals that regulate transendothelial migration. *Current opinion in immunology*. [Online] 38, 24–29. Available from: doi:10.1016/j.coi.2015.10.006.

Muller, W.A. & Randolph, G.J. (1999) Migration of leukocytes across endothelium and beyond: molecules involved in the transmigration and fate of monocytes. *Journal of leukocyte biology*. 66 (5), 698–704.

Muñoz, L., José Borrero, M., Ubeda, M., Lario, M., et al. (2012) Interaction between intestinal dendritic cells and bacteria translocated from the gut in rats with cirrhosis. *Hepatology*. [Online] 56 (5), 1861–1869. Available from: doi:10.1002/hep.25854.

Muñoz, L.E., Lauber, K., Schiller, M., Manfredi, A.A., et al. (2010) The role of defective clearance of apoptotic cells in systemic autoimmunity. *Nature Reviews Rheumatology*. [Online] 6 (5), 280–289. Available from: doi:10.4049/jimmunol.166.7.4498.

Nagata, S., Suzuki, J., Segawa, K. & Fujii, T. (2016) Exposure of phosphatidylserine on the cell surface. *Cell Death & Differentiation*. [Online] 23 (6), 952–961. Available from: doi:10.1038/cdd.2016.7.

Nguyen, K.-Q., Tsou, W.-I., Kotenko, S. & Birge, R.B. (2013) TAM receptors in apoptotic cell clearance, autoimmunity, and cancer. *Autoimmunity*. [Online] 46 (5), 294–297. Available from: doi:10.1016/j.bbamem.2008.05.006.

Nieto, J.C., Nieto, J.C., Sanchez, E., Sanchez, E., et al. (2015) Impaired innate immune response of leukocytes from ascitic fluid of patients with spontaneous bacterial peritonitis. *Journal of leukocyte biology*. [Online] 98 (5), 819–825. Available from: doi:10.1189/jlb.3AB0315-106R.

Nieto, J.C., Perea, L., Soriano, G., Zamora, C., et al. (2018) Ascitic fluid regulates the local innate immune response of patients with cirrhosis. *Journal of leukocyte biology*. [Online] Available from: doi:10.1002/JLB.3A0218-072R.

Nishi, C., Toda, S., Segawa, K. & Nagata, S. (2014) Tim4- and MerTK-Mediated Engulfment of Apoptotic Cells by Mouse Resident Peritoneal Macrophages. *Molecular and cellular biology*. [Online] 34 (8), 1512–1520. Available from: doi:10.1128/MCB.01394-13.

Nourshargh, S., Renshaw, S.A. & Imhof, B.A. (2016) Reverse Migration of Neutrophils: Where, When, How, and Why? *Trends in immunology*. [Online] Available from: doi:10.1016/j.it.2016.03.006.

Nüsse, O. (2011) Biochemistry of the Phagosome: The Challenge to Study a Transient Organelle. *The Scientific World JOURNAL*. [Online] 11, 2364–2381. Available from: doi:10.1100/2011/741046.

O'Brien, A.J., Fullerton, J.N., Massey, K.A., Auld, G., et al. (2014) Immunosuppression in acutely decompensated cirrhosis is mediated by prostaglandin E2. *Nature Medicine*. [Online] 20 (5), 518–523. Available from: doi:10.1038/nm.3516.

Ochodnicky, P., Lattenist, L., Ahdi, M., Kers, J., et al. (2017) Increased Circulating and Urinary Levels of Soluble TAM Receptors in Diabetic Nephropathy. *The American Journal of Pathology*. [Online] 187 (9), 1971–1983. Available from: doi:10.1016/j.ajpath.2017.05.004.

Oey, R.C., van Buuren, H.R., de Jong, D.M., Erler, N.S., et al. (2018) Bacterascites: A study of clinical features, microbiological findings, and clinical significance. *Liver International*. [Online] 38 (12), 2199–2209. Available from: doi:10.1111/liv.13929.

O'Grady, J. (2017) Con: Acute-on-chronic liver failure. *Liver Transplantation*. [Online] 23 (10), 1325–1327. Available from: doi:10.1002/lt.24809.

O'Grady, J.G., Alexander, G.J., Hayllar, K.M. & Williams, R. (1989) Early indicators of prognosis in fulminant hepatic failure. *YGAST*. 97 (2), 439–445.

O'Leary, J.G., Bajaj, J.S., Tandon, P., Biggins, S.W., et al. (2019) Outcomes After Listing for Liver Transplant in Patients With Acute-on-Chronic Liver Failure: The Multicenter North American Consortium for the Study of End-Stage Liver Disease Experience. *Liver Transplantation*. [Online] 25 (4), 571–579. Available from: doi:10.1002/lt.25426.

O'Leary, J.G., Reddy, K.R., Wong, F., Kamath, P.S., et al. (2015) Long-term Use of Antibiotics and Proton Pump Inhibitors Predict Development of Infections in Patients With Cirrhosis. *Clinical Gastroenterology and Hepatology*. [Online] 13 (4), 753-759.e2. Available from: doi:10.1016/j.cgh.2014.07.060.

Olson, J.C. (2019) Acute-on-chronic liver failure: management and prognosis. *Current Opinion in Critical Care*. [Online] 25 (2), 165–170. Available from: doi:10.1097/MCC.0000000000000595.

Orme, J.J., Du, Y., Vanarsa, K., Mayeux, J., et al. (2016) Heightened cleavage of Axl receptor tyrosine kinase by ADAM metalloproteases may contribute to disease pathogenesis in SLE. *Clinical Immunology*. [Online] 169, 58–68. Available from: doi:10.1016/j.clim.2016.05.011.

Ortega-Gómez, A., Perretti, M. & Soehnlein, O. (2013) Resolution of inflammation: an integrated view. *EMBO molecular medicine*. [Online] 5 (5), 661–674. Available from: doi:10.1002/emmm.201202382.

Oweira, H., Sadeghi, M., Volker, D., Mieth, M., et al. (2018) Serum Caspase-Cleaved Cytokeratin (M30) Indicates Severity of Liver Dysfunction and Predicts Liver Outcome. *Annals of Transplantation*. [Online] 23, 393–400. Available from: doi:10.12659/AOT.908031.

Pan, T., Zhou, T., Li, L., Liu, Z., et al. (2017) Monocyte programmed death ligand-1 expression is an early marker for predicting infectious complications in acute pancreatitis. *Critical Care*. [Online] 21 (1), 186. Available from: doi:10.1186/s13054-017-1781-3.

Panasiuk, A. (2005) Phagocytic and oxidative burst activity of neutrophils in the end stage of liver cirrhosis. *World Journal of Gastroenterology*. [Online] 11 (48), 7661. Available from: doi:10.3748/wjg.v11.i48.7661.

Panasiuk, A., Wysocka, J., Maciorkowska, E., Panasiuk, B., et al. (2005a) Phagocytic and oxidative burst activity of neutrophils in the end stage of liver cirrhosis. *World Journal of Gastroenterology*. [Online] 11 (48), 7661–7665. Available from: doi:10.3748/wjg.v11.i48.7661.

Panasiuk, A., Wysocka, J., Maciorkowska, E., Panasiuk, B., et al. (2005b) Phagocytic and oxidative burst activity of neutrophils in the end stage of liver cirrhosis. *World Journal of Gastroenterology*. [Online] 11 (48), 7661–7665. Available from: doi:10.3748/wjg.v11.i48.7661.

Park, H.-J., Baen, J.-Y., Lee, Y.-J., Choi, Y.-H., et al. (2012) The TAM-family receptor Mer mediates production of HGF through the RhoA-dependent pathway in response to apoptotic cells. *Molecular biology of the cell*. [Online] 23 (16), 3254–3265. Available from: doi:10.1091/mbc.E12-01-0029.

Pastore, M., Di Maira, G., Caligiuri, A., Petta, S., et al. (2018) Role of the protein tyrosine kinase Mer (MerTK) in the cross-talk between macrophages and hepatic stellate cells. *Journal of Hepatology*. [Online] 68, S407–S408. Available from: doi:10.1016/S0168-8278(18)31052-3.

Patel, V., Mcphail, M.J.W., Zamalloa, A., Støy, S., et al. (2018) Results of a placebo-controlled double blind randomised trial to investigate the efficacy of rifaximin-alpha versus placebo in improving systemic inflammation in patients with cirrhosis and chronic hepatic encephalopathy (RIFSYS Trial). *Journal of Hepatology*. [Online] 68, S107–S108. Available from: doi:10.1016/S0168-8278(18)30432-X.

Pearlman, D.S. (1999) Pathophysiology of the inflammatory response. *Journal of Allergy and Clinical Immunology*. [Online] 104 (4), s132–s137. Available from: doi:10.1016/S0091-6749(99)70308-8.

Peng, S., Sun, M., Sun, X., Wang, X., et al. (2018) Plasma levels of TAM receptors and ligands in severe preeclampsia. *Pregnancy Hypertension*. [Online] 13, 116–120. Available from: doi:10.1016/j.preghy.2018.05.012.

Peranzoni, E., Zilio, S., Marigo, I., Dolcetti, L., et al. (2010) Myeloid-derived suppressor cell heterogeneity and subset definition. *Current opinion in immunology*. [Online] 22 (2), 238–244. Available from: doi:10.1016/j.coi.2010.01.021.

Perea, L., Coll, M., Sanjurjo, L., Blaya, D., et al. (2017) Pentraxin-3 modulates lipopolysaccharide-induced inflammatory response and attenuates liver injury: Perea et al. *Hepatology*. [Online] 66 (3), 953–968. Available from: doi:10.1002/hep.29215.

Piano, S., Brocca, A., Mareso, S. & Angeli, P. (2018) Infections complicating cirrhosis. *Liver International*. [Online] 38 Suppl 1, 126–133. Available from: doi:10.1111/liv.13645.

Piano, S., Singh, V., Caraceni, P., Maiwall, R., et al. (2019) Epidemiology and Effects of Bacterial Infections in Patients With Cirrhosis Worldwide. *Gastroenterology*. [Online] 156 (5), 1368-1380.e10. Available from: doi:10.1053/j.gastro.2018.12.005.

Piano, S., Tonon, M., Vettore, E., Stanco, M., et al. (2017) Incidence, predictors and outcomes of acute-on-chronic liver failure in outpatients with cirrhosis. *Journal of Hepatology*. [Online] 67 (6), 1177–1184. Available from: doi:10.1016/j.jhep.2017.07.008.

Pillarisetty, V.G., Shah, A.B., Miller, G., Bleier, J.I., et al. (2004) Liver Dendritic Cells Are Less Immunogenic Than Spleen Dendritic Cells because of Differences in Subtype Composition. *The Journal of Immunology*. [Online] 172 (2), 1009–1017. Available from: doi:10.4049/jimmunol.172.2.1009.

Pinzani, M. & Macias-Barragan, J. (2010) Update on the pathophysiology of liver fibrosis. *Expert Review of Gastroenterology & Hepatology*. [Online] 4 (4), 459–472. Available from: doi:10.1586/egh.10.47.

Pinzello, G., Pinzello, G., Simonetti, R.G., Simonetti, R.G., et al. (1983) Spontaneous bacterial peritonitis: a prospective investigation in predominantly nonalcoholic cirrhotic patients. *Hepatology*. 3 (4), 545–549.

Polson, J. & Lee, W.M. (2005) AASLD position paper: The management of acute liver failure. *Hepatology*. [Online] 41 (5), 1179–1197. Available from: doi:10.1148/radiology.202.2.9015061.

Pugh, R.N.H., Murray-Lyon, I.M., Dawson, J.L., Pietroni, M.C., et al. (1973) Transection of the oesophagus for bleeding oesophageal varices. *British Journal of Surgery*. [Online] 60 (8), 646–649. Available from: doi:10.1002/bjs.1800600817.

Pulanco, M.C., Cosman, J., Ho, M.-M., Huynh, J., et al. (2017) Complement Protein C1q Enhances Macrophage Foam Cell Survival and Efferocytosis. *The Journal of Immunology*. [Online] 198 (1), 472–480. Available from: doi:10.4049/jimmunol.1601445.

Putignano, A. & Gustot, T. (2017) New concepts in acute-on-chronic liver failure: Implications for liver transplantation. *Liver transplantation : official publication of the American Association for the Study of Liver Diseases and the International Liver Transplantation Society*. [Online] 23 (2), 234–243. Available from: doi:10.1002/lt.24654.

Qi, N., Liu, P., Zhang, Y., Wu, H., et al. (2013) Development of a Spontaneous Liver Disease Resembling Autoimmune Hepatitis in Mice Lacking Tyro3, Axl and Mer Receptor Tyrosine Kinases David L. Boone (ed.). *PLoS ONE*. [Online] 8 (6), e66604. Available from: doi:10.1371/journal.pone.0066604.

Rainer, F., Horvath, A., Sandahl, T.D., Leber, B., et al. (2018) Soluble CD163 and soluble mannose receptor predict survival and decompensation in patients with liver cirrhosis, and correlate with gut permeability and bacterial translocation. *Alimentary Pharmacology & Therapeutics*. [Online] 47 (5), 657–664. Available from: doi:10.1111/apt.14474.

Rajaram, P. & Subramanian, R.M. (2018) *Adding to the Repertoire of Scoring Systems in Acute-on-Chronic Liver Failure: Will Simplicity Be Outdone by Complexity?* 2.

Randolph, G.J. (1998) Differentiation of Monocytes into Dendritic Cells in a Model of Transendothelial Trafficking. *Science*. [Online] 282 (5388), 480–483. Available from: doi:10.1126/science.282.5388.480.

Reddy, K.R., O'Leary, J.G., Kamath, P.S., Fallon, M.B., et al. (2015) High risk of delisting or death in liver transplant candidates following infections: Results from the North American consortium for the study of end-stage liver disease: Delisting or Death Following Infections. *Liver Transplantation*. [Online] 21 (7), 881–888. Available from: doi:10.1002/lt.24139.

Rimola, A., García-Tsao, G., Navasa, M., Piddock, L.J.V., et al. (2000) Diagnosis, treatment and prophylaxis of spontaneous bacterial peritonitis: a consensus document. *Journal of Hepatology*. [Online] 32 (1), 142–153. Available from: doi:10.1016/S0168-8278(00)80201-9.

Rolando, N., Wade, J.J., Stangou, A., Gimson, A.E.S., et al. (1996) Prospective study comparing the efficacy of prophylactic parenteral antimicrobials, with or without enteral decontamination, in patients with acute liver failure. *Liver Transplantation and Surgery*. [Online] 2 (1), 8–13. Available from: doi:10.1002/lt.500020103.

Rosciszewski, G., Cadena, V., Murta, V., Lukin, J., et al. (2017) Toll-Like Receptor 4 (TLR4) and Triggering Receptor Expressed on Myeloid Cells-2 (TREM-2) Activation Balance Astrocyte Polarization into a Proinflammatory Phenotype. *Molecular Neurobiology*. [Online] Available from: doi:10.1007/s12035-017-0618-z [Accessed: 31 May 2019].

Rostkowska, K.A., Szymanek-Pasternak, A. & Simon, K.A. (2018) Spontaneous bacterial peritonitis – therapeutic challenges in the era of increasing drug resistance of bacteria. *Clinical and Experimental Hepatology*. [Online] 4 (4), 224–231. Available from: doi:10.5114/ceh.2018.80123.

Rothbauer, M., Zirath, H. & Ertl, P. (2018) Recent advances in microfluidic technologies for cell-to-cell interaction studies. *Lab on a Chip*. [Online] 18 (2), 249–270. Available from: doi:10.1039/C7LC00815E.

Rothlin, C.V., Carrera-Silva, E.A., Bosurgi, L. & Ghosh, S. (2015) TAM Receptor Signaling in Immune Homeostasis. *Annual review of immunology*. [Online] Available from: doi:10.1146/annurev-immunol-032414-112103.

Rothlin, C.V., Ghosh, S., Zuniga, E.I., Oldstone, M.B.A., et al. (2007) TAM Receptors Are Pleiotropic Inhibitors of the Innate Immune Response. *Cell*. [Online] 131 (6), 1124–1136. Available from: doi:10.1016/j.cell.2007.10.034.

Rothlin, C.V. & Lemke, G. (2010) TAM receptor signaling and autoimmune disease. *Current opinion in immunology*. [Online] 22 (6), 740–746. Available from: doi:10.1016/j.coi.2010.10.001.

Ruiz, J., Kanagavelu, S., Flores, C., Romero, L., et al. (2016) Systemic Activation of TLR3-Dependent TRIF Signaling Confers Host Defense against Gram-Negative Bacteria in the Intestine. *Frontiers in Cellular and Infection Microbiology*. [Online] 5, 20431–11. Available from: doi:10.3389/fcimb.2015.00105.

Ruiz-Alcaraz, A.J., Carmona-Martínez, V., Tristán-Manzano, M., Machado-Linde, F., et al. (2018) Characterization of human peritoneal monocyte/macrophage subsets in homeostasis: Phenotype, GATA6, phagocytic/oxidative activities and cytokines expression. *Scientific Reports*. [Online] 8 (1), 12794. Available from: doi:10.1038/s41598-018-30787-x.

Ruiz-del-Arbol, L., Urman, J., Fernandez, J., González, M., et al. (2003) Systemic, renal, and hepatic hemodynamic derangement in cirrhotic patients with spontaneous bacterial peritonitis. *Hepatology*. [Online] 38 (5), 1210–1218. Available from: doi:10.1053/jhep.2003.50447.

Runyon, B.A. (1986) *Low-protein-concentration ascitic fluid is predisposed to spontaneous bacterial peritonitis*. [Online]. Gastroenterology. Available from: http://scholar.google.com/scholar?q=related:8cWwbHL_upYJ:scholar.google.com/&hl=en&num=20&as_sdt=0,5.

Runyon, B.A. (2012) *Management of Adult Patients with Ascites Due to Cirrhosis: Update 2012*. 96.

Runyon, B.A. (1988) Patients with deficient ascitic fluid opsonic activity are predisposed to spontaneous bacterial peritonitis. *Hepatology*. 8 (3), 632–635.

Saraiva, M. & O'Garra, A. (2010) The regulation of IL-10 production by immune cells. *Nature Reviews Immunology*. [Online] 10 (3), 170–181. Available from: doi:10.1038/nri2711.

Sarang, Z., Joós, G., Garabuczi, É., Rühl, R., et al. (2014) Macrophages engulfing apoptotic cells produce nonclassical retinoids to enhance their phagocytic capacity. *The Journal of Immunology*. [Online] 192 (12), 5730–5738. Available from: doi:10.4049/jimmunol.1400284.

Sargenti, K., Johansson, Å., Bertilsson, S., Mattsby-Baltzer, I., et al. (2016) Dysfunction of Circulating Polymorphonuclear Leukocytes and Monocytes in Ambulatory Cirrhotics Predicts Patient Outcome. *Digestive diseases and sciences*. [Online] Available from: doi:10.1007/s10620-016-4132-3.

Sargenti, K., Prytz, H., Nilsson, E. & Kalaitzakis, E. (2015) Predictors of mortality among patients with compensated and decompensated liver cirrhosis: the role of bacterial infections and infection-related acute-on-chronic liver failure. *Scandinavian Journal of Gastroenterology*. [Online] 50 (7), 875–883. Available from: doi:10.3109/00365521.2015.1017834.

Sather, S., Kenyon, K.D., Kenyon, K.D., Lefkowitz, J.B., et al. (2007) A soluble form of the Mer receptor tyrosine kinase inhibits macrophage clearance of apoptotic cells and platelet aggregation. *Blood*. [Online] 109 (3), 1026–1033. Available from: doi:10.1182/blood-2006-05-021634.

Sato, S., St-Pierre, C., Bhaumik, P. & Nieminen, J. (2009) Galectins in innate immunity: dual functions of host soluble β-galactoside-binding lectins as damage-associated molecular patterns (DAMPs) and as receptors for pathogen-associated molecular patterns (PAMPs). *Immunological Reviews*. [Online] 230 (1), 172–187. Available from: doi:10.1111/j.1600-065X.2009.00790.x.

Satsangi, S., Duseja, A., Sachdeva, M., Tomer, S., et al. (2018) Monocyte human leukocyte antigen - Antigen D related, neutrophil oxidative burst and cytokine analysis in patients of decompensated cirrhosis with and without acute-on chronic liver failure. *PLoS ONE*. [Online] 13 (7), e0200644. Available from: doi:10.1371/journal.pone.0200644.

Schlegel, J., Sambade, M.J., Sather, S., Moschos, S.J., et al. (2013) MERTK receptor tyrosine kinase is a therapeutic target in melanoma. *Journal of Clinical Investigation*. [Online] 123 (5), 2257–2267. Available from: doi:10.1172/JCI67816.

Schott, J., Reitter, S., Philipp, J., Haneke, K., et al. (2014) Translational Regulation of Specific mRNAs Controls Feedback Inhibition and Survival during Macrophage Activation Christine A. Wells (ed.). *PLoS Genetics*. [Online] 10 (6), e1004368. Available from: doi:10.1371/journal.pgen.1004368.

Schuppan, D. & Afdhal, N.H. (2008) Liver cirrhosis. *Lancet*. [Online] 371 (9615), 838–851. Available from: doi:10.1016/S0140-6736(08)60383-9.

Scott, R.S., Scott, R.S., McMahon, E.J., McMahon, E.J., et al. (2001) Phagocytosis and clearance of apoptotic cells is mediated by MER. *Nature*. [Online] 411 (6834), 207–211. Available from: doi:10.1038/35075603.

Seitz, H.M., Camenisch, T.D., Lemke, G., Earp, H.S., et al. (2007) Macrophages and Dendritic Cells Use Different Axl/Mertk/Tyro3 Receptors in Clearance of Apoptotic Cells. *The Journal of Immunology*. [Online] 178 (9), 5635–5642. Available from: doi:10.4049/jimmunol.178.9.5635.

Seki, S., Seki, S., Osada, S., Osada, S., et al. (1998) Role of liver NK cells and peritoneal macrophages in gamma interferon and interleukin-10 production in experimental bacterial peritonitis in mice. *Infection and Immunity*. 66 (11), 5286–5294.

Selvapatt, N., Singanayagam, A., Wendon, J. & Antoniades, C.G. (2014) Understanding infection susceptibility in patients with acute-on-chronic liver failure. *Intensive care medicine*. [Online] Available from: doi:10.1007/s00134-014-3349-x.

Sen, P., Wallet, M.A., Yi, Z., Huang, Y., et al. (2007) Apoptotic cells induce Mer tyrosine kinase-dependent blockade of NF- B activation in dendritic cells. *Blood*. [Online] 109 (2), 653–660. Available from: doi:10.1182/blood-2006-04-017368.

Senzolo, M., Cholongitas, E., Burra, P., Leandro, G., et al. (2009) beta-Blockers protect against spontaneous bacterial peritonitis in cirrhotic patients: a meta-analysis. *Liver International*. [Online] 29 (8), 1189–1193. Available from: doi:10.1111/j.1478-3231.2009.02038.x.

Sersté, T., Bert, F., Leflon-Guibout, V., Chauvet, C., et al. (2011) Detection of bacterial DNA in serum and ascitic fluid of asymptomatic outpatients with cirrhosis and non-neutrocytic ascites: BactDNA in ascites of asymptomatic outpatients. *Liver International*. [Online] 31 (4), 494–498. Available from: doi:10.1111/j.1478-3231.2011.02448.x.

Shahrara, S., Pickens, S.R., Dorfleutner, A. & Pope, R.M. (2009) IL-17 Induces Monocyte Migration in Rheumatoid Arthritis. *The Journal of Immunology*. [Online] 182 (6), 3884–3891. Available from: doi:10.4049/jimmunol.0802246.

Shalimar, Rout, G., Jadaun, S.S., Ranjan, G., et al. (2018) Prevalence, predictors and impact of bacterial infection in acute on chronic liver failure patients. *Digestive and liver disease : official journal of the Italian Society of Gastroenterology and the Italian Association for the Study of the Liver*. [Online] Available from: doi:10.1016/j.dld.2018.05.013.

Shapouri-Moghaddam, A., Mohammadian, S., Vazini, H., Taghadosi, M., et al. (2018) Macrophage plasticity, polarization, and function in health and disease. *Journal of Cellular Physiology*. [Online] 233 (9), 6425–6440. Available from: doi:10.1002/jcp.26429.

Shawcross, D.L., Wright, G.A.K., Stadlbauer, V., Hodges, S.J., et al. (2008) Ammonia impairs neutrophil phagocytic function in liver disease. *Hepatology*. [Online] 48 (4), 1202–1212. Available from: doi:10.1002/hep.22474.

Shetty, S., Lalor, P.F. & Adams, D.H. (2018) Liver sinusoidal endothelial cells — gatekeepers of hepatic immunity. *Nature Reviews Gastroenterology & Hepatology*. [Online] 15 (9), 555–567. Available from: doi:10.1038/s41575-018-0020-y.

Shetty, S., Weston, C.J., Adams, D.H. & Lalor, P.F. (2014) A Flow Adhesion Assay to Study Leucocyte Recruitment to Human Hepatic Sinusoidal Endothelium Under Conditions of Shear Stress. *Journal of Visualized Experiments*. [Online] (85), 51330. Available from: doi:10.3791/51330.

Shi, C. & Pamer, E.G. (2011) Monocyte recruitment during infection and inflammation. *Nature Reviews Immunology*. [Online] 11 (11), 762–774. Available from: doi:10.1038/nri3070.

Shibata, T. & Ato, M. (2017) A critical role of Gas6/Axl signal in allergic airway responses during RSV vaccine-enhanced disease. *Immunology and Cell Biology*. [Online] 95 (10), 906–915. Available from: doi:10.1038/icb.2017.61.

Shibata, T., Shibata, T., Habiel, D.M., Habiel, D.M., et al. (2014) Axl Receptor Blockade Protects from Invasive Pulmonary Aspergillosis in Mice. *The Journal of Immunology*. [Online] Available from: doi:10.4049/jimmunol.1401258.

Shimojima, M., Ikeda, Y. & Kawaoka, Y. (2007) The Mechanism of Axl-Mediated Ebola Virus Infection. *The Journal of Infectious Diseases*. [Online] 196 (s2), S259–S263. Available from: doi:10.1086/520594.

Shreiner, A.B., Kao, J.Y. & Young, V.B. (2015) The gut microbiome in health and in disease: *Current Opinion in Gastroenterology*. [Online] 31 (1), 69–75. Available from: doi:10.1097/MOG.0000000000000139.

Sica, A., Invernizzi, P. & Mantovani, A. (2013) Macrophage plasticity and polarization in liver homeostasis and pathology. *Hepatology*. [Online] 59 (5), 2034–2042. Available from: doi:10.1002/hep.26754.

Sica, A. & Mantovani, A. (2012) Macrophage plasticity and polarization: in vivo veritas. *Journal of Clinical Investigation*. [Online] 122 (3), 787–795. Available from: doi:10.1172/JCI59643.

Singh, S., D'mello, V., Henegouwen, P. van B. en & Birge, R.B. (2007) A NPxY-independent β5 integrin activation signal regulates phagocytosis of apoptotic cells. *Biochemical and Biophysical Research Communications*. [Online] 364 (3), 540–548. Available from: doi:10.1016/j.bbrc.2007.10.049.

Soehnlein, O. & Lindbom, L. (2010) Phagocyte partnership during the onset and resolution of inflammation. *Nature Reviews Immunology*. [Online] 10 (6), 427–439. Available from: doi:10.1038/nri2779.

Solt, L.A., Kamenecka, T.M. & Burris, T.P. (2012) LXR-mediated inhibition of CD4+ T helper cells. *PLoS ONE*. [Online] 7 (9), e46615. Available from: doi:10.1371/journal.pone.0046615.

Song, K.S., Park, Y.S. & Kim, H.K. (2000) Prevalence of anti-protein S antibodies in patients with systemic lupus erythematosus. *Arthritis & Rheumatism*. 43, 557–560.

Struecker, B., Raschzok, N. & Sauer, I.M. (2014) Liver support strategies: cutting-edge technologies. *Nature Reviews Gastroenterology & Hepatology*. [Online] 11 (3), 166–176. Available from: doi:10.1038/nrgastro.2013.204.

Subramanian, A., Tamayo, P., Mootha, V.K., Mukherjee, S., et al. (2005) Gene set enrichment analysis: A knowledge-based approach for interpreting genome-wide expression profiles. *Proceedings of the National Academy of Sciences*. [Online] 102 (43), 15545–15550. Available from: doi:10.1073/pnas.0506580102.

Sufit, A., Lee-Sherick, A.B., DeRyckere, D., Rupji, M., et al. (2016) MERTK Inhibition Induces Polyploidy and Promotes Cell Death and Cellular Senescence in Glioblastoma Multiforme Maria G Castro (ed.). *PLOS ONE*. [Online] 11 (10), e0165107. Available from: doi:10.1371/journal.pone.0165107.

Tacke, F. (2012) Functional role of intrahepatic monocyte subsets for the progression of liver inflammation and liver fibrosis in vivo. *Fibrogenesis & Tissue Repair*. [Online] 5 (S1), S27. Available from: doi:10.1186/1755-1536-5-S1-S27.

Tacke, F. & Zimmermann, H.W. (2014) Macrophage heterogeneity in liver injury and fibrosis. *Journal of Hepatology*. [Online] 60 (5), 1090–1096. Available from: doi:10.1016/j.jhep.2013.12.025.

Tang, Y., Wu, S., Liu, Q., Xie, J., et al. (2015) Mertk Deficiency Affects Macrophage Directional Migration via Disruption of Cytoskeletal Organization Alissa M Weaver (ed.). *PLoS ONE*. [Online] 10 (1), e0117787. Available from: doi:10.1371/journal.pone.0117787.g005.

Tan-Garcia, A., Wai, L.-E., Zheng, D., Ceccarello, E., et al. (2017) Intrahepatic CD206+ macrophages contribute to inflammation in advanced viral-related liver disease. *Journal of hepatology*. [Online] 67 (3), 490–500. Available from: doi:10.1016/j.jhep.2017.04.023.

Tapper, E.B. & Parikh, N.D. (2018) Mortality due to cirrhosis and liver cancer in the United States, 1999-2016: observational study. *BMJ*. [Online] k2817. Available from: doi:10.1136/bmj.k2817.

Tauber, A.I. (2003) Metchnikoff and the phagocytosis theory. *Nature Reviews: Molecular Cell Biology*. [Online] 4 (11), 897–901. Available from: doi:10.1038/nrm1244.

Taylor, J.V., Gordon, L.E. & Polk, H.C. (2000) Early decrease in surface expression of HLA-DQ predicts the development of infection in trauma patients. *Clinical and Experimental Immunology*. [Online] 122 (3), 308–311. Available from: doi:10.1046/j.1365-2249.2000.01397.x.

Terg, R., Casciato, P., Garbe, C., Cartier, M., et al. (2015) Proton pump inhibitor therapy does not increase the incidence of spontaneous bacterial peritonitis in cirrhosis: a multicenter prospective study. *Journal of Hepatology*. [Online] 62 (5), 1056–1060. Available from: doi:10.1016/j.jhep.2014.11.036.

Thaler, B., Hohensinner, P.J., Krychtiuk, K.A., Matzneller, P., et al. (2016) Differential in vivo activation of monocyte subsets during low-grade inflammation through experimental endotoxemia in humans. *Scientific Reports*. [Online] 6 (1), 30162. Available from: doi:10.1038/srep30162.

Thielens, N.M., Tedesco, F., Bohlson, S.S., Gaboriaud, C., et al. (2017) C1q: A fresh look upon an old molecule. *Molecular Immunology*. [Online] 89, 73–83. Available from: doi:10.1016/j.molimm.2017.05.025.

Thomas, G., Tacke, R., Hedrick, C.C. & Hanna, R.N. (2015) Nonclassical Patrolling Monocyte Function in the Vasculature. *Arteriosclerosis, Thrombosis, and Vascular Biology*. [Online] 35 (6), 1306–1316. Available from: doi:10.1161/ATVBAHA.114.304650.

Thorp, E., Vaisar, T., Subramanian, M., Mautner, L., et al. (2011) Shedding of the Mer Tyrosine Kinase Receptor Is Mediated by ADAM17 Protein through a Pathway Involving Reactive Oxygen Species, Protein Kinase Cδ, and p38 Mitogen-activated Protein Kinase (MAPK). *Journal of Biological Chemistry*. [Online] 286 (38), 33335–33344. Available from: doi:10.1074/jbc.M111.263020.

Tian, J., Yang, G., Chen, H.-Y., Hsu, D.K., et al. (2016) Galectin-3 regulates inflammasome activation in cholestatic liver injury. *The FASEB Journal*. [Online] 30 (12), 4202–4213. Available from: doi:10.1096/fj.201600392RR.

Titó, L., Rimola, A., Gines, P., Llach, J., et al. (1988) Recurrence of spontaneous bacterial peritonitis in cirrhosis: frequency and predictive factors. *Hepatology*. 8 (1), 27–31.

Tognarelli, J.M., Dawood, M., Shariff, M.I.F., Grover, V.P.B., et al. (2015) Magnetic Resonance Spectroscopy: Principles and Techniques: Lessons for Clinicians. *Journal of Clinical and Experimental Hepatology*. [Online] 5 (4), 320–328. Available from: doi:10.1016/j.jceh.2015.10.006.

Tornai, T., Vitalis, Z., Sipeki, N., Dinya, T., et al. (2016) Macrophage activation marker, soluble CD163, is an independent predictor of short-term mortality in patients with cirrhosis and bacterial infection. *Liver International*. [Online] 36 (11), 1628–1638. Available from: doi:10.1111/liv.13133.

Triantafyllou, E., Pop, O.T., Possamai, L.A., Wilhelm, A., et al. (2018a) MerTK expressing hepatic macrophages promote the resolution of inflammation in acute liver failure. *Gut*. [Online] 67 (2), 333–347. Available from: doi:10.1136/gutjnl-2016-313615.

Triantafyllou, E., Woollard, K.J., McPhail, M.J.W., Antoniades, C.G., et al. (2018b) The Role of Monocytes and Macrophages in Acute and Acute-on-Chronic Liver Failure. *Frontiers in Immunology*. [Online] 9, 2948. Available from: doi:10.3389/fimmu.2018.02948.

Tritto, G., Bechlis, Z., Stadlbauer, V., Davies, N., et al. (2011) Evidence of neutrophil functional defect despite inflammation in stable cirrhosis. *Journal of Hepatology*. [Online] 55 (3), 574–581. Available from: doi:10.1016/j.jhep.2010.11.034.

Tsiaoussis, G.I. (2015) Intestinal barrier dysfunction in cirrhosis: Current concepts in pathophysiology and clinical implications. *World Journal of Hepatology*. [Online] 7 (17), 2058. Available from: doi:10.4254/wjh.v7.i17.2058.

Turnbull, I.R., Gilfillan, S., Cella, M., Aoshi, T., et al. (2006) Cutting Edge: TREM-2 Attenuates Macrophage Activation. *The Journal of Immunology*. [Online] 177 (6), 3520–3524. Available from: doi:10.4049/jimmunol.177.6.3520.

Turner, M.D., Nedjai, B., Hurst, T. & Pennington, D.J. (2014) Cytokines and chemokines: At the crossroads of cell signalling and inflammatory disease. *Biochimica et Biophysica Acta (BBA) - Molecular Cell Research*. [Online] 1843 (11), 2563–2582. Available from: doi:10.1016/j.bbamcr.2014.05.014.

Tworkoski, K.A., Platt, J.T., Bacchiocchi, A., Bosenberg, M., et al. (2013) MERTK controls melanoma cell migration and survival and differentially regulates cell behavior relative to AXL. *Pigment Cell & Melanoma Research*. [Online] 26 (4), 527–541. Available from: doi:10.1111/pcmr.12110.

Verbeke, L., Nevens, F. & Laleman, W. (2011) Bench-to-beside review: acute-on-chronic liver failure - linking the gut, liver and systemic circulation. *Critical care (London, England)*. [Online] 15 (5), 233. Available from: doi:10.1186/cc10424.

Vergis, N., Khamri, W., Beale, K., Beale, K., et al. (2016) Defective monocyte oxidative burst predicts infection in alcoholic hepatitis and is associated with reduced expression of NADPH oxidase. *Gut*. [Online] Available from: doi:10.1136/gutjnl-2015-310378.

Viaud, M., Ivanov, S., Vujic, N., Duta-Mare, M., et al. (2018) Lysosomal Cholesterol Hydrolysis Couples Efferocytosis to Anti-Inflammatory Oxysterol Production. *Circulation Research*. [Online] 122 (10), 1369–1384. Available from: doi:10.1161/CIRCRESAHA.117.312333.

Waidmann, O., Brunner, F., Herrmann, E., Zeuzem, S., et al. (2013) Macrophage activation is a prognostic parameter for variceal bleeding and overall survival in patients with liver cirrhosis. *Journal of Hepatology*. [Online] 58 (5), 956–961. Available from: doi:10.1016/j.jhep.2013.01.005.

Wallet, M.A., Sen, P., Flores, R.R., Wang, Y., et al. (2008) MerTK is required for apoptotic cell–induced T cell tolerance. *The Journal of Experimental Medicine*. [Online] 205 (1), 219–232. Available from: doi:10.1084/jem.20062293.

Wang, J. & Kubes, P. (2016) A Reservoir of Mature Cavity Macrophages that Can Rapidly Invade Visceral Organs to Affect Tissue Repair. *Cell*. [Online] 165 (3), 668–678. Available from: doi:10.1016/j.cell.2016.03.009.

Wang, J., Vasaikar, S., Shi, Z., Greer, M., et al. (2017) WebGestalt 2017: a more comprehensive, powerful, flexible and interactive gene set enrichment analysis toolkit. *Nucleic Acids Research*. [Online] 45 (W1), W130–W137. Available from: doi:10.1093/nar/gkx356.

Wang, X., Malawista, A., Qian, F., Ramsey, C., et al. (2018) Age-related changes in expression and signaling of TAM receptor inflammatory regulators in monocytes. *Oncotarget*. [Online] 9 (11), 9572–9580. Available from: doi:10.18632/oncotarget.23851.

Wang, Y., Moncayo, G., Morin, P., Xue, G., et al. (2013) Mer receptor tyrosine kinase promotes invasion and survival in glioblastoma multiforme. *Oncogene*. [Online] 32 (7), 872–882. Available from: doi:10.1038/onc.2012.104.

Ward, N.S., Casserly, B. & Ayala, A. (2008) The Compensatory Anti-inflammatory Response Syndrome (CARS) in Critically Ill Patients. *Clinics in Chest Medicine*. [Online] 29 (4), 617–625. Available from: doi:10.1016/j.ccm.2008.06.010.

Wasmuth, H.E., Kunz, D., Yagmur, E., Timmer-Stranghöner, A., et al. (2005) Patients with acute on chronic liver failure display 'sepsis-like' immune paralysis. *Journal of Hepatology*. [Online] 42 (2), 195–201. Available from: doi:10.1016/j.jhep.2004.10.019.

Weston, C.J., Zimmermann, H.W. & Adams, D.H. (2019) The Role of Myeloid-Derived Cells in the Progression of Liver Disease. *Frontiers in Immunology*. [Online] 10, 893. Available from: doi:10.3389/fimmu.2019.00893.

Wiesner, R., Edwards, E., Freeman, R., Harper, A., et al. (2003) Model for end-stage liver disease (MELD) and allocation of donor livers. *Gastroenterology*. [Online] 124 (1), 91–96. Available from: doi:10.1053/gast.2003.50016.

Wiest, R., Krag, A. & Gerbes, A. (2011) Spontaneous bacterial peritonitis: recent guidelines and beyond. *Gut*. [Online] 61 (2), 297–310. Available from: doi:10.1136/gutjnl-2011-300779.

Wiest, R., Lawson, M. & Geuking, M. (2014) Pathological bacterial translocation in liver cirrhosis. *Journal of Hepatology*. [Online] 60 (1), 197–209. Available from: doi:10.1016/j.jhep.2013.07.044.

Williams, B.J.C., Williams, B.J.C., Craven, R.R., Craven, R.R., et al. (2009) TAM receptors are dispensable in the phagocytosis and killing of bacteria. *Cellular Immunology*. [Online] 259 (2), 128–134. Available from: doi:10.1016/j.cellimm.2009.06.006.

Williams, R. & Horton, R. (2013) Liver disease in the UK: a Lancet Commission. *Lancet (London, England)*. [Online] 382 (9904), 1537–1538. Available from: doi:10.1016/S0140-6736(13)62152-2.

Witowski, J., Książek, K., Warnecke, C., Kuźlan, M., et al. (2007) Role of mesothelial cell-derived granulocyte colony-stimulating factor in interleukin-17-induced neutrophil accumulation in the peritoneum. *Kidney International*. [Online] 71 (6), 514–525. Available from: doi:10.1038/sj.ki.5002082.

Wong, K.L., Wong, K.L., Yeap, W.H., Yeap, W.H., et al. (2012) The three human monocyte subsets: implications for health and disease. *Immunologic Research*. [Online] 53 (1–3), 41–57. Available from: doi:10.1007/s12026-012-8297-3.

Woodhouse, C.A., Patel, V.C., Singanayagam, A. & Shawcross, D.L. (2017) Review article: the gut microbiome as a therapeutic target in the pathogenesis and treatment of chronic liver disease. *Alimentary Pharmacology and Therapeutics*. [Online] Available from: doi:10.1111/apt.14397.

Wu, L., Deng, Z., Peng, Y., Han, L., et al. (2017) Ascites-derived IL-6 and IL-10 synergistically expand CD14+HLA-DR-/low myeloid-derived suppressor cells in ovarian cancer patients. *Oncotarget*. [Online] 8 (44), 76843–76856. Available from: doi:10.18632/oncotarget.20164.

Wu, Y., Lan, C., Ren, D. & Chen, G.-Y. (2016) Induction of Siglec-1 by Endotoxin Tolerance Suppresses the Innate Immune Response by Promoting TGF-β1 Production. *Journal of Biological Chemistry*. [Online] 291 (23), 12370–12382. Available from: doi:10.1074/jbc.M116.721258.

Xie, S., Li, Y., Li, X., Wang, L., et al. (2015) Mer receptor tyrosine kinase is frequently overexpressed in human non-small cell lung cancer, confirming resistance to erlotinib. *Oncotarget*. 6 (11), 14.

Xing, X., Yang, J., Yang, X., Wei, Y., et al. (2013) IL-17A Induces Endothelial Inflammation in Systemic Sclerosis via the ERK Signaling Pathway Shervin Assassi (ed.). *PLoS ONE*. [Online] 8 (12), e85032. Available from: doi:10.1371/journal.pone.0085032.

Xu, L., Hu, F., Zhu, H., Liu, X., et al. (2018) Soluble TAM receptor tyrosine kinases in rheumatoid arthritis: correlation with disease activity and bone destruction: sTAM in RA. *Clinical & Experimental Immunology*. [Online] 192 (1), 95–103. Available from: doi:10.1111/cei.13082.

Xue, J., Schmidt, S.V., Sander, J., Draffehn, A., et al. (2014) Transcriptome-Based Network Analysis Reveals a Spectrum Model of Human Macrophage Activation. *Immunity*. [Online] 40 (2), 274–288. Available from: doi:10.1016/j.immuni.2014.01.006.

Yona, S., Kim, K.-W., Wolf, Y., Mildner, A., et al. (2013) Fate Mapping Reveals Origins and Dynamics of Monocytes and Tissue Macrophages under Homeostasis. *Immunity*. [Online] 38 (1), 79–91. Available from: doi:10.1016/j.immuni.2012.12.001.

Zagórska, A., Través, P.G., Lew, E.D., Dransfield, I., et al. (2014) Diversification of TAM receptor tyrosine kinase function. *Nature immunology*. [Online] 15 (10), 920–928. Available from: doi:10.1074/jbc.M205663200.

Zhang, B., Fang, L., Wu, H.-M., Ding, P.-S., et al. (2016) Mer receptor tyrosine kinase negatively regulates lipoteichoic acid-induced inflammatory response via PI3K/Akt and SOCS3. *Molecular immunology*. [Online] 76, 98–107. Available from: doi:10.1016/j.molimm.2016.06.016.

Zhang, B., Lu, H., Jiang, A., Wu, H., et al. (2019) MerTK Downregulates Lipopolysaccharide-Induced Inflammation Through SOCS1 Protein but Does Not Affect Phagocytosis of Escherichia coli in Macrophages. *Inflammation*. [Online] 42 (1), 113–123. Available from: doi:10.1007/s10753-018-0877-5.

Zhang, C., Tang, K., Zhang, Y., Ma, Y., et al. (2017) Elevated Plasma Growth Arrest-Specific 6 Protein Levels Are Associated with the Severity of Disease During Hantaan Virus Infection in Humans. *Viral Immunology*. [Online] 30 (5), 330–335. Available from: doi:10.1089/vim.2016.0137.

Zhen, Y., Priest, S.O. & Shao, W.-H. (2016) Opposing Roles of Tyrosine Kinase Receptors Mer and Axl Determine Clinical Outcomes in Experimental Immune-Mediated Nephritis. *The Journal of Immunology*. [Online] 197 (6), 2187–2194. Available from: doi:10.4049/jimmunol.1600793.

Zigmond, E., Zigmond, E., Samia-Grinberg, S., Samia-Grinberg, S., et al. (2014) Infiltrating monocyte-derived macrophages and resident kupffer cells display different ontogeny and functions in acute liver injury. *Journal of immunology (Baltimore, Md. : 1950)*. [Online] 193 (1), 344–353. Available from: doi:10.4049/jimmunol.1400574.

Zimmermann, H.W., Bruns, T. & Weston, C.J. (2016) Bidirectional transendothelial migration of monocytes across hepatic sinusoidal endothelium shapes monocyte differentiation and regulates the balance between …. …. [Online] Available from: doi:10.1002/hep.28285/suppinfo.

Zizzo, G. & Cohen, P.L. (2018) Antibody Cross-Linking of CD14 Activates MerTK and Promotes Human Macrophage Clearance of Apoptotic Neutrophils: the Dual Role of CD14 at the Crossroads Between M1 and M2c Polarization. *Inflammation*. [Online] Available from: doi:10.1007/s10753-018-0864-x.

Zizzo, G. & Cohen, P.L. (2013) IL-17 stimulates differentiation of human anti-inflammatory macrophages and phagocytosis of apoptotic neutrophils in response to IL-10 and glucocorticoids. *Journal of immunology (Baltimore, Md. : 1950)*. [Online] 190 (10), 5237–5246. Available from: doi:10.4049/jimmunol.1203017.

Zizzo, G., Hilliard, B.A., Monestier, M. & Cohen, P.L. (2012) Efficient clearance of early apoptotic cells by human macrophages requires M2c polarization and MerTK induction. *Journal of immunology (Baltimore, Md. : 1950)*. [Online] 189 (7), 3508–3520. Available from: doi:10.4049/jimmunol.1200662.

Zou, Z., Xu, D., Li, B., Xin, S., et al. (2009) Compartmentalization and its implication for peripheral immunologically-competent cells to the liver in patients with HBV-related acute-on-chronic liver failure. *Hepatology Research*. [Online] 39 (12), 1198–1207. Available from: doi:10.4049/jimmunol.174.2.1055.

Zwaveling, J.H., Maring, J.K., Klompmaker, I.J., Haagsma, E.B., et al. (2002) Selective decontamination of the digestive tract to prevent postoperative infection: A randomized placebo-controlled trial in liver transplant patients: *Critical Care Medicine*. [Online] 30 (6), 1204–1209. Available from: doi:10.1097/00003246-200206000-00004.

9. APPENDIX

Appendix A: Standard Monoclonal Antibody Panel for PBMC Immunophenotype

Antibody	Fluorochrome	Source	Host Species	Clone	Isotype	Volume (µl)
TUBE 1						
CD14	PE-Cy7	BD Biosciences	Mouse	MϕP-9	IgG_{2b} κ	1.5
CD16	APC-H7	BD Biosciences	Mouse	3G8	IgG_1 κ	1.5
HLA-DR	PerCP-Cy5.5	ThermoFisher	Mouse	LN3	IgG_{2b} κ	2.5
MerTK	APC	R&D	Mouse	125518	IgG_1	2.5
Axl	Alexa-Fluor 488	R&D	Mouse	108724	IgG_1	3
Tyro3	PE	R&D	Mouse	96201	IgG_1	5
CD11b	Brilliant Violet 421	BioLegend	Mouse	ICRF44	IgG_1	5
Fixable Viability Dye	eFluor 506	ThermoFisher	N/A	N/A	N/A	N/A
TUBE 2						
CD14	PE-Cy7	BD Biosciences	Mouse	MϕP-9	IgG_{2b} κ	1.5
CD16	APC-H7	BD Biosciences	Mouse	3G8	IgG_1 κ	1.5
HLA-DR	PerCP-Cy5.5	ThermoFisher	Mouse	LN3	IgG_{2b} κ	2.5
CCR2	Alexa Fluor 647	BD Biosciences	Mouse	48607	IgG_{2b}	4
Axl	Alexa Fluor 488	R&D	Mouse	108724	IgG_1	3
CCR7	PE	BD Biosciences	Mouse	2-L1-A	IgG_1 κ	3.5
CCR5	Brilliant Violet 421	BioLegend	Rat	J418F1	IgG_{2b} κ	4
Fixable Viability Dye	eFluor 506	ThermoFisher	N/A	N/A	N/A	N/A

Appendix B: Monoclonal Antibody Panel for FACS Sorting of PBMCs & ACs

Antibody	Fluorochrome	Source	Host Species	Clone	Isotype	Volume (µl)
CD14	PE-Cy7	BD Biosciences	Mouse	MϕP-9	IgG_{2b} κ	1.5
CD16	APC-H7	BD Biosciences	Mouse	3G8	IgG_1 κ	1.5
HLA-DR	PerCP-Cy5.5	ThermoFisher	Mouse	LN3	IgG_{2b} κ	2.5
MerTK	APC	R&D	Mouse	125518	IgG_1	2.5
CD11b	PE	BD Biosciences	Mouse	ICRF44	IgG_1 κ	3
CD64	Brilliant Violet 421	BioLegend	Mouse	10.1	IgG_1 κ	2.5
Fixable Viability Dye	eFluor 506	ThermoFisher	N/A	N/A	N/A	N/A

Appendix C: Standard Monoclonal Antibody Panel for AC Immunophenotyping

Antibody	Fluorochrome	Source	Host Species	Clone	Isotype	Volume (µl)
TUBE 1: TAM Receptors						
CD14	PE-Cy7	BD Biosciences	Mouse	MϕP-9	IgG_{2b} κ	1.5
CD16	APC-H7	BD Biosciences	Mouse	3G8	IgG_1 κ	1.5
HLA-DR	PerCP-Cy5.5	ThermoFisher	Mouse	LN3	IgG_{2b} κ	2.5
MerTK	APC	R&D	Mouse	125518	IgG_1	2.5
Axl	Alexa-Fluor 488	R&D	Mouse	108724	IgG_1	3
Tyro3	PE	R&D	Mouse	96201	IgG_1	5
CD11b	Brilliant Violet 421	BioLegend	Mouse	ICRF44	IgG_1	5
Fixable Viability Dye	eFluor 506	ThermoFisher	N/A	N/A	N/A	N/A
TUBE 2: Homing Markers						
CD14	PE-Cy7	BD Biosciences	Mouse	MϕP-9	IgG_{2b} κ	1.5
CD16	APC-H7	BD Biosciences	Mouse	3G8	IgG_1 κ	1.5
HLA-DR	PerCP-Cy5.5	ThermoFisher	Mouse	LN3	IgG_{2b} κ	2.5
CCR2	Alexa Fluor 647	BD Biosciences	Mouse	48607	IgG_{2b}	4
Axl	Alexa Fluor 488	R&D	Mouse	108724	IgG_1	3
CCR7	PE	BD Biosciences	Mouse	2-L1-A	IgG_1 κ	3.5
CCR5	Brilliant Violet 421	BioLegend	Rat	J418F1	IgG_{2b} κ	4
Fixable Viability Dye	eFluor 506	ThermoFisher	N/A	N/A	N/A	N/A
TUBE 3: M-MDSC						
CD14	PE-Cy7	BD Biosciences	Mouse	MϕP-9	IgG_{2b} κ	1.5
CD16	APC-H7	BD Biosciences	Mouse	3G8	IgG_1 κ	1.5
HLA-DR	PerCP-Cy5.5	ThermoFisher	Mouse	LN3	IgG_{2b} κ	2.5
MerTK	APC	R&D	Mouse	125518	IgG_1	2.5
CD15	FITC	BD Biosciences	Mouse	HI98	IgM κ	3
CD11b	PE	BD Biosciences	Mouse	ICRF44	IgG_1 κ	3
CD64	Brilliant Violet 421	BioLegend	Mouse	10.1	IgG_1 κ	2.5
CD33	Brilliant Violet 510	BioLegend	Mouse	P67.6	IgG_1 κ	2.5
TUBE 4: Neutrophils						
CD66b	PE-Cy7	ThermoFisher	Mouse	G10F5	IgM κ	1.5
CD16	APC-H7	BD Biosciences	Mouse	3G8	IgG_1 κ	1.5
HLA-DR	PerCP-Cy5.5	ThermoFisher	Mouse	LN3	IgG_{2b} κ	2.5
CD177	Alexa Fluor 647	BD Biosciences	Mouse	MEM-166	IgG_1 κ	3
CD15	FITC	BD Biosciences	Mouse	HI98	IgM κ	3
CD11b	PE	BD Biosciences	Mouse	ICRF44	IgG_1 κ	3
CD64	Brilliant Violet 421	BioLegend	Mouse	10.1	IgG_1 κ	2.5
Miscellaneous (replacing antibodies on other panels)						
CD163	PE	BD Biosciences	Mouse	GHI/61	IgG_1 κ	3.5
CX_3CR1	PE	ThermoFisher	Rat	2A9-1	IgG_{2b} κ	3.5
CD86	PE	BD Biosciences	Mouse	IT2.2	IgG_{2b} κ	3
CD32	FITC	BD Biosciences	Mouse	FLI8.26	IgG_{2b} κ	3
PD-1	FITC	BD Biosciences	Mouse	MIH4	IgG_1 κ	3
CD206	Brilliant Violet 421	BioLegend	Mouse	15-2	IgG_1 κ	3

Appendix D: Monoclonal Antibody Panel for Ovarian Cancer AC Immunophenotype

Antibody	Fluorochrome	Source	Host Species	Clone	Isotype	Volume (µl)
TUBE 1						
CD14	PE-Cy7	BD Biosciences	Mouse	MϕP-9	IgG_{2b} κ	1.5
CD16	APC-H7	BD Biosciences	Mouse	3G8	IgG_1 κ	1.5
HLA-DR	PerCP-Cy5.5	ThermoFisher	Mouse	LN3	IgG_{2b} κ	2.5
MerTK	APC	R&D	Mouse	125518	IgG_1	2.5
Axl	Alexa-Fluor 488	R&D	Mouse	108724	IgG_1	3
Tyro3	PE	R&D	Mouse	96201	IgG_1	5
CD64	Brilliant Violet 421	BioLegend	Mouse	10.1	IgG_1 κ	2.5
Fixable Viability Dye	eFluor 506	ThermoFisher	N/A	N/A	N/A	N/A
TUBE 2						
CD14	PE-Cy7	BD Biosciences	Mouse	MϕP-9	IgG_{2b} κ	1.5
CD16	APC-H7	BD Biosciences	Mouse	3G8	IgG_1 κ	1.5
HLA-DR	PerCP-Cy5.5	ThermoFisher	Mouse	LN3	IgG_{2b} κ	2.5
Tie-2	APC	R&D	Mouse	83715	IgG_1 κ	3
PD-1	FITC	BD Biosciences	Mouse	MIH4	IgG_1 κ	3
CD163	PE	BD Biosciences	Mouse	GHI/61	IgG_1 κ	3.5
CD206	Brilliant Violet 421	BioLegend	Mouse	15-2	IgG_1 κ	3
Fixable Viability Dye	eFluor 506	ThermoFisher	N/A	N/A	N/A	N/A

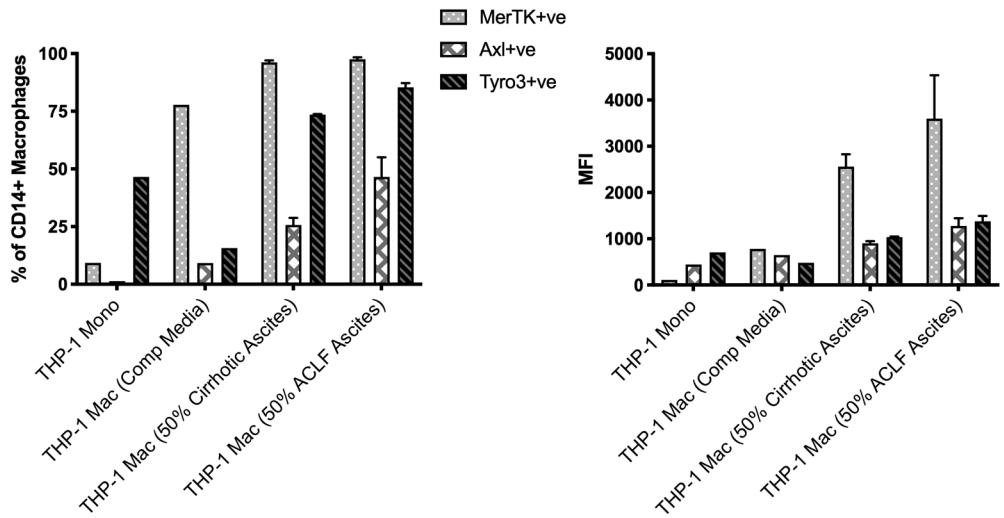
Appendix E: Absolute Count of MerTK+ and MerTK- after FACS Sorting

Cell Type	MerTK+	MerTK-
Ascitic Cells	220713	258649
	171696	73330
	428024	126328
	580882	204658
	54936	34565
	1897913	189193
	378709	390679
PBMC	64009	300947
	118763	200169
	99720	356157
Monocyte-derived Macrophages	497874	10441
	377697	287
	177965	3192

Appendix F: Antibody Panel for THP-1 Macrophages in Ascites Immunophenotyping

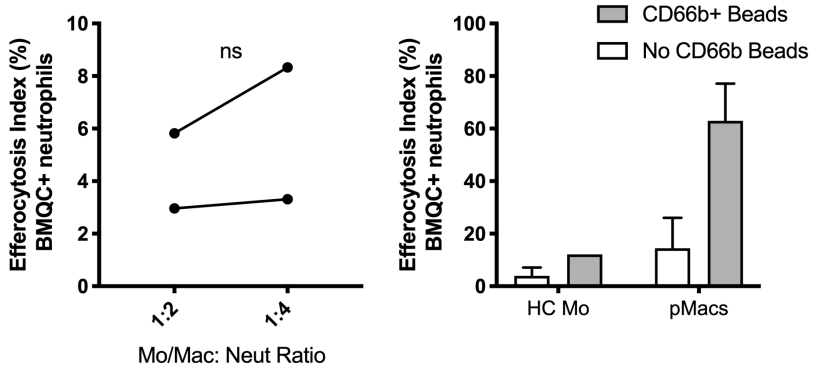
Antibody	Fluorochrome	Source	Host Species	Clone	Isotype	Volume (µl)
TUBE 1						
CD14	PE-Cy7	BD Biosciences	Mouse	MϕP-9	IgG_{2b} κ	1.5
CD16	APC-H7	BD Biosciences	Mouse	3G8	IgG_1 κ	1.5
HLA-DR	PerCP-Cy5.5	ThermoFisher	Mouse	LN3	IgG_{2b} κ	2.5
MerTK	APC	R&D	Mouse	125518	IgG_1	2.5
Axl	Alexa-Fluor 488	R&D	Mouse	108724	IgG_1	3
Tyro3	PE	R&D	Mouse	96201	IgG_1	5
CD64	Brilliant Violet 421	BioLegend	Mouse	10.1	IgG_1 κ	2.5
PD-1	Brilliant Violet	BD Biosciences	Mouse	EH12.1	IgG_1 κ	2.5
Fixable Viability Dye	eFluor 506	ThermoFisher	N/A	N/A	N/A	N/A
TUBE 2						
CD14	PE-Cy7	BD Biosciences	Mouse	MϕP-9	IgG_{2b} κ	1.5
CD16	APC-H7	BD Biosciences	Mouse	3G8	IgG_1 κ	1.5
HLA-DR	PerCP-Cy5.5	ThermoFisher	Mouse	LN3	IgG_{2b} κ	2.5
Tie-2	APC	R&D	Mouse	83715	IgG_1 κ	3
CD32	FITC	BD Biosciences	Mouse	FLI8.26	IgG_{2b} κ	3
CD163	PE	BD Biosciences	Mouse	GHI/61	IgG_1 κ	3.5
CCR5	Brilliant Violet 421	BioLegend	Rat	J418F1	IgG_{2b} κ	4
PD-1	Brilliant Violet	BD Biosciences	Mouse	EH12.1	IgG_1 κ	2.5
Fixable Viability Dye	eFluor 506	ThermoFisher	N/A	N/A	N/A	N/A

Appendix G: Effect of Ascites on THP-1 Macrophages



Appendix H: Optimisation of Macrophage Efferocytosis – Monocyte: Neutrophil Ratio and CD66b Magnetic Bead Selection - and Monoclonal Antibody Panel

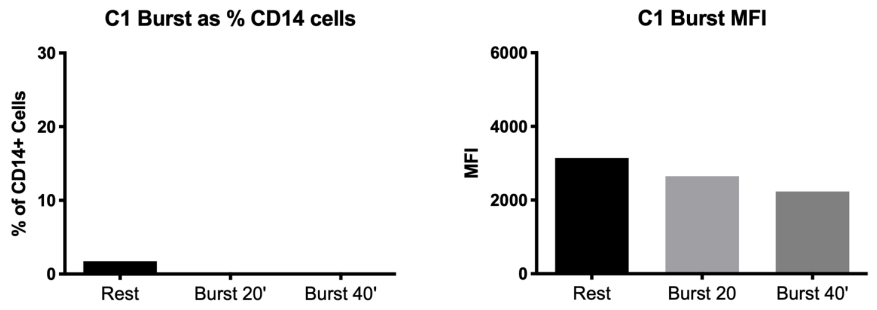
Antibody	Fluorochrome	Source	Host Species	Clone	Isotype	Volume (µl)
CD14	PE-Cy7	BD Biosciences	Mouse	MϕP-9	IgG_{2b} κ	1.5
CD16	Brilliant Violet 785	BD Biosciences	Mouse	3G8	IgG_1 κ	1.5
HLA-DR	PerCP-Cy5.5	ThermoFisher	Mouse	LN3	IgG_{2b} κ	2.5
MerTK	APC	R&D	Mouse	125518	IgG_1	2.5
Axl	Alexa-Fluor 488	R&D	Mouse	108724	IgG_1	3
BMQC Tracker	Violet 510	ThermoFisher	N/A	N/A	N/A	N/A
Fixable Viability Dye	eFluor 780	ThermoFisher	N/A	N/A	N/A	N/A



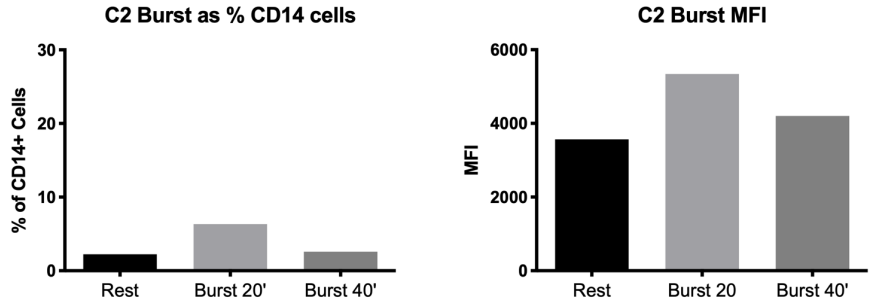
Appendix I: Monoclonal Antibody Panel for Immunophenotyping in pHrodo™ Assay

Antibody	Fluorochrome	Source	Host Species	Clone	Isotype	Volume (µl)
CD14	PE-Cy7	BD Biosciences	Mouse	MϕP-9	IgG_{2b} κ	1.5
CD16	Brilliant Violet 785	BD Biosciences	Mouse	3G8	IgG_1 κ	1.5
Axl	PerCP	R&D	Mouse	108724	IgG_1	5
MerTK	APC	R&D	Mouse	125518	IgG_1	2.5
BioParticles™	FITC	Life Technologies	N/A	N/A	N/A	N/A
HLA-DR	V500	BD Biosciences	Mouse	G46-6	IgG_{2a} κ	5
Zombie Violet FVD	Violet 450	BioLegend	N/A	N/A	N/A	N/A

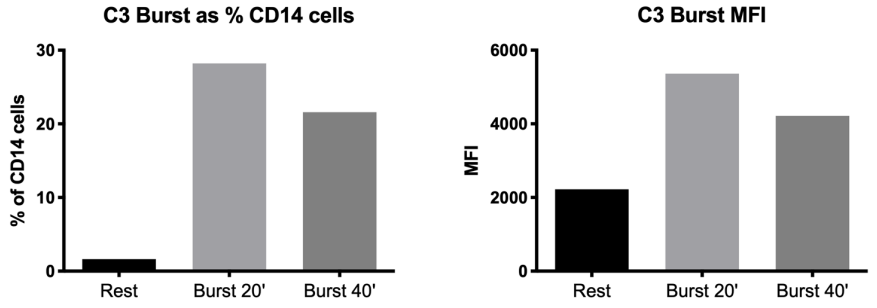
Appendix J: Optimization of Phagoburst Duration with 10% Autologous Ascites



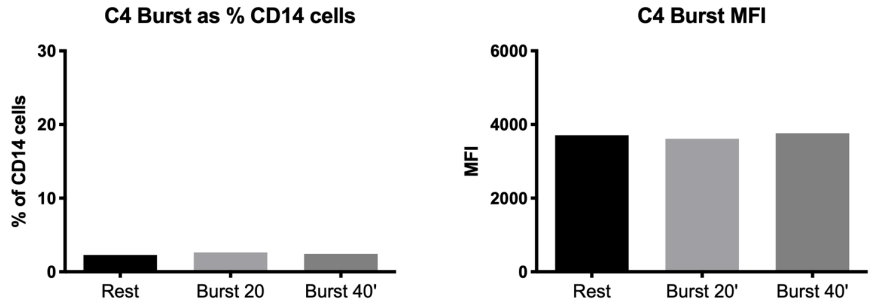
Child Pugh C12
MELD 31
protein ascites 16g/l



Child Pugh B9
MELD 8.5
protein ascites 23g/l

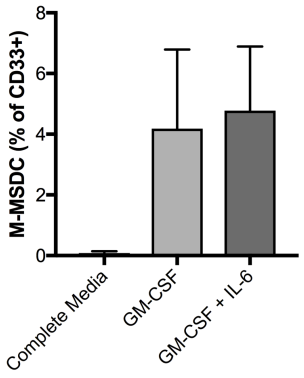


Child Pugh B7
MELD 11
protein ascites 33g/l

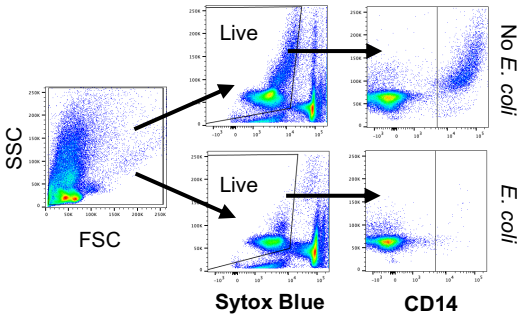


Child Pugh B7
MELD 14
protein ascites 37g/l

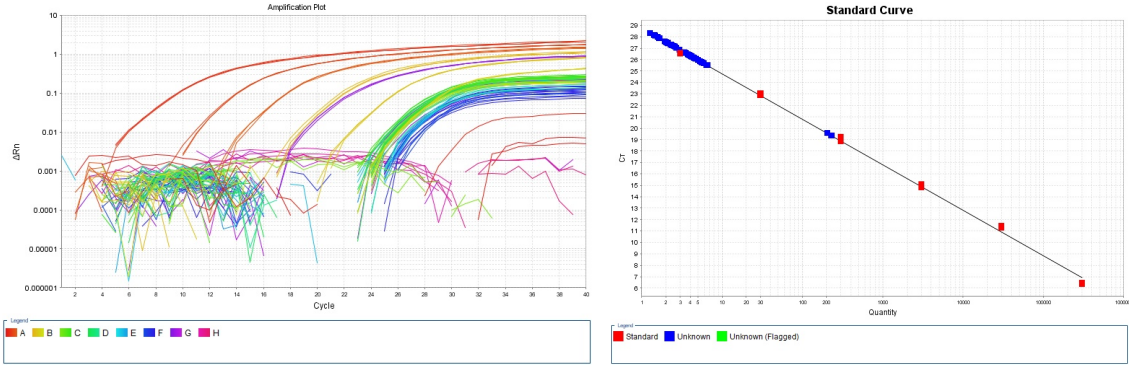
Appendix K: Effect of GM-CSF and IL-6 on M-MDSC Frequency



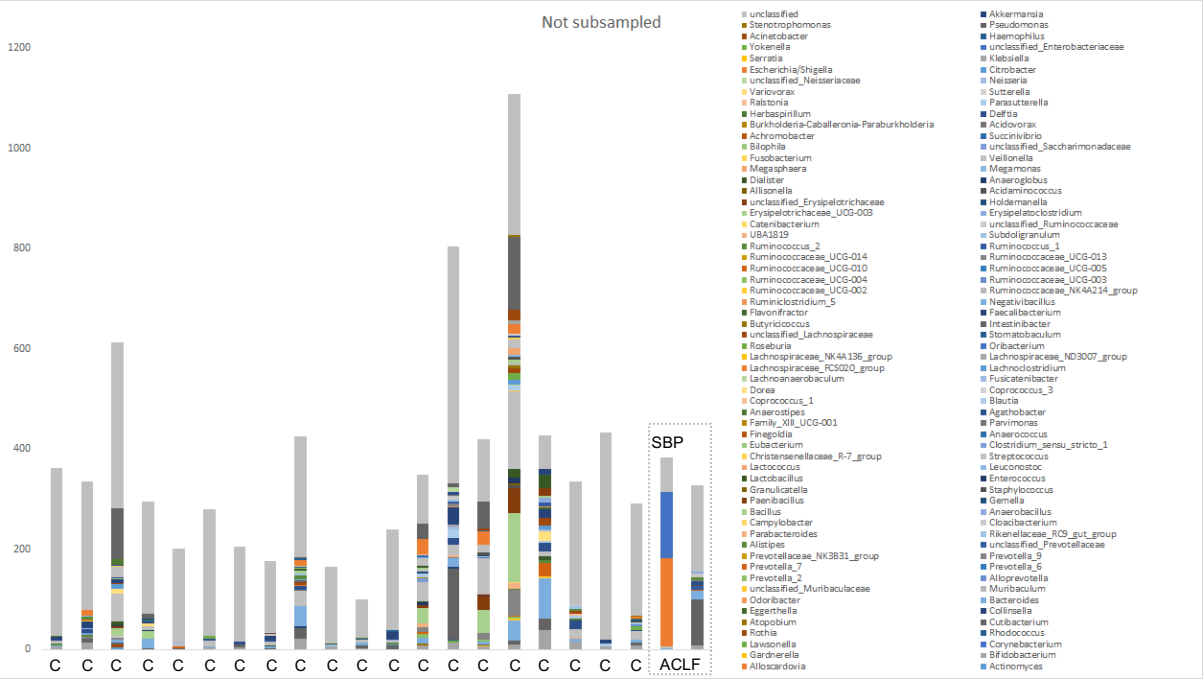
Appendix L: CellROX™ DeepRed Assay Gating and Evidence of CD14+ Cell Death



Appendix M: qPCR Standard Curve and Amplification Plots for Ascites Bacterial Quantification



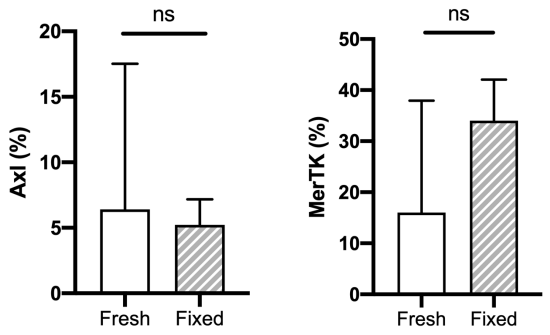
Appendix N: Bacterial Species Identified in Ascites on 16S rRNA Sequencing



Appendix O: Monoclonal Antibody Panel for Hepatic Macrophage Immunophenotyping

Antibody	Fluorochrome	Source	Host Species	Clone	Isotype	Volume (µl)
TUBE 1						
CD14	PE-Cy7	BD Biosciences	Mouse	M5E2	IgG_{2b} κ	1.5
CD16	APC-H7	BD Biosciences	Mouse	3G8	IgG_1 κ	1.5
HLA-DR	PerCP-Cy5.5	ThermoFisher	Mouse	LN3	IgG_{2b} κ	2.5
MerTK	APC	R&D	Mouse	125518	IgG_1	2.5
CCR7	FITC	BD Biosciences	Mouse	150503	IgG_{2a}	2
CD163	PE	BD Biosciences	Mouse	GHI/61	IgG_1 κ	3.5
TUBE 2						
CD14	PE-Cy7	BD Biosciences	Mouse	MϕP-9	IgG_{2b} κ	1.5
CD16	APC-H7	BD Biosciences	Mouse	3G8	IgG_1 κ	1.5
HLA-DR	PerCP-Cy5.5	ThermoFisher	Mouse	LN3	IgG_{2b} κ	2.5
MerTK	APC	R&D	Mouse	125518	IgG_1	2.5
CCR2	FITC	BioLegend	Mouse	K036C2	IgG_{2a} κ	3.5
CX_3CR1	PE	ThermoFisher	Rat	2A9-1	IgG_{2b} κ	3.5
CCR5	Brilliant Violet 421	BioLegend	Rat	J418F1	IgG_{2b} κ	4
CCR7	Brilliant Violet 510	BioLegend	Mouse	G043H7	IgG_{2a} κ	N/A
TUBE 3: M-MDSC						
CD14	PE-Cy7	BD Biosciences	Mouse	MϕP-9	IgG_{2b} κ	1.5
CD16	APC-H7	BD Biosciences	Mouse	3G8	IgG_1 κ	1.5
HLA-DR	PerCP-Cy5.5	ThermoFisher	Mouse	LN3	IgG_{2b} κ	2.5
MerTK	APC	R&D	Mouse	125518	IgG_1	2.5
CD32	FITC	BD Biosciences	Mouse	FLI8.26	IgG_{2b} κ	3
CD169	PE	BD Biosciences	Mouse	7-239	IgG_1 κ	3
CD11b	Brilliant Violet 421	BioLegend	Mouse	ICRF44	IgG_1	5
CD64	Brilliant Violet 510	BioLegend	Mouse	10.1	IgG_1 κ	2.5

Appendix P: Fixed vs. Fresh Hepatic Macrophage MerTK and Axl (%) Expression



Appendix Q: Monoclonal Antibody Panel for Phenotyping Monocytes in Migration Assay

Antibody	Fluorochrome	Source	Host Species	Clone	Isotype	Volume (µl)
TUBE 1						
CD14	PE-Cy7	BD Biosciences	Mouse	MϕP-9	IgG_{2b} κ	1.5
CD16	APC-H7	BD Biosciences	Mouse	3G8	IgG_1 κ	1.5
HLA-DR	PerCP-Cy5.5	ThermoFisher	Mouse	LN3	IgG_{2b} κ	2.5
MerTK	APC	R&D	Mouse	125518	IgG_1	2.5
CCR7	FITC	BioLegend	Mouse	G043H7	IgG_{2a} κ	2
CD163	PE	BD Biosciences	Mouse	GHI/61	IgG_1 κ	3.5
TUBE 2						
CD14	PE-Cy7	BD Biosciences	Mouse	MϕP-9	IgG_{2b} κ	1.5
CD16	APC-H7	BD Biosciences	Mouse	3G8	IgG_1 κ	1.5
HLA-DR	PerCP-Cy5.5	ThermoFisher	Mouse	LN3	IgG_{2b} κ	2.5
CCR2	Alexa Fluor 647	BD Biosciences	Mouse	48607	IgG_{2b}	4
CCR5	FITC	BioLegend	Rat	HEK1/85a	IgG_{2a} κ	3.5
CX_3CR1	PE	ThermoFisher	Rat	2A9-1	IgG_{2b} κ	3.5

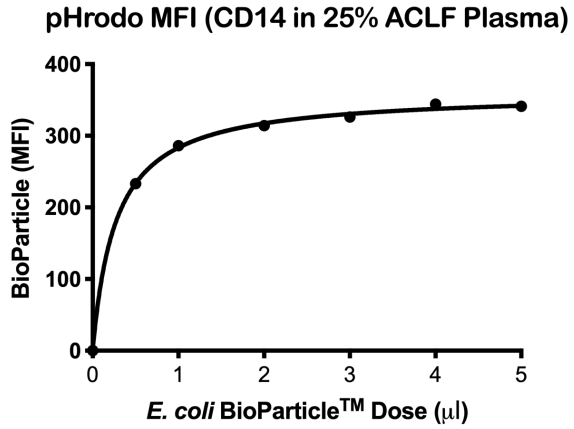
Appendix R: Monoclonal Antibody Panel for Monocyte Intracellular Cytokine Staining in Migration Assay

Antibody	Fluorochrome	Source	Host Species	Clone	Isotype	Volume (µl)
TUBE 1						
Extracellular Stain						
CD14	PE-Cy7	BD Biosciences	Mouse	MϕP-9	IgG_{2b} κ	1.5
CD16	APC-H7	BD Biosciences	Mouse	3G8	IgG_1 κ	1.5
HLA-DR	PerCP-Cy5.5	ThermoFisher	Mouse	LN3	IgG_{2b} κ	2.5
MerTK	PE	R&D	Mouse	125518	IgG_{2b}	2.5
Intracellular Stain						
TNF-α	APC	BD Biosciences	Mouse	MAb11	IgG_1 κ	2.5
TUBE 2						
Extracellular Stain						
CD14	PE-Cy7	BD Biosciences	Mouse	MϕP-9	IgG_{2b} κ	1.5
CD16	APC-H7	BD Biosciences	Mouse	3G8	IgG_1 κ	1.5
HLA-DR	PerCP-Cy5.5	ThermoFisher	Mouse	LN3	IgG_{2b} κ	2.5
MerTK	APC	R&D	Mouse	125518	IgG_1	2.5
Intracellular Stain						
IL-6	PE	BD Biosciences	Rat	MQ2-13A5	IgG_1	2.5

Appendix S: Monoclonal Antibody Panel for PBMC ICCS

Antibody	Fluorochrome	Source	Host Species	Clone	Isotype	Volume (µl)
Extracellular Stain						
CD14	PE-Cy7	BD Biosciences	Mouse	MϕP-9	IgG_{2b} κ	1.5
CD16	APC-H7	BD Biosciences	Mouse	3G8	IgG_1 κ	1.5
HLA-DR	PerCP-Cy5.5	ThermoFisher	Mouse	LN3	IgG_{2b} κ	2.5
MerTK	APC	R&D	Mouse	125518	IgG_1	2.5
Axl	Alexa-Fluor 488	R&D	Mouse	108724	IgG_1	3
Fixable Viability Dye	eFluor 506	ThermoFisher	N/A	N/A	N/A	N/A
Intracellular Stain						
TNF-α	PE	BD Biosciences	Mouse	MAb11	IgG_1 κ	2.5
IL-6	Brilliant Violet 421	BD Biosciences	Rat	MQ2-13A5	IgG_1	2.5

Appendix T: pHrodo™ BioParticle™ Dose Optimization



Appendix U: Permissions Granted for Copyrighted Figures

Page No.	Type of work:	Name of work	Source of work	Copyright holder and contact	Permission requested on	I have permission yes /no	Permission note
33	Table	Table 1.1 Definition of organ failures in patients with cirrhosis	Bacterial infections in cirrhosis: A position statement based on the EASL Special Conference 2013. Journal of Hepatology (2014), vol. 60: 1314	© 2014 Elsevier permissionshelpdesk@elsevier.com	19.09.19	yes	Licensed with a Creative Commons Attribution-NonCommercial-NoDerivatives 2.0 Generic (CC BY-NC-ND 2.0
47	Figure	Figure 1.1 Cirrhosis-associated Immune Dysfunction	Cirrhosis-associated immune dysfunction: Distinctive features and clinical relevance. Journal of Hepatology (2014), vol. 61: 1387.	© 2014 Elsevier permissionshelpdesk@elsevier.com	19.09.19	yes	Open Access content CC-BY 4.0 and permission granted (confirmation no. 11852448)
66	Figure	Figure 1.2 Schematic of TAM Receptor and Ligand Structure	Immunobiology of the TAM Receptors. Nature Reviews Immunology (2008), vol. 8: 328	© Nature Publishing Group, Springer Nature	19.09.19	yes	Order number 4672401001949
68	Figure	Figure 1.3 Schematic of TAM pathway signaling in innate immune cells.	Age-related changes in expression and signaling of TAM receptor inflammatory regulators in monocytes. Oncotarget (2018), vol. 9 (11): 9572-9580.	© Impact Journals forms@oncotarget.com	19.09.19	yes	Licensed with a Creative Commons Attribution 3.0 (CC BY 3.0) – open access
259	Part of Figure	Figure 7.1 MerTK+ hepatic macrophages are expanded in human and experimental APAP-induced acute liver injury	MerTK expressing hepatic macrophages promote the resolution of inflammation in acute liver failure. Gut (2018), vol. 67: 333-347	© 2018 BMJ Publishing Group bmj.permissions@bmj.com	23.09.19	yes	Open access content CC-BY-4.0 and permission granted (licence number 4674861419565)